



**HAL**  
open science

# Switched battery DC-DC converters for low-power applications

Carlos Augusto Berlitz

► **To cite this version:**

Carlos Augusto Berlitz. Switched battery DC-DC converters for low-power applications. Micro and nanotechnologies/Microelectronics. INSA de Lyon, 2023. English. NNT: 2023ISAL0118. tel-04689682

**HAL Id: tel-04689682**

**<https://theses.hal.science/tel-04689682v1>**

Submitted on 5 Sep 2024

**HAL** is a multi-disciplinary open access archive for the deposit and dissemination of scientific research documents, whether they are published or not. The documents may come from teaching and research institutions in France or abroad, or from public or private research centers.

L'archive ouverte pluridisciplinaire **HAL**, est destinée au dépôt et à la diffusion de documents scientifiques de niveau recherche, publiés ou non, émanant des établissements d'enseignement et de recherche français ou étrangers, des laboratoires publics ou privés.



# INSA

N°d'ordre NNT : 2023ISAL0118

## THESE de DOCTORAT DE L'INSA LYON, membre de l'Université de Lyon

**Ecole Doctorale 160**  
**Électronique, Électrotechnique, Automatique (EEA)**

**Spécialité/ discipline de doctorat :**  
Electronique, micro et nanoélectronique, optique et laser

Soutenue publiquement/à huis clos le 20/12/2023, par :  
**Carlos Augusto BERLITZ**

---

# Switched Battery DC-DC Converters for Low-Power Applications

---

Devant le jury composé de :

Vinassa, Jean-Michel	Professeur d'Université	Bordeaux INP	<b>Président</b>
Cousineau, Marc	Maître de Conférences	Toulouse INP	Rapporteur
Prodic, Aleksandar	Professeur d'Université	University of Toronto	Rapporteur
Vinassa, Jean-Michel	Professeur d'Université	Bordeaux INP	Examineur
Dumont, Romane	Ingénieure Docteur	ST Microelectronics	Examineur
Allard, Bruno	Enseignant chercheur	INSA Lyon	Directeur de thèse
Pillonet, Gaël	Directeur de Recherche	CEA-LETI	Co-directeur de thèse
Oukassi, Sami	Ingénieur Chercheur	CEA-LETI	Encadrant



Référence : TH1035\_BERLITZ Carlos Augusto

L'INSA Lyon a mis en place une procédure de contrôle systématique via un outil de détection de similitudes (logiciel Compilatio). Après le dépôt du manuscrit de thèse, celui-ci est analysé par l'outil. Pour tout taux de similarité supérieur à 10%, le manuscrit est vérifié par l'équipe de FEDORA. Il s'agit notamment d'exclure les auto-citations, à condition qu'elles soient correctement référencées avec citation expresse dans le manuscrit.

Par ce document, il est attesté que ce manuscrit, dans la forme communiquée par la personne doctorante à l'INSA Lyon, satisfait aux exigences de l'Établissement concernant le taux maximal de similitude admissible.

## Département FEDORA – INSA Lyon - Ecoles Doctorales

SIGLE	ECOLE DOCTORALE	NOM ET COORDONNEES DU RESPONSABLE
<b>CHIMIE</b>	<b><u>CHIMIE DE LYON</u></b> <a href="https://www.edchimie-lyon.fr">https://www.edchimie-lyon.fr</a> Sec. : Renée EL MELHEM Bât. Blaise PASCAL, 3e étage secretariat@edchimie-lyon.fr	<b>M. Stéphane DANIELE</b> C2P2-CPE LYON-UMR 5265 Bâtiment F308, BP 2077 43 Boulevard du 11 novembre 1918 69616 Villeurbanne <a href="mailto:directeur@edchimie-lyon.fr">directeur@edchimie-lyon.fr</a>
<b>E.E.A.</b>	<b><u>ÉLECTRONIQUE, ÉLECTROTECHNIQUE, AUTOMATIQUE</u></b> <a href="https://edeea.universite-lyon.fr">https://edeea.universite-lyon.fr</a> Sec. : Stéphanie CAUVIN Bâtiment Direction INSA Lyon Tél : 04.72.43.71.70 secretariat.edeea@insa-lyon.fr	<b>M. Philippe DELACHARTRE</b> INSA LYON Laboratoire CREATIS Bâtiment Blaise Pascal, 7 avenue Jean Capelle 69621 Villeurbanne CEDEX Tél : 04.72.43.88.63 <a href="mailto:philippe.delachartre@insa-lyon.fr">philippe.delachartre@insa-lyon.fr</a>
<b>E2M2</b>	<b><u>ÉVOLUTION, ÉCOSYSTÈME, MICROBIOLOGIE, MODÉLISATION</u></b> <a href="http://e2m2.universite-lyon.fr">http://e2m2.universite-lyon.fr</a> Sec. : Bénédicte LANZA Bât. Atrium, UCB Lyon 1 Tél : 04.72.44.83.62 secretariat.e2m2@univ-lyon1.fr	<b>Mme Sandrine CHARLES</b> Université Claude Bernard Lyon 1 UFR Biosciences Bâtiment Mendel 43, boulevard du 11 Novembre 1918 69622 Villeurbanne CEDEX <a href="mailto:sandrine.charles@univ-lyon1.fr">sandrine.charles@univ-lyon1.fr</a>
<b>EDISS</b>	<b><u>INTERDISCIPLINAIRE SCIENCES-SANTÉ</u></b> <a href="http://ediss.universite-lyon.fr">http://ediss.universite-lyon.fr</a> Sec. : Bénédicte LANZA Bât. Atrium, UCB Lyon 1 Tél : 04.72.44.83.62 secretariat.ediss@univ-lyon1.fr	<b>Mme Sylvie RICARD-BLUM</b> Institut de Chimie et Biochimie Moléculaires et Supramoléculaires (ICBMS) - UMR 5246 CNRS - Université Lyon 1 Bâtiment Raulin - 2ème étage Nord 43 Boulevard du 11 novembre 1918 69622 Villeurbanne Cedex Tél : +33(0)4 72 44 82 32 <a href="mailto:sylvie.ricard-blum@univ-lyon1.fr">sylvie.ricard-blum@univ-lyon1.fr</a>
<b>INFOMATHS</b>	<b><u>INFORMATIQUE ET MATHÉMATIQUES</u></b> <a href="http://edinfomaths.universite-lyon.fr">http://edinfomaths.universite-lyon.fr</a> Sec. : Renée EL MELHEM Bât. Blaise PASCAL, 3e étage Tél : 04.72.43.80.46 infomaths@univ-lyon1.fr	<b>M. Hamamache KHEDDOUCI</b> Université Claude Bernard Lyon 1 Bât. Nautibus 43, Boulevard du 11 novembre 1918 69 622 Villeurbanne Cedex France Tél : 04.72.44.83.69 <a href="mailto:hamamache.kheddouci@univ-lyon1.fr">hamamache.kheddouci@univ-lyon1.fr</a>
<b>Matériaux</b>	<b><u>MATÉRIAUX DE LYON</u></b> <a href="http://ed34.universite-lyon.fr">http://ed34.universite-lyon.fr</a> Sec. : Yann DE ORDENANA Tél : 04.72.18.62.44 yann.de-ordenana@ec-lyon.fr	<b>M. Stéphane BENAYOUN</b> Ecole Centrale de Lyon Laboratoire LTDS 36 avenue Guy de Collongue 69134 Ecully CEDEX Tél : 04.72.18.64.37 <a href="mailto:stephane.benayoun@ec-lyon.fr">stephane.benayoun@ec-lyon.fr</a>
<b>MEGA</b>	<b><u>MÉCANIQUE, ÉNERGÉTIQUE, GÉNIE CIVIL, ACOUSTIQUE</u></b> <a href="http://edmega.universite-lyon.fr">http://edmega.universite-lyon.fr</a> Sec. : Stéphanie CAUVIN Tél : 04.72.43.71.70 Bâtiment Direction INSA Lyon mega@insa-lyon.fr	<b>M. Jocelyn BONJOUR</b> INSA Lyon Laboratoire CETHIL Bâtiment Sadi-Carnot 9, rue de la Physique 69621 Villeurbanne CEDEX <a href="mailto:jocelyn.bonjour@insa-lyon.fr">jocelyn.bonjour@insa-lyon.fr</a>
<b>ScSo</b>	<b><u>ScSo*</u></b> <a href="https://edsciencessociales.universite-lyon.fr">https://edsciencessociales.universite-lyon.fr</a> Sec. : Mélina FAVETON INSA : J.Y. TOUSSAINT Tél : 04.78.69.77.79 melina.faveton@univ-lyon2.fr	<b>M. Bruno MILLY</b> Université Lumière Lyon 2 86 Rue Pasteur 69365 Lyon CEDEX 07 <a href="mailto:bruno.milly@univ-lyon2.fr">bruno.milly@univ-lyon2.fr</a>

\*ScSo : Histoire, Géographie, Aménagement, Urbanisme, Archéologie, Science politique, Sociologie, Anthropologie

# Abstract

With current popularization of portable electronic devices, wireless sensors, and the Internet of Things (IoT), the demand for efficient and adaptable power management solutions has risen to unprecedented heights. Low-power applications, spanning a broad spectrum of domains from healthcare to environmental monitoring, have become integral to our modern way of life. These applications, often operating on limited energy resources, present a unique set of challenges and opportunities in the realm of power electronics. While traditional DC-DC converters have demonstrated their efficacy in a myriad of scenarios, their conventional designs may no longer suffice to address the distinct and stringent requirements of low- and ultra-low-power systems. This thesis embarks on a comprehensive exploration of this intricate landscape, unveiling a tapestry of challenges, innovations, and solutions that define the domain of low-power DC-DC converters.

The pursuit of novel switched DC-DC converters specifically tailored to low-power applications is at the heart of this thesis. As technology advances, the call for power-efficient solutions becomes ever more compelling, driven by a confluence of factors that underscore the significance of this research endeavor.

Traditionally DC-DC converters rely on inductors or capacitors for high efficiency conversion. However, despite advances on plenty of domains of power electronics, some physical and intrinsic limitations are still present when dealing with low-power applications, like charge sharing loss or the difficulty of inductor miniaturization. Such constraints call for innovative solutions for this application field.

The manuscript starts by presenting DC-DC converters and the particular challenges that are faced by such solutions at low-power scenarios. It is followed by studying some of the solutions proposed to address such challenges and their limitations, serving as cornerstone to the remaining of the thesis. Having identified that some of the limitations of current solutions are intrinsic to the passive devices used, the next step is to propose a solution tackling this challenge, a new topology family of DC-DC converters based on batteries as flying passive device. This new family topology is then experimentally validated and compared to a more traditional solution at a simple scenario. In a next natural step the concept is further experimented to more advanced converter topologies, including promising control and regulation strategies. Ultimately it leads to exploring different battery chemistries and their impact on the topology but also other passive technologies like fuel cells. A new topology family for low frequency and low-power DC-DC converters is proposed and experimentally validated with advantages against traditional DC-DC converters at the same conditions. It also opens a new field of study for passive technologies not before

---

explored in this context.

# Résumé

Avec la popularisation recent des dispositifs électroniques portables, des capteurs sans fil et de l'Internet des objets (IoT en anglais), la demande de solutions de gestion d'alimentation efficaces et adaptables a atteint des sommets sans précédent. Les applications à faible puissance, couvrant un large éventail de domaines, de la santé à la surveillance environnementale, sont devenues essentielles à notre mode de vie moderne. Ces applications, souvent alimentées par des ressources énergétiques limitées, présentent un ensemble unique de défis et d'opportunités dans le domaine de l'électronique de puissance. Alors que les convertisseurs CC-CC traditionnels ont démontré leur efficacité dans de nombreuses situations, leurs conceptions conventionnelles pourraient ne plus suffire à répondre aux exigences distinctes et strictes des systèmes à faible et ultra-faible puissance. Cette thèse entreprend une exploration approfondie de ce paysage complexe, dévoilant une toile de défis, d'innovations et de solutions qui définissent le domaine des convertisseurs CC-CC à faible puissance.

La recherche des nouveaux convertisseurs CC-CC commuté spécifiquement adaptés aux applications à faible puissance est au cœur de cette thèse. À mesure que la technologie progresse, l'appel à des solutions économes en énergie devient de plus en plus pressant, sous l'impulsion d'une convergence de facteurs qui soulignent l'importance de ce domaine de recherche.

Traditionnellement, les convertisseurs CC-CC reposent sur des inducteurs ou des condensateurs pour une conversion à haute efficacité. Cependant, malgré les avancées dans des nombreux domaines de l'électronique de puissance, certaines limitations physiques et intrinsèques subsistent dans le domaine de faible-puissance, telles que les pertes de partage de charge ou la difficulté de miniaturisation des inducteurs. De telles contraintes appellent à des solutions innovantes pour ce genre d'application des convertisseurs CC-CC.

Le manuscrit commence par présenter les convertisseurs CC-CC et les défis particuliers auxquels sont confrontées de telles solutions dans des scénarios à faible puissance. Il est suivi par l'étude de certaines des solutions proposées pour relever de tels défis et leurs limitations, servant de pierre angulaire au reste de la thèse. Ayant identifié que certaines des limitations des solutions actuelles sont intrinsèques aux dispositifs passifs utilisés, l'étape suivante consiste à proposer une solution pour relever ce défi, une nouvelle famille de topologies de convertisseurs CC-CC basée sur des batteries en tant que dispositif passif volant. Cette nouvelle famille de topologies est ensuite validée expérimentalement et comparée à une solution plus traditionnelle dans un scénario simple. Dans une étape naturelle suivante, le concept est davantage expérimenté pour des topologies de convertisseurs plus avancées, y compris des possibles stratégies de



---

contrôle et de régulation. Cela conduit en fin de compte à explorer différentes chimies de batteries et leur impact sur la topologie, mais aussi d'autres technologies passives telles que les piles à combustible. Une nouvelle famille de topologies pour les convertisseurs CC-CC à basse fréquence et faible puissance est proposée et validée expérimentalement avec des avantages par rapport aux convertisseurs CC-CC traditionnels dans les mêmes conditions. Cela ouvre également un nouveau domaine d'étude pour les technologies passives jusqu'alors non explorées dans ce contexte.

# Résumé Étendu

## Chapitre 1 : Convertisseurs CC-CC commutée en basse et ultra-basse puissance

Ce chapitre fournit un aperçu des défis et des solutions liés aux convertisseurs CC-CC commutée en basse et ultra-basse puissance. Il commence par une revue des convertisseurs CC-CC en mettant l'accent sur les convertisseurs CC-CC commutée. Le chapitre explore les solutions prédominantes en matière de conversion CC-CC basse puissance, en mettant en avant les caractéristiques distinctives et les approches innovantes.

### Convertisseurs CC-CC commutées

Les convertisseurs CC-CC commutée sont essentiels dans l'électronique moderne pour la gestion efficace de l'énergie. Ils fonctionnent en stockant et en libérant périodiquement de l'énergie, ce qui permet la conversion de tension. Deux principaux types existent : les convertisseurs magnétiques (courants pour des puissances modérées à élevées) et les convertisseurs diélectriques (utilisés en basse puissance, y compris dans les applications émergentes à puissance plus fort ( $>100$  mW)).

### Paramètres et Caractéristiques

Les convertisseurs CC-CC sont définis par les niveaux de tension d'entrée/sortie, la capacité de gestion de puissance, l'efficacité et l'empreinte. L'efficacité reflète les performances et est affectée par les pertes internes, notamment les pertes par conduction et les pertes par commutation.

### Convertisseurs CC-CC Basse Puissance

Dans les applications basse puissance, il y a une demande en termes d'efficacité élevée et de densité de puissance. Les convertisseurs à condensateur commuté (SCC) sont envisagés, mais des compromis entre efficacité, densité de puissance et taille doivent être pris en compte, ce qui rend complexe le développement de convertisseurs basse puissance.

---

## État de l'Art

La conception de convertisseurs CC-CC basse puissance rencontre des défis en raison des pertes inhérentes et des limitations physiques. Les solutions actuelles sont analysées en tenant compte de paramètres tels que l'efficacité, la densité de puissance et la fréquence de fonctionnement.

### Solutions Actuelles pour les Convertisseurs CC-CC Basse Puissance

Les solutions CC-CC basse puissance sont limitées en raison des pertes inhérentes, notamment pour maintenir une efficacité élevée et une densité de puissance élevée. En général, l'efficacité diminue à des niveaux de puissance extrêmement bas. Les solutions inductives peuvent nécessiter une plus grande surface sur puce pour les inductances volumineuses, même si le circuit présente une conception compacte. Les solutions à base de condensateur obtiennent une efficacité compétitive mais rencontrent des limites intrinsèques en dessous d'un certain niveau de puissance de sortie. Les approches hybrides tentent de combiner la capacitance et l'inductance, cependant, il est souvent constaté que l'efficacité élevée n'est présente qu'à des puissances de sortie plus élevées.

Lors de l'analyse de l'efficacité maximale par rapport à la densité de puissance pour les convertisseurs récents, les solutions à base d'inductance utilisent souvent des inductances externes pour atteindre une efficacité élevée, réduisant la densité de puissance de la solution complète. Les solutions à base de condensateur, bien qu'elles soient plus intégrées, peuvent avoir une efficacité maximale plus faible.

La fréquence de fonctionnement est un facteur majeur pour les performances à de telles puissances. Les convertisseurs basse puissance réduisent les fréquences de commutation pour maintenir une efficacité élevée, mais cela limite la densité de puissance. Le choix général entre les convertisseurs à inductance et à condensateur dépend des compromis nécessaires pour une application spécifique.

### Limitations des Solutions Actuelles

Les solutions à base d'inductance se comportent bien mais ont une empreinte plus importante. Les convertisseurs à base de condensateur rencontrent des défis pour atteindre plusieurs rapports de conversion avec un contrôle grossier uniquement. Des stratégies pour augmenter la granularité de contrôle existent mais peuvent introduire des pertes supplémentaires.

Historiquement, les convertisseurs à condensateur commuté (SCC) en basse puissance fonctionnaient dans la limite de commutation lente (SSL), mais les applications modernes exigent également une opération dans la limite de commutation rapide (FSL). La FSL nécessite une densité de capacitance plus élevée, souvent à partir de dispositifs exotiques tels que les technologies de tranchées profondes, limitant l'intégration complète des passifs. Pour surmonter ces limitations, des dispositifs passifs alternatifs tels que les batteries à l'état solide sont explorés. Ils offrent une densité d'énergie plus élevée mais peuvent nécessiter une densité de puissance plus élevée pour une opération même en faible puissance.

---

## Chapitre 2 : Topologie proposée - Convertisseur à Batterie Commutée

Dans les convertisseurs CC-CC, le choix du composant de stockage d'énergie intermédiaire a un impact significatif sur les performances du convertisseur. En général, les convertisseurs utilisent des inductances ou des condensateurs, mais ces derniers présentent des limitations en termes de puissance et de densité énergétique. Les condensateurs, bien qu'ils soient plus faciles à intégrer, ont une densité énergétique plus faible, tandis que les inductances sont difficiles à intégrer sur une seule puce et offrent une faible densité énergétique et de puissance en raison de leur nature magnétique. Pour surmonter ces limitations, nous proposons une nouvelle famille de convertisseurs appelée "Convertisseurs à Batterie Commutée" (SBC en anglais), inspirée du concept des "Convertisseurs à Condensateur Commuté" (SSB).

### La Batterie en tant que Dispositif de Stockage d'Énergie Volant

Les batteries, traditionnellement utilisées pour le stockage d'énergie à long terme, sont désormais envisagées pour des applications à plus court terme grâce aux avancées technologiques. Contrairement aux condensateurs qui stockent de l'énergie sous forme de charge ou aux inductances qui stockent de l'énergie dans un champ magnétique, les batteries sont des dispositifs pour stockage d'énergie chimique de long terme. Les batteries ont un profil de décharge unique où la tension reste relativement constante sur une plage de niveaux de charge, donc pas directement proportionnel à la quantité de charge stockée. Cette caractéristique pour faire des batteries un candidat prometteur pour le stockage d'énergie dans les convertisseurs CC-CC, offrant une densité d'énergie et de puissance plus élevée à de basses fréquences de fonctionnement.

### Puissance et Densité Énergétique

Les batteries excellent en densité d'énergie par rapport aux condensateurs et aux inductances, ce qui les rend adaptées au stockage d'énergie. Cependant, leur capacité de délivrance de puissance est limitée par leurs capacités en courant. Par contre, à de basses fréquences de fonctionnement, les batteries peuvent fournir une densité de puissance plus élevée que les composants passifs traditionnels grâce à une indépendance de la fréquence pour les batteries. Cette observation suggère que les batteries peuvent être un ajout précieux aux convertisseurs CC-CC, en particulier dans les applications à faible puissance.

### Intégration sur Puce

Les récentes avancées dans la technologie des batteries à état solide ont ouvert la voie à des solutions de batterie compactes et intégrées. Les batteries à état solide peuvent être directement intégrées sur des substrats en silicium, offrant une densité d'énergie et de puissance plus élevée, une meilleure sécurité et une durée de vie plus longue. Cette intégration améliore l'efficacité de la conversion d'énergie dans des facteurs de forme réduits.

---

## Défis et Contraintes

L'incorporation de batteries dans les convertisseurs CC-CC commutés introduit des défis. Les batteries sont conçues pour un fonctionnement continu, et leurs performances peuvent se dégrader avec des commutations fréquentes. Elles ont également des plages de tension limitées et des réponses dynamiques plus lentes que les composants passifs traditionnels. De plus, les batteries ont un nombre fini de cycles de charge-décharge, ce qui peut affecter leur durée de vie et les performances globales du système.

Pour relever ces défis, des investigations expérimentales sont nécessaires pour comprendre comment les batteries se comportent dans le contexte des convertisseurs CC-CC commutés. Le Chapitre 3 décrira les expériences et les résultats obtenus pour évaluer la faisabilité de l'utilisation de batteries comme dispositifs de stockage d'énergie intermédiaire dans ce contexte.

## Topologie du Convertisseur à Batterie Commutée (SBC)

Le SBC (Convertisseur à Batterie Commutée) est une nouvelle famille de convertisseurs CC-CC conçue pour améliorer la densité d'énergie et de puissance dans les applications à faible puissance. Inspiré des topologies de convertisseurs à condensateur commuté (SCC), le SBC intègre des batteries en tant que composants passifs volants dans le convertisseur. Cette configuration unique introduit des défis liés à la définition de séquences d'états optimales et à la garantie que les batteries restent dans des limites de tension sûres.

Un défi majeur est de concevoir une séquence d'états qui empêche les batteries de dépasser leurs seuils de tension de sécurité, garantissant ainsi leur longévité et leurs performances optimales. Cette séquence est cruciale car la contribution ionique des batteries est un avantage clé par rapport aux autres composants passifs.

Le maintien de l'équilibre des charges est tout aussi important, car les batteries servent de dispositifs de stockage d'énergie intermédiaire. L'équilibre des charges garantit que les batteries ne sont ni surchargées ni déchargées pendant le fonctionnement à l'état stable, préservant ainsi leurs performances et leur longévité.

## Fonctionnement en Micro-Cycles

Pendant le fonctionnement du SBC, les batteries connaissent un modèle d'utilisation différent par rapport aux cycles de décharge profonde traditionnels. Ce modèle implique des phases de charge et de décharge alternées, appelées "micro-cycles" ( $\mu$ -cycles). Chaque  $\mu$ -cycle a un impact minimal sur l'état de charge (SoC) de la batterie, préservant ainsi sa tension et sa durée de vie.

La limitation de la profondeur de décharge (DoD) dans chaque  $\mu$ -cycle réduit le stress sur la batterie, atténue les réactions secondaires et améliore ses performances et sa fiabilité. Une faible DoD réduit également la génération de chaleur dans la batterie, réduisant le stress thermique.

L'utilisation de  $\mu$ -cycles optimise les stratégies de gestion de batterie, garantissant des niveaux de tension cohérents et permettant à la batterie de supporter beaucoup plus de cycles que les cycles de décharge profonde traditionnels.

---

## Séquençage

Le SBC utilise une séquence de phases avec des batteries connectées en série pour conserver le SoC et maintenir la tension de sortie. Chaque phase doit répondre à des critères spécifiques, notamment la présence d'au moins une batterie en série, la satisfaction de l'exigence de tension de sortie et aussi la conservation du SoC.

La séquence se répète pendant le fonctionnement à l'état stable, optimisant l'utilisation des batteries et la stabilité du système. La durée de phase brève et la faible DoD garantissent que les batteries fonctionnent en toute sécurité dans leur plage de tension.

En respectant ces principes, le SBC minimise la variation de tension, réduit les pertes, élimine le besoin d'un condensateur de sortie et optimise les performances des batteries.

## Efficacité Énergétique

L'efficacité énergétique du SBC dépend principalement des pertes de conduction. Contrairement aux SCC, le SBC ne souffre pas de pertes de partage de charge en raison des caractéristiques uniques des batteries. Il subit plutôt des pertes dominées par la conduction.

Le circuit fonctionne principalement dans la limite de commutation rapide (FSL) en raison de la grande capacité de stockage d'énergie des batteries. Par conséquent, les pertes sont principalement liées à la résistance à l'état ouvert des commutateurs et à la résistance interne des batteries.

Pour estimer les pertes de conversion, une équation simplifiée incorporant des paramètres structuraux est utilisée. Cette approche évite le besoin d'analyses de réseau complexes ou de simulations.

$$R_{out} = \sum_i R_i \cdot D_i + \sum_k R_{int,k} \cdot D_k \quad (1)$$

Ici  $R_{out}$  est la résistance équivalente de sortie du SBC,  $R_i$  la résistance de conduction du  $i^{eme}$  commutateur,  $D_i$  sont rapport cyclique.  $R_{int,k}$  est la résistance de interne de la  $k^{eme}$  batterie, avec  $D_k$  sont rapport cyclique ou elle est en conduction.

## Exploration de la Topologie

La topologie du SBC fonctionne de manière similaire aux SCC, utilisant différents cycles pour différentes ratios de conversion de tension. L'identification de cycles fonctionnels qui répondent aux conditions de la Section de sequençage est essentielle pour la mise en œuvre des circuits SBC.

Pour explorer les possibilités, nous avons conçu un algorithme semi-exhaustif adapté à la recherche de phases valides qui satisfont ces conditions. Cet algorithme analyse systématiquement les combinaisons de phases pour identifier celles qui fonctionnent. Pour optimiser l'efficacité et réduire le temps de calcul, nous avons imposé des contraintes et des préférences supplémentaires. Cette approche simplifie la recherche de configurations de phase adaptées, améliorant les performances du circuit SBC.

---

## Obtention de Phases Valides pour le SBC

Les phases valides du SBC impliquent des connexions spécifiques entre les dispositifs, garantissant qu'au moins une batterie se connecte en série à la sortie. Chaque phase doit répondre aux critères décrits avant. Nous autorisons également jusqu'à deux groupes de batteries, chacun ayant une valeur de tension distincte. Cependant, il est possible que les deux groupes aient la même tension, simplifiant la conception. Cette adaptabilité à différentes configurations de batterie est une caractéristique clé du SBC.

## Obtention et Exploration de Cycles de Travail

Pour trouver des cycles de travail, nous utilisons un algorithme qui part des phases valides obtenues précédemment. Il explore les combinaisons de ces phases pour établir des cycles qui remplissent les conditions de la Section II. L'équilibre des charges est un critère crucial pour les cycles de travail, où la variation totale de charge doit être nulle pour toutes les batteries de chaque groupe.

Des cycles équivalents, qui utilisent les mêmes phases dans un ordre différent, peuvent également être trouvés. Ces cycles maintiennent l'équilibre des charges mais offrent des avantages pratiques, tels que l'optimisation de l'utilisation des commutateurs et la minimisation des variations de l'état de charge au sein des batteries.

Nous pouvons classer les cycles de travail en fonction de critères tels que la longueur (nombre de phases) et le nombre de batteries, ce qui permet une optimisation pour différents objectifs. Les cycles plus courts réduisent les pertes et l'encombrement, tandis que la réduction du nombre de batteries améliore l'intégrabilité.

L'algorithme d'optimisation peut être aussi simple que de trouver le cycle de travail le plus court parmi les cycles explorés.

## Chapitre 3 : Validation expérimentale du SBC

Ce chapitre aborde la validation expérimentale de la topologie SBC introduite dans le chapitre 2. Ce processus de validation implique le choix de la technologie de batterie appropriée pour le SBC et la comparaison de ses performances avec un convertisseur traditionnel à base de condensateur dans des conditions similaires.

### Options de Batterie

Trois principales options de batterie sont envisagées et étudiées : les batteries Nickel-Métal-Hydrure (NiMH), les batteries Lithium-Ion (Li-ion) et les batteries à état solide (SSB).

#### Nickel-Metal-Hydrure (NiMH)

Les batteries NiMH offrent des avantages tels qu'une densité d'énergie élevée, un coût relativement bas et un impact environnemental réduit par rapport à d'autres types de batteries. Elles ont un taux

---

de auto-décharge modéré, ce qui les rend adaptées à une utilisation intermittente. Les batteries NiMH fournissent une tension stable pendant la majeure partie de leur cycle de décharge, ce qui est bénéfique pour les applications à basse puissance. Cependant, elles ont une densité d'énergie inférieure par rapport aux batteries Li-ion et peuvent souffrir de l'effet mémoire si elles ne sont pas correctement gérées.

### **Lithium-Ion (Li-ion)**

Les batteries Li-ion sont connues pour leur haute densité d'énergie et leur efficacité de charge/décharge, ce qui les rend adaptées à une utilisation intermittente. Elles offrent une tension stable et peuvent fournir des courants de décharge élevés. Cependant, elles ont une tension nominale élevée, ce qui peut être limitant pour certaines applications, ainsi que des préoccupations en matière de sécurité, notamment la sensibilité à la surcharge et à la surchauffe.

### **Batterie à État Solide (SSB)**

Les batteries à état solide sont une technologie prometteuse avec une sécurité améliorée, une densité d'énergie plus élevée et une durée de vie de cycle plus longue. Elles utilisent des électrolytes solides, réduisant le risque de fuite et de surchauffe. Les SSB peuvent fonctionner à des températures plus élevées et ont le potentiel d'offrir une plus grande densité d'énergie et de puissance. Cependant, des défis subsistent pour atteindre des densités relatives élevées avec les conceptions actuelles à base de particules.

Le choix de la batterie la plus adaptée pour l'évaluation initiale du SBC est déterminé expérimentalement en raison de l'absence de modèles appropriés. Chaque option de batterie a ses propres avantages et limites, et la sélection dépendra des exigences spécifiques et des objectifs de performance du SBC.

### **Validation de la Batterie**

Dans cette section, nous explorons la validation des batteries pour une utilisation dans les Convertisseurs à Batterie Commutée (SBC). Les SBC diffèrent considérablement des applications de batterie traditionnelles, il est donc essentiel d'évaluer le comportement de la batterie dans ces conditions uniques. Nous avons choisi un modèle de batterie NiMH disponible dans le commerce avec une tension nominale de 1,2 V pour nos expériences.

Pour évaluer cela, nous avons mené des expériences en utilisant une Batterie Sous Test (BUT) soumise à des cycles de microCoulombs à milliCoulombs, imitant le fonctionnement du SBC. Cela impliquait un petit déplacement de charge/décharge ( $Q_E$ ) qui ne représente qu'une fraction de la capacité de la batterie, se produisant autour d'un point de polarisation spécifique sur la courbe tension-capacité (V-Q).

Nous avons également réalisé une analyse d'impédance à l'aide de la Spectroscopie d'Impédance Electrochimique (EIS) sur différents échantillons du SoC de la BUT pour comprendre le comportement de la batterie dans diverses conditions de fonctionnement. Cependant, pour valider pleinement les performances de la batterie dans des conditions de SBC, nous avons besoin d'une validation expérimentale à grand signal, reproduisant le fonctionnement réel du SBC.



---

## Impédance de la Batterie

Comprendre l'impédance interne de la batterie à différents États de Charge (SoC) est crucial pour évaluer sa pertinence pour les SBC. Nous avons utilisé l'EIS pour analyser le profil d'impédance interne d'une batterie NiMH à différents niveaux de SoC. Le comportement de la batterie a indiqué une augmentation de l'impédance près des extrêmes de SoC, ce qui a des implications sur la densité de puissance et l'efficacité. La batterie a montré une relation linéaire entre la résistance interne et le SoC, avec la résistance la plus élevée près de la décharge complète et de la charge complète.

## Batterie dans un $\mu$ -Cycle

Pour imiter étroitement le fonctionnement du SBC, nous avons soumis la batterie à un  $\mu$ -cycle, qui impliquait une forme d'onde de courant rectangulaire avec une valeur moyenne nulle. Cette forme d'onde reproduisait le fonctionnement du SBC, avec un point de polarisation spécifique fixé à 50% de SoC pour assurer une performance efficace.

Lors de l'analyse du  $\mu$ -cycle, nous avons observé deux composantes de tension significatives : la chute de tension ohmique IR, due à la résistance interne de la batterie, et la tension redox, attribuée aux réactions redox pendant le cycle. La chute de tension ohmique IR présentait une relation linéaire avec le courant, et sa pente fournissait des informations sur la résistance de la batterie dans des conditions de  $\mu$ -cycle.

Nous avons constaté que le comportement de la batterie pendant les  $\mu$ -cycles était influencé par le niveau de courant, la tension redox et la chute IR augmentaient avec des courants plus élevés. Une faible influence de la fréquence est observé dans la chute de tension IR et une relation logarithmic avec la tension redox. De plus, la tension moyenne de la batterie s'approchait étroitement du potentiel à circuit ouvert relaxé (OCRV) dans diverses conditions, indiquant une stabilité remarquable sur des  $\mu$ -cycles étendus.

## Performances du SBC

L'évaluation des performances du SBC implique sa comparaison avec un SCC doté de circuits d'étage de puissance identiques, fonctionnant aux mêmes niveaux de puissance et de fréquence. Des composants disponibles dans le commerce avec des dimensions similaires sont utilisés, y compris un condensateur à haute capacité, et le SBC est implémenté à l'aide d'un circuit intégré LM2663.

Le SBC fonctionne dans une topologie 2 :1 avec deux phases. Dans la première phase ( $\phi_1$ ), la source de tension d'entrée ( $V_{in}$ ) charge le dispositif passif volant (batterie ou condensateur), et dans la deuxième phase ( $\phi_2$ ), le dispositif passif volant est connecté directement à la sortie, délivrant sa charge.

Le circuit intégré LM2663 dispose d'un oscillateur interne réglable, permettant de contrôler la fréquence de commutation. La batterie utilisée est une NiMH V6HR avec une tension à circuit ouvert de 1,2 V. Le condensateur volant est un condensateur électrolytique en aluminium polymère de 100  $\mu$ F.

La résistance de sortie équivalente du SBC est d'environ 6,4  $\Omega$  et est principalement influencée par la résistance interne de la batterie. Les comparaisons de performances portent sur différentes fréquences de fonctionnement et courants de sortie, couvrant une large gamme de conditions de fonctionnement.

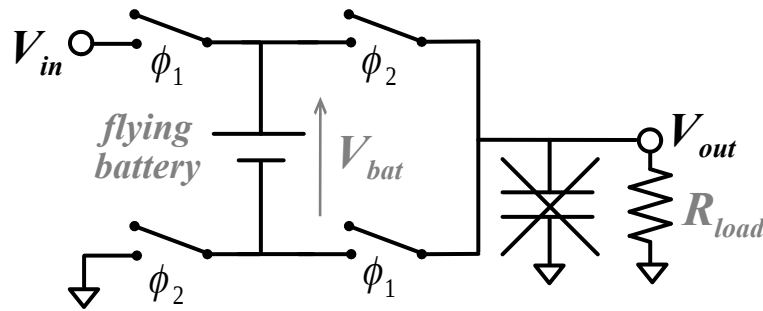


FIGURE 1 | Circuit de puissance du convertisseur SBC 2 :1

### Fonctionnement à l'État Stable

En fonctionnement à l'état stable, le SBC 2 :1 démontre un comportement cohérent, maintenant une tension de sortie moyenne, bien que présentant une légère ondulation initiale. Deux types d'ondulations,  $V_{IR}$  et  $V_{redox}$ , sont observés dans la forme d'onde de la tension de batterie ( $V_{bat}$ ).  $V_{IR}$  est une chute de tension ohmique due à la résistance interne de la batterie, tandis que  $V_{redox}$  résulte de réactions redox pendant les  $\mu$ -cycles. Ce comportement est distinct du SCC, qui présente une forme d'onde d'ondulation typique de type RC.

### Ondulation

Le SBC, même sans condensateur de sortie, atteint une faible ondulation de tension de sortie (inférieure à 5%) à basses fréquences (100 Hz) et à un courant de sortie de 20 mA, surpassant le SCC. Le SCC nécessite un condensateur de sortie pour réduire l'ondulation à 100 Hz, tandis que le SBC maintient une faible ondulation sans en avoir. L'ondulation de tension de sortie du SBC reste inférieure à 9% même à un courant de sortie de 30 mA.

### Efficacité

Le SBC présente une efficacité élevée, dépassant 90%, sur une large plage de courants de sortie, jusqu'à 20 mA. Cette haute efficacité est atteinte même à de basses fréquences, où le SCC subit des pertes significatives. La résistance interne de la batterie contribue moins aux pertes par rapport aux SCC à basses fréquences.

### Auto-Ajustement de la Tension de la Batterie (BVSA)

Le processus BVSA permet à la tension de la batterie de s'adapter à la valeur stable souhaitée dictée par la topologie du SBC. Ce comportement est distincte du comportement traditionnel des batteries, où est la batterie qui impose sa tension sur le circuit. Ce comportement est cohérent sur différentes fréquences, améliorant la polyvalence et la facilité de conception du SBC.

---

## Équilibre de Charge

Avoir un équilibre de charge est très important pour le SBC. Le SBC maintient le fonctionnement à l'état stable même dans très longue durée de fonctionnement. Même avec une certaine asymétrie du rapport cyclique le SBC retiens sont équilibre de charge, car la batterie ajuste sa tension pour atteindre cet équilibre. De petites asymétries pendant une opération régulière ont des effets négligeables sur les valeurs de tension à l'état stable.

## Durée de Vie

Le fonctionnement unique du SBC se traduit par un nombre de cycles de batterie significativement plus élevé par rapport à l'utilisation de batterie conventionnelle. Les expériences à long terme n'ont montré aucune dégradation significative des performances de la batterie. Le composant capacitif du mécanisme de transfert de charge de la batterie et les faibles niveaux de courant contribuent à prolonger la durée de vie de la batterie.

Dans l'ensemble, le SBC présente des caractéristiques de performance prometteuses, le rendant adapté à diverses applications à basse puissance.

## Chapitre 4 : Topologies Avancées de Convertisseurs à Batterie

Dans ce chapitre, nous explorons le potentiel des SBC au-delà de la validation expérimentale initiale et leurs avantages par rapport aux SCC traditionnels. Nous examinons les topologies des SBC qui intègrent plusieurs batteries volantes pour atteindre des taux de conversion plus élevés et élargir leur gamme d'applications.

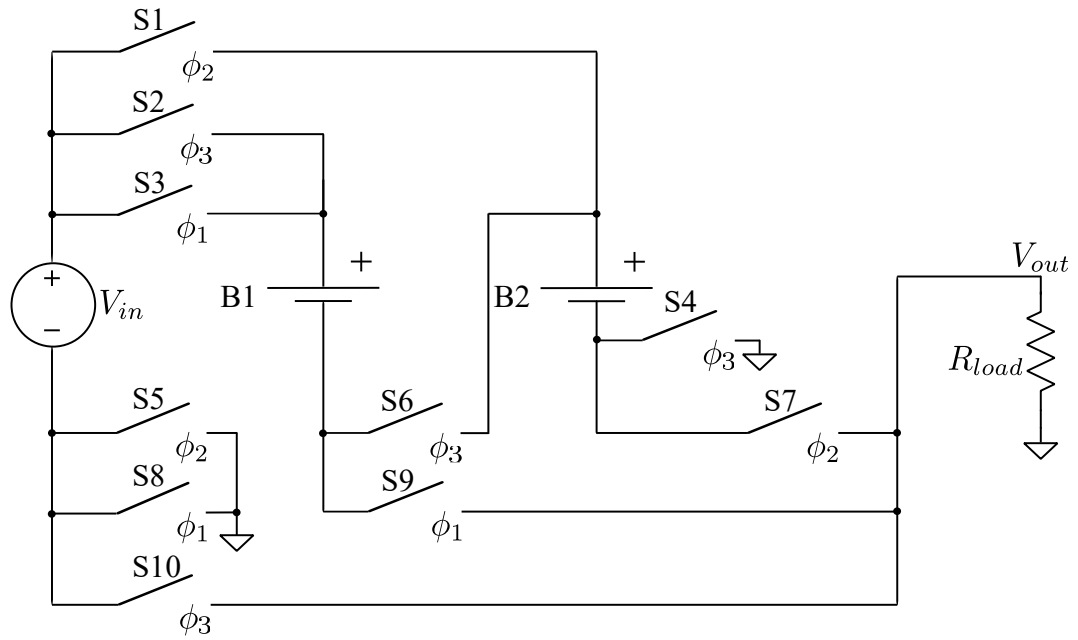
Nous examinons également les stratégies de contrôle et de régulation des circuits SBC en configurations à boucle fermée pour améliorer leurs performances, leur stabilité et leur efficacité pour des applications pratiques.

### Exploration à Batteries Multiples

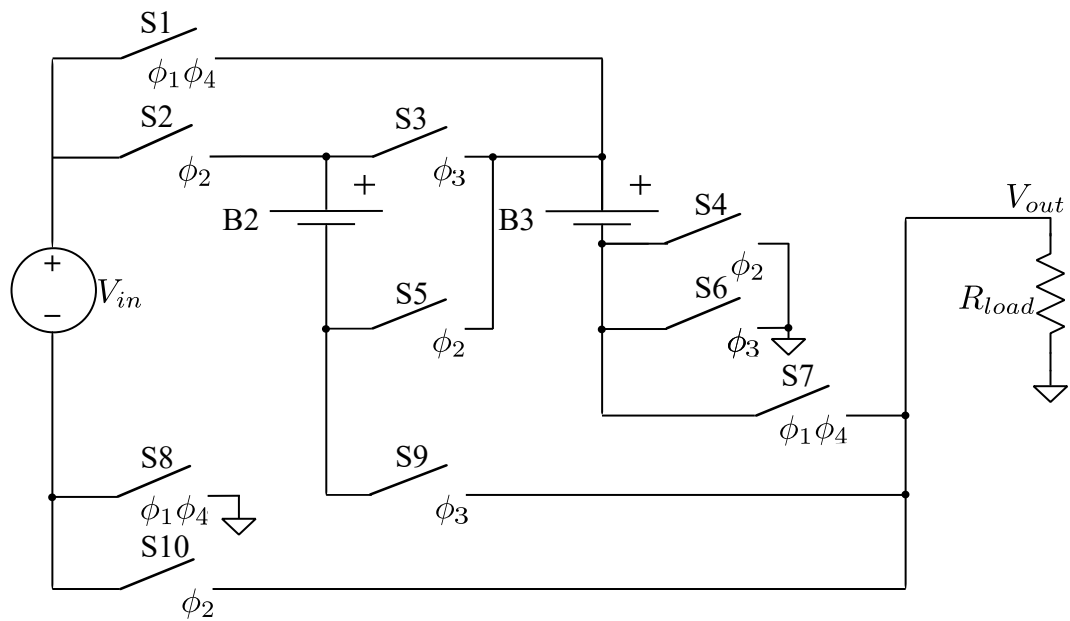
Pour explorer les SBC avec plusieurs batteries, nous effectuons une recherche semi-exhaustive avec les algorithmes proposées dans le chapitre 2 pour trouver des topologies qui répondent aux exigences de cycle et remplissent des conditions spécifiques.

### Topologies Proposées

Nous sélectionnons des topologies spécifiques de SBC pour une validation expérimentale. La première est une SBC 3 :1, où deux batteries fonctionnent au même niveau de tension ( $2 \cdot V_{out}$ ). Elle maintient l'équilibre de charge sur trois phases pour atteindre un rapport de conversion de 3 :1. La deuxième topologie est une SBC 4 :1 qui utilise de manière deux batteries avec des niveaux de tension différents (une à  $2 \cdot V_{out}$  et l'autre à  $3 \cdot V_{out}$ ).



(a)



(b)

FIGURE 2 | Diagramme électrique du (a) 3 :1 SBC et (b) 4 :1 SBC

---

Les deux topologies présentent un comportement non conventionnel pendant des phases spécifiques, avec la source d'entrée recevant de l'énergie. Mais ce comportement permet aux SBC de surmonter les contraintes traditionnelles et de fonctionner efficacement avec plusieurs batteries.

Ces expériences mettent en lumière la faisabilité pratique et les avantages des SBC avec plusieurs batteries, ouvrant la voie à diverses applications du SBC.

La configuration 3 :1 SBC, comme illustrée dans la Fig. 2a, est choisie pour la validation expérimentale. Cette configuration minimise le nombre de phases et de batteries nécessaires. Elle utilise les batteries  $V_{bat,1}$  et  $V_{bat,2}$  au même niveau de tension de  $2 \cdot V_{out}$ , résultant en  $V_{bat,i}/V_{out}$  de 2 pour les deux batteries. Le système fonctionne en trois phases :  $\phi_1$  et  $\phi_2$  impliquent la charge des batteries B1 et B2, respectivement, tandis que la phase  $\phi_3$  voit les deux batteries libérer de la charge vers le circuit. Des charges égales sont échangées au cours de ces phases, assurant l'équilibre de charge tout au long du cycle. Le circuit de l'étage de puissance nécessite peu de commutations, avec une tension maximale aux commutateurs de  $V_{in}/3$ .

En plus de la SBC 3 :1, une configuration SBC 4 :1 est explorée, comme on le voit dans la Fig. 2b. Cette configuration utilise les batteries B2 et B3 à des niveaux de tension différents ( $2 \cdot V_{out}$  et  $3 \cdot V_{out}$ , respectivement). L'opération implique quatre phases :  $\phi_1$  et  $\phi_4$  chargent la batterie B3,  $\phi_2$  transfère la charge de B3 à B2, et  $\phi_3$  libère de la charge des deux batteries vers le circuit. Toutes les phases ont une durée égale ( $t_{\phi_1} = t_{\phi_2} = t_{\phi_3} = t_{\phi_4}$ ), et des charges égales sont échangées, maintenant l'équilibre de charge. Les exigences de tension des commutateurs sont relativement faibles, avec un maximum de  $V_{in}/2$ , réduisant les pertes de puissance par rapport à certains convertisseurs traditionnels.

La configuration 4 :1 SBC présente également une phase répétitive, qui peut être optimisée en utilisant trois phases de durée différente tout en préservant l'équilibre de charge. Cette adaptation améliore l'efficacité et met en évidence la flexibilité des SBC pour atteindre différents rapports de conversion.

## Validation Expérimentale

Pour valider les SBC à l'aide de plusieurs batteries, nous avons mis en œuvre les configurations proposées de SBC 3 :1 et 4 :1, en utilisant des batteries spécifiques dans leurs plages de fonctionnement. La SBC 3 :1 utilisait les batteries B1 et B2, tandis que la SBC 4 :1 utilisait B2 et B3. Ces configurations permettaient une conversion de tension de 3,75 V à 1,25 V et de 5 V à 1,25 V respectivement. Le comportement BVSA des batteries permettait une certaine flexibilité dans les tensions, à condition qu'ils restent dans des limites spécifiées de la batterie et le rapports de conversion de tension est retenu.

Nous avons utilisé un commutateur analogique CMOS disponible dans le commerce (MAX4678) pour les deux SBC, en générant les phases de contrôle nécessaires de manière externe. La SBC 3 :1 a présenté une résistance de sortie équivalente de 8,7  $\Omega$ , avec une contribution de 31% des batteries à cette résistance. La SBC 4 :1 avait une résistance de sortie équivalente de 9,4  $\Omega$ , avec 52% attribués à la résistance interne de la batterie.

Les deux SBC ont présenté un temps d'établissement avant d'atteindre un fonctionnement en régime permanent en raison du comportement BVSA. Pendant le fonctionnement en régime permanent, ils ont maintenu des tensions de sortie stables avec de légères variations.

---

## Ondulation

Nous avons évalué l'ondulation de la tension de sortie pour les SBC 3 :1 et 4 :1 à 100 Hz et 1 kHz sans condensateur de sortie. La SBC 3 :1 maintenait une ondulation inférieure à 5% même à 100 Hz, tandis que la SBC 4 :1 présentait moins de 9% d'ondulation à la même fréquence. La fréquence de commutation plus élevée de la SBC 3 :1 contribuait à une ondulation plus faible par rapport à la SBC 2 :1.

## Efficacité

L'efficacité de la conduction a été évaluée à 100 Hz et 1 kHz pour les SBC 3 :1 et 4 :1. Les mesures et les calculs de l'efficacité étaient étroitement alignés, la SBC 3 :1 atteignant une efficacité >90% au-dessus de 10 mA de courant de sortie et fournissant une puissance de sortie de 15 mW. La SBC 4 :1 maintenait une efficacité >90% jusqu'à 10 mA de courant de sortie et produisait une puissance de sortie de 13 mW, bien qu'avec une densité de puissance volumique plus faible en raison de batteries plus grandes et de complexité.

Les deux configurations de SBC présentaient une faible ondulation de tension de sortie et une efficacité élevée, même à de basses fréquences. Elles ont maintenu leurs performances sur des millions de cycles, ce qui indique une stabilité à long terme. De plus, le comportement BVSA permettait une certaine flexibilité dans les rapports de conversion de tension avec les mêmes batteries, élargissant la plage opérationnelle de ces topologies de SBC.

## Approches de Contrôle

Actuellement, les circuits SBC fonctionnent en mode à boucle ouverte, mais l'exploration de configurations à boucle fermée pour réguler la tension de sortie est essentielle pour la recherche future. Diverses approches de contrôle traditionnelles peuvent être envisagées pour mettre en œuvre la famille de topologies SBC. Cependant, la constante de temps du SBC est étroitement liée au comportement lent de la batterie, ce qui peut poser des défis pour la régulation en boucle fermée en raison de la réponse plus rapide du convertisseur par rapport aux batteries.

Comme pour les SCC, le SBC peut bénéficier d'une stratégie de contrôle à deux niveaux : le contrôle à gros grains et le contrôle à fins grains. Le contrôle à gros grains consiste à modifier la configuration de phase du circuit, permettant au convertisseur de fonctionner près du rapport optimal pour maximiser l'efficacité. Le contrôle à fins grains se concentre sur la modulation directe de la résistance de sortie pour atteindre la tension de sortie exacte souhaitée. Cependant, le contrôle à fins grains s'accompagne de pertes de puissance, similaires à un régulateur linéaire.

## Modulation de Fréquence

La modulation de fréquence, couramment utilisée dans les SCC, offre une régulation à fins grains en variant la fréquence de commutation sur une large plage. Cette approche peut maintenir une efficacité constante pour une tension de sortie régulée donnée et peut être combinée à d'autres technologies pour

---

des réponses plus rapides. Cependant, elle peut augmenter l'ondulation de la tension de sortie et est moins pratique pour les SBC en raison de leur impédance de sortie indépendante de la fréquence et de leur plage de fréquence de fonctionnement limitée.

### **Modulation du Rapport Cyclique**

La modulation du rapport cyclique, souvent mise en œuvre par la modulation de largeur d'impulsion (PWM), a été utilisée dans les SCC lorsqu'ils fonctionnent dans la région de FSL. Elle permet une régulation à fins grains dans une plage limitée et peut atteindre un équilibre symétrique entre les périodes de charge et de décharge. Cependant, elle peut entraîner un fonctionnement déséquilibré dans les SBC, ce qui a un impact sur l'efficacité et l'ondulation de la tension de sortie.

L'impact de la modulation du rapport cyclique sur l'efficacité des SBC est notable, en particulier à des niveaux d'asymétrie élevés et lorsqu'ils fonctionnent près du potentiel de tension physique de la batterie. De plus, elle affecte l'ondulation de la tension de sortie, car les changements de la tension moyenne de la batterie modifient proportionnellement la différence de tension entre l'entrée et la sortie.

### **Approches Hybrides**

Une approche alternative consiste à ajouter une inductance de sortie et à appliquer une modulation du rapport cyclique à celle-ci. Cette approche hybride combine les avantages de la modulation du rapport cyclique avec des composants supplémentaires pour atténuer certaines de ses limitations.

En conclusion, bien que les stratégies de contrôle à boucle fermée présentent des avantages pour les SBC, le choix de l'approche de contrôle doit tenir compte des caractéristiques et des limites uniques du SBC, notamment son impédance de sortie indépendante de la fréquence et sa plage de fréquence de fonctionnement limitée. La modulation du rapport cyclique et les approches hybrides semblent plus adaptées au contrôle à fins grains dans les SBC par rapport à la modulation de fréquence.

## **Chapitre 5 : Exploration de l'Impact des Différentes Technologies de Batterie**

Dans ce chapitre, nous examinons la pertinence de diverses technologies de batterie pour le concept du SBC. Nous explorons leur impact sur les performances du SBC, en mettant l'accent sur les batteries au lithium-ion (Li-Ion), les batteries à l'état solide (SSB), et les batteries à films minces à l'échelle du millimètre. Ces technologies offrent différentes caractéristiques et avantages, ce qui en fait des candidats potentiels pour une intégration dans le cadre du SBC. Le chapitre explore aussi la possibilité d'utiliser des cellules à combustible dans le cadre du convertisseur CC-CC à faible fréquence.

---

## Impact des Différentes Chimies

### Batteries au Lithium-ion (Li-Ion)

Les batteries au lithium-ion (Li-Ion) sont bien connues pour leur densité de stockage d'énergie, leur conception légère et leurs capacités rechargeables, ce qui en fait un choix populaire pour les applications électroniques. Dans nos expériences, nous avons utilisé une batterie Li-Ion avec une tension nominale de 1,5 V et une capacité de 2,5 mAh. Malgré sa plage de tension de fonctionnement plus élevée par rapport à d'autres batteries, la batterie Li-Ion a démontré une efficacité dépassant 90% pour une plage de courant de sortie de 2 mA à des fréquences de 100 Hz et 1 kHz. Elle a atteint une efficacité maximale de 97%, ce qui en fait une option viable pour le SBC. Cependant, elle a présenté une ondulation de tension de sortie plus élevée en raison de sa capacité plus faible.

### Batteries à l'État Solide (SSB)

Les batteries à l'état solide (SSB en anglais), qui utilisent des électrolytes solides, offrent une sécurité améliorée, une densité énergétique plus élevée et une durée de vie de cycle prolongée par rapport aux batteries à électrolyte liquide traditionnelles. Nous avons examiné une batterie à film mince (TFB) prête à l'emploi et une TFB à l'échelle du millimètre développée par le CEA-Leti. La TFB prête à l'emploi avait une tension nominale de 3,9 V et une capacité de 1 mAh, tandis que la TFB à l'échelle du millimètre avait une capacité plus faible de 4,8  $\mu$ Ah. Les deux TFB ont montré une efficacité plus faible par rapport à d'autres technologies de batterie, principalement en raison de leur résistance interne élevée. La SSB commerciale a atteint une efficacité maximale de 76,8% à 100 Hz pour un courant de sortie de 2 mA. L'efficacité maximale de la TFB Leti était inférieure à 10%, principalement parce que le circuit utilisé n'est pas optimisée pour un fonctionnement à faible puissance. Cependant, elle a présenté une densité volumétrique de puissance élevée, ce qui indique un potentiel pour des améliorations futures.

### Exploration des MFC Faibles

Les piles à combustible, semblables aux batteries, sont des cellules électrochimiques qui convertissent l'énergie chimique en électricité grâce à des réactions d'oxydoréduction. Cependant, les piles à combustible diffèrent des batteries en ce qu'elles nécessitent un apport continu de combustible et d'agents oxydants pour leur fonctionnement. Cela permet aux piles à combustible, telles que les piles à combustible microbiennes (MFC), de générer de l'électricité en continu tant que le combustible et les agents oxydants sont disponibles.

### Pile à Combustible Microbienne (MFC)

Les MFC sont un type de pile à combustible qui fonctionne de manière similaire à d'autres variantes de piles à combustible. Ils se composent de deux types principaux : les MFC à chambre unique et les MFC à double chambre. Dans une MFC à chambre unique, il n'y a pas de membrane séparant les compartiments anodique et cathodique, ce qui les rend adaptées à notre étude.



---

Dans une MFC à chambre unique, des micro-organismes forment un biofilm sur la surface de l'anode et oxydent la matière organique en l'absence d'oxygène. Les électrons produits lors de cette oxydation circulent à travers un conducteur jusqu'à la cathode, où ils réagissent avec l'oxygène, générant de l'électricité. La puissance générée par les MFC est continue mais influencée par des facteurs tels que la disponibilité de matière organique et le transport des ions hydrogène vers la membrane d'échange.

Les MFC sont utilisées pour la récupération d'énergie et l'alimentation de capteurs. Différents types de MFC, tels que les MFC benthiques, les MFC végétales et les MFC à base d'eaux usées, présentent des conceptions et des performances électriques différentes. La densité de puissance varie généralement de 50 mW/m<sup>2</sup> à 2000 mW/m<sup>2</sup>, ce qui les rend adaptées aux charges de capteurs. La combinaison de plusieurs MFC peut permettre d'atteindre des tensions ou des niveaux de puissance plus élevés, mais des schémas de compensation actifs peuvent être nécessaires pour traiter la variabilité entre eux.

L'analyse du comportement électrique des MFC implique l'étude de leurs courbes I-V (courant-tension). Les méthodes potentiostatiques sont couramment utilisées pour cette caractérisation. Les MFC présentent un comportement similaire aux caractéristiques I-V typiques, avec des tensions à circuit ouvert variant de 0,2 V à 1,2 V et des impédances internes variant de 100 Ω à 1000 Ω. À mesure que les MFC s'affaiblissent, leurs performances se dégradent, en particulier dans les réacteurs en mode batch. Les variations de température peuvent également affecter leurs performances.

La récupération efficace d'énergie à partir des MFC nécessite l'établissement de conditions de Point de Puissance Maximale (PPM). Différentes topologies de convertisseurs CC-CC ont été explorées à cette fin, mais les circuits intégrés commercialement disponibles ont souvent des exigences élevées en tension à circuit ouvert, ce qui les rend inadaptés aux MFC à faible puissance. Cependant, le concept d'un convertisseur de pile à combustible commutée (SFC) explore l'utilisation de MFC faibles comme dispositifs de stockage d'énergie intermédiaire. Bien que les MFC faibles ne puissent pas fournir une alimentation électrique continue, elles peuvent néanmoins contribuer à l'efficacité énergétique globale d'un système SFC.

## **Convertisseur de Pile à Combustible Commutée (SFC)**

Le SFC étend la topologie à condensateur commuté utilisée dans les batteries aux MFC, en utilisant une MFC à chambre unique comme stockage d'énergie intermédiaire. Ici l'application utilisée est d'un circuit élévateur de tension pour doubler la tension de sortie. Le SFC présente une efficacité remarquable, atteignant une puissance de sortie maximale de 1,4 mW avec des rendements dépassant 90%. Même à des puissances de sortie modestes, il maintient une efficacité élevée, ce qui souligne sa robustesse. La fréquence de fonctionnement affecte l'efficacité, avec des fréquences plus élevées entraînant de meilleures performances. La MFC dans le SFC se comporte différemment d'un condensateur standard, comme en témoigne son efficacité plus élevée par rapport à un condensateur équivalent.

Le potentiel du SFC réside dans sa capacité à récupérer efficacement de l'énergie à partir de MFC faibles ou épuisées, offrant une solution innovante pour résoudre les défis posés par leurs caractéristiques électriques. Le SFC peut prolonger la durée de vie des batteries primaires et extraire l'énergie résiduelle des batteries presque épuisées, en faisant une technologie prometteuse pour les systèmes IoT économiques.

---

## Conclusion

Dans la quête de solutions énergétiques efficaces et durables pour l'électronique moderne, cette recherche s'est concentrée sur les convertisseurs CC-CC à basse puissance. Ces convertisseurs sont essentiels pour transformer l'énergie électrique entre différents niveaux de tension dans les dispositifs électroniques. Pour adresser des difficultés des convertisseurs CC-CC à faible puissance cette recherche propose une nouvelle topologie de convertisseur appelé Convertisseur à Batterie Commutée (SBC). Le travail s'est étalé sur cinq chapitres, chacun contribuant à l'avancement de la conversion d'énergie à basse puissance base sur les batteries commutées.

Le Chapitre 1 a posé les bases en mettant en avant la demande croissante de solutions énergétiques efficaces dans notre monde dépendant de l'électronique. Il a introduit deux types de convertisseurs CC-CC : linéaires et commutés, en mettant l'accent sur les convertisseurs commutés. Ces convertisseurs utilisent des condensateurs et des inductances pour des transformations de tension précises. Il a exploré les défis des convertisseurs CC-CC commutés à basse puissance. Ensuite il a souligné l'importance de l'efficacité, de la puissance et de l'encombrement de ces convertisseurs, qui trouvent des applications dans diverses industries.

Le Chapitre 2 mettre en avant les limites des passives traditionnels dans la conversion CC-CC commutée. Pour ça la topologie du Convertisseur à batterie Commutée est proposée. La topologie est détaillée théoriquement pour préparer la base d'une validation expérimentale.

Le Chapitre 3 a présenté une vérification expérimentale des Convertisseurs à Batterie Commutée (SBC) dans des scénarios à basse fréquence et basse puissance, démontrant leur performance supérieure par rapport aux convertisseurs traditionnels.

Le Chapitre 4 s'est penché sur les configurations de SBC avec plusieurs batteries, démontrant leur potentiel pour étendre les rapports de conversion et les applications. Il a également discuté des stratégies de contrôle pour les circuits SBC.

Le Chapitre 5 a exploré différentes compositions de batteries, telles que les batteries Li-Ion et les batteries à état solide, ainsi que leur intégration dans le cadre des SBC. Il a également examiné l'utilisation des piles à combustible microbiennes (MFC) comme dispositifs de stockage d'énergie.

En conclusion, ce voyage de recherche a contribué au développement de convertisseurs CC-CC à basse puissance, en particulier la topologie SBC. Il a élargi notre compréhension de la conversion d'énergie et ouvert de nouvelles possibilités pour des solutions énergétiques durables et efficaces dans l'électronique à basse puissance. Les orientations futures de la recherche promettent d'améliorer davantage les capacités des SBC et leurs applications dans un avenir plus vert et plus efficace.



# Contents

<b>Abstract</b>	<b>v</b>
<b>Résumé</b>	<b>vii</b>
<b>Résumé Étendu</b>	<b>ix</b>
<b>Contents</b>	<b>xxvii</b>
<b>List of Figures</b>	<b>xxxix</b>
<b>List of Tables</b>	<b>xxxv</b>
<b>Introduction</b>	<b>xxxvii</b>
<b>1 Low- and Ultra-Low Power Switched DC-DC Converters</b>	<b>1</b>
I Switched DC-DC Converters . . . . .	1
a Parameters and characteristics . . . . .	2
i Input and output voltage levels . . . . .	3
ii Power . . . . .	3
iii Efficiency and losses . . . . .	3
iv Footprint . . . . .	4
b Low-power DC-DC converter . . . . .	4
II State of the Art . . . . .	5
a Current solutions for low-power DC-DC converters . . . . .	5
b Limitations of current solutions . . . . .	8
III Conclusion . . . . .	10
Bibliography . . . . .	13
<b>2 Proposed Topology: Switched Battery Converter</b>	<b>17</b>
I Battery as a Flying Energy Storage Device . . . . .	17
a Power and Energy Density . . . . .	18

## CONTENTS

---

b	On-chip integration . . . . .	21
c	Challenges and Restrictions . . . . .	21
i	Voltage limits . . . . .	22
ii	Operating frequency . . . . .	22
iii	Cycling operation and lifespan . . . . .	23
II	Switched-Battery Converter (SBC) Topology . . . . .	23
a	Micro-cycle . . . . .	25
b	Sequencing . . . . .	26
c	Power Efficiency . . . . .	28
III	Topology Exploration . . . . .	31
a	Obtaining valid phases for the SBC . . . . .	31
b	Obtaining and exploring working cycles . . . . .	34
IV	Conclusion . . . . .	36
	Bibliography . . . . .	39
<b>3</b>	<b>Experimental validation of SBC</b>	<b>41</b>
I	Battery Options . . . . .	41
a	Nickel Metal Hydrate (NiMH) . . . . .	42
b	Lithium Ion (Li-ion) . . . . .	44
c	Solid-State Battery (SSB) . . . . .	45
II	Battery validation . . . . .	46
a	Battery impedance . . . . .	46
b	Battery in a $\mu$ -cycle . . . . .	49
III	SBC performance . . . . .	52
a	Steady-State Operation . . . . .	54
b	Output Voltage Ripple . . . . .	56
c	Power Efficiency . . . . .	57
d	Battery Voltage Self-Adjustment . . . . .	59
e	Charge Balance . . . . .	60
f	Lifetime . . . . .	62
IV	Conclusion . . . . .	63
	Bibliography . . . . .	65
<b>4</b>	<b>Advanced Battery-Based Converters Topologies</b>	<b>67</b>
I	Multiple-Battery Exploration . . . . .	67
a	Proposed Topologies . . . . .	69
i	3:1 Battery Based Converter . . . . .	69
ii	4:1 Battery Based Converter . . . . .	71
b	Experimental validation . . . . .	74

## CONTENTS

---

i	Ripple . . . . .	78
ii	Efficiency . . . . .	80
iii	Overall Performances . . . . .	82
II	Possible control approaches . . . . .	82
a	Frequency Modulation . . . . .	83
b	Duty Cycle Modulation . . . . .	84
III	Conclusion . . . . .	86
	Bibliography . . . . .	89
<b>5</b>	<b>Different Passive Technologies Exploration and Impact</b>	<b>91</b>
I	Impact of Different Chemistries . . . . .	91
a	Lithium-ion (Li-Ion) . . . . .	92
b	Solid-state batteries (SSBs) . . . . .	93
II	Exploration of weak MFCs . . . . .	98
a	Microbial Fuel-Cell . . . . .	98
i	Common Applications of MFCs . . . . .	99
ii	MFC's Electrical Behavior and Performance . . . . .	99
iii	Energy Scavenging and DC-DC Converter for MFCs . . . . .	99
b	Switched Fuel-Cell Converter (SFC) . . . . .	102
i	Experimental Setup . . . . .	103
ii	Performance . . . . .	104
III	Conclusion . . . . .	108
	Bibliography . . . . .	111
	<b>Conclusion</b>	<b>113</b>

## CONTENTS

---

xxx

# List of Figures

1	Circuit de puissance du convertisseur SBC 2 :1 . . . . .	xvii
2	Diagramme électrique du (a) 3 :1 SBC et (b) 4 :1 SBC . . . . .	xix
1.1	Switched DC-DC converter . . . . .	2
1.2	Summary of the relation between size and power density of low-power DC-DC converters. . . . .	6
1.3	Peak efficiency vs power density at peak efficiency of recent published solutions for low- and ultra-low-power switched DC-DC converters. . . . .	7
1.4	Recursive topology pseudo-code generator (top left). An example of 4-bit RSC operation across four different ratios (top right). Implemented 4-bit RSC block diagram (bottom). [22]	8
1.5	(a) Power cell design and (b) Combination of power cells to achieve 24 voltage conversion ratios. [11] . . . . .	9
1.6	Summary of current solutions for low power switched capacitor converters . . . . .	10
2.1	Battery voltage profile as a function of its state of charge and the effect of temperature. [2]	19
2.2	Battery power density advantage at low operating frequency . . . . .	20
2.3	Switched DC-DC converter using battery as passive device . . . . .	24
2.4	Battery voltage behavior in $\mu$ -cycle operation . . . . .	27
2.5	Model of SBC converter . . . . .	29
2.6	Possibilities of connection by the elements of SBC for each phase . . . . .	32
2.7	Algorithm exploring valid phases . . . . .	33
2.8	Algorithm for obtaining working cycles . . . . .	35
2.9	Algorithm classifying working cycles by length . . . . .	37
3.1	Ragone plot of various rechargeable battery technologies [3] . . . . .	43
3.2	Structure of (a) Li/LiPON/Si <sub>1-x</sub> Ti <sub>x</sub> half-cell, (b) Si <sub>1-x</sub> Ti <sub>x</sub> /LiPON/LiCoO <sub>2</sub> full-cell. [15] . . . . .	45
3.3	Battery internal resistance pattern by SoC. . . . .	47
3.4	V6HR experimental impedance around 50% SoC (a) magnitude and (b) phase . . . . .	48
3.5	(a) Battery V-Q characteristic under $\mu$ -cycle (b) Schematic battery voltage response to microcycles. . . . .	49



LIST OF FIGURES

---

3.6	IR drop voltage relation to output current. [11] . . . . .	50
3.7	Ionic voltage component related to frequency. [11] . . . . .	51
3.8	Mean voltage value of the battery (relaxed). [11] . . . . .	52
3.9	(a) 2:1 converter power stage electrical schematic and (b) implementation of 2:1 SBC using LM2663 and V6HR . . . . .	53
3.10	Experimental steady-state operation of the 2:1 SBC at 100 Hz: (a) output and battery voltages and (b) battery voltage ripple . . . . .	55
3.11	Comparison of relative output voltage ripple between 2:1 SBC and 2:1 SCC . . . . .	56
3.12	Experimental efficiency of the 2:1 SBC (without output capacitance): (a) independence of frequency and (b) advantage against SCC at 100 Hz with output capacitance . . . . .	58
3.13	Impact of frequency and current on the battery voltage evolution during power-on dynamics in the 2:1 SBC . . . . .	60
3.14	Steady-state operation with duty cycle asymmetry of (a) 45-55 and (b) 40-60 . . . . .	61
3.15	Long charge and discharge cycle of battery after more than $10^7$ $\mu$ -cycles . . . . .	63
4.1	SBC conversion ratios depending on $V_{bat,1}/V_{out}$ and/or $V_{bat,2}/V_{out}$ . Yellow dots denote a possible conversion ratio with at most 17 phases. . . . .	68
4.2	3:1 SBC topology: (a) electrical schematic with two batteries of similar voltage and (b) minimum number of operating phases . . . . .	70
4.3	Simplest 4:1 SBC topology: (a) electrical schematic and (b) operating phases of the shortest cycle . . . . .	73
4.4	Transient behavior of (a) 3:1 SBC and (b) 4:1 SBC demonstrating BVSA at 1 kHz and output current of 1 mA . . . . .	76
4.5	Output voltage of (a) 3:1 SBC and (b) 4:1 SBC during steady-state operation at 1 kHz and output current of 2.5 mA with no output capacitor . . . . .	77
4.6	Output voltage ripple of (a) 3:1 SBC and (b) 4:1 SBC at 100 Hz and 1 kHz respectively . . . . .	79
4.7	Conversion efficiency of (a) 3:1 SBC and (b) 4:1 SBC at 100 Hz and 1 kHz, respectively . . . . .	81
4.8	Positive and negative duty cycle asymmetries on 2:1 SBC. . . . .	84
4.9	2:1 SBC battery voltage and output voltage variation due to duty cycle modulation at 100 Hz and output current of 2.5 mA. . . . .	85
4.10	Duty cycle modulation impact on efficiency of a 2:1 SBC at 100 Hz and output current of 2.5 mA. . . . .	86
5.1	Ragone plot of various storage chemistries. Diagonal perforated lines represent the relation between energy and power. [1] . . . . .	92
5.2	Relative output voltage ripple of 2:1 SBC using TS621E Li-ion battery at different operating frequencies . . . . .	93
5.3	Efficiency of 2:1 SBC using TS621E Li-ion battery at different operating frequencies . . . . .	94

## LIST OF FIGURES

---

5.4	Relative output voltage ripple of 2:1 SBC using off-the-shelf EFL1K0AF39 thin-film battery at different operating frequencies . . . . .	95
5.5	Efficiency of 2:1 SBC using off-the-shelf EFL1K0AF39 thin-film battery at different operating frequencies . . . . .	96
5.6	Efficiency of 2:1 SBC using millimeter-scale Leti thin-film battery at 100 Hz and 1 kHz operating frequency. . . . .	97
5.7	Electrical behaviour of an MFC under sudden changes of the output resistive load. 3 min delay is introduced between successive changes. [2] . . . . .	100
5.8	MFC typical I-V characteristic. [2] . . . . .	101
5.9	Electrical performances of a single-chamber batch-mode MCF with various level of acetate density. [2] . . . . .	102
5.10	Switched DC-DC voltage doubler using MFC. . . . .	103
5.11	Electrical circuit under study. . . . .	103
5.12	Comparison between an SFC and an SCC with corresponding conditions at 4.2 Hz. . . . .	105
5.13	Efficiency of voltage-doubler SFC against output power at different frequencies. . . . .	106
5.14	Output voltage ripple of SFC (a) comparison against SCC and (b) response to operating frequency . . . . .	107

## LIST OF FIGURES

---

# List of Tables

2.1	Off-the-shelf devices sample with $\text{mm}^3$ volume . . . . .	20
3.1	Capacitor network value for operation of LM2663 . . . . .	54
4.1	Voltage across switches and battery charge movement in each phase of 3:1 SBC operation	71
4.2	Voltage across switches and battery charge movement in each phase of 4:1 SBC operation	74
5.1	Capacitor network value for operation of LM2663 with the MFC . . . . .	104

## LIST OF TABLES

---

# Introduction

In today's landscape of modern electronic systems, the demand for highly efficient power management solutions has escalated in response to the widespread adoption of battery-powered devices, the evolution of energy harvesting technologies, and the global commitment to sustainable energy practices. The central role played by DC-DC converters in facilitating the intricate tasks of power conversion and regulation cannot be overstressed. These converters serve as base to the effective conversion of electrical energy across varying voltage levels, facilitating integration and optimal performance of a wide spectrum of electronic components.

However, this increase also comes with the demand for performance in low- and ultra low-power operation. The driving force behind the advancement of low-power DC-DC converters lies in the essential need for optimizing energy utilization and raising overall system efficiency. In an environment where battery lifespan and operational endurance are of utmost importance, such converters emerge as main drivers for ensuring effective energy management. These converters play a vital role not only in ensuring efficient energy management, but also enabling prolonged device operation and minimizing energy waste. As a result, the research endeavors in this particular domain are directed towards creating converters that not only showcase high efficiency but also feature compact designs, enhanced power densities, improved responsiveness to rapid changes in power demand and solid reliability.

The realm of applications for low-power DC-DC converters spans a vast spectrum across industries and disciplines. Consider medical devices seeking compact and energy-conserving power supply solutions, wireless sensor networks reliant on energy scavenging, or portable consumer electronics in need of prolonged battery life. These converters are the foundational elements underpinning the operational essence of numerous modern innovations. This thesis explores the realm of low-power DC-DC converters, shedding light on the primary challenges that this domain poses and proposing an innovative solution to tackle them. The journey begins with a succinct recapitulation of DC-DC converters, with a specific focus on switched DC-DC converters and their unique characteristics. How they fit into the low- and ultra-low-power demands and challenges, and identify current strategies to address them. Continuing to identify the limits of current solutions on the physical limits of current flying passives. It then proposes a new and innovative solution on a form of a new topology family, going through with practical validation. In the end culminating into possibilities of further expansion of the concept.

Chapter 1 serves as the foundational cornerstone, providing an introduction to the challenges and

---

potential solutions in the low-power DC-DC converter landscape. It offers a concise overview of the current state of the art in DC-DC converters operating at low- and ultra-low-power levels, laying the groundwork for the distinctive features and innovative approaches that are under scrutiny in this thesis.

In Chapter 2, it delves deeper into the heart of DC-DC converters by scrutinizing the central energy transfer passive devices, which play a pivotal role in determining the converter's footprint and efficiency. Traditionally, DC-DC converters have been classified into two main categories based on the choice of intermediate storage components: inductors and capacitors. It explores the technological and physical factors that influence power and energy density, making the selection of the appropriate intermediate storage component a critical decision in the design process.

The emergence of Switched Capacitor Converters (SCCs), with recent developments such as 3D capacitors, has dominated the landscape of high-power density converters, particularly in low-power applications. However, in the quest to push the boundaries of volumetric power and energy density in DC-DC converters, this thesis proposes a novel topology family known as the Switched Battery Converter (SBC). Drawing inspiration from SCC topologies, the SBC employs at least one battery as the flying passive component, presenting a promising alternative for achieving unprecedented performance levels in low-power conversion. Chapter 3 begins a new step in the thesis, as it begins the experimental validation of the SBC topology introduced in Chapter 2. To substantiate its potential as a solution for high-efficiency low-power delivery, it first considers and evaluate various battery technology options. The chosen battery technology is subjected to SBC conditions in an isolated scenario. Subsequently, it is incorporated in a fully operational SBC circuit and subjected to rigorous testing. Its performance is compared against a traditional capacitor-based converter operating under similar conditions.

The Chapter 4 journey continues the study of the SBC topology evaluating its performance when dealing with multiple flying batteries. Delving into the realm of multiple flying batteries it aims to confirm the benefits and expand the capabilities of the SBC, unlocking the potential for higher conversion ratios and a broader range of applications. Additionally, it explores strategies for control and regulation of SBC circuits in closed-loop configurations, further enhancing its practical utility.

Chapter 5 confronts a key challenge associated with the SBC, its strong correlation between the output voltage and the battery voltage. The chapter explores potential solutions to this constraint, including the adoption of alternative battery chemistries like Lithium-Ion, or solid-state thin film batteries. This exploration not only diversifies output voltage possibilities but also introduces advantages and disadvantages associated with different battery technologies within the SBC framework. Furthermore, the SBC concept is extended to other energy storage devices sharing similar attributes, such as fuel cells. It not only has the potential of broadening the scope of low-frequency DC-DC converters but also can offer additional uses to this energy storage devices.

We conclude this journey by synthesizing the findings, discussing the implications of our research, and proposing future directions for the field of low-power DC-DC converters. This thesis not only contributes to the ever-evolving landscape of energy-efficient electronics but also underscores the potential of the SBC and similar innovative topologies in revolutionizing low-power conversion technologies.

---

Through a blend of theoretical insights and rigorous experimentation, this thesis aims to catalyze advancements in low-power DC-DC converters, offering solutions that address the evolving demands of modern electronics while driving us towards a more sustainable and energy-efficient future.





# CHAPTER 1

## Low- and Ultra-Low Power Switched DC-DC Converters

This chapter introduces the primary challenges associated with low- and ultra-low power switched DC-DC converters, while also providing insights into potential solutions aimed at achieving the desired specifications. It begins with a concise review of DC-DC converters, with a specific emphasis on switched DC-DC converters and their inherent features. Following this, it delivers a succinct outline of the prevailing solutions in the realm of DC-DC converters operating at extremely low power levels – essentially delving into the current state of the art in this domain. Subsequently, it accentuates the distinctive characteristics under investigation and the innovative approaches being pursued to address this emerging requirement.

### I Switched DC-DC Converters

In today's landscape of modern electronic systems, the demand for highly efficient power management solutions has escalated in response to the widespread adoption of battery-powered devices, the evolution of energy harvesting technologies, and the global commitment to sustainable energy practices. DC-DC converters play a central role in enabling modern systems' operation by providing an effective conversion of electrical energy across varying voltage levels and with highly dynamic operation.

Broadly speaking, there exist two primary archetypes of DC-DC converters: the linear and the switched varieties. Linear DC-DC converters leverage the principle of resistive voltage drop to generate and regulate a designated output voltage. Conversely, switched DC-DC converters operate through the periodic storage and subsequent release of input energy: this energy being released at a different voltage level. In this chapter, our focus is the domain of switched DC-DC converters for their higher efficiency and generally better power density.

Switched DC-DC converters operate around one or more central passive components and a network of switches that are connected and disconnected in a certain pattern, transferring energy from the input to the output as shown in Fig. 1.1. These converters rely on a cyclical process of energy storage, where energy is stored and accumulated in the passive devices over a defined interval and then later released

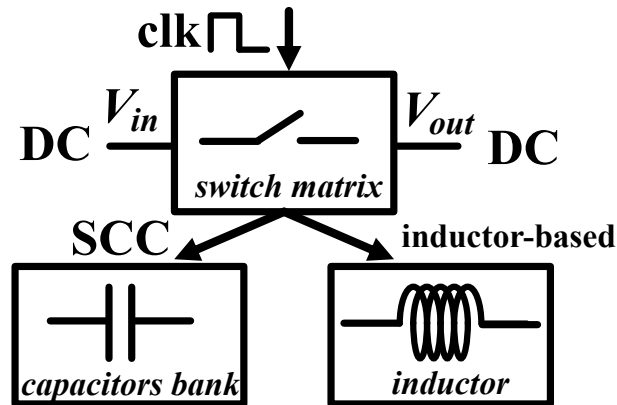


Figure 1.1 | Switched DC-DC converter

to the output at a voltage level that has been adjusted as needed. The pattern in which the switches make the connections is cyclical and determines what will be the ratio of the output voltage value with respect to the input one. This method of operation allows for the efficient transfer of power between input and output, resulting in the desired voltage conversion. There are two main families of switched DC-DC Converters:

- Magnetic: these are switched DC-DC converters where the central passive element is of the magnetic nature, the most common one being an inductor. In general lines, this solutions tend to dominate moderate to high power applications ( $>100$  mW).
- Dielectric: this family of switched DC-DC converters operates using an intermediate passive device that stores temporarily the energy in a dielectric material, the most common proponent device being a capacitor. Traditionally this family is more easily integrated into single chip solutions and has been historically used on low power applications ( $<100$  mW). New developments are demonstrated at over 100 mW applications as well thanks to GaN capabilities and the increase in capacitance density of new technologies.

As noted the latter family of converters has at its core a flying passive device, traditionally an inductor or a capacitor, which serves as a temporary energy storage device during the conversion. The significance of switched DC-DC converters stems from their versatility and ability to address a wide range of applications, from portable electronic devices demanding extended battery life to energy harvesting systems requiring efficient power extraction from ambient sources. As electronic systems continue to evolve, the design and optimization of switched DC-DC converters hold paramount importance in meeting the ever-growing demands for efficient energy utilization and seamless electronic integration.

## a Parameters and characteristics

A DC-DC converter is characterized by a defined set of parameters and characteristics that enable meaningful comparisons between different converter designs. Some of the main attributes that define a

DC-DC converter's behavior are outlined below.

### **i Input and output voltage levels**

The input and output voltage values that a DC-DC converter can handle significantly influence the choice of components utilized within the converter's circuit. For instance, the selection of switches and capacitors in the power stage impacts their voltage ratings, which in turn establish the operational voltage boundaries of the converter. Furthermore, the converter's output voltage is also contingent upon the chosen topology for the power stage. Optimal topology selection aim to ensure that the converter can generate the requisite output voltage at the desired input voltage level. The relationship between output and input voltages is a pivotal factor that plays a prominent role in determining the appropriate converter topology.

### **ii Power**

DC-DC converters are typically engineered to cater to specific output power ranges. For low- and ultra-low power applications it highly limits design choices and significantly shapes the component selection process.

Traditionally the thermal constraints imposed on these components define the upper limits of the converter's power-handling capacity. However, in the specific context of this study's targeted application, the demand for extremely low output power (on the  $\mu\text{W}$  range) can lighten such demands. Nevertheless, for a possible single-chip integration or other highly dense solutions, thermal demands regain importance even at such low power.

### **iii Efficiency and losses**

Efficiency stands as another crucial facet when describing a DC-DC converter as it is related to the internal losses. Efficiency serves as a valuable metric to portray a DC-DC converter's performance under steady-state conditions. Since efficiency directly connect to output power, we can see how this pair of characteristics are usually intrinsically connected on design and performance evaluation.

These losses in the converter operation emanate from diverse phenomena within each component. For example, magnetic components present core losses due to the magnetic flux circulating within its core. On the other hand, capacitor based converters are impacted by charge sharing losses.

In general, main intrinsic losses can be clustered in two groups, conduction losses and switching losses. Conduction losses can be more easily described as the losses while the DC-DC converter is on full conduction and are related to the on-resistance of the switches in the circuit, as well as parasitic ohmic resistances of other passives and devices, like the capacitors ESR, for example. They tend to dominate the overall losses in the power stage of DC-DC converters when they are operating at lower frequencies. The switching losses, on the other hand, are the losses related to the converter's transition from one conduction

state to another, such as losses due to charging MOSFETs gates. They tend to dominate the losses for operation at higher switching frequencies.

#### iv Footprint

The primary passive devices within switched DC-DC converters wield substantial influence over the overall circuit footprint. The energy storage capability of these components is directly related to their physical size [24]. In essence, larger passive components can store more energy under similar conditions. Consequently, the size of these passive components emerges as a significant contributor to the total footprint of the entire circuit. The aim of this study is for converters in the  $\text{mm}^2$  range, as they are to be integrated in compact solutions as wireless sensors and IoT devices.

#### b Low-power DC-DC converter

In the realm of low-power electronic applications, especially within circuits designed for wake-up mechanisms and continuous "always-on" functionality, there is a growing demand for DC-DC converters that possess both exceptional efficiency and substantial power density [8, 9]. This demand intensifies as power budgets dwindle. To illustrate, achieving a 90% power efficiency at a  $1 \mu\text{W}$  power output entails managing a loss power budget as meager as  $100 \text{ nW}$ . At these ultra-low-power levels, previously insignificant factors such as leakage and switching losses rise to prominence.

In this context, Switched Capacitor Converters (SCCs) have garnered substantial attention as a prominent solution for achieving remarkable power density in low-power applications [13, 18]. The output impedance of SCCs scales inversely with the operating frequency and the capacitance values of flying capacitors [15, 23]. However, power efficiency is directly influenced by switching losses, which tend to escalate with higher operating frequencies. A dilemma arises wherein efforts to maintain high efficiency at low input power might inadvertently result in a larger converter footprint as previously mentioned. The integration of cutting-edge technologies involving high-density capacitors doesn't necessarily translate into significant enhancements in SCC power density or efficiency, primarily due to intrinsic limitations associated with charge-sharing losses. If focusing on inductor-based converters the relation between operating frequency, losses and footprint is also present. As shown in [4], the reduction in switching frequency even below hundreds of kHz already implies the need of bulky inductors even for lower output power levels.

In essence, the development of low-power switched DC-DC converters represents a multifaceted development. To keep high efficiency and high power density, it involves not only the pursuit of advanced engineering solutions but also the delicate navigation of trade-offs between efficiency, power density, and physical size. All of this provides different approaches to develop low-power switched DC-DC converters which will be explored in the state of the art presented in the next section.

## II State of the Art

As presented earlier, the design of low-power DC-DC converters presents several additional challenges. To better understand such challenges, an interesting approach is to study current solutions addressing some of these challenges.

To analyze existing solutions several aspects are taken into account, based on the previously established parameters and characteristics defining DC-DC converters.

### a Current solutions for low-power DC-DC converters

While the domain of DC-DC converters is vast, the availability of low-power solutions remains relatively limited. This scarcity can be attributed to inherent losses associated with various converter topologies and technologies, compounded by fundamental physical limitations. Maintaining both high efficiency and substantial power density in low-power converters presents a formidable challenge.

Fig. 1.2 shows the experimental results of recently published low- and ultra-low power DC-DC converters ( $\mu\text{W}$  range) and illustrates the complexity of this challenge. Sustaining a consistent power density of  $10 \text{ mW}/\text{mm}^2$  proves challenging below the  $\text{mW}$  power range, plummeting to  $100 \text{ nW}/\text{mm}^2$  at the lowest explored output power levels [12, 16]. Inductive solutions often necessitate significant on-chip surface for bulky  $\mu\text{H}$  inductors to achieve acceptable efficiency at low-frequency operation [6, 26], even when aiming for a compact chip design. For inductive solutions, even frequencies under the  $\text{MHz}$  range can be already considered low, but for this study we focus on even lower frequencies ( $> 1\text{kHz}$ ). It's important to note that off-chip inductor surface is not always explicitly considered when presenting the converter's surface in the literature. This underscores the impact of reducing surface area in inductance-based converters, which exhibit lower power density at such power and surface scales, demanding higher operating frequencies that can hinder efficiency [27].

On the other hand, capacitor-based solutions can more consistently explore full on-chip integration but tend to face a power density limit at output power levels below  $1 \text{ mW}$  [2, 12, 19, 16]. The latter solutions typically achieve peak efficiencies under  $75\%$ , with the exception in [19], with  $82\%$ . Even when not fully on-chip integrated SCC solutions still maintain on-chip capacitors using external support for other blocks, like clock generation [11]. Another approach in energy conversion are hybrid solutions, blending capacitance and inductance in the same converter. [17] uses such hybrid approach with both passives as external devices. It operates in the  $\text{mW}$  range of output power, where technologies consistently offer higher power density and acceptable efficiency.

Figure 1.3 provides an overview of peak efficiency versus power density at peak efficiency for recent low- and ultra-low-power switched DC-DC converters. Inductive solutions often rely on external inductors to achieve high-efficiency conversions due to the challenges of on-chip integration. In order to keep such high efficiency on low-power, these solutions employ double-mode [7] or even triple-mode [21] control, for example, combining pulse-width modulation (PWM) and pulse-frequency modulation (PFM). Other approaches aim to limit internal power consumption with the use of double delay lines in a double chain

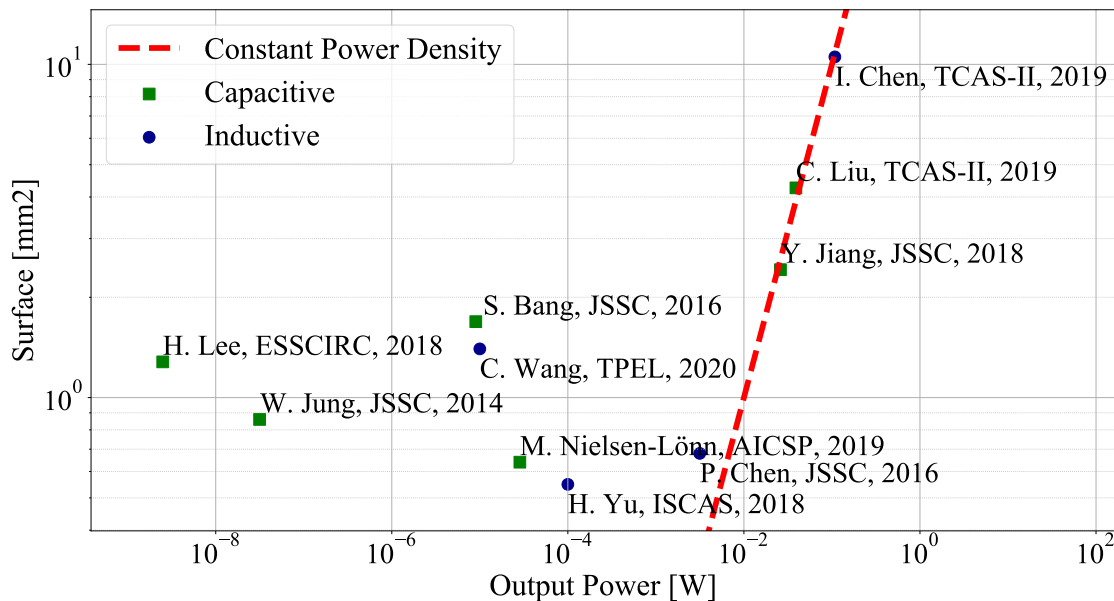


**Figure 1.2** | Summary of the relation between size and power density of low-power DC-DC converters.

digital PWM [14] or providing a precise control of peak inductor current and zero detection [25]. What can also be highlighted is that despite being able to operate in ultra-low-power they do not display peak efficiency, or even acceptable efficiencies in some cases, if not operating closer to higher power outputs. [25] can operate even at an output power of 5 nW but presents peak efficiency at 22 mW (146  $\mu\text{W}/\text{mm}^2$ ). Despite good efficiency demonstrated by some inductor-based solutions, they rely on off-chip passives, highlighting the difficulty of miniaturization of such solutions. It makes SCC the go-to approach in low-power high density DC-DC converters. For this fact, this study will focus more in capacitor-based DC-DC converters.

In contrast to inductor-based converter, capacitor-based converters approach of full on-chip integration improves the required footprint of the complete solution. And such solutions are still able to present competitive efficiency and power delivery capabilities. However, intrinsic losses may limit performance. Some topologies focus on reducing such intrinsic charge sharing and bottom plate parasitic losses to reach acceptable levels of efficiency. For example, by optimizing an algebraic equation [10] proposes an algebraic series-parallel converter, which builds on improving other strategies like two dimensions series-parallel.

Despite presenting good peak efficiency SCC may present sub-optimal performance when trying to achieve multiple conversion ratios. A common approach to broaden capacitor-based converters' conversion ratio is a coarse-grain gear-box control strategy. It consists in combining different topologies and using the appropriate one for the desired conversion ratio depending on input and output levels. Some topologies try to provide a fine-grain control by advancing this concept like successive approximation SCC topologies, but they can introduce additional losses, like cascading losses. [22] attempts to tackle the latter issue via a

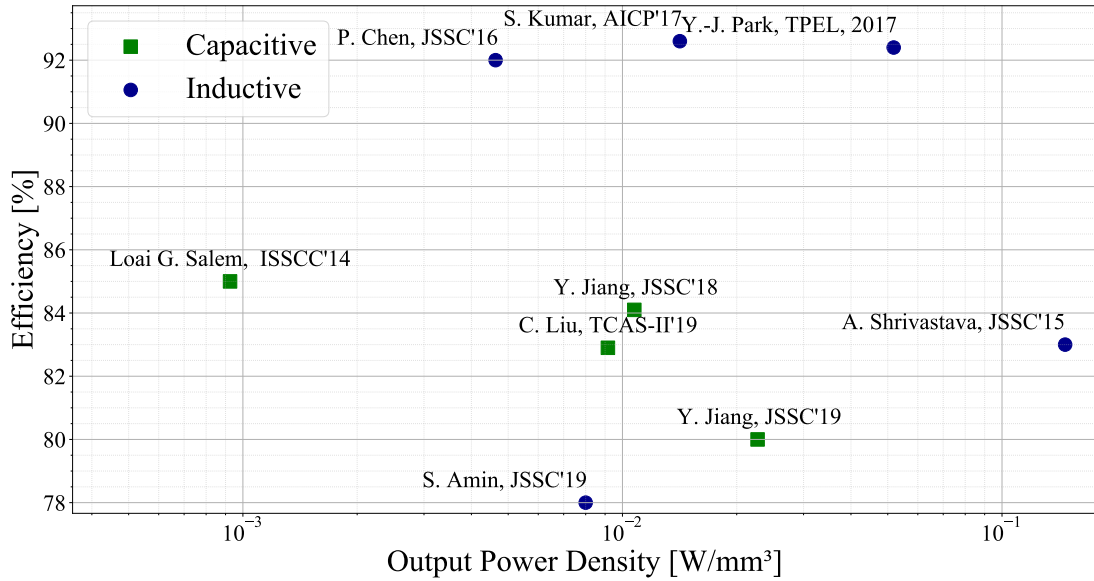


**Figure 1.3** | Peak efficiency vs power density at peak efficiency of recent published solutions for low- and ultra-low-power switched DC-DC converters.

recursive switching capacitor (RSC) strategy shown in Fig. 1.4, aiming to fully use every flying capacitor on every configuration and limiting series connections to improve efficiency and footprint. A fine-grain control can also be performed by combining different topology approaches like [11], using a partitionable power stage with power cells (shown in Fig. 1.5a) inspired by Dickson and series-parallel topologies. They all aim to broaden the power output levels in which the converter can maintain acceptable efficiency.

Despite strategies to reduce losses and broaden acceptable efficiency power levels, operation frequency remains directly connected to a DC-DC converter's performance. It is not rare to see operating frequencies on the hundreds of MHz with some solutions even operating on the order of GHz [20] to limit converters footprint and deliver good power output and efficiency. However, for low-power solutions such high frequencies imply in higher losses and, thus, low efficiency.

Figure 1.6 provides a summary of current solutions' operating frequencies at peak efficiency and output power density for low-power DC-DC converters. Typically, low-power switched DC-DC converters maintain high efficiency by drastically reducing switching frequencies. At this conditions, energy transfer per cycle remains relatively constant compared to Watt-level converters, making passive device size no longer directly correlated with the output power. Although inductive solutions rely on off-chip passives making it easier on footprint requirements, they remain limited in operating frequency, as reducing it in inductor-based converters can significantly increase saturation losses.

Reducing the operating frequency to keep acceptable levels of efficiency can even be done inside the same circuit. [10] reduces the operating frequency by more than tenfold between peak efficiency (at an output power of 20 mW) and the lowest power output of 1.2 mW.



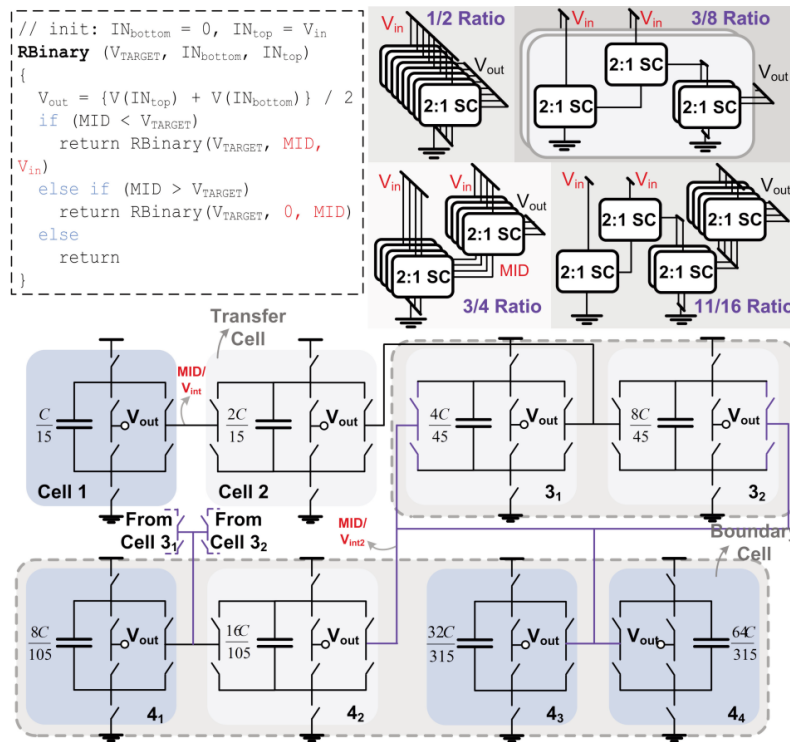


**Figure 1.4** | Recursive topology pseudo-code generator (top left). An example of 4-bit RSC operation across four different ratios (top right). Implemented 4-bit RSC block diagram (bottom). [22]

## b Limitations of current solutions

Inductor-based solutions do perform adequately in low-power scenarios. However, they come with a significant trade-off in terms of footprint size, which tends to be larger compared to their capacitor-based counterparts. This size disparity persists even when the on-chip surface area is relatively comparable. This challenge arises from the inherent difficulty of miniaturizing inductor-based converters. As a result, for low-power applications with a focus on high power density, SCCs often emerge as the preferred choice.

Capacitor-based solutions, while promising, encounter their own set of challenges, particularly when aiming to achieve multiple conversion ratios. Typically, these circuits employ a strategy akin to a gearbox to adapt to varying voltage ratios. However, at a fundamental level, this approach offers only coarse-grained control. To achieve finer control over the conversion process, some strategies have been devised, such as successive approximation SCC topologies. The latter approaches provide better control granularity but can introduce additional losses, including cascading losses. An intriguing approach, as seen in the work of [22], involves a recursive switching strategy called recursive switching capacitor (RSC). This strategy aims to maximize the utilization of every flying capacitor configuration, thus minimizing the need for series connections. To further enhance control granularity, various topological approaches can be combined. For instance, [11] utilizes a partitionable power stage with cells inspired by Dickson and series-parallel topologies. It uses a combination of identical power cells divided between main cells (MCs) and auxiliary cells (ACs) based on connection possibilities to the other power cells. Such power 20 power

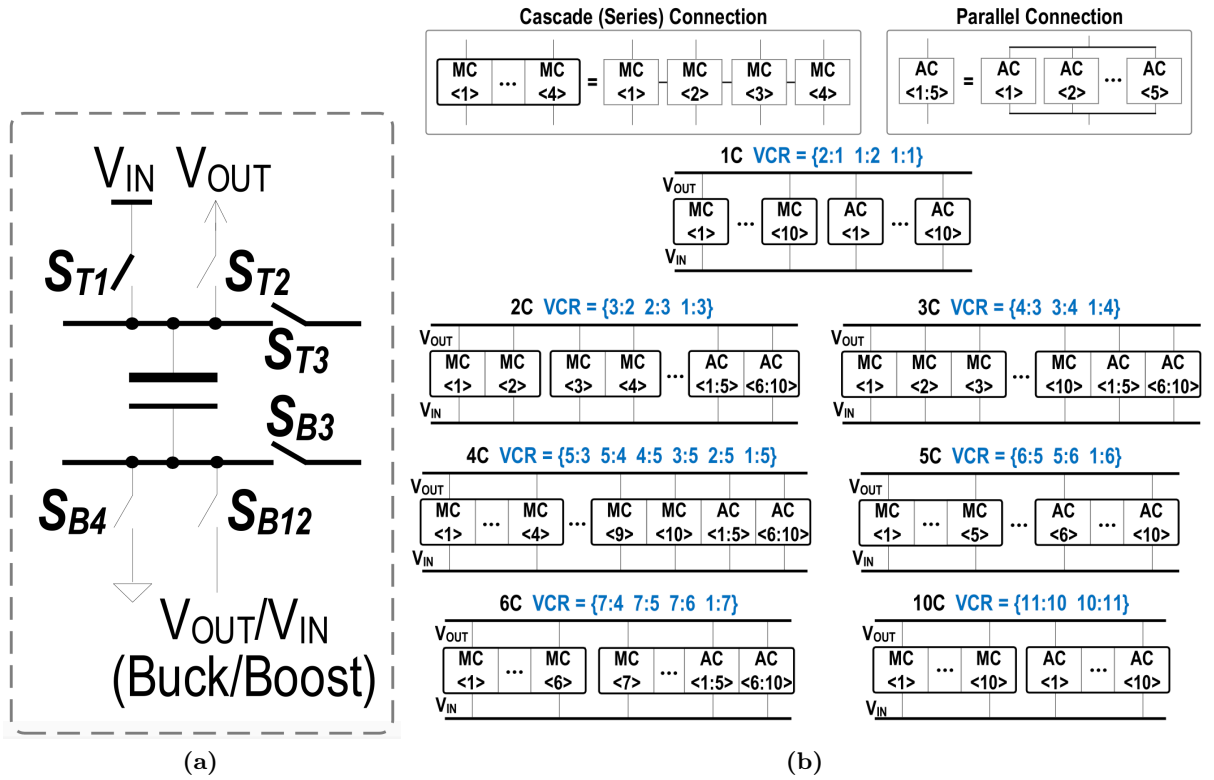


Figure 1.5 | (a) Power cell design and (b) Combination of power cells to achieve 24 voltage conversion ratios. [11]

cells can be combined to generate 24 different voltage conversion ratios as shown in Fig. 1.5b. While these genre of strategies represent significant advancements, they still represent a discrete granularity. They cannot match the continuous granularity offered by inductor-based solutions or linear converters like Low Drop-Out (LDO) regulators.

Historically, SCC circuits were predominantly assumed to operate in the Slow Switching Limit (SSL) region. In SSL, during each clock semi-period, the charge is entirely transferred from one pumping capacitor to the next. Conversely, in the Fast Switching Limit (FSL) region, during each clock semi-period, the charge is not entirely transferred from one pumping capacitor to the other [1]. Both operational regimes are discussed in greater detail in Chapter 2.

As charge-sharing losses dominate in SSL, further miniaturization of SCCs becomes inherently limited by the switching frequency [3]. In SSL, the output impedance is inversely proportional to the product of the flying capacitor value and switching frequency. To reduce the footprint without altering the switching frequency, flying capacitors with higher capacitance density must be employed. However, increasing the switching frequency impacts power efficiency negatively, particularly at low output power levels.

Modern applications often necessitate DC-DC converters to operate in the FSL region. In the FSL region, not all the energy stored in the flying capacitor is delivered every cycle. This requires capacitors to

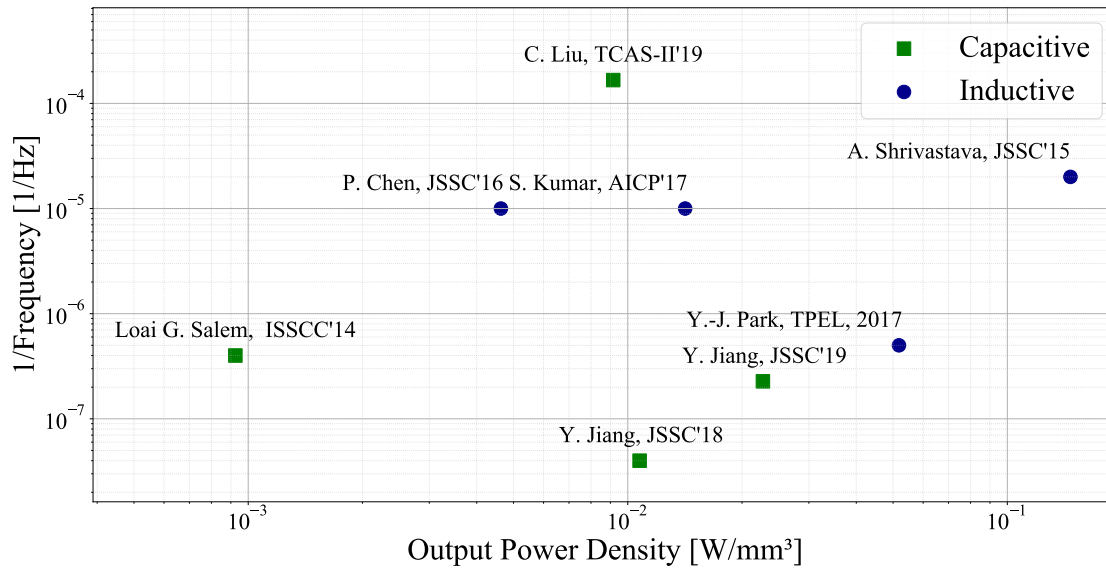


**Figure 1.6** | Summary of current solutions for low power switched capacitor converters

store more energy for the same output power at the same operating frequency. This increase in energy storage capacity can be achieved through larger capacitors or capacitors with higher capacitance density. Increasing the operating frequency aims to reduce footprint, making higher density capacitors essential. However, achieving such capacitance density typically involves the adoption of more exotic devices, like deep-trench technologies. This path may reduce the feasibility of fully integrating passives into low-power DC-DC converters. Increasing the technological complexity and impacting the overall cost of the solution.

To overcome the inherent limitations of inductor and capacitor-based converters at low power levels, the exploration of alternative passive devices presents a promising avenue. Solid-state batteries, in particular, exhibit significantly higher energy density compared to their power capability. While this limitation may be a concern in higher-power applications, it may not be a hindrance in the context of low-power converters. Recent research has also delved into the on-chip integration capabilities and scalability of solid-state batteries [5]. Their operation at low frequencies and low power levels makes them a potential candidate as flying devices in switched DC-DC converters.

### III Conclusion

This chapter approached low- and ultra-low-power DC-DC converters, beginning with an understanding of the ever-growing demand for efficient power solutions. It highlights the pivotal role played by DC-DC converters in enabling the efficient transformation of electrical energy between different voltage levels, thereby facilitating the seamless operation of diverse electronic components.

Two main categories of DC-DC converters were introduced: linear and switched topologies. While

### III. CONCLUSION

---

linear converters rely on resistive voltage drops for voltage regulation, switched converters store and release energy periodically to achieve voltage transformation. The focus falls to switched DC-DC converters, which revolve around central passive devices, traditionally capacitors and inductors.

The chapter addressed the specific challenges of low-power switched DC-DC converters. Exploring how the demand for heightened efficiency, reduced form factors, enhanced power density, and improved transient response intensifies as power budgets shrink.

Efficiency, power, and footprint emerge as defining characteristics of low-power DC-DC converters. Remembering that maintaining high efficiency at ultra-low power levels can be particularly challenging due to the dominance of previously insignificant factors like leakage and switching losses.

SCCs took center stage as a promising solution for achieving high power density in low-power applications. However, the balance between efficiency and footprint is still key in SCCs. Efforts to maintain high efficiency often lead to larger converter footprints, and integration of high-density capacitors does not always yield significant enhancements in power density or efficiency.

The review of the state of the art about low-power DC-DC converters evaluated the performance of various solutions, by studying mainly efficiency, power density, and operating frequencies. Inductor-based solutions, though acceptable at low power, were shown to have larger footprints, making SCCs the preferred choice. Capacitor-based solutions, while promising, still grapple with sub-optimal performance when aiming for multiple conversion ratios.

Historically, SCCs operated in the Slow Switching Limit region, posing challenges related to charge-sharing losses and miniaturization. The transition to the Fast Switching Limit region, necessitated by modern applications, may require capacitors with higher capacitance density. While this presents opportunities to reduce footprint, it also demands more exotic devices, technology complexity, and design risks, potentially limiting full passive integration.

The chapter concluded by introducing the prospect of alternative passive devices, specifically solid-state batteries, as potential solutions to break through the limitations of traditional inductor and capacitor-based converters. These batteries, with their significantly higher energy density, may hold the key to unlocking new frontiers in low-power DC-DC conversion. And the possibilities offered by this exploration are explored in the next chapters.



# Bibliography

- [1] Andrea Ballo, Alfio Dario Grasso, Gaetano Palumbo, and Toru Tanzawa. Charge pumps for ultra-low-power applications: Analysis, design, and new solutions. *IEEE Transactions on Circuits and Systems II: Express Briefs*, 68(8):2895–2901, 2021.
- [2] Suyoung Bang, David Blaauw, and Dennis Sylvester. A successive-approximation switched-capacitor dc–dc converter with resolution of  $v_{in}/2^N$  for a wide range of input and output voltages. *IEEE Journal of Solid-State Circuits*, 51(2):543–556, 2016.
- [3] Y. Beck, Nir Eden, Shira Sandbank, S. Singer, and Keyue Smedley. On loss mechanisms of complex switched capacitor converters. *IEEE Transactions on Circuits and Systems I: Regular Papers*, 62:1–10, 09 2015.
- [4] Armande Capitaine. *Récupération d'énergie à partir de piles à combustible microbiennes benthiques*. PhD thesis, Universite de Lyon, 11 2017.
- [5] Jacopo Celè, Sylvain Franger, Yann Lamy, and Sami Oukassi. Minimal architecture lithium batteries: Toward high energy density storage solutions. *Small*, 19, 01 2023.
- [6] I.-Chou Chen, Che-Wei Liang, and Tsung-Heng Tsai. A single-inductor dual-input dual-output dc–dc converter for photovoltaic and piezoelectric energy harvesting systems. *IEEE Transactions on Circuits and Systems II: Express Briefs*, 66(10):1763–1767, 2019.
- [7] Po-Hung Chen, Chung-Shiang Wu, and Kai-Chun Lin. A 50 nW-to-10 mW output power tri-mode digital buck converter with self-tracking zero current detection for photovoltaic energy harvesting. *IEEE Journal of Solid-State Circuits*, 51(2):523–532, 2016.
- [8] Gajendranath Chowdary and Shouri Chatterjee. A 300-nW sensitive, 50-nA DC-DC converter for energy harvesting applications. *IEEE Transactions on Circuits and Systems I: Regular Papers*, 62(11):2674–2684, 2015.
- [9] J. Deng, J-L Nagel, L. Zahnd, M. Pons, D. Ruffieux, C. Arm, P. Persechini, and S. Emery. Energy-autonomous mcu operating in sub-vt regime with tightly-integrated energy-harvester: A SoC for IoT smart nodes containing a mcu with minimum-energy point of 2.9 pJ/cycle and a harvester with output power range from sub- $\mu$ W to 4.32mW. In *2019 IEEE/ACM International Symposium on Low Power Electronics and Design (ISLPED)*, pages 1–4, 2019.

- [10] Yang Jiang, Man-Kay Law, Zhiyuan Chen, Pui-In Mak, and Rui P. Martins. Algebraic series-parallel-based switched-capacitor dc–dc boost converter with wide input voltage range and enhanced power density. *IEEE Journal of Solid-State Circuits*, 54(11):3118–3134, 2019.
- [11] Yang Jiang, Man-Kay Law, Pui-In Mak, and Rui P. Martins. Algorithmic voltage-feed-in topology for fully integrated fine-grained rational buck–boost switched-capacitor dc–dc converters. *IEEE Journal of Solid-State Circuits*, 53(12):3455–3469, 2018.
- [12] Wanyeong Jung, Sechang Oh, Suyoung Bang, Yoonmyung Lee, Zhiyoong Foo, Gyouho Kim, Yiqun Zhang, Dennis Sylvester, and David Blaauw. An ultra-low power fully integrated energy harvester based on self-oscillating switched-capacitor voltage doubler. *IEEE Journal of Solid-State Circuits*, 49(12):2800–2811, 2014.
- [13] Marko Krstic, Suzan Eren, and Praveen Jain. Analysis and design of multiphase, reconfigurable switched-capacitor converters. *IEEE Journal of Emerging and Selected Topics in Power Electronics*, 8(4):4046–4059, 2020.
- [14] Sandeep Kumar, Jin-Woong Choi, and Hanjung Song. An ultra-low power cmos dc–dc buck converter with double-chain digital PWM technique. *Analog Integrated Circuits and Signal Processing*, 92:141–149, 2017.
- [15] Alexander Kushnerov. Multiphase Fibonacci switched capacitor converters. *IEEE Journal of Emerging and Selected Topics in Power Electronics*, 2(3):460–465, 2014.
- [16] Hyeonji Lee, Eunsang Jang, Hassan Saif, Yongmin Lee, Minsun Kim, Muhammad Bilawal Khan, and Yoonmyung Lee. A sub-nw fully integrated switched-capacitor energy harvester for implantable applications. In *ESSCIRC 2018 - IEEE 44th European Solid State Circuits Conference (ESSCIRC)*, pages 50–53, 2018.
- [17] Chi-Wei Liu, Yi-Lun Chen, Pei-Chun Liao, Shiau-Pin Lin, Ting-Wei Wang, Ming-Jie Chung, Po-Hung Chen, Ming-Dou Ker, and Chung-Yu Wu. An 82.9%-efficiency triple-output battery management unit for implantable neuron stimulator in 180-nm standard CMOS. *IEEE Transactions on Circuits and Systems II: Express Briefs*, 66(5):788–792, 2019.
- [18] Yan Lu, Junmin Jiang, and Wing-Hung Ki. Design considerations of distributed and centralized switched-capacitor converters for power supply on-chip. *IEEE Journal of Emerging and Selected Topics in Power Electronics*, 6(2):515–525, 2018.
- [19] Martin Nielsen-Lönn, Pavel Angelov, J.J. Wikner, and Atila Alvandpour. Self-powered micro-watt level piezoelectric energy harvesting system with wide input voltage range. *Analog Integrated Circuits and Signal Processing*, 98, 03 2019.
- [20] Alessandro Novello, Gabriele Atzeni, Giorgio Cristiano, Mathieu Coustans, and Taekwang Jang. 17.3 a 1.25ghz fully integrated dc-dc converter using electromagnetically coupled class-d lc oscillators. In *2021 IEEE International Solid- State Circuits Conference (ISSCC)*, volume 64, pages 260–262, 2021.
- [21] Young-Jun Park, Ju-Hyun Park, Hong-Jin Kim, Hocheol Ryu, SangYun Kim, YoungGun Pu, Keum Cheol Hwang, Youngoo Yang, Minjae Lee, and Kang-Yoon Lee. A design of a 92.4% ef-

## BIBLIOGRAPHY

---

- efficiency triple mode control dc–dc buck converter with low power retention mode and adaptive zero current detector for IoT/wearable applications. *IEEE Transactions on Power Electronics*, 32(9):6946–6960, 2017.
- [22] Loai G. Salem and Patick P. Mercier. 4.6 an 85%-efficiency fully integrated 15-ratio recursive switched-capacitor DC-DC converter with 0.1-to-2.2 V output voltage range. In *2014 IEEE International Solid-State Circuits Conference Digest of Technical Papers (ISSCC)*, pages 88–89, 2014.
- [23] Michael D. Seeman, Vincent W. Ng, Hanh-Phuc Le, Mervin John, Elad Alon, and Seth R. Sanders. A comparative analysis of Switched-Capacitor and inductor-based DC-DC conversion technologies. In *2010 IEEE 12th Workshop on Control and Modeling for Power Electronics (COMPEL)*, pages 1–7, June 2010. ISSN: 1093-5142.
- [24] Michael Douglas Seeman. *A Design Methodology for Switched-Capacitor DC-DC Converters*. PhD thesis, EECS Department, University of California, Berkeley, May 2009.
- [25] Aatmesh Shrivastava, Nathan E. Roberts, Osama U. Khan, David D. Wentzloff, and Benton H. Calhoun. A 10 mV-input boost converter with inductor peak current control and zero detection for thermoelectric and solar energy harvesting with 220 mV cold-start and  $-14.5$  dBm, 915 MHz RF kick-start. *IEEE Journal of Solid-State Circuits*, 50(8):1820–1832, 2015.
- [26] Chuang Wang, Kai Zhao, Zunchao Li, and Qi Xiong. Single-inductor dual-input triple-output buck–boost converter with clockless shortest power path control strategy for IoT nodes. *IEEE Transactions on Power Electronics*, 35(2):2044–2052, 2020.
- [27] Hengwei Yu, Mingyi Chen, Chundong Wu, Kea-Tiong Tang, and Guoxing Wang. A batteryless and single-inductor DC-DC boost converter for thermoelectric energy harvesting application with 190 mV cold-start voltage. In *2018 IEEE International Symposium on Circuits and Systems (ISCAS)*, pages 1–4, 2018.



## BIBLIOGRAPHY

---

## CHAPTER 2

# Proposed Topology: Switched Battery Converter

The passive device involved in the intermediate energy transfer inside a DC-DC converter is crucial as it plays a significant role in determining the converter's footprint. DC-DC converters are traditionally classified into two main categories (or a mix of both if resonance is explored) based on the intermediate storage components: inductors and capacitors. The power and energy density are factor of technology and root physics laws (storing energy on a magnetic flux, or as electrostatic charges, for example). Therefore, selecting an appropriate intermediate storage component is critical in designing an efficient and compact DC-DC converter. Inductors are challenging to integrate onto a single chip and exhibit low power and energy density due to the nature of storing energy as a magnetic flux. Conversely, capacitors are comparatively easier to integrate (into a single chip) than inductors, and advancements in technology enable them to deliver superior energy and power densities at single chip level.

For fully integrated on-chip high power density converters, even more for low power application, the popular and promising solution is the SCC, even more with current improvements of 3D capacitors [8, 5]. However, recent development in the miniaturization of solid-state batteries present the possibility of fully integrated on-chip batteries with high energy density [9]. Aiming to increase the volumic power and energy density of DC-DC converters we propose a new topology family of switching DC-DC converters. This topology family, inspired by the SCC topologies uses at least one battery as the flying passive component and is named the switched-battery converter (SBC).

### I Battery as a Flying Energy Storage Device

Batteries serve as long-term (minutes or hours) chemical energy storage devices, unlike capacitors that store energy as charge in their plates and inductors that store energy in a magnetic field. Traditionally, batteries have been predominantly utilized as energy storage systems, allowing for the accumulation and subsequent discharge of stored energy. Even with recent advancements exploring the possibility of employing batteries at the point of load or in close proximity to energy harvesting systems, expanding their applications beyond conventional long-term energy storage functions.

Compared to the traditional passive device that more resembles the battery, the capacitor exhibits

voltage that is proportional to the stored charges on its two electrodes. However, the voltage between a battery's terminals is not directly related to the stored charge inside the device, although there is still a slight relation between them in large operation range (called later the voltage plateau). As shown in Fig. 2.1, a battery's discharge profile presents a region in which the voltage is approximately constant, reducing the direct correlation between stored energy (or extracted charge  $Q$ ) and the voltage between the battery's terminals. In this region the slope ( $V/Q$ ) of the battery is very small, so the charging or discharging of the battery does not imply a change in its voltage. If we wanted to obtain the same slope using a capacitor, for instance, we would need a surface for the capacitor 1000 or even 10000 larger than the one for a battery. Furthermore, the strong relationship between the voltage between the capacitor's terminals and the stored charge is the reason behind charge sharing loss in SCC operation, a predominant source of losses. Again, the solution would be to design converters with much larger capacitors, reducing power density, or, in this case, working at a higher switching frequency, but it would imply greater switching losses. Exploiting this fact helps in cementing the interest in exploring batteries as a viable new flying passive device in DC-DC converters and break this trade-off.

We also need to keep in mind the particularities of batteries, one that is constantly brought forward is that the C-rate is often used to determine charging and discharging times. The use of C-rate is also common to define other battery's power characteristics, since it is relative to a battery's capacity (and batteries main application continues to be as energy storage device). Regarding C-rate, a current of 1 CA means that the battery will charge (or discharge) in one hour, thus a battery of 10 mAh when working at 1 CA can provide 10 mA during one hour, at 2 CA it would provide 20 mA, but only for 30 minutes, and so on.

### a Power and Energy Density

In terms of energy density, batteries outperform traditional passives of similar size by more than four orders of magnitude, as depicted in Table 2.1. This superior energy density makes batteries highly suitable for energy storage applications, despite advancements in capacitance density achieved by technologies like deep-trench capacitors, which can reach around 200 nF/mm<sup>2</sup> [3] or even 1  $\mu$ F/mm<sup>2</sup> at very low voltages. However, it is important to note that the higher energy density of batteries does not necessarily translate into a higher power density, as it does in traditional passives. The power delivery of batteries is often severely constrained by their limited current delivery capability. For continuous operation, the maximum current of batteries rarely exceeds a few units of CA, and even in pulsed operation, it seldom reaches 10 CA. Therefore, the power delivery of batteries is inherently more heavily tied to their current delivery limit than to their absolute energy storage capacity and density.

If we center the analysis of power delivery to low operating frequencies, the higher energy density of batteries can be translated into a higher power density. Focusing on low operating frequencies allows us to reduce switching losses, as in fully integrated on-chip solutions the approach to retain high power density is commonly to work at higher frequencies at the cost of higher switching losses.

As shown by (2.1), output power  $P_{out}$  can be described as a product of delivered energy  $E_{del}$  and

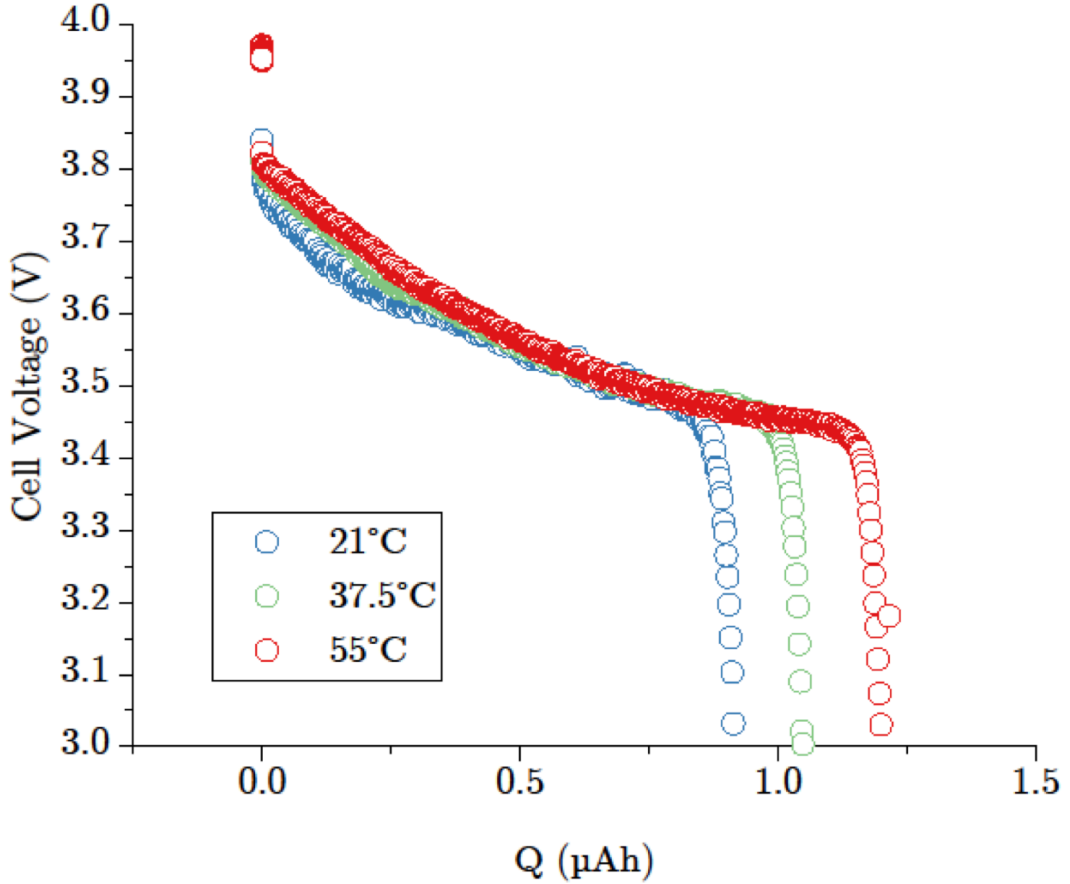


**Figure 2.1** | Battery voltage profile as a function of its state of charge and the effect of temperature. [2]

the operating frequency  $f_{op}$ . From such relationship we can establish the first-order correlation between power density and operating frequency shown in Fig. 2.2. In contrast to traditional passive devices, where power delivery capability is directly proportional to operating frequency, batteries (at first-order) are only subject to limitations imposed by their current delivery capabilities and not (2.1). So, at sufficiently low operating frequencies (such as some units of Hz as shown in Fig. 2.2), batteries can exhibit a greater power delivery density compared to conventional alternatives. At such low frequencies, the required footprint for a capacitor in a SCC can heavily impact a lower power and energy density, while the battery dimension is not impacted by operating frequency but only by power demands.

$$P_d = E_{sto} \cdot f \quad (2.1)$$

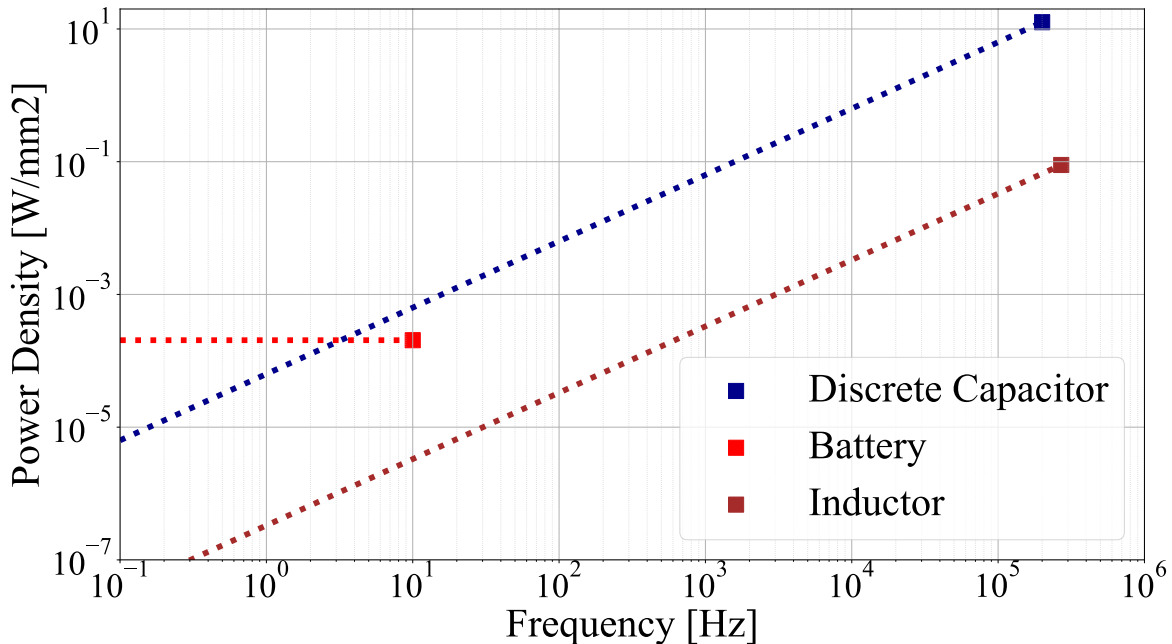
This observation serves to reinforce the significance of investigating batteries as a potential third option for intermediate energy storage within the framework of DC-DC converters, particularly in the context of low-power applications. By exploiting the unique characteristics of batteries, such as their high energy density, we can explore their suitability as intermediate storage element rather than long-term energy storage device. The fact that batteries can outperform traditional passive devices in terms of power density

**TABLE 2.1** | OFF-THE-SHELF DEVICES SAMPLE WITH  $\text{mm}^3$  VOLUME

Passive	Metric	Energy density [ $J.\text{mm}^{-3}$ ]	Power density [ $W.\text{mm}^{-3}$ ]	Power density [ $\mu W.\text{mm}^{-3}$ ]	Voltage/ Current rating	ESR [ $\Omega$ ]	Surface [ $\text{mm}^2$ ]	Volume [ $\text{mm}^3$ ]
	Frequency	-	@ SRF/10	@ 1 Hz				
Battery (V6HR)		$3.6 \times 10^{-1}$	N.A	360	0.018 A	6	35.2	74
Capacitor [6]		$33 \times 10^{-6}$	2	33	6.3 Vdc	0.015	31.4	60
Inductor [7]		$70 \times 10^{-9}$	0.01	0.07	0.145 A	2.9	16	69

at low frequencies and low power amplifies the interest and motivation to study their integration (as flying battery) within the switched DC-DC converter concept, an approach that, to the best of my knowledge, has not been explored so far in the literature.

Considering the potential benefits of utilizing batteries for energy storage in low-power scenarios, it becomes increasingly pertinent to delve deeper into their performance characteristics and explore how they can be optimally employed. Further investigations into the interplay between operating frequency, power density, and the current delivery limitations of batteries will contribute to a better understanding of their capabilities and limitations. Consequently, the study of batteries as an intermediate energy storage option within the realm of DC-DC converters holds great promise for enabling efficient and effective energy management in various low-power applications.


**Figure 2.2** | Battery power density advantage at low operating frequency

## b On-chip integration

In the past, the miniaturization of batteries has been a challenge due to their sub-linear scaling behavior. This means that reducing the volume of a battery to a tenth would result in significantly less than a tenth of its original energy storage capacity. Consequently, achieving fully integrated solutions with high energy density using batteries has been difficult. However, recent advancements and trends in the miniaturization of solid-state batteries (SSBs) have shown remarkable energy density even at the scale of cubic millimeters, indicating a paradigm shift in this area [9]. Reduction of packaging and the development of SSB paved the way for the development of compact and integrated battery solutions with improved performances.

Liquid electrolyte batteries, although typically requiring larger packaging solutions, generally offer higher output power compared to their solid-state counterparts. Conversely, solid-state thin film batteries (TFBs) with a total thickness as low as 100  $\mu\text{m}$  [9] can be directly integrated onto silicon substrates. This integration enables the realization of significantly higher energy and power densities. The use of SSBs also brings forth other promising characteristics when compared to liquid electrolyte batteries, such as improved safety and longer cycle life and lifespan. When combined with their higher energy density and power capabilities, SSBs present the potential for small packaging battery-based DC-DC converters that can deliver efficient power conversion [2].

The emergence of solid-state batteries as a viable solution for compact and efficient energy storage systems offers numerous advantages. Their integration directly onto silicon substrates not only facilitates miniaturization but also enables seamless integration with other electronic components, leading to more compact and space-efficient designs. Additionally, the improved safety and longer cycle life of SSBs make them highly desirable for applications where reliability and longevity are critical factors [2].

Furthermore, the integration of solid-state batteries within DC-DC converters holds promise for achieving high energy and power densities in small form factors. The combination of enhanced energy density, power delivery capabilities, and the ability to operate directly on silicon substrates opens up new possibilities for the design and implementation of efficient power conversion systems. These advancements in battery technology, particularly in the realm of solid-state batteries, have paved the way for the development of integrated and high-performance energy storage solutions that can enable small packaging battery based DC-DC converters.

## c Challenges and Restrictions

Batteries have historically been associated with continuous operation scenarios and are not typically used in periodic operation. However, the introduction of batteries into switched applications brings a whole new set of challenges and restrictions that differ from their conventional usage and that need to be taken into account.

Traditionally, batteries have been designed and optimized for continuous operation, where they provide a steady and consistent power supply over an extended period of time. In continuous operation, the batteries are typically discharged at a relatively constant rate, allowing for predictable performance and reliable power delivery.

In contrast, switched operation involves frequent on-off cycles, where the batteries are intermittently connected and disconnected from the load. This on-off pattern also makes the battery to be intermittently charged and discharged. This introduces a dynamic aspect to battery usage, as the power demand fluctuates depending on the switching intervals and durations. Such dynamic behavior poses challenges for batteries, as they need to respond quickly to sudden changes in load, while also managing their energy storage and discharge characteristics effectively.

Furthermore, when batteries are used in switched operation, certain restrictions come into play. For example, the battery's cycle life and efficiency may be affected due to the increased number of charge and discharge cycles associated with frequent switching. This can lead to accelerated degradation of the battery's capacity and overall performance over time. Additionally, the design and integration of battery management systems become crucial to monitor and control the battery's state of charge, voltage levels, and temperature variations during switching operations.

Overall, the incorporation of batteries in switched operation brings a shift in their traditional usage, requiring specific considerations to address the challenges posed by dynamic power demands and potential limitations in battery performance.

### **i Voltage limits**

Traditional passive devices regularly present broad voltage operating ranges. Capacitors, in particular, exhibit flexibility in voltage operation, ranging from 0 V to their specified voltage breaking safety limit, which can exceed 1000 V. This wide range allows capacitors to adapt to various voltage conditions.

In contrast, batteries have a more limited voltage range determined by their electrochemical mechanisms. The voltage range for batteries is well-defined and narrow, with a cut-off voltage typically well above 0 V. For instance, traditional Li-Ion batteries have a cut-off voltage around 3.0 V and a maximum voltage of 4.2 V. Crossing this voltage range not only affects battery performance but also poses a risk to the battery's integrity, or requires series of battery connections to withstand the voltage, reducing energy density and power capability of the solution.

It is crucial to adhere to the specified voltage range for batteries to ensure optimal functionality and prevent damage. Operating a battery beyond its recommended voltage limits can lead to reduced performance, decreased lifespan, and potentially dangerous outcomes. Therefore, careful consideration of the voltage range is essential in the design and operation.

### **ii Operating frequency**

Battery chemistry plays a crucial role in dictating the speed at which ions can physically move between the anode and cathode within a battery. This movement is vital for the ions to participate in the reaction, fully using the battery's volume to exploit all potential energy density. However, when the operating frequency exceeds a certain threshold (around single Hz), the ions fail to reach the opposite terminal in sufficient flow, leading to a reduction in the chemical reaction. Consequently, only a portion of the energy transfer is allowed to occur, mainly involving what can be referred to as the capacitive part of the battery,

dramatically reducing the energy density offered in the classical battery operation mode. The unique chemical technology offered by the battery is not fully utilized in such scenarios.

The conversion of chemical energy into electrical energy, when compared to other traditional passive devices, is slower than of electrostatic and electromagnetic context. This slower speed can be expressed as a higher electrical time constant, hindering the dynamic response of batteries. Electrostatic and electromagnetic devices outperform batteries in terms of dynamic response, as they are capable of faster energy conversion. Consequently, batteries introduce inherent limitations on the switching frequency of DC-DC converters (in the range of Hz or at most kHz), as their slower response times restrict the rate at which energy can be efficiently transferred.

The impact of this slower dynamic response is particularly significant in the context of DC-DC converters. These converters rely on fast and efficient energy conversion to regulate the voltage levels and ensure smooth power transmission. However, due to the slower response of batteries, the achievable switching frequency of the DC-DC converter is constrained, otherwise the battery is used as capacitors, resulting sub-utilization of the battery capability, as explained earlier. This limitation necessitates careful consideration and optimization of the converter design to ensure compatibility with the slower dynamics of batteries. Balancing the desired switching frequency with the capabilities of the battery chemistry becomes crucial to achieve optimal performance and reliable operation of the DC-DC converter using battery as intermediate energy storage device.

### iii Cycling operation and lifespan

Limited number of cycles is a significant characteristic that distinguishes batteries from other devices used in DC-DC converters. Traditional battery technologies typically offer a finite number of charge-discharge cycles, usually on the order of  $10^3$  cycles.

Despite advancements in battery technology as the development of new chemistries and designs aimed at improving cycle life due to the use of new electrode materials, electrolyte formulations, and improved cell designs, it is still limited. Therefore, it becomes imperative to develop strategies for the proposed use of the battery in a DC-DC converter that minimizes battery cycling or work in a manner that extends its cycle life and lifespan.

Following such specific challenges and considerations of using batteries as intermediate energy storage device in DC-DC converters, Section II explores a family of topologies addressing such restrictions. However, current battery models do not reflect batteries' behaviors in the context of intermediate storage for switched DC-DC converters, guiding us to an experimental approach to evaluate the battery in such conditions and validate its use on the DC-DC topology. Chapter 3 will describe the experiments and results obtained.

## II Switched-Battery Converter (SBC) Topology

In order to enhance the energy and power density of DC-DC conversion in low-power applications, a new family of switched DC-DC converters called SBC (Switched-Battery Converter) is proposed. Drawing



inspiration from SCC (Switched-Capacitor Converter) topologies, the SBC topology integrates at least one battery as the flying passive component within the converter, as depicted in Fig. 2.3. This modification plays a central role in the design and introduces a fresh set of challenges, particularly in terms of defining an appropriate state sequence and to find the boundaries of batteries operation in this unconventional mode of operation.

One of the primary challenges associated with designing the SBC topology is establishing a state sequence that ensures the batteries remain within their designated voltage operating limits. This is crucial to safeguard the batteries' longevity, overall performance and to ensure that the battery's ionic contribution is properly used. Since the ionic contribution is the batteries' most straightforward performance advantage against other passives. To address this challenge, it is necessary to identify a set of phases in which the arrangement of components effectively maintains the output voltage at the desired level. By determining these phases, the state sequence can be designed to regulate the converter's operation and prevent the batteries from exceeding their safe voltage thresholds.

Maintaining charge balance throughout the entire converter cycle is another critical aspect that must be considered. As the battery does not work as an energy source to the system, rather as an intermediate energy storage, when transferring energy from input (that can be another battery) to the source, the charge balance ensures that the battery is not discharged during steady-state operation. Furthermore, since the batteries' function as flying passive components in the SBC topology, maintaining charge equilibrium is essential to avoid imbalances that could degrade battery performance or lead to premature failure. Consequently, the devised state sequence must be carefully designed to ensure charge balance.

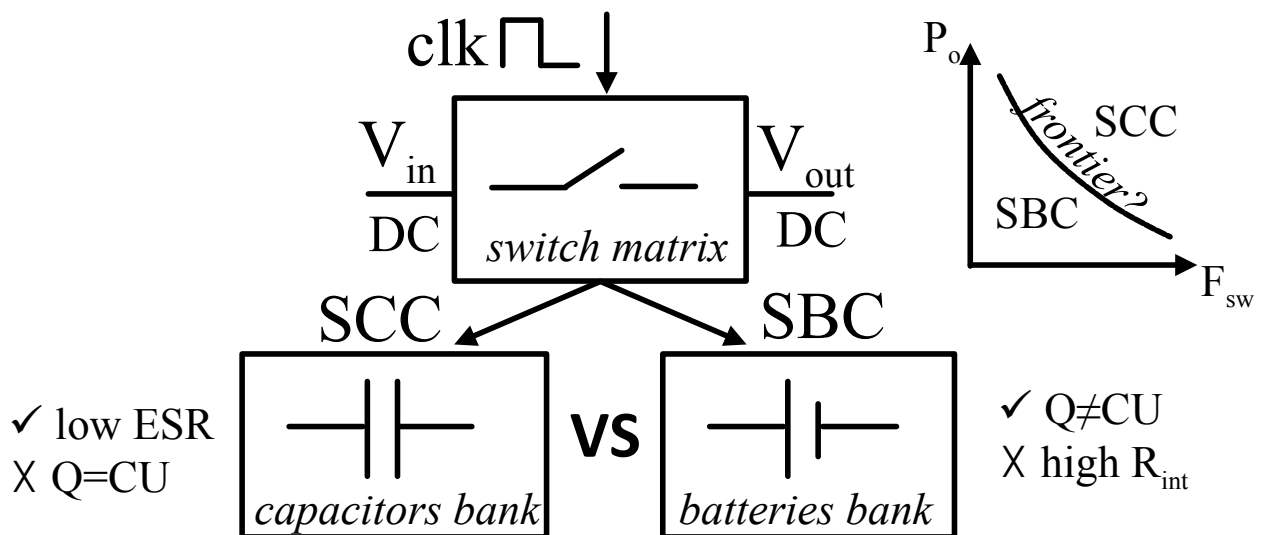


Figure 2.3 | Switched DC-DC converter using battery as passive device

### a Micro-cycle

During SBC operation, batteries are subjected to a significantly different pattern of use compared to regular deep depth of discharge (DoD) utilization in long term energy storage applications. The usage profile during SBC steady-state operation involves alternating charging and discharging phases, but the amount of charge passing through the battery during each phase is much smaller than the battery's overall state of charge (SoC). This cycling of energy through the battery in such a shallow DoD without significantly altering SoC is referred to as a  $\mu$ -cycle [10].

One of the primary objectives of employing  $\mu$ -cycles during SBC operation is to ensure that the battery's average voltage remains unaffected (working on the weak slope region as shown in Fig. 2.1). Another one is to address the cycle life limit intrinsic to batteries when operating in prolonged periods of charging and discharging with larger DoD. By limiting the DoD in each  $\mu$ -cycle, the battery also experiences less stress and strain, leading to reduced degradation and improved cycle life [4]. Additionally, the reduced DoD helps mitigate undesirable side reactions, such as electrolyte decomposition or material degradation, which can occur during extended operation at higher DoD levels.

The use of  $\mu$ -cycles in SBC operation is an example of optimizing battery management strategies to maximize performance and reliability while enabling the SBC implementation. By carefully controlling the charge and discharge processes and keeping them within narrow limits, the battery can maintain its average voltage and reduce voltage ripple (a main limiting factor in SCC operation due to charge sharing loss) while enduring significantly more cycles than it would in standard-cycle operation (with significant DoD).

Fig. 2.4 illustrates the voltage pattern of the battery during  $\mu$ -cycle operation in SBC's steady-state operation. In this mode, the battery is already charged and polarized at a stable voltage point. The figure shows how the battery's voltage changes during a complete  $\mu$ -cycle.

During the charging phase of the  $\mu$ -cycle, the battery receives a relatively small quantity of charge  $\Delta Q$ . This charge value is significantly smaller than the battery's SoC at the beginning of the cycle. Despite the small charge input, we can consider that the battery's voltage increases as it absorbs the energy. However, since the charge input is much smaller than the overall SoC, the voltage increase during this phase remains extremely limited, specially if the battery operates in the voltage plateau by being set to the proper SoC before the beginning of operation.

To ensure that the battery returns to its initial SoC before starting the next cycle, a discharging phase of equal duration follows the charging phase. The discharge occurs under the same conditions as the charging phase, maintaining a consistent discharge rate and discharge current. In this discharging phase, the battery releases a quantity of charge equal to the negative of the charge received in the previous charging phase ( $-\Delta Q$ ).

By discharging the same amount of charge as received during the charging phase, the battery's SoC returns to its initial level, thus the battery serves as intermediate storage component, and not as an input source (as there is no long term SoC variation). This ensures that the battery is ready for the next cycle, starting from the same SoC as before. The voltage during the discharging phase gradually decreases as the

energy is released from the battery. But again, as the discharge is also limited due to the small quantity of charge involved, the voltage drop is extremely low. For a 1 mAh battery working at 1 Hz with an output current of 1 mA (equivalent to 1 CA), the  $\mu$ -cycle would represent a DoD lower than 0.03% ( $\Delta Q = 1mC$ ), incurring in a negligible voltage drop between the battery's terminal due to charge/discharge principle.

Overall, the voltage pattern during the  $\mu$ -cycle operation shows a slight increase during the charging phase and a subsequent decrease during the discharging phase, ultimately returning to the battery's initial SoC. This controlled pattern allows the battery to maintain a steady average voltage and prevents significant deviations in its SoC. Such careful management of charge and discharge quantities within the  $\mu$ -cycle operation contributes to extending the battery's cycle life and ensuring its optimal performance over an extended period of time.

Despite the benefits of a low DoD it incurs in a trade-off with the SBC's output current and consequentially power. At same frequency a higher output current incurs in a directly proportional higher DoD of the battery. Using the same  $\mu$ -cycle as above, with the circuit provides an output current of 2 mA (2 CA) instead of 1 mA at the same frequency of 1 Hz, the  $\mu$ -cycle would represent a DoD of almost 0.06%. To preserve the same DoD the battery would need to have double the capacity, generally impacting in higher footprint and possible reduction of power density. If considering a linear scaling factor of the battery, the power density would be preserved, but there is possible impact in losses and efficiency.

Expanding on voltage variation throughout a  $\mu$ -cycle, batteries do not present the direct linear relation between stored charge and voltage (as do capacitors, for example), this characteristic when combined to a very small DoD (in relation to the battery's overall SoC) allows the voltage between the battery's terminals to remain near constant. The constant behavior of battery's voltage induces reduced losses, improved performance (efficiency and ripple) but, more critically, it allows the battery to operate consistently inside its narrow voltage range, enabling its use inside a DC-DC converter.

One significant benefit of employing  $\mu$ -cycle operation is its ability to greatly extend the cycle life of batteries. In typical commercial batteries used in applications with large DoD, the cycle life is generally around 1000 cycles. However, if each  $\mu$ -cycle were equivalent to a full cycle with a large DoD, the concept of SBC would be impractical. For instance, operating at a frequency of 100 Hz would quickly exhaust the cycle limit of most commercial batteries within a mere 10 seconds.

By significantly extending the battery's cycle life, the concept of SBC becomes viable and practical. It enables frequent charging and discharging cycles without prematurely degrading the battery. This is particularly advantageous in applications where rapid and frequent energy transfer is required, such as in electric vehicles or grid-scale energy storage systems.

## b Sequencing

The SBC utilizes a series of distinct topology phases, in which each phase represents a predetermined configuration of connections among the devices, ensuring that at least one battery is connected in series. These phases are meticulously arranged in a specific sequence, collectively forming a cycle that plays a crucial role in preserving the SoC of every battery within the system. The primary objective of this

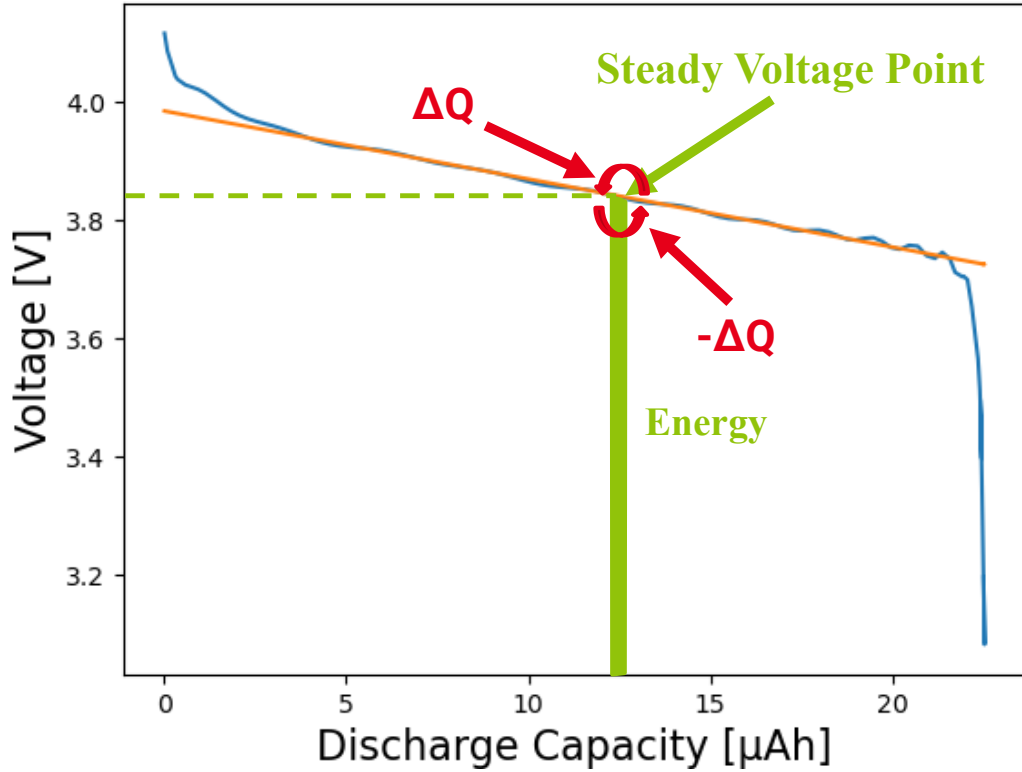


Figure 2.4 | Battery voltage behavior in  $\mu$ -cycle operation

cyclic arrangement is to ensure that the SoC of each battery, by the end of a cycle, matches its initial SoC at the beginning of that particular cycle. This repetitive cycle persists throughout the steady-state operation of the system, enabling efficient conservation and management of the batteries' SoC. By carefully orchestrating the sequence and flow of energy through each phase, the SBC optimizes the utilization of the battery resources while maintaining the desired performance and stability of the system.

Each phase satisfy certain criteria and adhere to specific requirements to be considered for valid and explored into the construction of a valid SBC cycle. It is important to acknowledge that while a phase may be valid, it may not necessarily be optimal or suitable for integration into a functional cycle.

To be considered valid, a phase must incorporate at least one battery connected in series with the load. This battery can be connected in series with the input voltage source, in one of both polarities (positive or negative), and the voltage generated by this arrangement must be equal to the desired SBC output voltage. This fundamental characteristic of having at least one battery connected in series distinguishes the SBC as a battery-based DC-DC converter and sets it apart from other topologies like the SCC family.

The fulfillment of the required SBC output voltage by each phase eliminates the need for a bulky output decoupling capacitor within the system, even more considering the focus on low frequency operation. This feature streamlines the design and operation of the SBC, simplifying its implementation. Moreover, the SBC's unique advantage lies in its ability to connect the input voltage source across multiple phases, rather than restricting it to a single phase. This flexibility grants greater freedom in the creation of valid

phases and, consequently, functional cycles, remaining a key principle of the SBC's operation.

For a cycle to be convenient in the SBC, it has to fulfill the following criteria:

1. the average voltage across each battery has to remain fixed around their operational voltage (dictated by the battery's electrochemical reaction);
2. the energy given/received by each battery has to achieve balance during one cycle (preserving SoC);
3. the voltage created by a battery network arrangement and the input source has to be equal to the output voltage in all phases removing the necessity of an output capacitor.

During the operation of a working cycle within the SBC, each phase is intentionally kept brief in order to conserve a small DoD. This practice results in the battery operating on a  $\mu$ -cycle basis, as previously described. The primary purpose of this approach is to preserve the battery's operational voltage range, ensuring its longevity and preventing any potential safety risks to the overall system.

By adhering to the specified operational voltage range, the SBC guarantees that each battery operates within its safe and efficient limits. This not only safeguards the battery but also eliminates the need for supplementary or parallel phases to recharge or discharge the battery during the working cycle. This streamlined approach enhances the system's overall efficiency and reliability while maintaining a stable and steady-state operation.

Since each phase ensures that the required SBC output voltage is met, this behavior is also valid for the SBC working cycle. This design facilitates energy balance and preserving SoC of the batteries within the system.

One notable benefit of operating on  $\mu$ -cycles is the minimal variation in voltage between the terminals of the batteries. This reduces losses within the system and significantly improves the overall efficiency of the SBC. Additionally, this operating mode facilitates more efficient internal behavior within the batteries themselves, including diffusion and other ionic reactions, further optimizing their performance.

In summary, by adhering to the brief phase duration, conserving a small DoD, and operating on  $\mu$ -cycles, the SBC ensures that batteries work within their safe voltage range, improves energy balance, eliminates the need for additional phases, avoids the use of an output capacitor, enhances system efficiency, and optimizes the behavior and performance of the batteries themselves.

### c Power Efficiency

For evaluating the achievable SBC power efficiency, we will first study its intrinsic losses. As the SBC topology borrows inspiration from the SCC, we approach such analysis proposing an equivalent SBC model similar to the SCC, assuming an ideal DC voltage conversion ratio under no load condition, represented by an ideal transformer and all conversion losses caused by an output impedance  $R_{out}$  creating an output voltage drop as shown in Fig. 2.5 [12]. From such model if we consider a resistive load  $R_{load}$  we can easily obtain the expression that defines the circuit efficiency as:

$$\eta = \frac{R_{load}}{R_{out} + R_{load}} \quad (2.2)$$

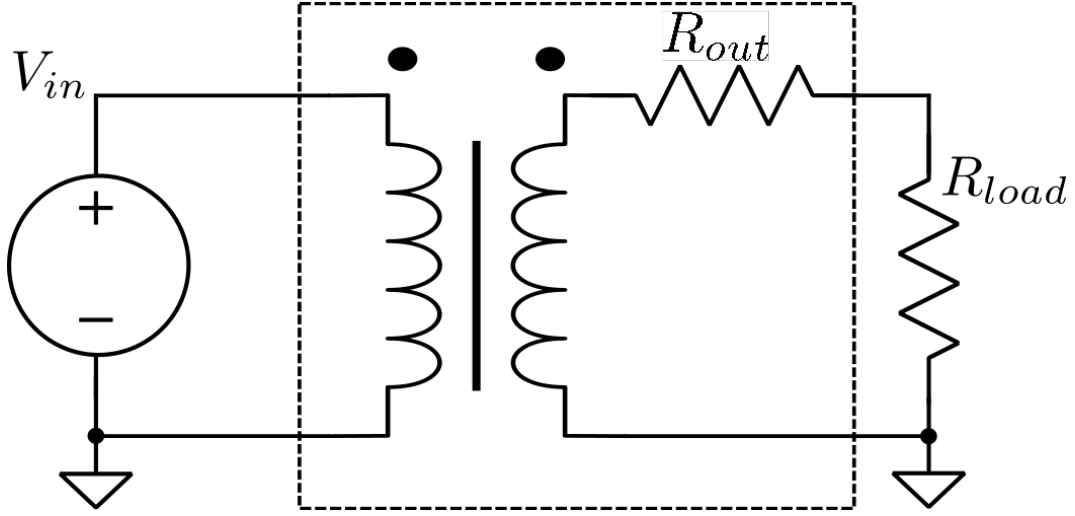


Figure 2.5 | Model of SBC converter

The SBC and SCC present similarities in topology, however both systems present distinct loss mechanisms. However, as the SCC present a well established and studied formalism and method, we start the analysis of the SBC dynamic loss from the SCC approach. As presented in [13], SCC circuits operate in either one of two operating conditions, or in between them. One of such conditions refers to low switching frequencies, where losses and the output impedance are dominated by the amount of charge that can be transferred by the capacitors (hard charging operation). This regime is denoted as the slow switching limit (SSL), however the SSL behavior of SCC is not present in SBC, as batteries do not present the linear relation between stored charge and voltage that is present in capacitors, and thus the battery's voltage drop during operation is negligible and presenting no charge sharing loss. Charge sharing loss being an intrinsic loss in SCC circuits and predominant in SSL regime, due to the voltage difference between the switched capacitor(s) before and after the switch between them is closed (the transport of charges to achieve equipotential is inherently lossy) [1]. The other operating regime is known as fast switching limit (FSL) under high operating frequency in SCCs. This soft-charging regime leads to the output impedance and losses to be dominated by the switch on-state resistances.

The frequency of the inflection point between FSL and SSL ( $f_{lim}$ ) is given by [13] as the inverse of the product between the switch on-state resistance ( $R_{on}$ ) and the capacitance of the flying capacitor ( $C_{fly}$ ) as shown in (2.3). The circuit is considered to be operating in FSL if the operating frequency is greater than  $f_{lim}$ , and in SSL otherwise. As detailed earlier, batteries feature a much higher energy storage capacity than capacitor. Since the SBC uses a battery as the flying passive, for effects of determining  $f_{lim}$  we consider the SBC's equivalent capacitance for  $C_{fly}$  to be infinite and thus  $f_{lim}$  is equal to 0 and the circuit is always operating in FSL.

$$f_{lim} = \frac{1}{R_{on} \cdot C_{fly}} \quad (2.3)$$

With the lack of SSL behavior even at low operating frequency, the SBC losses are dominated by the

conduction losses, and it is natural to start the analysis of SBC losses by the FSL equivalent resistance for general SCC circuits presented in [13] given by:

$$R_{FSL} = \sum_i \sum_j^n \frac{R_i (a_{r,i}^j)^2}{D_j} \quad (2.4)$$

Where  $R_i$  is the on-resistance of the  $i^{th}$  switch,  $D_j$  is the duty cycle of the  $j^{th}$  phase for a converter with  $n$  phases and  $a_{r,i}^j$  is the normalized charge flow through switch  $i$  during phase  $j$ . The values for  $a_{r,i}^j$  are determined typically by circuit inspection and normalized by the total output charge,  $q_{out}$ , similarly to [13]. The values of  $a_{r,i}^j$  for switches that are off are zero and are independent of duty cycle in steady-state as they only represent charges flowing through the switches ensuring conservation on the flying component.

For the SBC if we consider an equal charge flow in each phase  $j$ , differing only in direction for each switch, we adjust it and work with the vector  $a_{r,i}$  instead of  $a_{r,i}^j$ , representing only the charge through each switch when the  $i^{th}$  switch is on. And assuming equal duration of each  $n$  phase instead of using a phase duty cycle, we rather consider the amount of time that each switch will be used, as they can be reused in different phases, and we work with  $D_i$  as the duty cycle of the  $i^{th}$  switch. For the specific case of the SBC we can simplify the FSL impedance in (2.4) to:

$$R_{FSL} = n \sum_i R_i |a_{r,i}| D_i \quad (2.5)$$

However, as capacitors' ESR are generally negligible against the on-resistance of the switches, the proposed  $R_{FSL}$  for SCCs does not take into account the flying passive series resistance. Since batteries have higher internal impedance than the ESR of regularly used flying capacitors, it can have a meaningful impact on the overall equivalent series resistance of the SBC. Adjusting (2.5) to include the impact of batteries' internal resistance gives the equivalent output resistance of the SBC converter as:

$$R_{out} = n \sum_i R_i |a_{r,i}| D_i + n \sum_k R_{int,k} |a_{b,k}| D_k \quad (2.6)$$

Where  $R_{int,k}$  is the internal resistance of the  $k^{th}$  battery,  $D_k$  is the duty cycle in which the  $k^{th}$  battery is utilized and  $a_{b,k}$  is the normalized charge flow through the battery while it is being used. Circuit inspection is used to obtain the value of  $a_{b,k}$  and later is normalized by the total output charge,  $q_{out}$  similarly to  $a_{r,i}$ . This result allows to estimate SBC's conversion losses using only structural parameters.

For further simplification, we can expand the concept of equal charge considering only series connections between switches when in on state, so that in each phase  $n$  will have the charge flow of  $q_{out}/n$  and we can further simplify (2.6) as:

$$R_{out} = \sum_i R_i \cdot D_i + \sum_k R_{int,k} \cdot D_k \quad (2.7)$$

Similar to (2.6), (2.7) allows us to use only structural parameters of the SBC to estimate conversion

losses and efficiency, not requiring complicated network analysis or simulations, as simulations using batteries imply even higher costs than with capacitors.

### III Topology Exploration

The SBC topology, similar to SCCs, operates by utilizing different cycles for various voltage conversion ratios. Each conversion ratio requires a unique combination of phases to ensure efficient operation. The identification of functional cycles that satisfy the conditions outlined in Section II-b is crucial for the successful implementation of SBC circuits.

To explore the range of possibilities, we developed a semi-exhaustive algorithm specifically designed to search for valid phases that meet the aforementioned restrictions and requirements. This algorithm systematically analyzes and evaluates different phase possibilities to identify those that satisfy the specified conditions. By determining the valid phases, we can subsequently attempt to establish working cycles that achieve the desired voltage conversion ratio(s).

To optimize the algorithm's efficiency and reduce computational time, we imposed additional restrictions and preferences (it is one of the main reasons that it is a semi-exhaustive exploration instead of an exhaustive one). These constraints help streamline the search process and we can focus the algorithm's efforts on most promising and viable solutions. Through this approach, we can effectively explore the design space of the SBC topology, identify suitable phase configurations, and improve the overall performance of SBC circuits.

#### a Obtaining valid phases for the SBC

Each SBC valid phase is a particular strict set of fixed connections between the devices (mainly batteries and the input source and the output load), in which there needs to have at least one battery connected in series to the output. To be considered a valid phase for the SBC, each explored phase  $j$  needs to fulfill the conditions described in Section II-b and also satisfy:

$$V_{out,j} = a_{0,j} \cdot V_{in} + \sum_i a_{i,j} \cdot V_{bat,i,j} \quad (2.8)$$

Here  $V_{out}$  refers to the output voltage of the  $j^{th}$  phase (which should be equal among different phases),  $V_{bat,i,j}$  is the battery voltage of the  $i^{th}$  battery during the  $j^{th}$  phase, and  $a_{i,j} = -1/0/+1$  represents the  $i^{th}$  element during the  $j^{th}$  phase (here the element 0 is the voltage source). The value of  $a_{i,j}$  signifies that the element (either the voltage source or one of the batteries) is disconnected (0), connected in series to the load in a positive orientation (1), or a negative orientation (-1). We consider a positive orientation when the element adds voltage with respect to the ground towards a higher  $V_{out}$  and a negative orientation when it subtracts voltage towards a lower  $V_{out}$  as shown in Fig. 2.6. We also require that for each phase, at least one of the batteries is connected to the load.

In the exploration of valid phases for the SBC, a limitation was imposed to allow the use of at most



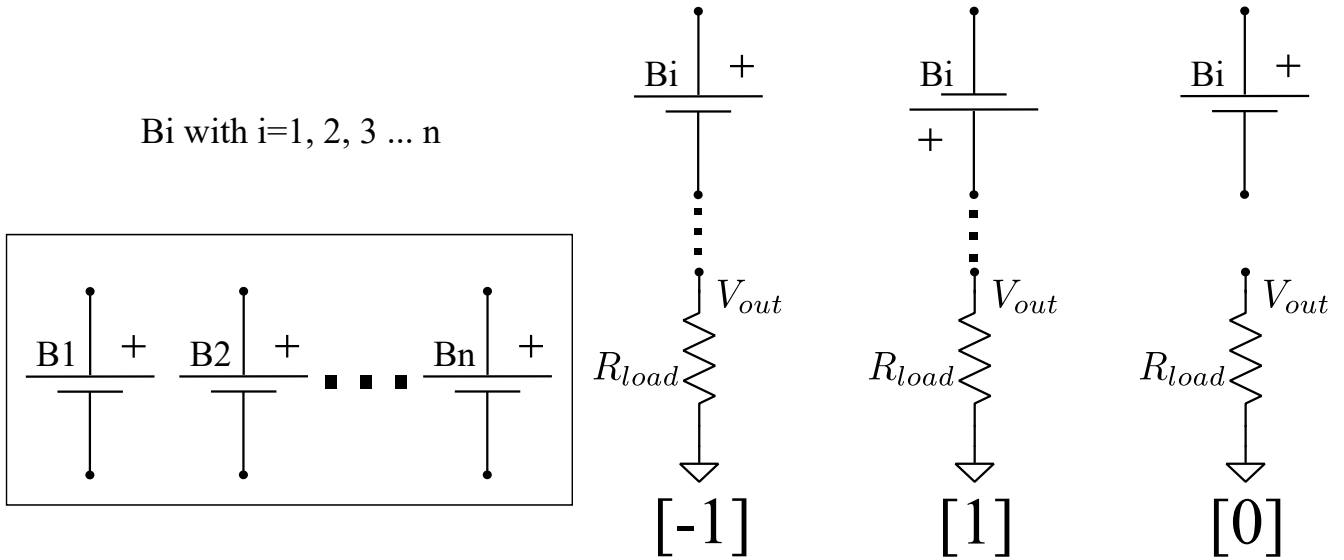


**Figure 2.6** | Possibilities of connection by the elements of SBC for each phase

two groups of batteries, with each group having a distinct DC voltage value. This limitation simplifies the design and analysis process. However, it is worth noting that despite this restriction, there is still the possibility of having both groups with the same voltage value, meaning that both groups are composed of battery with the same chemistry (redox couple).

When both groups have the same voltage value, it essentially means that only one group of batteries is required. This simplifies the overall design by reducing the complexity associated with managing and balancing two distinct voltage levels.

Additionally, when exploring different voltage ratios, it is not uncommon to encounter cases where one group has a voltage value that is an integer multiple of the other group. In such scenarios, it is also possible to have both groups with the same voltage value. This further highlights the versatility of the system, as it can accommodate different battery cell configurations and still achieve optimal SBC performance.

The ability of the system to adapt and work with various battery configurations is a valuable characteristic of the SBC. It offers flexibility in accommodating different battery types, capacities, and configurations. This versatility is particularly beneficial in applications where battery cells with similar voltage values or specific voltage ratios are available or desirable.

The semi-extensive algorithm shown in Fig 2.7 demonstrates the exploration of valid phases for a given set of  $V_{in}$  and  $V_{out}$ . The algorithm will navigate the number of batteries for individual groups. With such values it will validate which obtained combinations satisfy (2.8). Combinations that satisfy the  $V_{out}$  criteria will be stored in a  $P$  vector in order to be used later in establishing working cycles. The algorithm has a limited number of loops based on the maximum number of batteries in each group  $N_{i,max}$ .

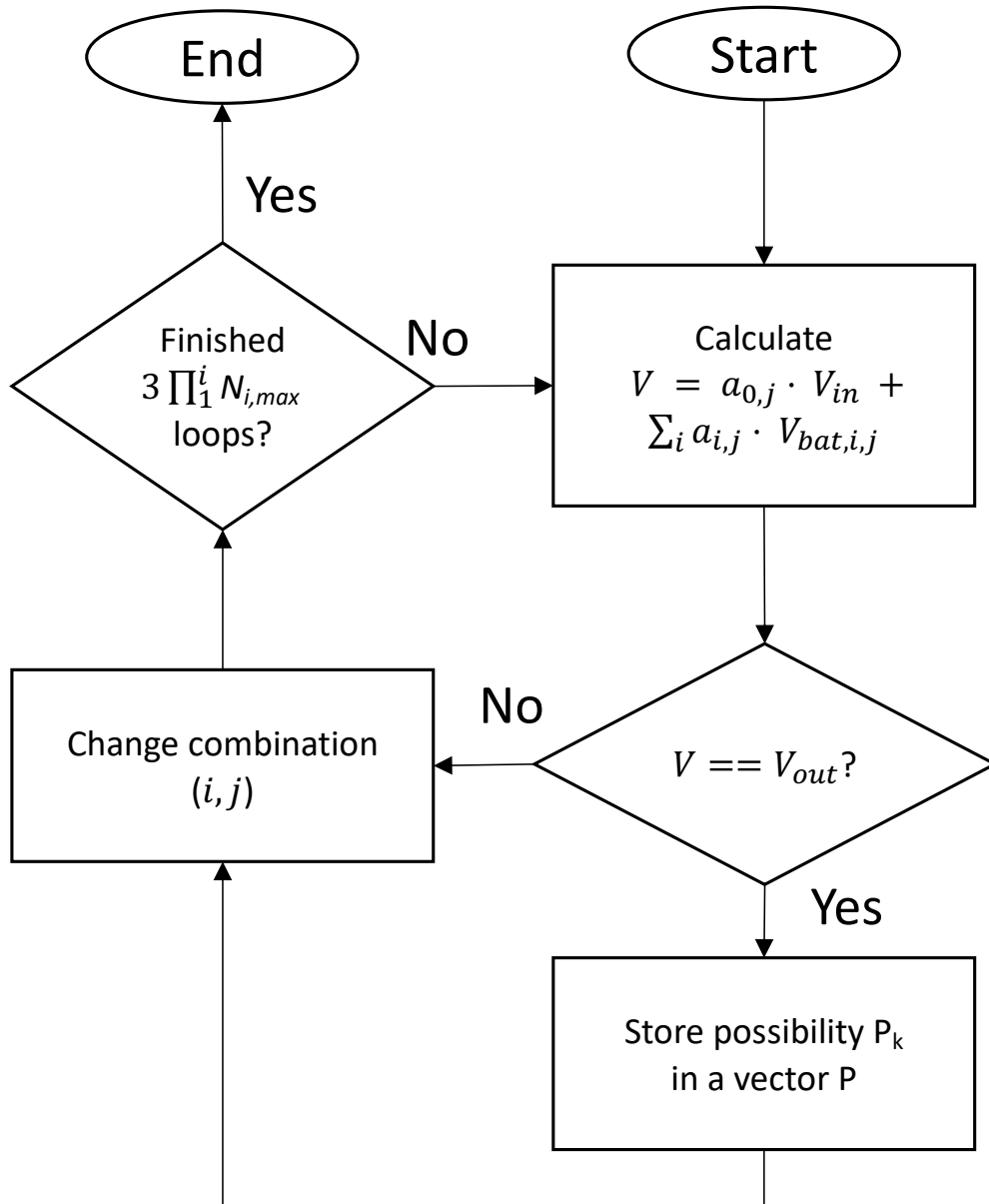


Figure 2.7 | Algorithm exploring valid phases

An obtained  $P$  vector represents all valid phases found by the semi-exhaustive algorithm for a set of  $V_{in}$  and  $V_{out}$ , consequentially a voltage conversion ratio  $V_{out}/V_{in}$ . The larger the  $P$  vector for a given voltage conversion ratio, the greater the probability of finding a working cycle for that particular voltage conversion ratio, however it is not guaranteed. It is possible that even a large set of valid phases is not capable of forming a working phase.

## b Obtaining and exploring working cycles

The exploration of a working cycle tries to establish SBC cycles that satisfy the conditions established in Section II. For the exploration of such cycles the semi-exhaustive algorithm shown in Fig. 2.8 starts from the vector  $P$ , obtained from the algorithm shown Fig. 2.7. The vector  $P$  has  $P_N$  possibilities represented as  $P_k$ .

After loading vector  $P$  the algorithm generates a vector  $C_i$  with  $N^i$  combinations having length of  $i$  phases, it will then navigate and combine phases  $P_k$  from vector  $P$  picking different cycle possibilities  $C_{i,j}$ . To evaluate if charge balance is achieved for a given combination  $C_{i,j}$  we evaluate  $\Delta Q$  for each battery  $h$  of group  $g$  in that combination as:

$$\Delta Q_g = \sum_{h=1}^N bat_{g,h} \quad (2.9)$$

From (2.9) we establish that a working cycle achieves charge balance if the following condition is met:

$$\Delta Q == 0 \iff \forall(\Delta Q_g = 0) \quad (2.10)$$

If charge balance is achieved, combination  $C_{i,j}$  from vector  $C_i$  is stored in a vector  $W$  as a closed working cycle. As shown in Fig. 2.8, the algorithm continues exploring all possible combinations of length  $i$  before incrementing  $i$  and progress to explore longer cycles. It continues exploring cycles until reaching the configured length limit  $i_{max}$ .

It is possible that multiple twin cycles are found, cycles that use the same phases only in a different order. These equivalent cycles can be identified from a charge balance point of view, the order of phases is effectively unimportant. However, while charge balance is maintained regardless of the phase order, there are practical implications to consider. The order of phases can be optimized for different purposes. It can also be optimized to minimize the switching activities of some switches, reducing driving losses by not activating the switches twice, but rather rearranging the sequence of phases. Or it can be optimized to minimize charge state variations throughout the cycle in each individual battery, by strategically arranging the phases, it is possible to reduce the likelihood of providing charge for a single battery in consecutive phases.

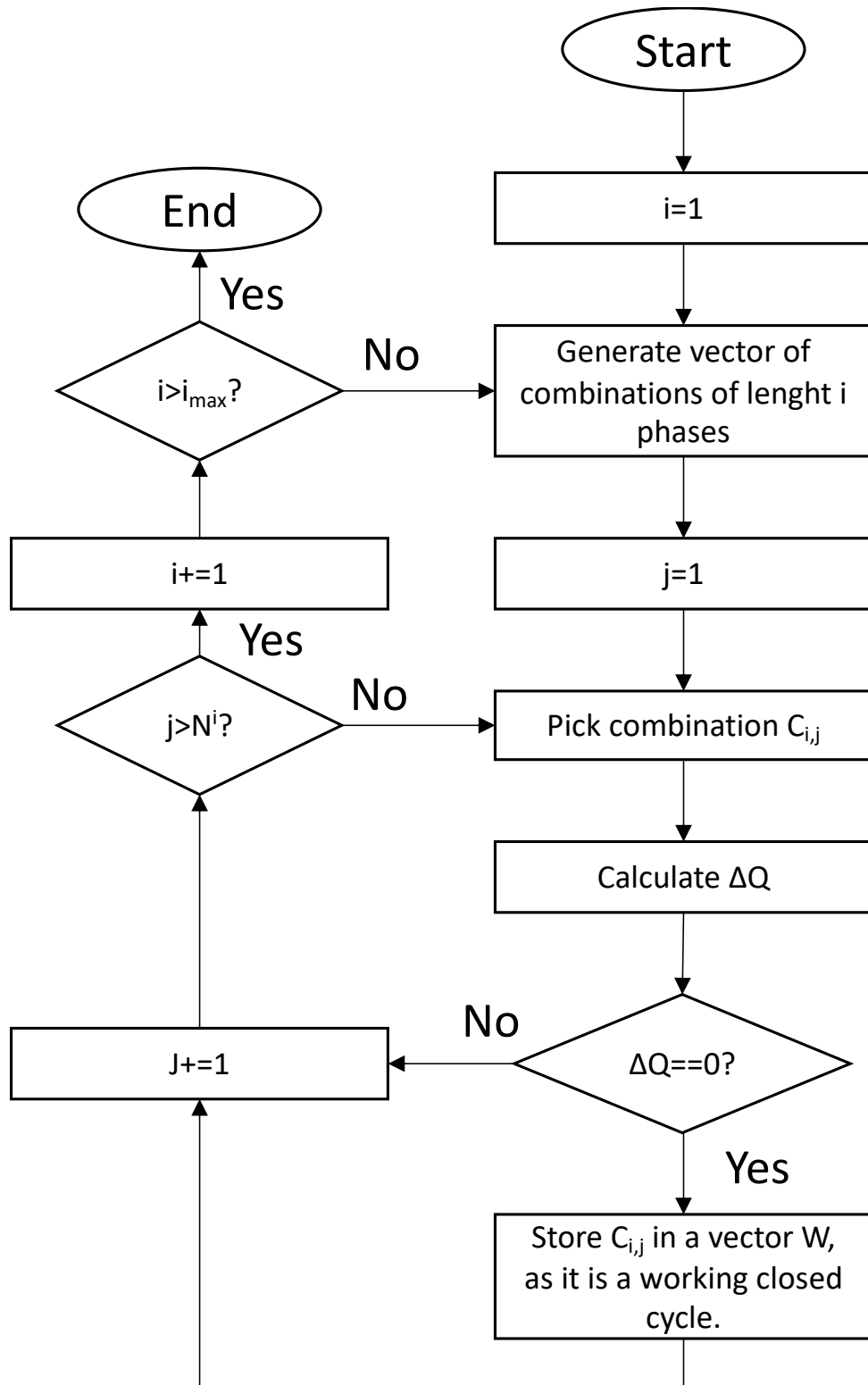


Figure 2.8 | Algorithm for obtaining working cycles

Avoiding consecutive charge phases for a single battery helps limit charge state variations throughout the cycle. When a battery receives charge in succession, it can lead to imbalances and potentially affect its performance and lifespan (even on a  $\mu$ -cycle steady-state operation). For example, by spreading out the charge delivery across different non-consecutive phases, the charge state variations within each battery can be minimized, promoting a more balanced steady-state operation (and longer cycle life).

With vector  $W$  obtained from the algorithm in Fig. 2.8 we have  $F$  working cycles (which are previous explored combinations  $C_{i,j}$ ). We can classify obtained working cycles  $W_f$  using different criteria. Some of the main criteria are length (number of phases) and number of batteries, both for a single group and in general. A shortest cycle implies less phases, decreasing the number of times that the energy storing elements are switched, minimizing losses by switching and even in charge movements. If the optimization is based on minimizing the number of batteries, the advantage in reducing the footprint occupied by the converter, allowing higher energy density and a greater integrability of the circuit.

For example, if we optimize the obtained cycles by length we search the shortest working cycle (the one with less phases). The optimization algorithm can be as simple as the one shown in Fig. 2.9, where we navigate the obtained vector  $W$  and obtain the length for each working cycle  $W_f$ . This length is compared to the previous shortest length found for cycle  $W_{opt}$ . If it is longer, we go to the next working cycle in the vector, if it is shorter, this cycle is then stored as  $W_{opt}$ . We perform this action until we reach the last stored cycle in vector  $W$  ( $W_F$ ) and have as output the shortest working cycle found in the previous exploration.

The principle of DC-DC topologies using batteries as flying energy storage devices are patented in [11] describing requirements and strategies for the exploration of possible topologies. The algorithms presented in this chapter are put in practice in Chapter 4 for the exploration of SBC topologies in different conversion ratios.

## IV Conclusion

This chapter explores the concept of incorporating batteries as the central intermediate energy storage device in DC-DC converters. For low power applications an approach to reduce losses is to work at low frequencies. Since batteries output power is frequency independent at first order, it presents an advantage against capacitor and inductor based converters at low frequencies. At such low frequencies traditional passive technologies require huge footprints, incurring in low power density, highlighting the interest of batteries. Batteries power output is limited by its inherent size and chemistry.

By studying the possibility of incorporating batteries as the central intermediate energy storage device in DC-DC converters, it explores the limitations associated with batteries and their consequential impact on the specific use of switched converters. Despite their many advantages, batteries possess inherent limitations that affect their insertion within converter systems. These limitations are analyzed in detail, shedding light on the challenges and considerations that must be taken into account when designing converter architectures utilizing batteries as the intermediate energy storage device.

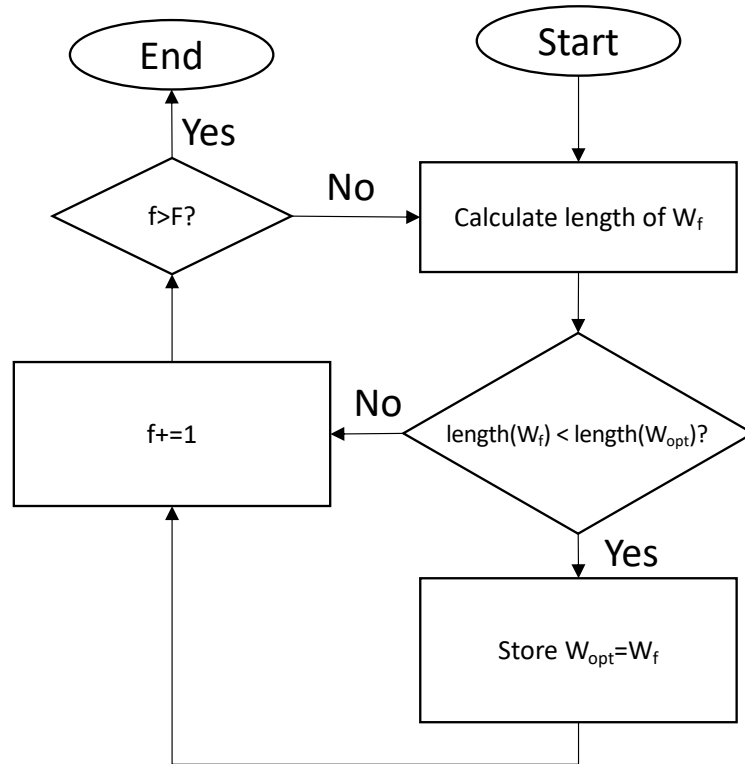


**Figure 2.9** | Algorithm classifying working cycles by length

In response to these limitations, a novel family of converter topologies is introduced in this chapter, the SBC. This new family of converters utilizes batteries as flying energy storage devices, presenting an alternative approach to address the challenges of low frequency and low power applications. The chapter goes on to provide a comprehensive explanation of the process required to achieve valid phases and working cycles within these converter topologies, emphasizing the importance of establishing reliable and efficient operational modes.

Moreover, the chapter delves briefly into the realm of possible optimization for these cycles, outlining potential strategies to enhance their practical implementation and physical performance. These optimization techniques aim to improve the overall efficiency, reliability, integrability and effectiveness of the converter systems employing batteries as flying passive devices. The proposed algorithms for exploration and optimization are put into practice in Chapter 4.

The chapter also sets the stage for the subsequent chapter by highlighting the primary focus of the upcoming discussion: experimental implementation and a comparative analysis of the new converter topologies against existing SCC architectures. This comparative evaluation aims to assess the performance and viability of the novel battery-based converter topologies in practical scenarios, providing valuable

insights for further advancements in the field of DC-DC converters.

The impact of batteries' initial State of Charge (SoC) is not mentioned in this chapter. Neither is the study of batteries output current or some key performance benchmarks of DC-DC converters as output voltage ripple. A study of the impact of such different parameters in SBC performance is needed. Chapter 3 approaches the experimental validation of batteries in  $\mu$ -cycle operation and the impact of such parameters. It also experimentally compares SBC against SCC in a 2:1 DC-DC converter using such performance benchmarks. In Chapter 4 higher complexity SBC topologies are experimentally explored.

# Bibliography

- [1] B. Allard. *Power Systems-On-Chip: Practical Aspects of Design*. Wiley, 2016.
- [2] Jacopo Celè, Sylvain Franger, Yann Lamy, and Sami Oukassi. Minimal architecture lithium batteries: Toward high energy density storage solutions. *Small*, 19, 01 2023.
- [3] Leland Chang, Robert K. Montoye, Brian L. Ji, Alan J. Weger, Kevin G. Stawiasz, and Robert H. Dennard. A fully-integrated switched-capacitor 2:1 voltage converter with regulation capability and 90% efficiency at 2.3A/mm<sup>2</sup>. In *2010 Symposium on VLSI Circuits*, pages 55–56, June 2010. ISSN: 2158-5636.
- [4] James W. Evans, Bernard Kim, Seiya Ono, Ana C. Arias, and Paul K. Wright. Multicycle testing of commercial coin cells for buffering of harvested energy for the iot. *IEEE Internet of Things Journal*, 8(12):10047–10051, 2021.
- [5] Marko Krstic, Suzan Eren, and Praveen Jain. Analysis and design of multiphase, reconfigurable switched-capacitor converters. *IEEE Journal of Emerging and Selected Topics in Power Electronics*, 8(4):4046–4059, 2020.
- [6] Murata Manufacturing Co. Ltd. ECASD40J107M015K00.
- [7] Murata Manufacturing Co. Ltd. LQH44NN471K03.
- [8] Yan Lu, Junmin Jiang, and Wing-Hung Ki. Design considerations of distributed and centralized switched-capacitor converters for power supply on-chip. *IEEE Journal of Emerging and Selected Topics in Power Electronics*, 6(2):515–525, 2018.
- [9] S. Oukassi, A. Bazin, C. Secouard, I. Chevalier, S. Poncet, S. Poulet, J-M. Boissel, F. Geffraye, J. Brun, and R. Salot. Millimeter scale thin film batteries for integrated high energy density storage. In *2019 IEEE International Electron Devices Meeting (IEDM)*, pages 26.1.1–26.1.4, December 2019.
- [10] Emeric Perez, Carlos Augusto Berlitz, Yasser Moursy, Bruno Allard, Sami Oukassi, and Gaël Pillonnet. Ultra-low frequency dc-dc converters using switched batteries. In *2022 IEEE Energy Conversion Congress and Exposition (ECCE)*, pages 1–7, 2022.
- [11] Gaël Pillonnet, Bruno Allard, Carlos Augusto Berlitz, and Sami Oukassi. Device for converting dc-dc based on batteries, October 13 2022. US Patent App. 17/704,596.



## BIBLIOGRAPHY

---

- [12] Michael D. Seeman and Seth R. Sanders. Analysis and optimization of switched-capacitor dc–dc converters. *IEEE Transactions on Power Electronics*, 23(2):841–851, 2008.
- [13] Michael Douglas Seeman. *A Design Methodology for Switched-Capacitor DC-DC Converters*. PhD thesis, EECS Department, University of California, Berkeley, May 2009.

## CHAPTER 3

# Experimental validation of SBC

The SBC described in Chapter 2 proposed a new family of topology specially interesting at an ultra-low operating frequency aiming to a potential solution to maintain high efficiency in cases of low power delivery. Such new topology have to be validated and tested experimentally.

For experimental validation of such topology, the first step is to evaluate different battery technology options with respect to SBC operating conditions. Next we incorporate it into a SBC working circuit and compare its performance against a traditional capacitor based converter under similar conditions.

## I Battery Options

Since a main characteristic of the SBC is to employ batteries as an intermediate energy storage device, choosing the appropriate battery for an SBC proof of concept is a key aspect of evaluating the system's viability.

In brief, batteries operate based on an electrochemical reaction that involves the movement of charged ions between electrodes and an electrolyte. The positive electrode (cathode) and negative electrode (anode) composition is the main feature defining batteries performance and characteristics. The electrolyte is a conductive medium that allows the transport of lithium ions between the anode and cathode, but despite its importance, is not as well referenced when choosing appropriate battery technology. As batteries are complex electrochemical devices, their selection process involves careful consideration of several factors such as battery chemistry, capacity, voltage range, energy density, charging and discharging characteristics, overall efficiency, among others.

Battery chemistry is a critical aspect when choosing a battery for an SBC. Different chemistries, such as lead-acid, lithium-ion, nickel-cadmium, and nickel-metal hydride, offer varying characteristics in terms of energy density, cycle life, self-discharge rates, and safety considerations. Thus, the choice of chemistry depends on factors such as desired energy storage capacity, aimed operating temperature and voltage range, cost-effectiveness, and required safety parameters.

Informed by battery chemistry some characteristics as capacity and voltage range are crucial factors to consider when selecting a battery for an SBC. The capacity determines the amount of energy that can be

stored and subsequently supplied to the load, while the voltage range should align with the SBC's input and output voltage requirements. It is essential to ensure that the battery capacity is sufficient to meet the energy demands and DoD of the system and that its voltage range is compatible with the converter's voltage specifications.

Another contributing factor is the charging and discharging characteristics of the battery, which significantly impact the performance of the SBC during  $\mu$ -cycle operation. These characteristics include charge acceptance rate, discharge rate capability, and efficiency during charge and discharge cycles (key aspect of switched application). An SBC should be able to efficiently charge the battery while avoiding overcharging or undercharging, which can degrade the battery life or compromise its performance.

Overall efficiency is another crucial consideration when choosing a battery for any power application. The battery's chemistry efficiency affects the energy conversion process within the SBC, as well as the overall system efficiency. Higher battery efficiency translates into better utilization of the stored energy and reduced losses during charge and discharge cycles, resulting in improved overall performance and extended battery life.

Fortunately, the demand for efficient and environmentally friendly energy storage systems has driven extensive research and development in the field of battery technology providing us with multiple choices.

### **a Nickel Metal Hydrate (NiMH)**

Nickel-Metal Hydrate (NiMH) batteries have emerged as a popular rechargeable battery technology in late 20<sup>th</sup> century due to their advantageous features and applications in various applications. Among the various types of rechargeable batteries, NiMH batteries have gained significant attention due to their favorable characteristics, including high energy density, relatively low cost, and reduced environmental impact compared to other battery chemistries at the time. Despite their reduced environmental impact, NiMH batteries remain liquid electrolyte batteries, posing environmental risks but also presenting other characteristics common to such batteries.

The cathode of a NiMH battery typically consists of a nickel oxyhydroxide (NiOOH) active material, while the anode comprises a hydrogen-absorbing alloy, usually based on rare earth metals. During discharge, the cathode releases hydroxyl ions (OH<sup>-</sup>) while the anode generates hydrogen ions (H<sup>+</sup>). These ions travel through the electrolyte, and the overall reaction produces electrical energy. During recharge, the reaction is reversed, and the battery stores energy.

Their constructions uses various components, including the positive and negative electrodes mentioned earlier, but also separators, electrolyte, and current collectors. The cathode is typically made of a pressed powder mixture of nickel hydroxide (Ni(OH)<sub>2</sub>), a conductive additive, and a binder. The negative electrode is composed of a hydrogen-absorbing alloy, which allows the storage of hydrogen ions during charging. Separators, usually made of microporous plastic films, are used to keep the electrodes apart while enabling the movement of ions. The electrolyte in NiMH batteries is typically a potassium hydroxide (KOH) solution. The current collectors, made of conductive materials such as nickel or stainless steel, facilitate the flow of electrons between the battery and the external circuit.

## I. BATTERY OPTIONS

Several performance characteristics define the capabilities and limitations of NiMH batteries. As shown in Fig. 3.1 NiMH batteries typically offer higher gravimetric energy and gravimetric power density than their predecessors, such as Nickel-Cadmium (NiCd) batteries. However, they present lower specific power when compared to some Lithium-ion (Li-ion) technologies. They also represent longer cycle life than previous technologies, contributing to their widespread application.

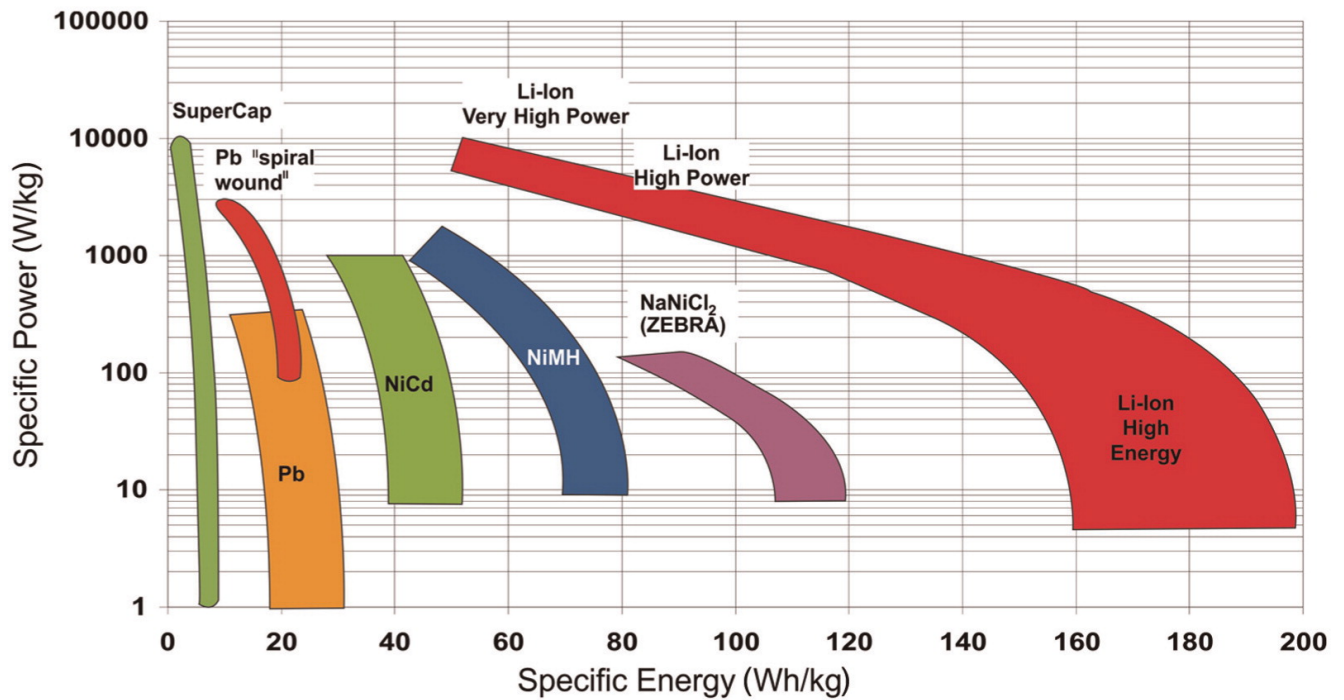


Figure 3.1 | Ragone plot of various rechargeable battery technologies [3]

NiMH batteries have a moderate self-discharge rate compared to some other rechargeable batteries. The self-discharge rate of NiMH batteries typically ranges from 1% to 3% per day, depending on factors such as temperature and state of charge, making them well suited for intermittent use. They also exhibit good performance at low temperatures opening new application possibilities.

Another important characteristic for a battery to be used in a SBC is its voltage characteristic. NiMH batteries have a nominal voltage of around 1.2 V per cell, which is lower than that of NiCd batteries, for instance. NiMH batteries can also deliver a relatively stable voltage throughout most of their discharge cycle, providing a consistent power supply to devices, and wider plateau for  $\mu$ -cycle operation. The voltage level is interesting for low power applications and modern microelectronic nodes. Ultimately, NiMH batteries can deliver high discharge currents, which is very well suited for DC-DC switched converter applications.

Despite their advantages, NiMH batteries also face certain limitations. One significant drawback is their lower energy density compared to Li-ion batteries, limiting their use in high-energy-demanding applications. NiMH batteries also suffer from a phenomenon called memory effect, which can reduce their usable capacity if not properly managed. Furthermore, their performance can degrade over time due

to factors such as self-discharge and electrode degradation, but this is a common future to commercial batteries. Overcharging or deep discharge can also lead to the loss of battery capacity and overall lifespan, but they tend to be avoided in SBC operation.

## **b Lithium Ion (Li-ion)**

Lithium-ion (Li-ion) batteries have revolutionized the world of portable electronics and are widely used in various applications, ranging from smartphones and laptops to electric vehicles and renewable energy storage systems. They offer a unique combination of high energy density, lightweight design, and rechargeable capabilities, making them a preferred choice for many modern applications.

Li-ion batteries operate based on the movement of lithium ions between two electrodes, typically made of a lithium-containing compound (such as lithium cobalt oxide ( $\text{LiCoO}_2$ ), lithium manganese oxide ( $\text{LiMn}_2\text{O}_4$ ), or lithium iron phosphate ( $\text{LiFePO}_4$ )) as cathode and a carbon material (regularly graphite) as anode, which also contains a conductive additive to enhance electron transfer. The electrolyte, is usually a liquid or gel-like substance containing a lithium salt, such as lithium hexafluorophosphate ( $\text{LiPF}_6$ ), dissolved in an organic solvent. It facilitates the ionic movement between the electrodes during charge and discharge cycles. [13]

One of the main characteristics for which Li-ion batteries are well known and adopted is that they offer one of the highest energy densities among rechargeable battery technologies [6]. Particularly for battery cells, this means that they can store a significant amount of energy relative to their size and weight. High energy density enables Li-ion batteries to power portable devices for longer durations, improving their usability and convenience.

However, in the context of DC-DC converters, an important aspect of Li-ion batteries is their high charge/discharge efficiency, typically ranging from 90% to 95%. [10] Allied to a low self-discharge rate of only about 1% to 2% per month [10], makes them an interesting option for intermittent usage.

For low-power switched DC-DC converters Li-ion battery cells present the inconvenience of having a high nominal voltage level (around 3.6 to 3.7 V). For step-down converters this high voltage level tends to limit applications, or implies an increase of converter and system complexity. However, it can be considered as a positive characteristic for overall energy and power density.

Despite some known advantages, Li-ion batteries are still well known for being sensitive to overcharging, overheating, and physical damage, which can lead to safety hazards such as thermal runaway and cell rupture. Although extensive research and development have improved the safety of Li-ion batteries, they are still hazardous material, and present a huge environmental risk, both in production as well as disposing. The extraction and processing of lithium and other materials used in Li-ion batteries have associated environmental impacts. Proper recycling and disposal methods are crucial to minimize the environmental footprint of Li-ion [16].

### c Solid-State Battery (SSB)

Solid-state batteries (SSBs) have emerged as a promising technology for next-generation energy storage systems, offering advantages such as improved safety, higher energy density, and longer cycle life [4]. These batteries utilize solid-state electrolytes instead of liquid electrolytes, which enables enhanced performance and opens up new possibilities for battery design and functionality.

One of the primary advantages of solid-state batteries is their enhanced safety profile, as different from liquid electrolyte batteries, SSBs employ solid electrolytes, which can be ceramic, polymer, or composite materials, to transport ions between the cathode and anode. The use of solid electrolytes highly reduce one of the main risks of liquid electrolyte batteries, the leakage and thermal runaway, thus enhancing the battery's safety [14]. Moreover, solid-state batteries can operate at higher temperatures, as solid-state electrolytes are inherently more stable and less prone to leakage or combustion, opening up opportunities for applications in electric vehicles (EVs), aerospace industry and grid storage systems [15]. The use of solid electrolytes also enables the integration of batteries upon silicon substrates as shown in Fig. 3.2 for Li/LiPON/Si<sub>1-x</sub>Ti<sub>x</sub> half-cell and Si<sub>1-x</sub>Ti<sub>x</sub>/LiPON/LiCoO<sub>2</sub> full-cell technologies, allowing greater power and energy density. [15]

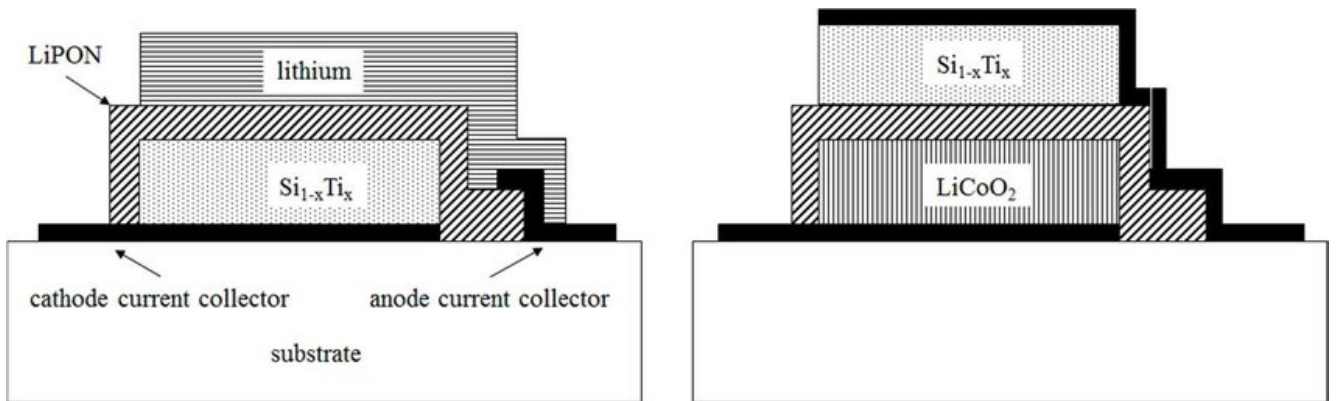


**Figure 3.2** | Structure of (a) Li/LiPON/Si<sub>1-x</sub>Ti<sub>x</sub> half-cell, (b) Si<sub>1-x</sub>Ti<sub>x</sub>/LiPON/LiCoO<sub>2</sub> full-cell. [15]

Solid electrolytes also have fewer side effects than their liquid counterparts, which leads to a longer life expectancy of solid-state batteries [9]. Such side effect and reactions also impact charging and discharging rates, and as SSBs exhibit improved kinetics and are less prone to side reactions, they can feature higher cycling performance. Higher charge and discharge rates translate into higher power density.

However, some challenges still remain in the development and commercialization of solid-state batteries. A particular one is the challenge to achieve high relative densities with current particle-based architectures, as they are limited by high interfacial resistances and the need to mix active material slurries with solid electrolyte particles and inactive particles for stability [6]. As mentioned in [4], such grains boundary remains one of the main limitation in solid state composite electrodes despite important recent progress [8].

All in all, despite the limitations of particle-based electrode designs, there are several promising new

architectures that show potential for SSBs such as thicker and denser electrodes exploring Li [6] or the advances of other materials. Considering the constant trend for portability and miniaturization of electronic devices while demanding increasingly high power, SSBs place themselves for increasing relevancy in the field [9].

Given these proposed battery electrochemical technologies, next Section explores the most suitable of them for initial SBC evaluation. Given the lack of appropriate models, such analysis is made experimentally.

## II Battery validation

In Chapter 2, it was demonstrated that batteries offer advantages over traditional passive devices in the Hertz range. However, the operation of batteries in the context of SBC systems involves a significantly different usage profile compared to traditional large DoD and State of Charge (SoC) scenarios, which has not been explored in previous research to the best of my knowledge. The lack of appropriate battery models to capture such conditions necessitates an experimental approach.

To evaluate this innovative battery usage, a Battery Under Test (BUT) was subjected to cycling in the range of microCoulombs ( $\mu\text{C}$ ) to milliCoulombs ( $\text{mC}$ ) at a timescale that mimics SBC operation mode. This unique usage profile involves a small charge/discharge displacement  $Q_E$ , which represents only a fraction of the battery capacity ( $\ll 1\%$  of SoC). This displacement occurs around a selected bias point on the voltage-capacity (V-Q) characteristic, as explained in more detail in Chapter 2.

To determine the optimal steady-state operating point of the battery, an impedance analysis was conducted using Electrochemical Impedance Spectroscopy (EIS) on different BUT samples. This small-signal analysis provides valuable insights into the impedance behavior of the battery under different operating conditions. However, to complement the findings from the small-signal analysis and validate the battery's performance under SBC operation conditions, a large-signal experimental validation is necessary. This involves subjecting a selected BUT to  $\mu$ -cycle conditions with higher output currents, replicating the actual operating conditions of the SBC.

### a Battery impedance

The SBC operates around a given SoC. Determining the potential impact of the initial SoC on SBC performance and identify the optimal SoC value, is crucial to evaluate the viability of the battery as a passive device in DC-DC converters. The internal impedance of the battery plays a significant role in power density and efficiency, making it a valuable benchmark for assessing the influence of the SoC value. To obtain insights into this, Electrochemical Impedance Spectroscopy (EIS) was employed to analyze the internal impedance profile of the battery at different SoC levels.

To evaluate the potential of commercially available off-the-shelf batteries, a NiMH battery with a nominal voltage of 1.2 V is selected as the battery model. Fig. 3.3 illustrates the general behavior of the internal resistance with respect to different SoC values. The internal resistance increases near the extremes of SoC, indicating two distinct phenomena. As the battery approaches full discharge (SoC of

0%), the lack of available ions for discharge leads to increased impedance. Similarly, when the battery is nearly fully charged (SoC of 100%), the majority of intercalation sites are already filled, resulting in higher internal resistance.

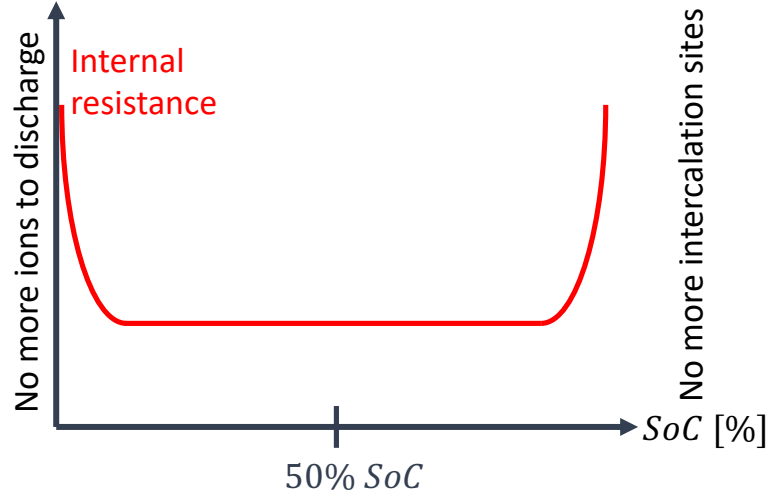


Figure 3.3 | Battery internal resistance pattern by SoC.

Further experimentation focuses on a commercially available NiMH battery model called V6HR, which has a volume of  $74 \text{ mm}^3$ . This battery falls within the power range required for the system and has a nominal voltage of  $1.2 \text{ V}$  ( $V_{bat}$ ). It is a single-cell NiMH battery with a nominal capacity of  $6 \text{ mAh}$ . The manufacturer specifies a DC current limit ( $I_{lim}$ ) at  $3C$ , equivalent to  $18 \text{ mA}$ , and provides a DC resistance ( $R_{int}$ ) value of  $6 \Omega$ . Choosing this battery aligns with the initial requirement of delivering power in the milliwatt range.

Considering that the power density of the SBC is inherently limited by the impedance of the battery, it is crucial to evaluate the impact of SoC on the battery's impedance. To achieve this, a small-signal impedance  $Z_{bat}$  is experimentally obtained through EIS around the 50% SoC point. The 50% SoC is chosen because it exhibits minimal internal resistance, as shown in Fig. 3.3. However, it should be noted that 50% SoC is not an absolute value but a practical selection.

Fig. 3.4 presents the experimental impedance results for the V6HR battery around the 50% SoC. At frequencies below the kHz range, the real part of the impedance dominates and is approximately equal to the DC resistance of the battery. The magnitude of the impedance varies around  $6 \Omega$ , with only a factor of 3 over over four decades of frequency. The battery can be utilized up to tens of kHz, with a resonance frequency around a hundred kHz. As an initial approximation, the maximum achievable battery output power  $P_{max}$  is limited to  $V_{bat}^2/4Z_{bat}$ , resulting in  $60 \text{ mW}$ .

The phase is almost constant throughout the studied frequency span, with an increase at high frequencies. At low frequencies the battery presents the mass transport phenomena, when the ions are the ones transporting charge, at high enough frequencies this transport is limited and we enter in a regimen of charge-transfer [7]. However, at high enough frequencies the battery behavior is somewhat



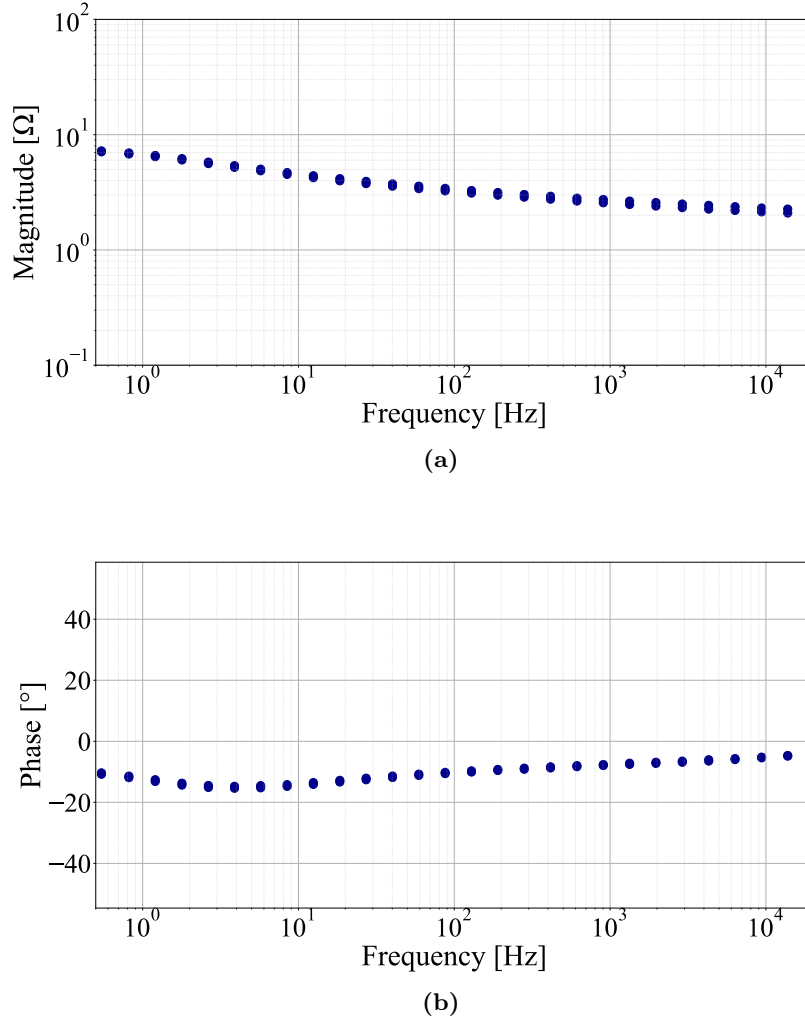


**Figure 3.4** | V6HR experimental impedance around 50% SoC (a) magnitude and (b) phase

altered (in an small-signal analysis), and it starts presenting an impedance similar to an inductance (with phase higher than  $0^\circ$ ). However, it is important to note that small-signal analysis does not consider various electrochemical limitations, as it involves currents much lower than 1 CA. The quasi-static current limit ( $I_{lim}$ ) is determined by the electrochemical stability potential window of the battery electrolyte, constraining the maximum output power level under full charging/discharging conditions. In practice, a better prediction for the achievable quasi-static battery power would be given by  $V_{bat} \times I_{lim}$ , which in this case is 22 mW, lower than the calculated  $P_{max}$ . The power indicated for the battery in Chapter 2 is slightly higher as it corresponds to the tested power under  $\mu$ -cycle conditions. With the power delivery capabilities of the battery being limited primarily by the  $I_{lim}$  instead of the internal resistance, it became one of the major features for selecting an appropriate battery. However, it is important to note that the  $I_{lim}$  provided by manufacturers often considers a constant DC current, which diverges from the  $\mu$ -cycle

behavior and can change the effective  $I_{lim}$ .

In addition to the previously mentioned factors, it is essential to consider that the battery impedance is not only influenced by the state of charge and voltage but also by the current level during operation. At higher operating currents, exceeding 1 CA, the rate of ion transfer becomes limited, resulting in changes in the battery's impedance and overall performance.

To comprehensively understand and validate the behavior of the battery during  $\mu$ -cycle operation, both small-signal and large-signal analyses are necessary. While small-signal analysis provides insights into the battery's response to small perturbations around the bias point, it does not fully represent the battery's behavior under the operating conditions of the SBC, particularly when the battery is subjected to high currents and stronger charge/discharge  $\mu$ -cycles.

### b Battery in a $\mu$ -cycle

The large signal validation plays a crucial role in closely resembling the operation of  $\mu$ -cycles. This experimental validation is performed on the BUT described earlier, specifically the V6HR model. To ensure accurate results, the battery is preemptively charged to a bias point  $Q_{DC}$  set at SoC of 50% of its total capacity as shown in Fig. 3.5a. To obtain the particular battery voltage profile as a function of SoC a couple of charge and discharge cycles are performed prior. Such cycles are long (around 10 hours of a charge cycle and 10 hours of discharge), using currents on the order of 0.1 CA.

As detailed earlier, the specific SoC of 50% of its total capacity is chosen strategically to avoid operating near the extremes of charge and discharge, which typically exhibit higher internal impedance and steeper V-Q slopes. At SoC of 50% we can expect close to minimal resistance and V-Q slope, contributing to the battery performance and an efficient operation with lower risks.

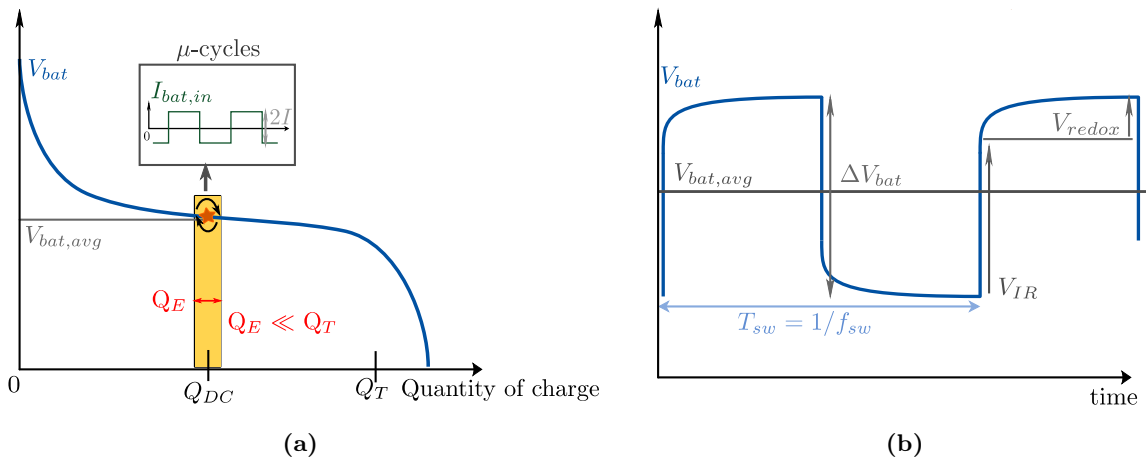


**Figure 3.5** | (a) Battery V-Q characteristic under  $\mu$ -cycle (b) Schematic battery voltage response to microcycles.

To characterize the large-signal behavior of the battery, a rectangular current waveform is applied by the potentiostat to the BUT. This waveform has an amplitude  $I_{bat,in}$  in the milliamperere range and a

frequency  $f_{sw}$  in the Hertz range. Importantly, the waveform has a zero mean value to accurately replicate the  $\mu$ -cycle operation of the SBC. Fig. 3.5a provides a detailed representation of the SBC  $\mu$ -cycle operation, while Fig. 3.5b displays the resulting voltage response obtained during the experimental study.

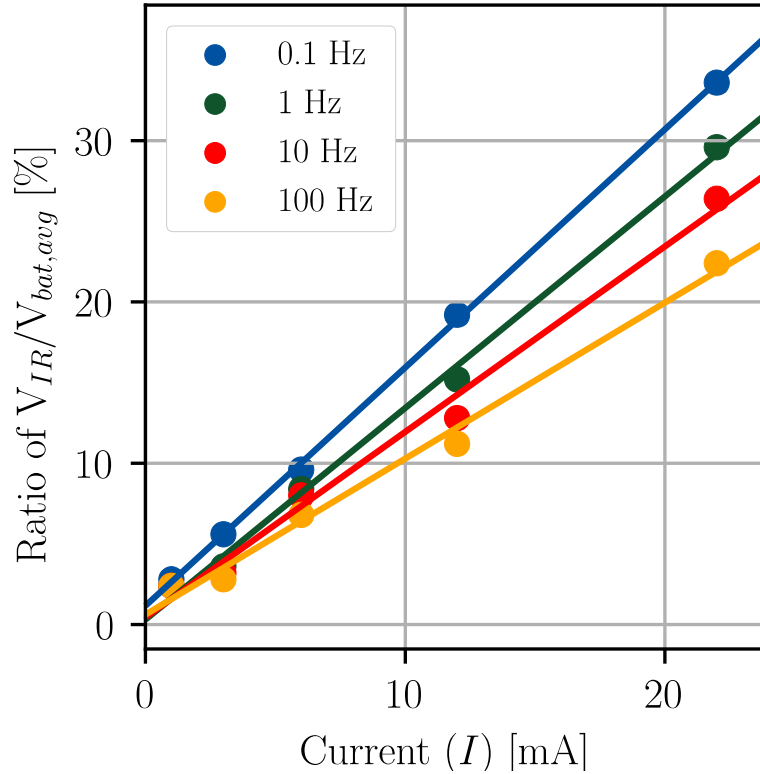


**Figure 3.6** | IR drop voltage relation to output current. [11]

Analyzing the response of the BUT shown in Fig. 3.5b, two major voltage components that represent the large-signal behavior of the battery can be identified, as introduced in [11]:

1. the ohmic IR drop  $V_{IR}$  is an almost instantaneous voltage drop due to the BUT internal resistance
2. the redox voltage  $V_{redox}$  is caused by the redox reactions due to the  $\mu$ -cycling

The first component ( $V_{IR}$ ), as expected, exhibits a linear correlation with the applied current, as depicted in Fig. 3.6. The slope of the plot in Fig. 3.6 provides valuable information about the resistance of the battery under the specific operating conditions of the  $\mu$ -cycle. The resistance extracted from the slope, denoted as  $R_{\mu c}$ , is found to be approximately  $7 \Omega$ , with a tolerance of  $\pm 15\%$  over three decades of frequency. It is worth noting that  $R_{\mu c}$  may slightly deviate from the previously determined small-signal impedance ( $R_{int}$ ), underscoring the importance of conducting large-signal characterization to obtain a comprehensive understanding of the battery's behavior in SBC operating conditions.

During the analysis of the large-signal validation, a slight frequency dependence is observed in the IR drop, which aligns with the findings from the previous small-signal analysis shown in Fig. 3.4. This frequency dependence suggests that the IR drop is influenced by certain chemical mechanisms within

## II. BATTERY VALIDATION

the battery. Additionally, the redox voltage exhibits a logarithmic frequency relationship, indicating the superposition of two distinct chemical processes, as detailed in [1]:

1. a ion diffusion phenomenon, which is described by a function of the square root of time.
2. a charge transfer process, corresponding to a small displacement on the V-Q characteristic.

Furthermore, it is observed that the redox voltage shows a nearly linear relationship with current ( $R^2=0.99$  at 10 Hz), as depicted in Fig. 3.7. In summary, the ionic voltage decreases with increasing frequency, while both the redox voltage and IR drop increase with higher current levels.

Another interesting observation is that the battery's average voltage ( $V_{bat,avg}$ ) under the rectangular current waveform input closely approximates the open-circuit relaxed potential (OCRV) in steady-state conditions. This value remains consistent regardless of the current level or the frequency of the waveform, as illustrated in Fig. 3.8. This finding represents a novel result in the study of battery behavior. Furthermore,  $V_{bat,avg}$  demonstrates remarkable stability over  $10^7$   $\mu$ -cycles while operating at the battery's current limit under the rectangular current waveform. This indicates an extended cycle life for batteries subjected to  $\mu$ -cycles compared to the typical cycle life of NiMH batteries rated by the manufacturer (approximately  $10^3$  cycles of full charge and discharge), as reported in [5]. With the findings that the battery can handle a  $\mu$ -cycle regimen as required by the SBC, next Section the battery is inserted into a proper converter structure. The SBC performance is then compared to the performance of a classic SCC circuit.

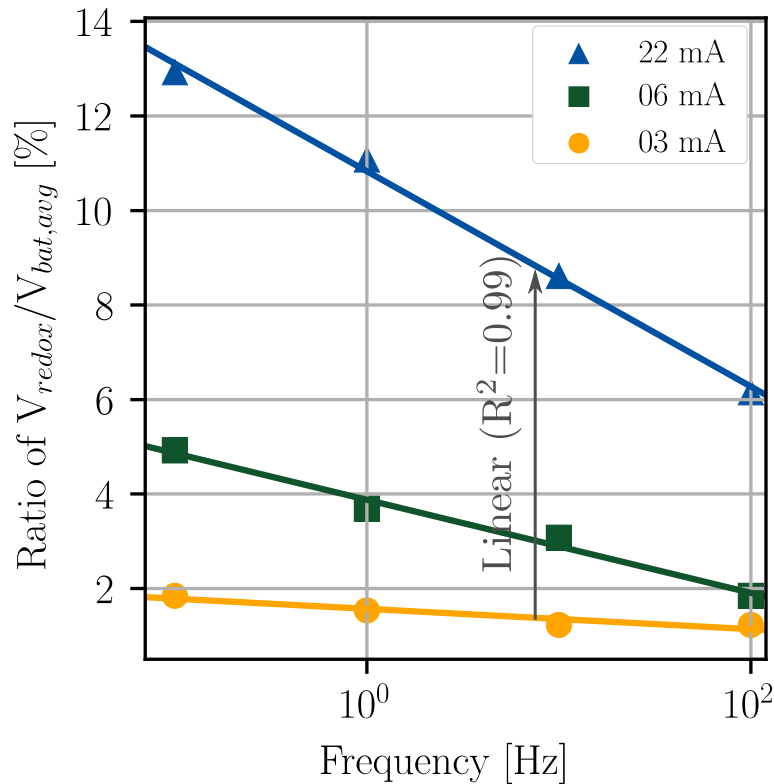


**Figure 3.7** | Ionic voltage component related to frequency. [11]

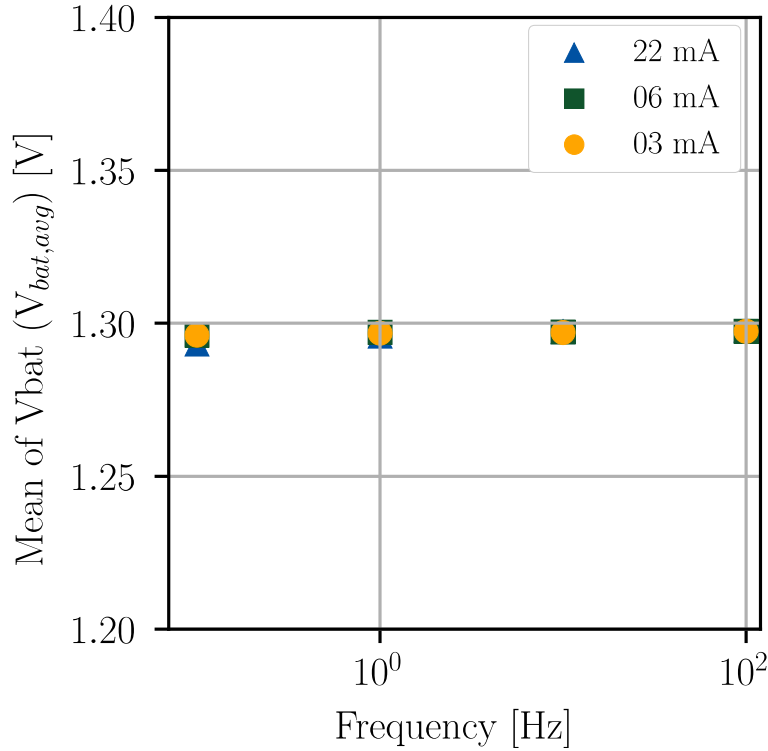


Figure 3.8 | Mean voltage value of the battery (relaxed). [11]

### III SBC performance

To evaluate the performance of the SBC, it is compared to a SCC using the same power stage circuit, shown in Fig. 3.9a, at the same output power levels and operating frequencies. For fairness of comparison, BUT and capacitor are off-the-shelf components featuring similar dimensions both in surface and volume. A high capacitance (for the dimensions) with suitable voltage rating capacitor is chosen. The SBC is shown in Fig. 3.9b and is implemented using a commercial switched-capacitor voltage converter integrated circuit (LM2663).

The circuit implements a 2:1 topology that operates in two phases. In phase  $\phi_1$ , the input voltage source  $V_{in}$  supplies charges ( $Q_{\phi_1}$ ) to the flying passive device, which is the battery for the SBC configuration and the capacitor for the SCC configuration. In phase  $\phi_2$ , the flying passive device is directly connected to the output, delivering the charge  $Q_{\phi_2}$ .

The off-the-shelf IC LM2663 features an internal oscillator with an adjustable frequency, which can be externally controlled using a network of capacitors. The footprint of the IC is approximately  $19 \text{ mm}^2$ , which is equivalent to the dimensions of the BUT and the flying capacitor used in the experiment. Table 3.1 shows the equivalent capacitance in the capacitor network for tuning the LM2663 switching frequency.

For the experimental setup, the BUT chosen is the NiMH device known as V6HR, described in detail previously. The NiMH battery offers an open circuit voltage of  $1.2 \text{ V} \pm 10\%$ , which is suitable for the implemented 2:1 topology that converts the input voltage  $V_{in}$  of  $2.6 \text{ V}$  to an output voltage  $V_{out}$  of  $1.3 \text{ V}$ .

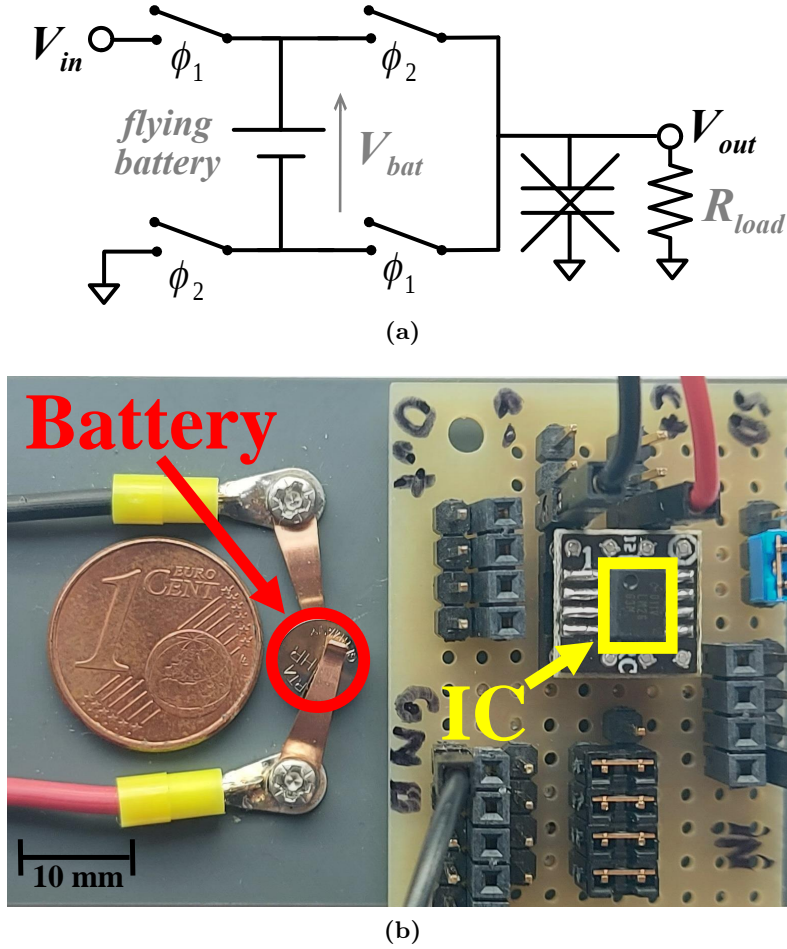


**Figure 3.9** | (a) 2:1 converter power stage electrical schematic and (b) implementation of 2:1 SBC using LM2663 and V6HR

The flying capacitor used in the experiment is a 100  $\mu\text{F}$  polymer aluminum electrolytic capacitor (ECASD40J107M015K00). This capacitor has a volume of 60  $\text{mm}^3$  (surface of 31.4  $\text{mm}^2$ ) and is rated for 6.3 V. It exhibits an ESR of 0.015  $\text{m}\Omega$ , much lower than the ohm scale internal resistance presented by the battery.

The equivalent output resistance of the SBC, calculated using equation (2.7), is 6.4  $\Omega$ . As discussed in Chapter 2, this value is independent of the switching frequency at first order but is significantly influenced by the internal resistance of the battery, which contributes approximately 90% to the total equivalent output resistance.

To compare the performance of the converters, various operating frequencies spanning multiple orders of magnitude and output currents ranging from 100  $\mu\text{A}$  to 30 mA are examined. These current values correspond to 1/6 CA up to 5 CA, representing a range within its regular operating limits. As the goal is to focus on low-power applications, despite the studied operating frequencies spanning through different orders of magnitude, they remain on the low end for switched DC-DC converters. Such conditions are not ideal for the SCC and might be considered unfavorable to optimal performance for this family of

**TABLE 3.1** | CAPACITOR NETWORK VALUE FOR OPERATION OF LM2663

Frequency [Hz]	10	100	1k	10k
Capacitance [nF]	405	22.5	3.5	0.4

topologies.

### a Steady-State Operation

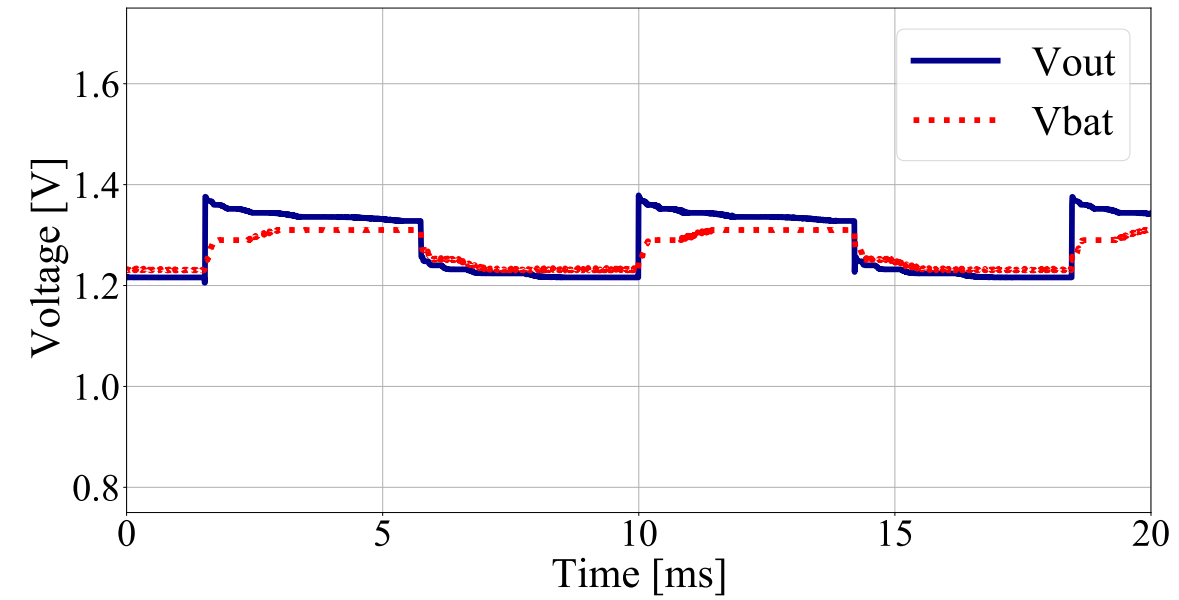
A typical operation curve of the 2:1 SBC configuration (without output capacitance) in steady-state 2:1 is shown in Fig. 3.10a. The output voltage  $V_{out}$  presents a similar behavior during both phases,  $\phi_1$  and  $\phi_2$ , with a small difference in average value between the two phases.

During phase  $\phi_1$ , the output voltage  $V_{out}$  results from the voltage difference between the input voltage  $V_{in}$  and the battery voltage  $V_{bat}$ . On the other hand, during phase  $\phi_2$ , the battery is directly connected to the output, leading to a direct transfer of its voltage to  $V_{out}$ . This difference in behavior between the two phases is evident in the plot of  $V_{bat}$  over one cycle, shown in Fig. 3.10b. It closely resembles the signal shown in Fig. 3.5b, validating the the large signal  $\mu$ -cycle experiment presented in Section b, which mimicks the SBC steady-state operation.

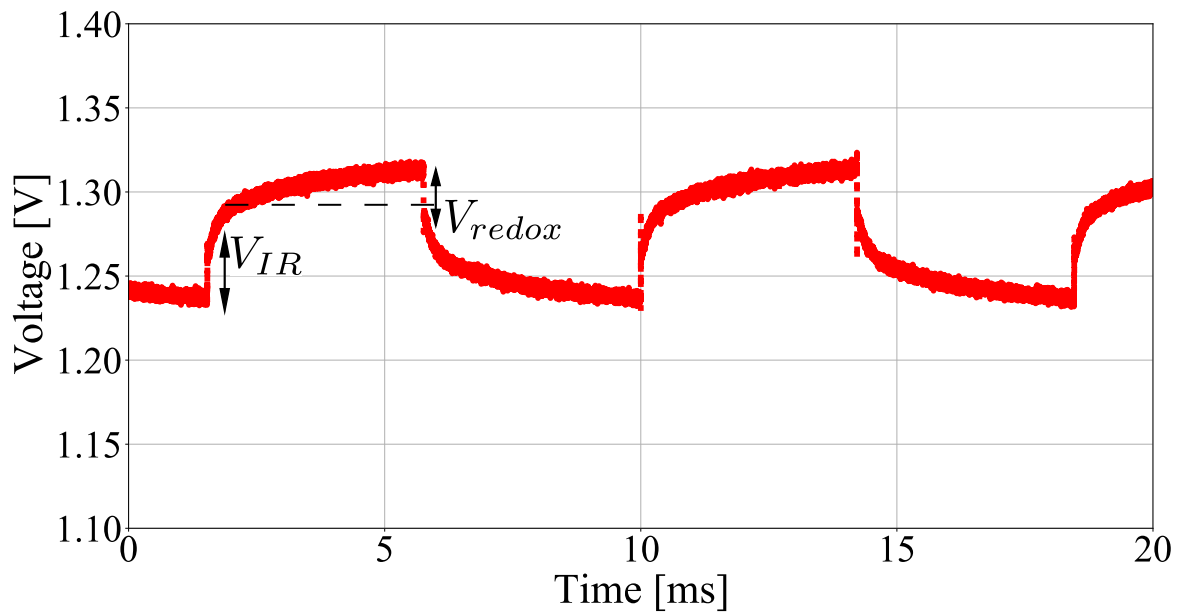
The behavior of  $V_{bat}$  during a cycle highlights the presence of two types of ripple, as introduced in [11] and described in the previous section. Fig. 3.10b exhibits the characteristic pattern observed in  $V_{bat}$ , consistent with the findings from Figure 3.5b. The plot shows an almost instantaneous ohmic voltage drop, referred to as  $V_{IR}$ , which arises due to the internal resistance of the battery (BUT). Alongside the ohmic IR drop, there is another voltage component termed  $V_{redox}$ , attributed to redox reactions occurring during  $\mu$ -cycling [11]. This  $V_{redox}$  is associated with the slow variation in battery voltage and contributes to the particular form of the output voltage ripple.

Such waveform behavior is distinct from the SCC steady-state operation, despite also presenting the similar symmetry between  $\phi_1$  and  $\phi_2$ . The ripple on the battery's terminals is low and highly independent of the operating frequency, limiting charge-sharing losses. On the other hand, for the SCC the ripple waveform presents the characteristic RC curve, reaching even linear behavior for appropriate conditions. Such behavior is highly dependant of the operating frequency, making charge-sharing losses invariably dominant at low operating frequency.

The presence of  $V_{IR}$  and  $V_{redox}$  components during steady-state operation provides valuable insights into the behavior of the SBC configuration. Understanding the variations in  $V_{bat}$  during the different phases can provide insights not only for optimizing the converter's performance and efficiency but also for optimization of batteries for SBC operation.



(a)



(b)

**Figure 3.10** | Experimental steady-state operation of the 2:1 SBC at 100 Hz: (a) output and battery voltages and (b) battery voltage ripple



## b Output Voltage Ripple

In most applications of DC-DC converters, a large output voltage ripple ( $\gg 5\%$ ) is considered unacceptable [2], making it a crucial performance benchmark. In the case of SCCs, besides the output capacitance value, the output voltage ripple is significantly affected by the operating frequency, especially for a given passive component size. Therefore, it is essential to ensure for the SBC to maintain an acceptable output voltage ripple, as it not only operates at low and ultra-low frequencies but also does not require an output capacitor.

Fig. 3.11 illustrates the relative output voltage ripple with respect to the output current for both the SBC and SCC at frequencies of 0.1 kHz and 10 kHz. The SBC, operating without any output capacitance, demonstrates an output voltage ripple of less than 5% even at a frequency as low as 100 Hz while delivering 20 mA to the load. In contrast, the SCC, lacking an output capacitor for fair comparison (keeping same volume), experiences an output voltage ripple that reaches over 30% under similar conditions requiring to use an output capacitor to reduce the ripple to a comparable level. For the same 20 mA output current, with a bulky 5.0 F output capacitor (PHV-5R4H505-R, being around 100x bigger than the flying capacitor), the SCC presents a bit over 3% of output voltage ripple at 100 Hz. The SBC offers relative ripple under 9% even for output currents over 30 mA and operating at 100 Hz without the need for any output capacitance. The SCC presents high ripple for low current at 10 kHz due to a resonance phenomena.

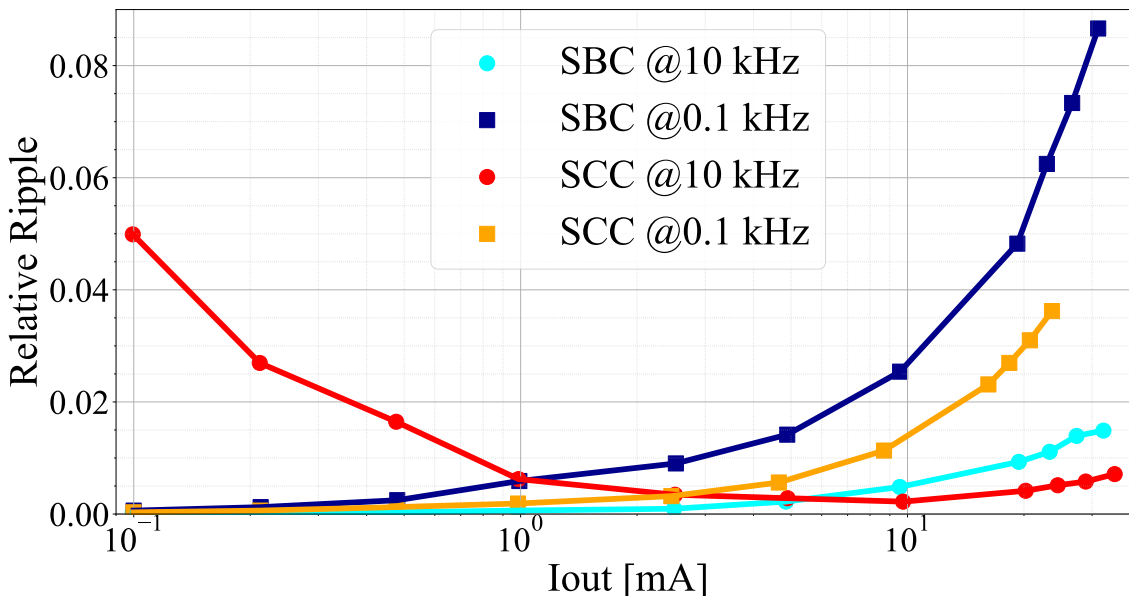


Figure 3.11 | Comparison of relative output voltage ripple between 2:1 SBC and 2:1 SCC

The significant difference in output voltage ripple between the SBC and SCC at low frequencies can be attributed to the fundamental principles of their respective constructions. In the SCC, the voltage across the terminals of the capacitor is directly dependent on the stored charge according to the relationship

$Q = CV$ . As a result, the output voltage ripple in the SCC arises from variations in the charge stored in the capacitor.

On the other hand, the SBC does not rely on the direct dependence of the voltage between the battery terminals on the transferred charge, as explained earlier. Even without the presence of an output capacitor, the SBC exhibits lower output voltage ripple at low operating frequencies, leading to reduced losses. This lower ripple can be attributed to the battery's higher electrical inertia compared to that of a capacitor. The slow variation in battery voltage is associated with the effect of  $V_{redox}$ , as observed in Fig. 3.10b.

The SBC is even capable of presenting acceptable levels of relative output voltage ripple ( $\sim 12\%$  at 25 mW) when working at unconventional ultra-low frequencies (0.1 Hz to 10 Hz) as demonstrated in [11]. The reduced output voltage ripple in the SBC, even without an output capacitor, enhances its suitability for applications where low ripple is a critical requirement. The SBC's ability to maintain a stable output voltage with acceptable ripple even without output capacitance contributes to improved efficiency and performance in power conversion systems.

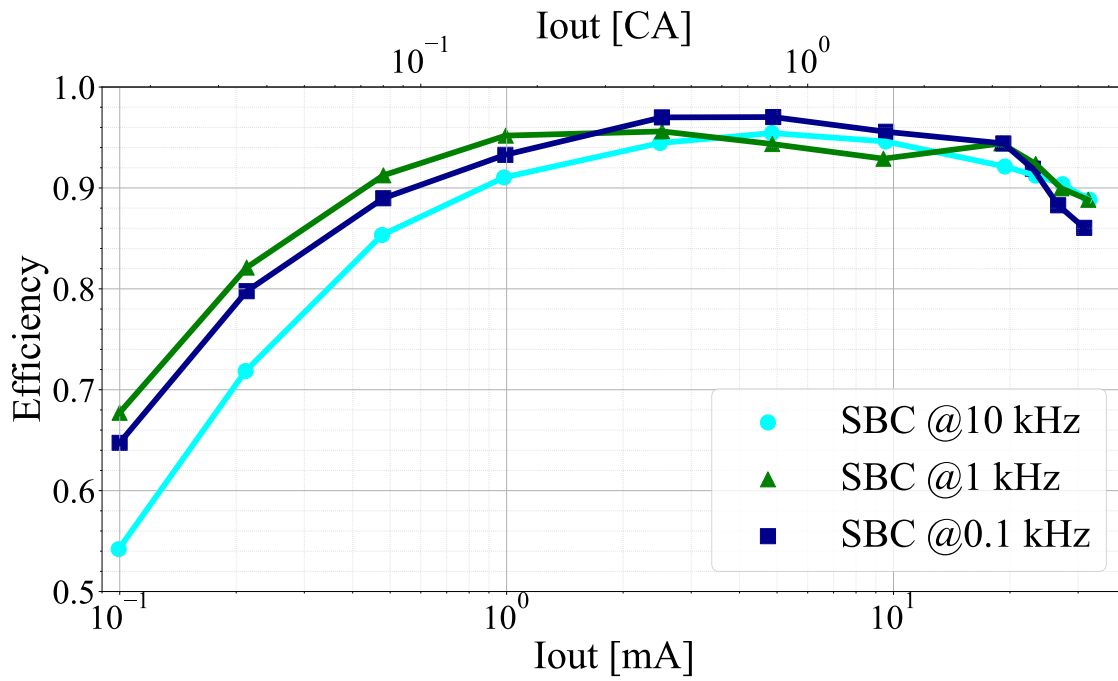
### c Power Efficiency

The efficiency of the SBC is evaluated at various frequencies and different current amplitudes, as shown in Fig. 3.12a. As discussed in Chapter 2, the conduction losses and overall efficiency of the SBC are largely independent of the switching frequency. However, a small difference can be observed for low output currents, primarily due to the quiescent current of the active circuit itself, which ranges from 30  $\mu\text{A}$  to 50  $\mu\text{A}$ .

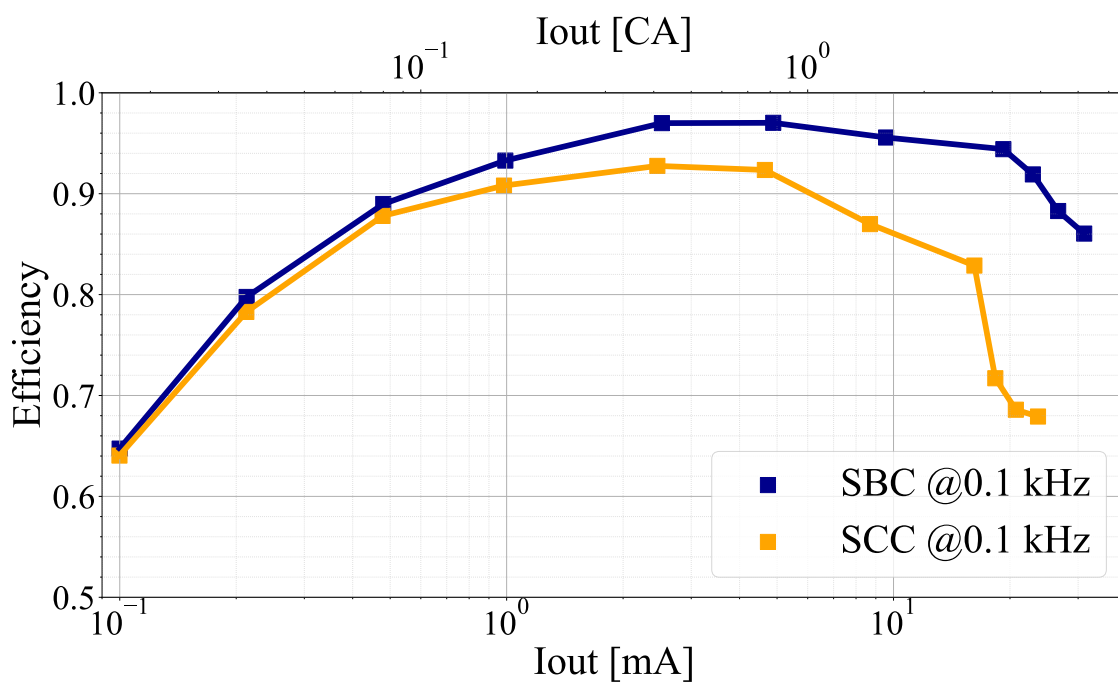
As the whole circuit is powered by  $V_{in}$ , the input power includes the control of the switches, the oscillator and overall quiescent consumption of the off-the-shelf IC.

Fig. 3.12b illustrates the performance difference between the SBC with the SCC at a frequency of 100 Hz. Comparing both configurations, the SBC, which operates without an output capacitor, exhibits better efficiency than the SCC, which utilizes a large output decoupling capacitor (100x bigger than the flying capacitor). This advantage of the SBC is particularly noticeable at low operating frequencies, where the SCC operates close to SSL, thus experiencing significant losses related to charge sharing and other factors traditionally associated with a slow switching capacitor regimen. In contrast, the SBC does not feature such losses as charge-sharing and can allow drastic reduction on driving losses due to the charge and discharge of MOSFETs' gates on future implementations.

The efficiency of the SBC is significantly influenced by the internal resistance of the battery. Although the battery's internal resistance is significantly higher than the ESR of the capacitor used in the SCC, it remains less significant in terms of overall losses compared to the switched-capacitor regime of the SCC at low frequencies. There is always a frequency low enough for the SBC to present competitive performance. The objective here is to quantify it for a particular exemple.



(a)



(b)

**Figure 3.12** | Experimental efficiency of the 2:1 SBC (without output capacitance): (a) independence of frequency and (b) advantage against SCC at 100 Hz with output capacitance

The efficiency gain of the SBC over the SCC is more pronounced at higher output currents (still in low power range), especially at moderate and low frequencies when operating without an output capacitor. At high frequencies, the equivalent output resistance of the SCC is dominated by the FSL effects, aligning with the analysis presented in Chapter 2 and presenting similar losses and performance tendencies as the SBC.

The SBC configuration demonstrates high efficiency, exceeding 90%, across a respectable range of output currents, reaching up to 20 mA (more than 3 CA for the V6HR). The SBC can maintain this high efficiency while delivering a maximum output power of approximately 27 mW at 100 Hz and 32 mW at 1 kHz and 10 kHz. A rough estimation indicates a power volume density of approximately 364  $\mu\text{W}/\text{mm}^3$  at 100 Hz and 432  $\mu\text{W}/\text{mm}^3$  at 1 kHz and 10 kHz, calculated based solely on battery volume.

The high efficiency and power density of the SBC make it a promising solution for low-power applications, where maximizing efficiency and conserving space are critical factors.

#### d Battery Voltage Self-Adjustment

The Battery Voltage Self-Adjustment (BVSA) process in the SBC allows the battery voltage to adapt and converge towards the steady-state value dictated by the topology. Different than regular battery usage, where it imposes the voltage value on the circuit, during SBC operation the topology imposes the voltage value on the battery, such as in the 2:1 configuration where  $V_{bat} = V_{in}/2$ . This BVSA behavior is similar to how capacitors adjust their voltage in a SCC, highlighting the battery/capacitor behavior during  $\mu$ -cycle operation. It is important to note that this self-adjustment seems to not pose risks to the battery's lifespan as long as the voltage remains within the battery's allowable limits for charging and discharging.

As the BVSA causes the battery voltage to converge towards the steady-state value imposed by the SBC topology, the battery voltage gradually approaches such steady-state value, resulting in a constant average output voltage. However, during the convergence time there may be some initial ripple in the battery and output voltage as the convergence occurs. This ripple diminishes as the BVSA process progresses and eventually reaches a minimum point. This mechanism demonstrates that the battery functions as a steady voltage provider in the short term while exhibiting adjustable voltage characteristics, akin to a capacitor, over longer periods.

The efficiency of the SBC during such power-on dynamic can be influenced by the BVSA process, depending on the initial voltage of the battery. If the battery's initial voltage is higher than the required steady-state value, the efficiency will start at a high value and gradually decrease until it reaches the steady-state. Conversely, if the battery's initial voltage is lower than the required steady-state value, the efficiency will start lower and gradually increase until it reaches the steady-state. However, it still offers a mechanism for the battery voltage to self-adjust to the conditions demanded by the circuit in which it is inserted, which to the best of my knowledge has not been investigated in the literature so far.

The large electric inertia of batteries results in longer settling times to reach a steady-state voltage. Empirical observation shows that the settling time for BVSA is independent of operating frequency in the 2:1 topology, however, it is not independent of output current. As shown in Fig. 3.13, the output current

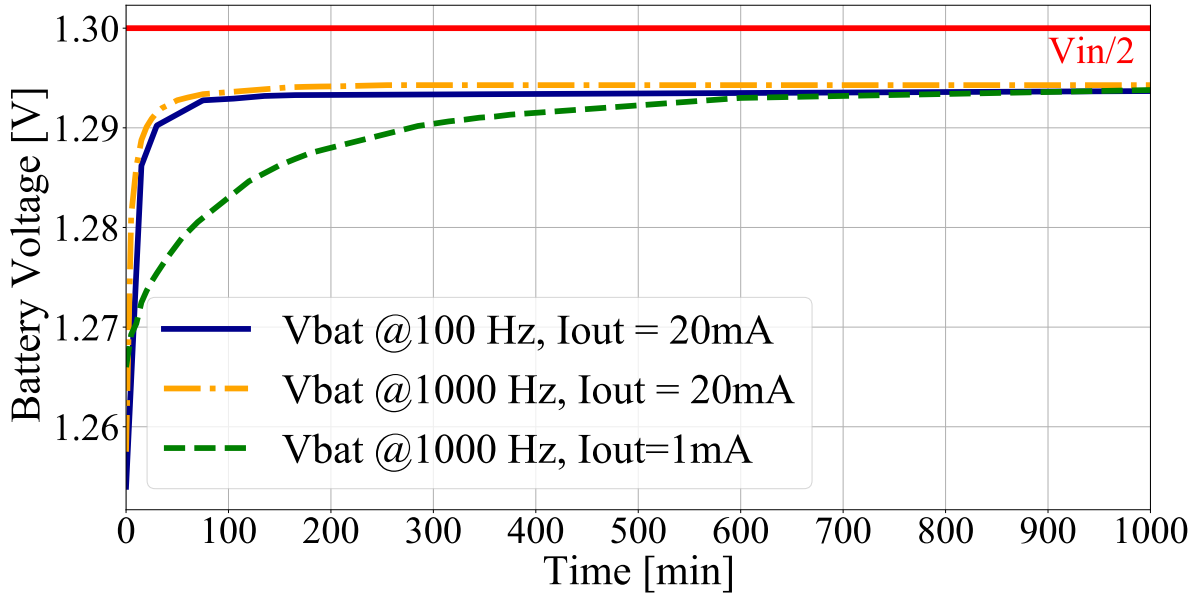


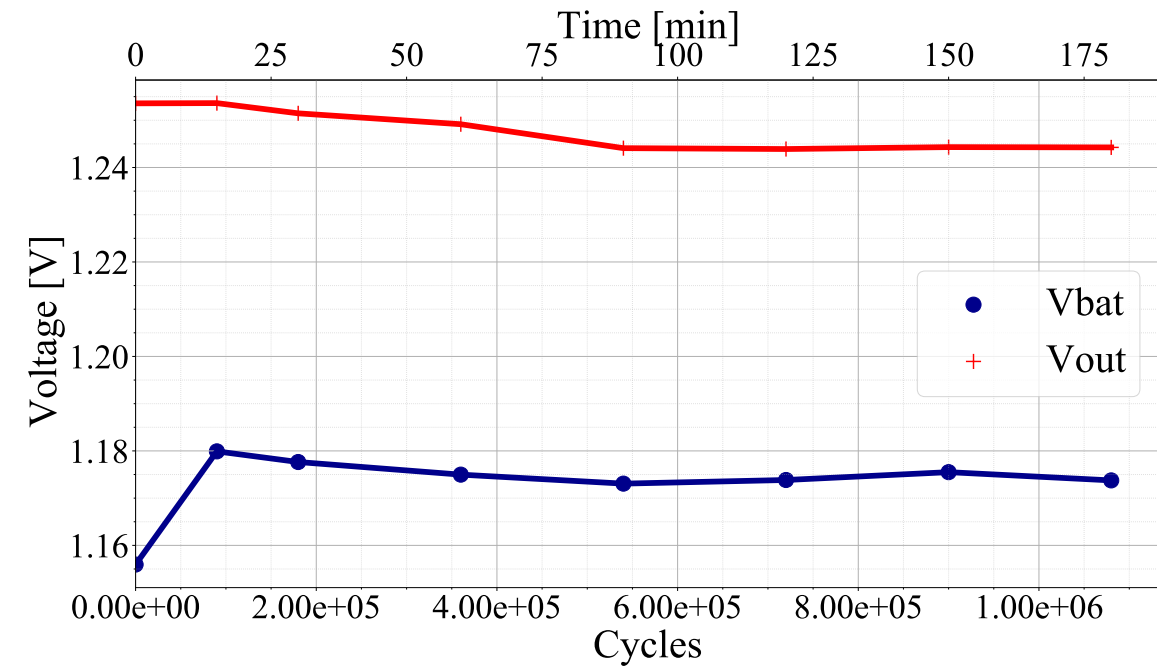
**Figure 3.13** | Impact of frequency and current on the battery voltage evolution during power-on dynamics in the 2:1 SBC

does impact the transient behavior of the output voltage during the power-on dynamic, while frequency impact is negligible. For instance, at an output current of 20 mA, it takes over 85 minutes (500 thousand cycles) to reach the steady-state voltage at 100 Hz, while it takes approximately half that time at 1000 Hz, which is ten times the frequency. The initial voltage of the battery at both frequencies is similar, around 1.254 V at 100 Hz and 1.257 V at 1000 Hz. At a fixed frequency (1000 Hz), the current and transferred charge play crucial roles in the evolution of the output and battery voltage. For example, at 20 mA, the battery voltage increases by approximately 24 mV in around 5 minutes (300 thousand cycles), whereas at 1 mA, it takes about 50 minutes (3 million cycles) to achieve a gain of 13 mV, 10 times slower for half the voltage increase, at 0.5% of the current. These observations correspond to the exponential phase of the voltage increase starting at similar voltages.

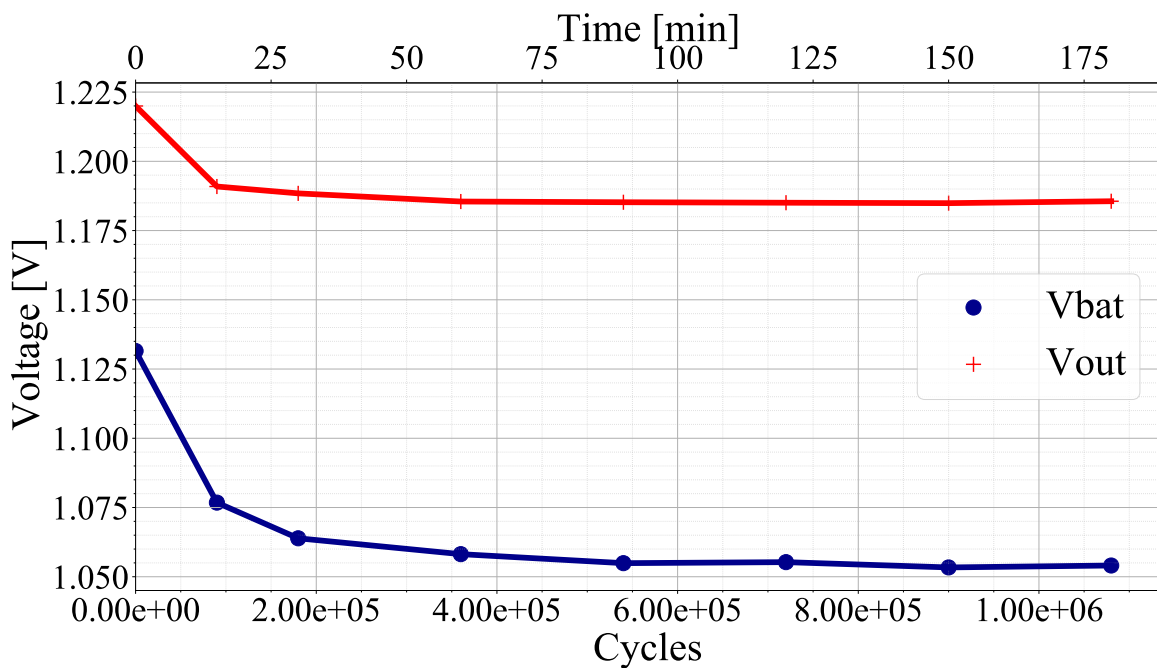
The BVSA allows the battery to self-adapt to conditions imposed by the SBC topology, widening the use cases of the topology family. The independence to frequency is interesting to ensure that even at low frequency (the target operation for the SBC) it features the same behavior and expected BVSA transient.

### e Charge Balance

Battery charge balance is a crucial aspect of the SBC operation, as the battery must receive the same amount of charge that it supplies to the load. As here the battery is not used as energy storage device, rather as an intermediate energy storage.



(a)



(b)

Figure 3.14 | Steady-state operation with duty cycle asymmetry of (a) 45-55 and (b) 40-60

However, achieving perfect charge balance over each complete cycle is not always possible, especially in symmetrical cycles (where each phase has the same duration). Even with a slightly duty-cycle imbalance, despite  $\mu$ -cycle operation, due to the operating frequency, the battery could be discharged or overcharged after few hours/days. Despite this, experimental data has shown that even with imbalances on duty cycles the SBC is able to achieve steady-state operation. This is due to the self-balancing behavior of the battery, which adjusts its voltage to reach the required charge balance.

In steady-state operation, the voltage of the flying batteries changes towards the steady-state operation voltage value imposed by the topology. This behavior presents no risk to battery life as long as the value is still inside the battery's voltage limits for charge and discharge. In Fig. 3.14a we see the circuit reaching a steady-state operation with an asymmetry of 45-55, meaning that  $\phi_1$  has 45% of the duration of the cycle, while  $\phi_2$  has 55%. The circuit stabilizes with  $V_{out}$  at a voltage value roughly 90% of the one in a symmetrical duty-cycle. Accordingly, an asymmetry of 40-60 reaches steady-state operation with  $V_{out}$  at a voltage value roughly 80% as shown in Fig. 3.14b. Smaller values of asymmetry (or small imbalances on a symmetrical) duty-cycle have negligible impact on the steady-state voltage values of the SBC, and continue to operate during long ranges of time. Furthermore, comparison of relaxed open circuit voltage of battery before and after long SBC operations show no significant change, indicating no change of the battery's SoC.

## f Lifetime

While battery lifetime is a significant concern in DC-DC converters, with typical lifespans ranging from  $10^3$  to  $10^4$  fully charge/discharge cycles, the battery used in the SBC configuration experiences a significantly higher number of cycles due to its Hz-range operation. Even at a conservative frequency of 1 Hz, the battery would need to support nearly one billion cycles over a 10-year period. However, it is important to note that the SBC introduces a unique scenario compared to conventional battery usage. It operates with an extremely low DoD ( $\ll 1\%$ ). This characteristic fundamentally changes the perspective when evaluating battery lifetime within the context of SBC operation.

To address concerns about battery lifetime, a comprehensive long-term experiment was conducted over several weeks at a frequency of 1 kHz, subjecting the battery to over one billion  $\mu$ -cycles. During the experiment the steady-state output and battery voltages were monitored, with no significant change. Following the experiment, the battery's performance was evaluated by analyzing the batteries Q-V behavior. A long full cycle of charge and discharge was performed in the fully discharged battery with a current of 0.6 mA (representing 0.1 CA) with the result shown in Fig. 3.15. Comparing the full cycle to the charge and discharge characteristics and the results obtained with a brand new battery, no significant degradation was observed. This finding suggests that the impact of SBC operation on battery performance differs significantly from regular battery usage, which involves nearly full charge/discharge cycles.

Moreover, as mentioned in Section d, the capacitive component of the battery's charge transfer mechanism plays a role in extending its lifetime by reducing electrochemical stress. The battery in the SBC operates not only in battery mode but also in capacitive mode, effectively mitigating its electrochemical

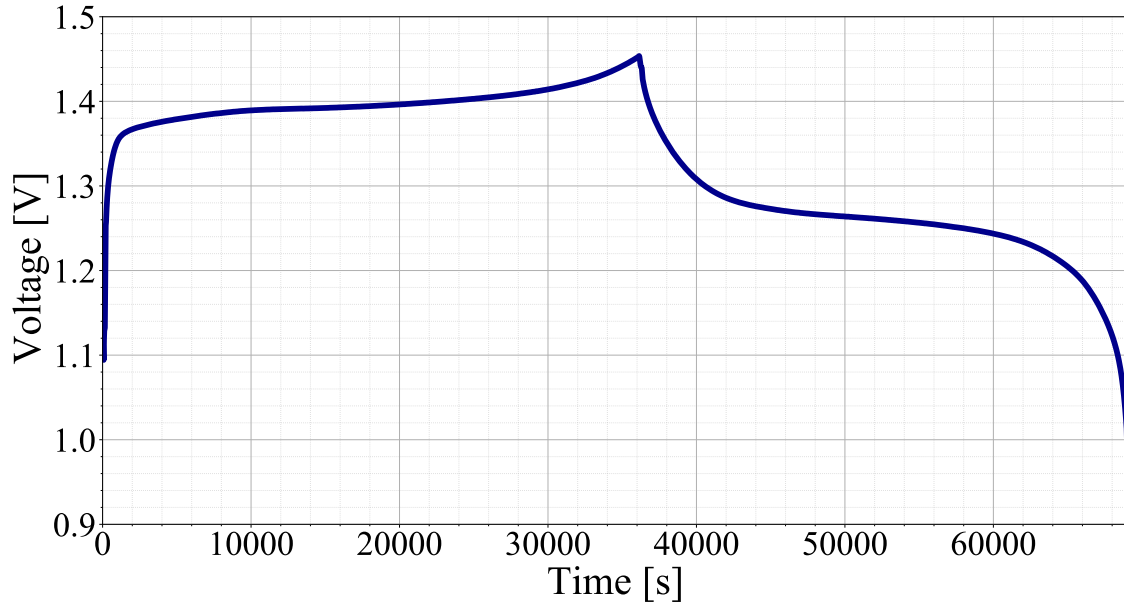


**Figure 3.15** | Long charge and discharge cycle of battery after more than  $10^7$   $\mu$ -cycles

degradation. Additionally, the relatively low current levels used in the SBC, compared to typical battery usage, may also contribute to reducing degradation over time [5]. However, it is important to acknowledge that battery degradation is a complex and multifactorial phenomenon, and further research may be necessary to fully understand the long-term impact of SBC operation on battery performance.

## IV Conclusion

The experimental validation of the SBC has provided substantial evidence of its viability. The SBC has demonstrated its ability to deliver efficient and reliable power conversion, particularly in the low-frequency range where it outperforms the SCC in terms of output voltage ripple, efficiency, and power density.

The successful validation of the SBC in an open-loop 2:1 converter configuration has laid the foundation for further exploration and development of the SBC topology family highlighting its performance advantages over traditional SCCs. Moreover, the unique characteristics of the SBC, such as the BVSA mechanism and its operation with an extremely low DoD, present new perspectives on battery lifetime and performance. Preliminary results indicate that SBC operation with a low DoD may significantly extend battery lifetime compared to traditional charge/discharge cycles. However, further research is needed to fully understand the long-term impact of SBC operation on battery performance and degradation.

While the initial validation presented on this chapter focused on single flying element configurations, it sets the scenario for Chapter 4 exploration of SBC topologies featuring multiple flying batteries using the algorithms presented in Chapter 2. By incorporating more than one flying battery, higher conversion ratios can be achieved, thereby expanding the range of potential applications for the SBC (even more



working in tandem with the BVSA mechanism). This exploration based on principles patented in [12] enable us to fully leverage the advantages offered by the SBC and further solidify its position as a promising alternative to conventional DC-DC converters in low power and low frequency scenarios.

Furthermore, the study of closed-loop operation and control strategies for SBC circuits is crucial to maximize their performance and stability. By exploring control and regulation strategies for SBC closed-loop operation we can enhance the SBC's application scenarios and expand across a wide range of load conditions.

In addition to investigating advanced topologies, there is a growing interest in understanding the impact of different battery chemistries on the performance and operation of the SBC, which will be explored in Chapter 5.

# Bibliography

- [1] Anup Barai, Kotub Uddin, W. D. Widanage, Andrew McGordon, and Paul Jennings. A study of the influence of measurement timescale on internal resistance characterisation methodologies for lithium-ion cells. *Sci Rep*, 8(1):21, January 2018.
- [2] Tom Van Breussegem and Michiel Steyaert. A 82voltage doubler. In *2009 Symposium on VLSI Circuits*, pages 198–199, 2009.
- [3] Heide Budde-Meiwes, Julia Drillkens, Benedikt Lunz, Jens Muennix, Susanne Rothgang, Julia Kowal, and Dirk Uwe Sauer. A review of current automotive battery technology and future prospects. *Proceedings of the Institution of Mechanical Engineers, Part D: Journal of Automobile Engineering*, 227(5):761–776, 2013.
- [4] Jacopo Celè, Sylvain Franger, Yann Lamy, and Sami Oukassi. Minimal architecture lithium batteries: Toward high energy density storage solutions. *Small*, 19, 01 2023.
- [5] James W. Evans, Bernard Kim, Seiya Ono, Ana C. Arias, and Paul K. Wright. Multicycle testing of commercial coin cells for buffering of harvested energy for the iot. *IEEE Internet of Things Journal*, 8(12):10047–10051, 2021.
- [6] A.C. Johnson, A.J. Dunlop, R.R. Kohlmeyer, C.T. Kiggins, A.J. Blake, S.V. Singh, E.M. Beale, B. Zahiri, A. Patra, X. Yue, J.B. Cook, P.V. Braun, and J.H. Pikul. Strategies for approaching one hundred percent dense lithium-ion battery cathodes. *Journal of Power Sources*, 532:231359, 2022.
- [7] Leon Katzenmeier, Manuel Gößwein, Leif Carstensen, Johannes Sterzinger, Michael Ederer, Peter Müller-Buschbaum, Alessio Gagliardi, and Aliaksandr S Bandarenka. Mass transport and charge transfer through an electrified interface between metallic lithium and solid-state electrolytes. *Communications Chemistry*, 6(1):124, 2023.
- [8] Ju Young Kim, Seungwon Jung, Seok Hun Kang, Myeong Ju Lee, Dahee Jin, Dong Ok Shin, Young-Gi Lee, and Yong Min Lee. All-solid-state hybrid electrode configuration for high-performance all-solid-state batteries: Comparative study with composite electrode and diffusion-dependent electrode. *Journal of Power Sources*, 518:230736, 2022.
- [9] Cong Li, Zhen yu Wang, Zhen jiang He, Yun jiao Li, Jing Mao, Ke hua Dai, Cheng Yan, and Jun chao Zheng. An advance review of solid-state battery: Challenges, progress and prospects. *Sustainable Materials and Technologies*, 29:e00297, 2021.

## BIBLIOGRAPHY

---

- [10] David Linden and Thomas B. Reddy, editors. *Handbook of Batteries*. McGraw-Hill, New York, 3rd edition, 2002.
- [11] Emeric Perez, Carlos Augusto Berlitz, Yasser Moursy, Bruno Allard, Sami Oukassi, and Gaël Pillonnet. Ultra-low frequency dc-dc converters using switched batteries. In *2022 IEEE Energy Conversion Congress and Exposition (ECCE)*, pages 1–7, 2022.
- [12] Gaël Pillonnet, Bruno Allard, Carlos Augusto Berlitz, and Sami Oukassi. Device for converting dc-dc based on batteries, October 13 2022. US Patent App. 17/704,596.
- [13] Bruno Scrosati and Jürgen Garche. Lithium batteries: Status, prospects and future. *Journal of Power Sources*, 195(9):2419–2430, 2011.
- [14] Chunwen Sun, Jin Liu, Yudong Gong, David P. Wilkinson, and Jiujuun Zhang. Recent advances in all-solid-state rechargeable lithium batteries. *Nano Energy*, 33:363–386, 2017.
- [15] A Suzuki, S Sasaki, and T Jimbo. Development of all-solid-state thin-film secondary battery for mems and iot device. *Journal of Physics: Conference Series*, 1407(1):012037, nov 2019.
- [16] Martin Winter, Brian Barnett, and Kang Xu. Before li-ion batteries. *Chemical Reviews*, 118(23):11433–11456, 2018.

## CHAPTER 4

# Advanced Battery-Based Converters Topologies

In this chapter, we continue our investigation into the potential of SBC topologies following the primary experimental validation and their performance advantages over traditional SCCs. While the previous validation focused on the local isolated battery behavior and the use of a battery in an open-loop 2:1 SBC converter. The 2:1 SBC was directly inspired from SCC topology, as they both involve a single flying element, bringing a need to further explore SBC topologies, as topologies that incorporate multiple flying batteries. This exploration aims to confirm the benefits and expand the capabilities of the SBC, particularly in terms of achieving higher conversion ratios and broadening the range of potential applications.

We then explore and investigate possible strategies that can be further explored for control and regulation of SBC circuits in closed-loop. By addressing these control challenges, we aim to offer possibilities to enhance the performance, stability, and efficiency of the SBC, making it even more suitable for a wide range of practical applications.

## I Multiple-Battery Exploration

To explore SBC using multiple batteries, it is imperative that we find topologies that fulfill the cycle requirements described in Chapter 2, Section II-b. Additionally, the condition expressed in (2.8) must be fulfilled.

We employ a semi-exhaustive search using the algorithms proposed in Section III in Chapter 2 to explore possible conversion ratios for the SBC. We focus on voltage step-down conversion. To streamline the algorithms and reduce computation time, the search is limited to the use of two groups of batteries ( $V_{bat,1}$  and  $V_{bat,2}$ ). Furthermore,  $V_{bat,i}/V_{out}$  is restricted to be between 1 and 10, to limit the working voltages of batteries based on the output voltage. From such inputs and limitations the algorithm first searches for phases (a set of fixed connections between the batteries, the input source and the output load) that fulfill requirements detailed in Chapter 2. And then explore obtained phases to get a working cycle (a sequence of phases that achieves charge balance and a desired voltage conversion ratio).

Figure 4.1 provides a visualization of the attainable conversion ratios  $V_{in}/V_{out}$  for the SBC, plotted against the  $V_{bat,i}/V_{out}$  ratio. It shows only working cycles, so on top of fulfilling the condition expressed

in (2.8) (which is not sufficient, but still mandatory) it also fulfills the remaining conditions. Here,  $V_{bat,i}$  corresponds to the value of  $V_{bat,1}$  and/or  $V_{bat,2}$ , as some cycles may involve both batteries at the same voltage level. For instance, when selecting  $V_{in}/V_{out} = 3$  (a 3:1 SBC), various options for  $V_{bat,i}/V_{out}$  are available. However, not all combinations of  $V_{bat,1}$  and/or  $V_{bat,2}$  can result in a functional cycle. For instance, a working cycle may be feasible with one group at  $4 \cdot V_{out}$  and the other at  $1 \cdot V_{out}$ , but not with  $4 \cdot V_{out}$  and  $2 \cdot V_{out}$ . This means, for example, that for  $V_{in} = 3$  V we have  $V_{out} = 1$  V, hence a battery of 4 V can be combined with a battery of 2 V.

As described in Chapter 2, from all this working cycles we can optimize different parameters. If we chose a conversion ratio (3:1 as above) and optimize cycles with minimal length (fewest number of phases) the algorithms will provide us with a set of cycles that feature this characteristic, with the smaller number of phases (for a 3:1 SBC being of 3 phases). The cycles feature different number of batteries, with the one with less batteries using only 2 ( $V_{bat,1}/V_{out} = V_{bat,2}/V_{out} = 2$  and the one with the larger number using as much as 7 batteries ( $V_{bat,1}/V_{out} = 4$  and  $V_{bat,2}/V_{out} = 2.5$  or  $V_{bat,1}/V_{out} = 1.25$  and  $V_{bat,2}/V_{out} = 1.5$ ).

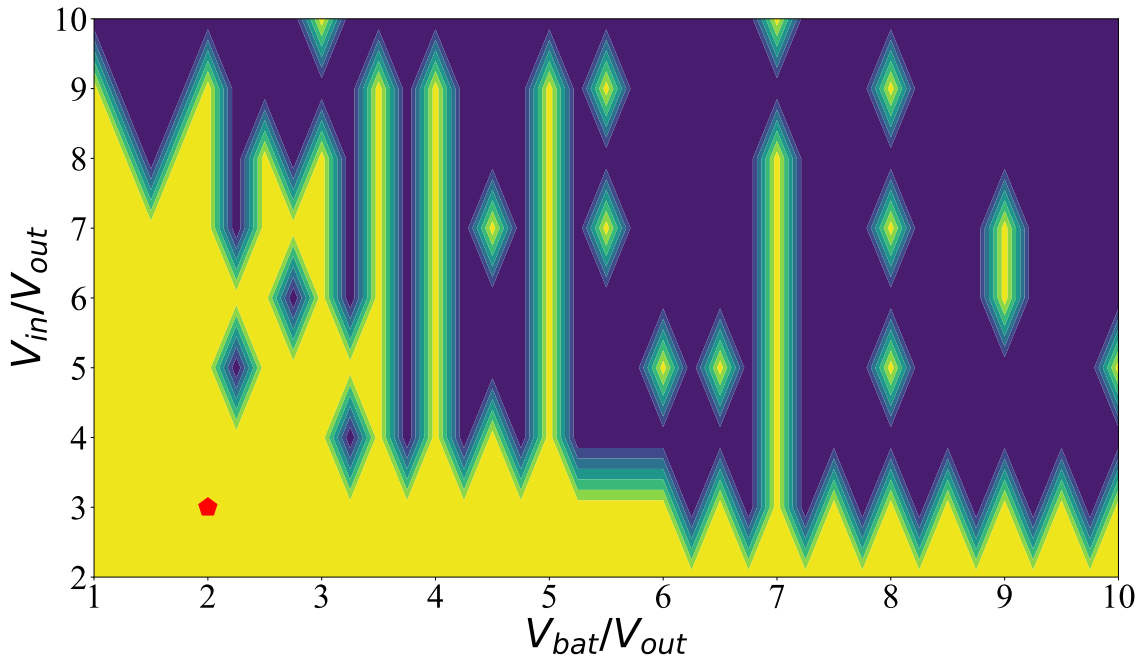


**Figure 4.1** | SBC conversion ratios depending on  $V_{bat,1}/V_{out}$  and/or  $V_{bat,2}/V_{out}$ . Yellow dots denote a possible conversion ratio with at most 17 phases.

From such options we can choose one that optimizes another characteristic, for example minimizing the number of batteries required (to reduce costs and increase power density), or focusing in the ones that best match voltage values inside a chosen battery range. We explore such options in next section with the proposed topologies.

## a Proposed Topologies

The exploration presented in Fig. 4.1 provides us with a range of SBC topologies to choose from, allowing us to explore various conversion ratios. This reinforces the versatility and potential of SBCs in a wider array of applications. By selecting specific topologies, we can focus on validating the operational performance of SBCs utilizing multiple batteries through experimental testing.

The selected SBC topologies represent distinctive cycles that require experimental validation and respect the following criteria, respecting previous constraints:

1. the average voltage between the terminals of each battery remains fixed around their operational voltage (dictated by the battery's electrochemical reaction);
2. the energy given and received by each battery achieves balance for each cycle (preserving SoC);
3. the voltage created by a battery network arrangement and the input source is equal to the output voltage in all phases.

Studying such cycles offer valuable insights into the behavior and efficiency of SBCs when multiple batteries are involved. By conducting experiments on these chosen configurations, we aim to further demonstrate the advantages and practical feasibility of SBCs in various real-world scenarios.

## i 3:1 Battery Based Converter

The first configuration chosen to be experimentally validated is the one highlighted in Fig. 4.1, which corresponds to a 3:1 SBC ( $V_{in}/V_{out}$  of 3). The chosen topologies is the one that not only minimizes the number of phases but also the number of total batteries required. This configuration utilizes  $V_{bat,1}$  and  $V_{bat,2}$  at the same voltage level of  $2 \cdot V_{out}$ , resulting in  $V_{bat,i}/V_{out}$  of 2 for both batteries. The implemented configuration involves both groups, with a single flying battery in each one (B1 and B2), operating in three phases as depicted in Fig. 4.2b. During phases  $\phi_1$  and  $\phi_2$ ,  $V_{in}$  supplies charges ( $Q_{\phi_1}$  and  $Q_{\phi_2}$ ) to batteries B1 and B2, respectively. In phase  $\phi_3$ , both batteries release charge  $Q_{\phi_3}$  to the circuit. Since the duration of all three phases are equal ( $t_{\phi_1} = t_{\phi_2} = t_{\phi_3}$ ) and  $I_{out}$  remains constant throughout the cycle, it follows that  $Q_{\phi_1} = Q_{\phi_2} = Q_{\phi_3}$ . Exchanging equal charges over the three phases, B1 and B2 maintain charge balance throughout the cycle, preserving SoC through energy balance, as explained in Chapter 2, Section b.

Figure 4.2b provides additional insights into the operation of the 3:1 SBC topology. Notably, during phase  $\phi_3$ , the voltage source is connected in the opposite polarity to  $V_{out}$  and receives energy from the circuit. This behavior deviates from the typical operation of DC-DC converters, where the voltage source primarily provides energy to the circuit only. However, this unorthodox behavior is essential for the 3:1 SBC configuration to achieve charge balance and reduce the strict relationship between  $V_{bat}$  and  $V_{out}$ .

The power stage circuit for the 3:1 SBC is illustrated in Fig. 4.2a. In this implementation, the current flowing through the switches is either  $I_{out}$  or 0, depending on their respective conducting phases. Each switch conducts only during one phase, as chosen in this specific configuration.

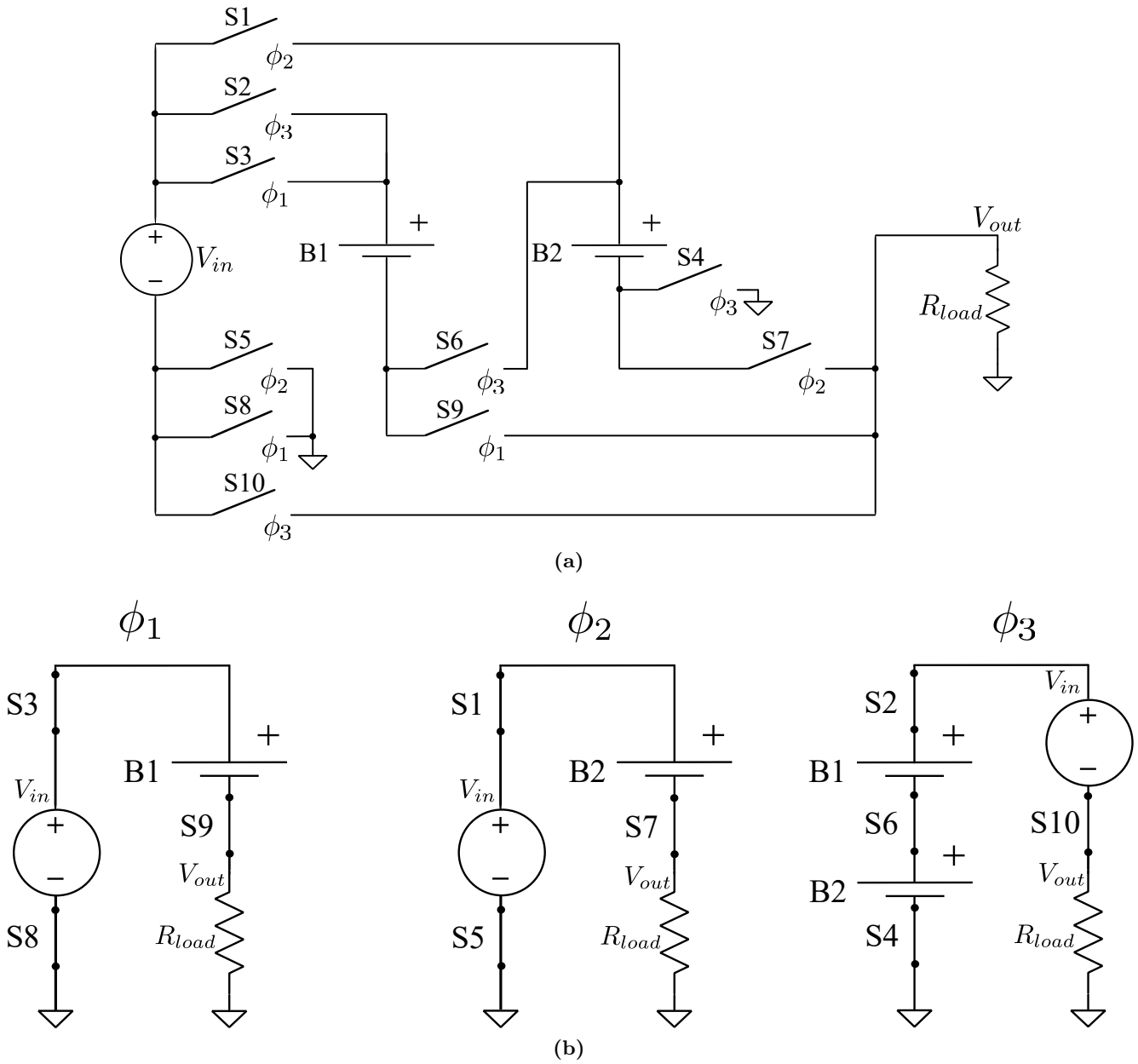


**Figure 4.2** | 3:1 SBC topology: (a) electrical schematic with two batteries of similar voltage and (b) minimum number of operating phases

Table 4.1 provides information about the respective voltages across the terminals of the switches in the 3:1 SBC. It is important to note that due to the discrete nature of the switches used in the circuit, certain switches have floating terminals during specific phases. For example, during phase  $\phi_1$ , the negative terminal of battery B2 is floating (as well as the positive terminal of B2), resulting in high impedance for switches  $S_4$  and  $S_7$  as one of their terminals is floating. Consequently, precise floating voltage values cannot be determined between the terminals of these switches during this phase.

Nonetheless, Table 4.1 indicates that the maximum voltage across the terminals of the switches is equal to  $V_{in}/3$ . This observation highlights the low-power and low-voltage requirement of the switches in the 3:1 SBC. To provide a comparison, consider a 3:1 series-parallel SCC where certain switches must hold a voltage of  $2/3 \cdot V_{in}$  across their terminals when open, while still conducting a current equal to  $I_{out}$  when closed. In contrast, the 3:1 SBC requires lower voltage levels over the switches, contributing to reduce power losses and potentially improving overall efficiency.

**TABLE 4.1** | VOLTAGE ACROSS SWITCHES AND BATTERY CHARGE MOVEMENT IN EACH PHASE OF 3:1 SBC OPERATION

Phase	Voltage across terminals										Charge	
	S1	S2	S3	S4	S5	S6	S7	S8	S9	S10	B1	B2
$\phi_1$	Z	0	0	Z	0	Z	Z	0	0	$V_{in}/3$	$+Q$	0
$\phi_2$	0	Z	Z	$V_{in}/3$	0	Z	0	0	Z	$V_{in}/3$	0	$+Q$
$\phi_3$	0	0	0	0	$V_{in}/3$	0	$V_{in}/3$	$V_{in}/3$	$V_{in}/3$	0	$-Q$	$-Q$

Conducting experimental validation on the 3:1 SBC topology, offers valuable insights into its practical performance and effectiveness. This empirical verification is crucial for demonstrating the capabilities and benefits of SBCs utilizing multiple batteries, paving the way for broader application in diverse fields.

## ii 4:1 Battery Based Converter

In addition to exploring the 3:1 SBC topology, we also investigated other possible SBC configurations to broaden our understanding of the SBC using multiple batteries. Fig. 4.1 provides an overview of the feasible converter topologies with different conversion ratio. It shows that a converter with  $V_{in}/V_{out}$  equal to 4 (4:1 SBC) is possible using different combinations of  $V_{bat}/V_{out}$ . Optimizing the possible 4:1 SBC topologies to the shortest cycle (fewest number of phases) with the fewest number of batteries, leads to of a 4:1 SBC topology that operates with two batteries.

In the chosen 4:1 SBC configuration, there is a significant difference with regard to the 3:1 configuration as the two batteries, B2 and B3, operate at different voltage levels. Specifically, B2 operates at  $2 \cdot V_{out}$  while B3 operates at  $3 \cdot V_{out}$ . For practical implementation the use of two batteries with distinct voltage values can increase difficulty and complexity in a practical implementation, as such voltage ratios are not always possible with batteries nominal voltages. However, the dynamic adaptive behavior of batteries (BVSA) presented in Chapter 3 is a possible way to facilitate it. The inquiry remain if the BVSA behavior will respect each battery's voltage level or if it will impose the same voltage level for both batteries.

An option to use batteries with distinct voltage values and reduce BVSA demands is to use of batteries of same chemistry but with different number of cells connected in series. The operating phases of the



chosen 4:1 SBC are illustrated in Fig. 4.3b.

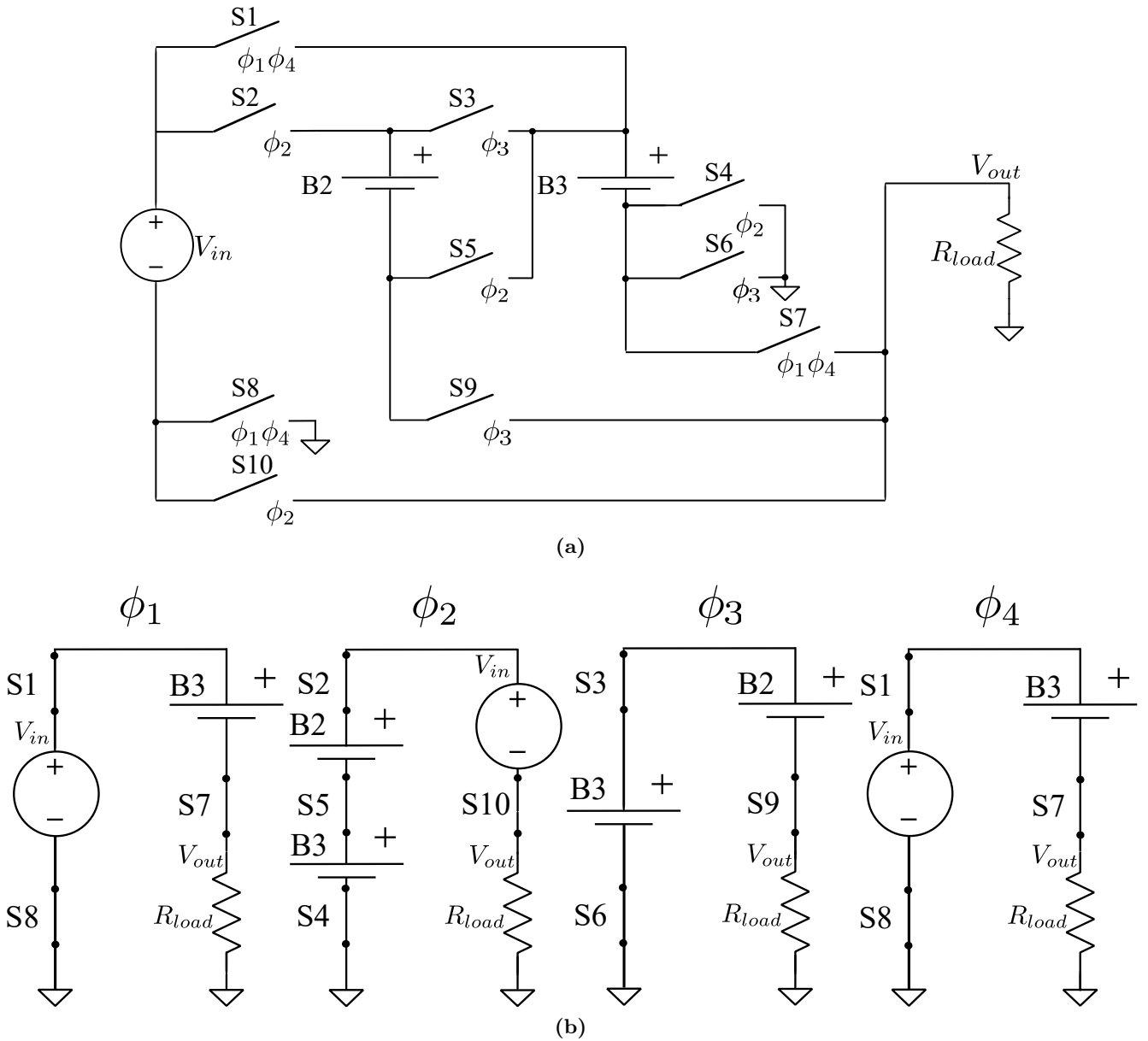
During phases  $\phi_1$  and  $\phi_4$ ,  $V_{in}$  supplies charges  $Q_{\phi_1}$  (equal to  $I_{out} \cdot t_{\phi_1}$ ) and  $Q_{\phi_4}$  (equal to  $I_{out} \cdot t_{\phi_4}$ ) to battery B3, respectively. In phase  $\phi_2$ , B3 transfers charge  $Q_{\phi_2}$  ( $I_{out} \cdot t_{\phi_2}$ ) to battery B2. Finally, during phase  $\phi_3$ , both batteries release charge  $Q_{\phi_3}$  ( $I_{out} \cdot t_{\phi_3}$ ) back to the circuit. It is important to denote that all phases have ideally equal duration ( $t_{\phi_1} = t_{\phi_2} = t_{\phi_3} = t_{\phi_4}$ ), and the output current  $I_{out}$  remains constant throughout the entire cycle. As a result, the charges involved in each phase are equal, leading to the condition  $Q_{\phi_1} = Q_{\phi_2} = Q_{\phi_3} = Q_{\phi_4}$ . This equal distribution of charge ensures that both batteries, B2 and B3, maintain charge equilibrium during the proposed cycle. It also satisfies the other previously established restrictions: having each battery to retain an average voltage inside their operation voltage, and the output voltage in all phases being equal to the voltage creation by battery network arrangement and the input source.

Figure 4.3a shows the schematic circuit of the 4:1 SBC power stage. Similarly to the 3:1 SBC topology, the 4:1 SBC exhibits a singular characteristic during one of its phases ( $\phi_2$  for the 4:1 SBC and  $\phi_3$  for the 3:1 configuration). In this phase, the input voltage source is connected in the opposite polarity to  $V_{out}$ , resulting in the input voltage source receiving energy and charge from the circuit. This behavior deviates from the typical operation of DC-DC converters, where the input voltage source typically acts as a power provider rather than an energy receiver. It can have an impact on efficiency as some charge provided by the input will return to it without performing effective work to the output.

However, this unorthodox behavior is precisely what allows the 3:1 and 4:1 SBC configurations to achieve charge balance and break away from the strict relationship between  $V_{bat}$  and  $V_{out}$ . By allowing energy transfer in both directions, these topologies enable the SBC effective utilization of multiple batteries with different voltage levels to achieve the desired conversion ratios.

Table 4.2 presents the information about the voltages across the terminals of the switches in the 4:1 SBC with four equally timed phases. As with the 3:1 SBC, certain switches have floating terminals during specific phases. It is due to the discrete nature of the switches used in the circuit, making it impossible to determine the precise voltage between the terminals of some switches during certain phases. Although it can be presumed that some nodes will be determined by the batteries open circuit voltage in some configurations (not taken into account here).

Table 4.2 shows that the maximum voltage across the terminals of the switches when opened is of  $V_{in}/2$ . When closed, each switch conducts a current equal to  $I_{out}$ . This power requirements are lower than in some traditional DC-DC solutions. For comparison, in a 4:1 series-parallel SCC, certain switches must hold a voltage of  $3/4 \cdot V_{in}$  while still having to deliver a current equal to  $I_{out}$ . Such reduction in power demands represent a reduction in power losses and a contribution towards higher efficiency.



**Figure 4.3** | Simplest 4:1 SBC topology: (a) electrical schematic and (b) operating phases of the shortest cycle

However, due to the requirement of the input voltage source to operate in both polarities, some switches are required to be bidirectional. Possibly increasing complexity when implementing the topology over non-discrete switches, as to ensure that they will operate correctly on both polarities. For a fully on-chip solution, all switches can be easily integrated on a single die, reducing footprint. A discrete implementation of an ultra-low-power converter have several limitations and low generalization principle, for example large switches preventing the study of driving losses, among other issues. Nevertheless it is an useful tool and requirement for early proof of concept demonstration.

**TABLE 4.2** | VOLTAGE ACROSS SWITCHES AND BATTERY CHARGE MOVEMENT IN EACH PHASE OF 4:1 SBC OPERATION

Phase	Voltage across terminals										Charge	
	S1	S2	S3	S4	S5	S6	S7	S8	S9	S10	B2	B3
$\phi_1$	0	Z	Z	$V_{in}/4$	Z	$V_{in}/4$	0	0	Z	$V_{in}/4$	0	+Q
$\phi_2$	$V_{in}/2$	0	$V_{in}/4$	0	0	0	$V_{in}/4$	$V_{in}/4$	$V_{in}/2$	0	-Q	-Q
$\phi_3$	Z	Z	0	0	$V_{in}/2$	0	$V_{in}/4$	Z	0	Z	+Q	-Q
$\phi_4$	0	Z	Z	$V_{in}/4$	Z	$V_{in}/3$	0	0	Z	$V_{in}/4$	0	+Q

Another interesting feature of the 4:1 SBC topology, distinguishing it from the 3:1 configuration, is the repetition of one switching phase. As can be seen in Fig. 4.3a and Table 4.2, phases  $\phi_1$  and  $\phi_4$  use the same devices and connections, effectively repeating one another. In order to optimize the design and improve efficiency, the timing of the switching phases is modified. Instead of employing four equally timed phases, the circuit is implemented using three phases only, but of different durations. One of the three phases in the 4:1 SBC combines the characteristics of both phases  $\phi_1$  and  $\phi_4$ . This particular phase has a duration twice as long as the other two phases (which are equally timed). This adjustment, ensures the preservation of charge balance throughout the entire cycle.

It is important to note that the chosen topology can work with four equally timed phases (with phases  $\phi_1$  and  $\phi_4$  being identical) and still achieve good performance. However, this optimization allows for more efficient operation of the 4:1 SBC, reducing dynamic switching losses, making it a more viable and effective solution for achieving the desired conversion ratio, and highlights the versatility of the SBC. Carefully considering the timing and duration of the switching phases, allows to maximize a little bit the performance of the 4:1 SBC while maintaining the charge balance between the batteries.

## b Experimental validation

The presented topologies are implemented to experimentally validate the SBC using multiple batteries. The performances are compared to the ones of traditional series-parallel SCC for the same appropriate conversion ratio.

The proposed 3:1 SBC configuration is implemented using two batteries, B1 and B2 (2V15H), with an operating range between 2 V and 2.8 V. With both batteries operating at  $2 \cdot V_{out}$ , this configuration allows for voltage conversion from 3 V to 1 V, up to 4.2 V to 1.4 V. For our implementation, we chose a battery voltage of 2.5 V, resulting in the 3:1 SBC converting an input voltage of 3.75 V to an output voltage of 1.25 V. Due to the BVSA (explained in Chapter 3) the chosen batteries allow a conversion from

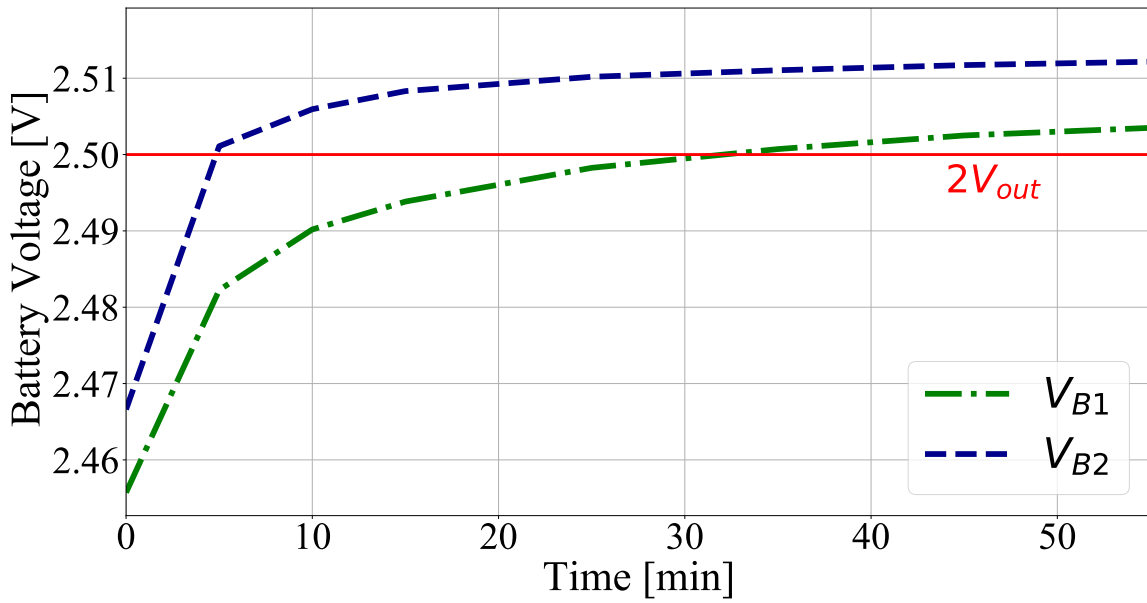
6 V down to 2 V up to 9 V down to 3 V. However it is paramount to retain that the voltage conversion ratio is kept strict as the BVSA only allows batteries' voltage fluctuation keepin the structural topology imposed voltages.

In the case of the 4:1 SBC, we employed battery B2 (2V15H), which can operate from 2 V to 2.8 V, and battery B3 (3V40H) with an operating range of 3 V to 4.2 V. With the proposed 4:1 topology presented earlier, B2 works at  $2 \cdot V_{out}$  and B3 works at  $3 \cdot V_{out}$ , so to convert an input voltage of 5 V into an output voltage of 1.25 V, B2 is set to operate at 2.5 V and B3 at 3.75 V. Although these values are not the batteries' exact open circuit nominal voltages, they fall within the operating limits indicated by the battery manufacturer.

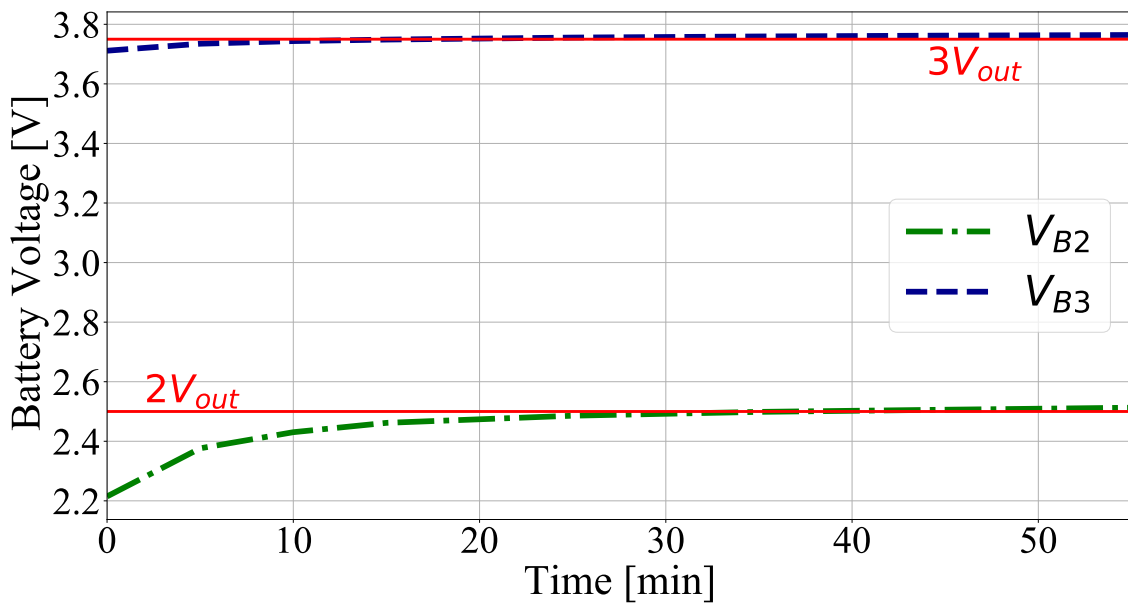
To build the 3:1 and 4:1 SBC circuits, we used a commercially available off-the-shelf CMOS analog switch IC (MAX4678). An external control is used to generate the circuit phases. It generates the three phases of equal duration for the 3:1 SBC and another is responsible for the three phases required for the 4:1 operation, with two phases having equal duration and one phase with double duration, as mentioned earlier. Incorporating these structural parameters into the equation for the simplified equivalent output resistance (2.7), we calculated the equivalent output resistance for the 3:1 SBC as  $8.7 \Omega$ . It is worth noting that batteries' internal resistance contribution to this is significant, accounting for 31% of the total output resistance. This contribution, while lower than that of the 2:1 SBC, remains higher than the contribution of the capacitor ESR in any SCC circuit. Using the same equation (2.7), we determined the equivalent output resistance of the 4:1 SBC to be  $9.4 \Omega$ , with 52% of this value attributed to the internal resistance of the batteries. As detailed in Chapter 2, the batteries' internal resistance are a major contributor to the equivalent resistance of the SBC topologies.

Both the 3:1 and 4:1 SBC topologies exhibit a settling time of a couple of minutes before reaching steady-state operation as shown in Fig. 4.4. Such settling time is related to the the self-adjustment behavior described in Chapter 3, the BVSA. In the case of the 3:1 SBC, as shown in Fig. 4.4a, both batteries, B1 and B2, despite not having exactly equal open-circuit voltages prior to the experiment, eventually reached a voltage of 2 times the output voltage as required by the topology. In steady-state they present only a minor voltage difference of less than 10 mV between them.

Similarly, the batteries B2 and B3 in the 4:1 SBC also exhibit the BVSA behavior defined in Chapter 3, as shown in Fig. 4.4b, wherein both batteries adjust their voltages to match the requirements of the circuit. During the settling time, these batteries align their voltages to 2 times and 3 times the output voltage, respectively, as dictated by the 4:1 SBC topology. This self-adjustment mechanism ensures that the SBC operates efficiently and effectively once the steady-state condition is achieved.

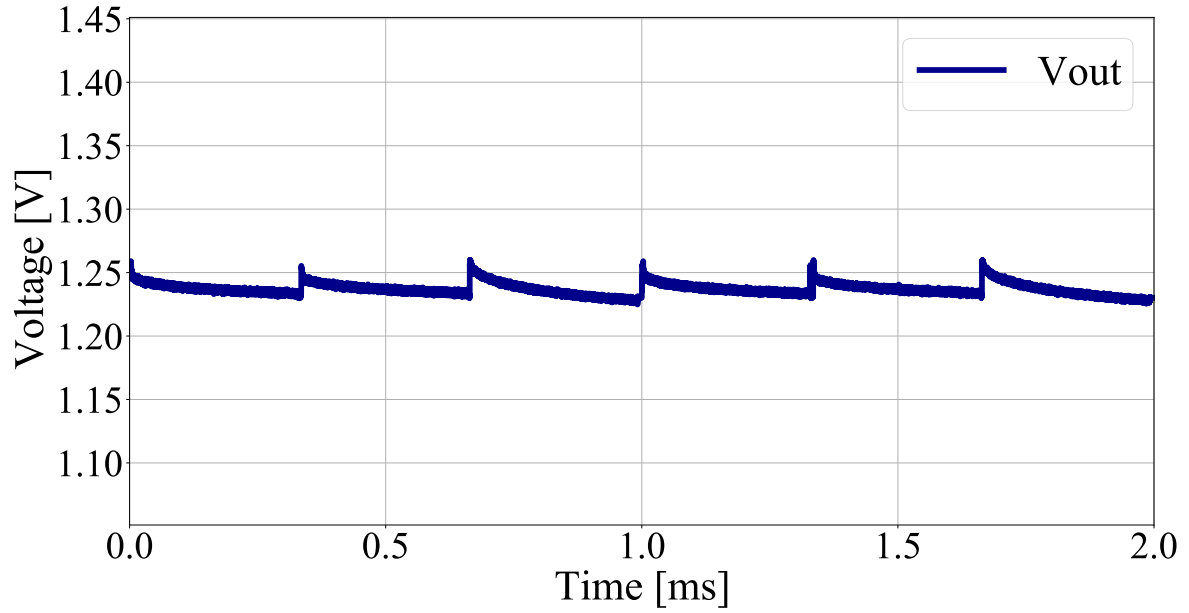


(a)

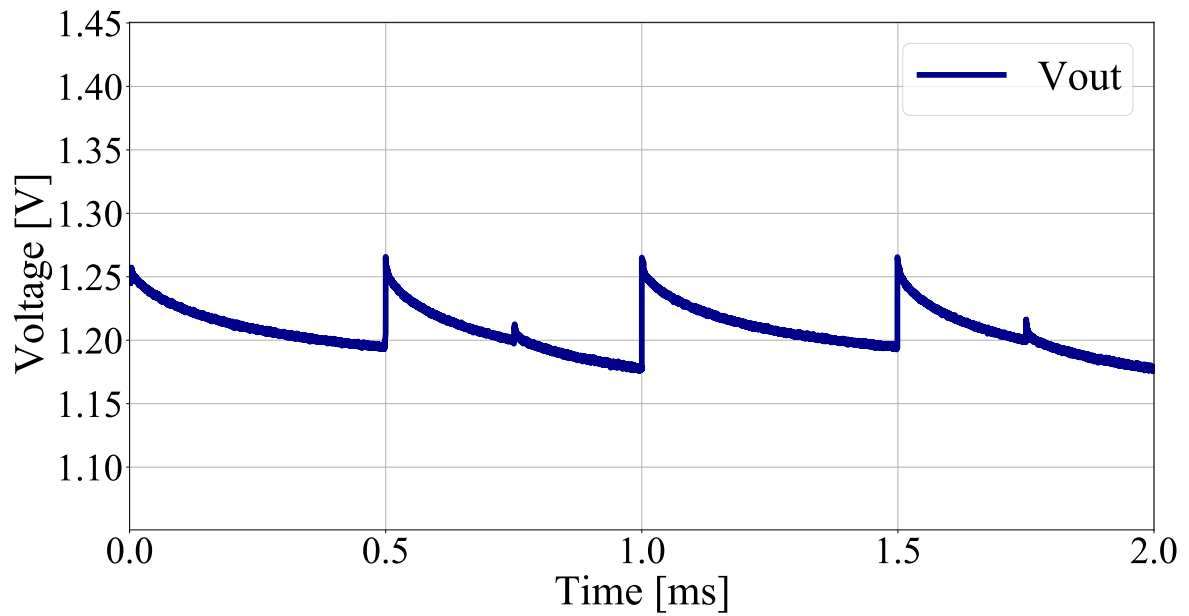


(b)

Figure 4.4 | Transient behavior of (a) 3:1 SBC and (b) 4:1 SBC demonstrating BVSA at 1 kHz and output current of 1 mA



(a)



(b)

**Figure 4.5** | Output voltage of (a) 3:1 SBC and (b) 4:1 SBC during steady-state operation at 1 kHz and output current of 2.5 mA with no output capacitor

Fig. 4.5 shows the two proposed topologies during steady-state operation at 1 kHz and an output current of 2.5 mA. The 3:1 SBC waveform shown in Fig. 4.5a has the three phases of equal duration and similar form. However, as shown in Fig. 4.5b, the 4:1 SBC present a unequal duration of its phases as explained earlier. Due to the heterogeneous phases and different batteries, we can see distinct behavior of the output voltage in the different phases. Either way, such different behavior between phases still form a stable working cycle, and is less prominent with weaker output currents.

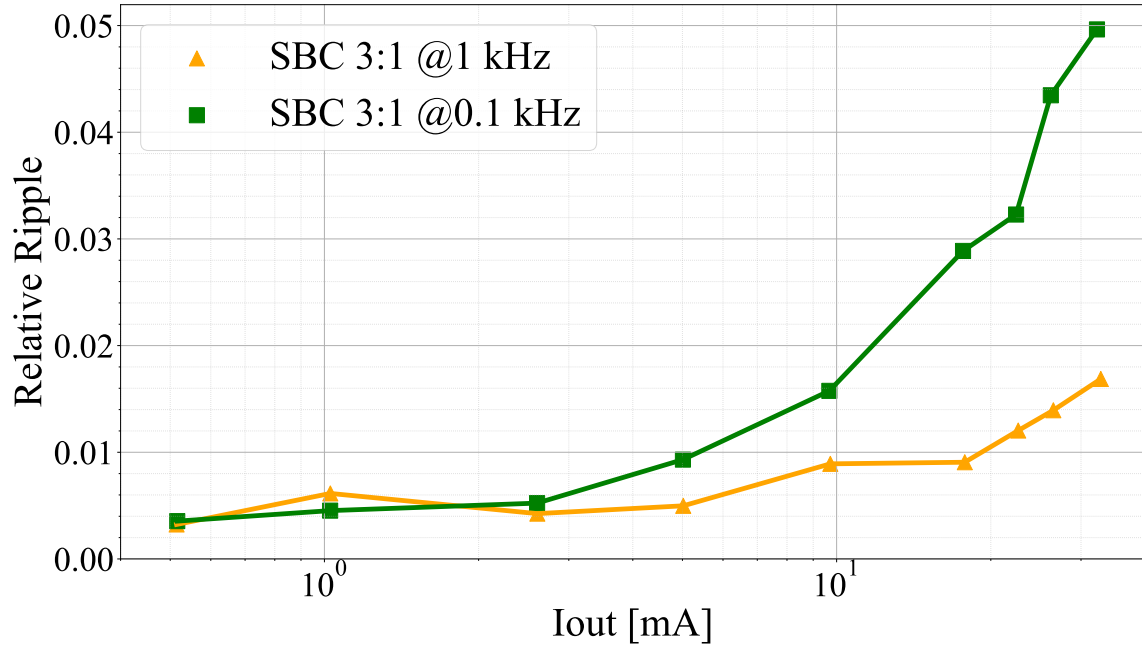
The two proposed SBC topologies operated with a range of frequency from 100 Hz up to 10 kHz. Similarly to the approach taken with the 2:1 SBC, the performance analysis of these configurations primarily centers around evaluating the output voltage ripple and efficiency. These key parameters provide crucial insights into the overall effectiveness and stability of the SBC circuits during operation.

### i Ripple

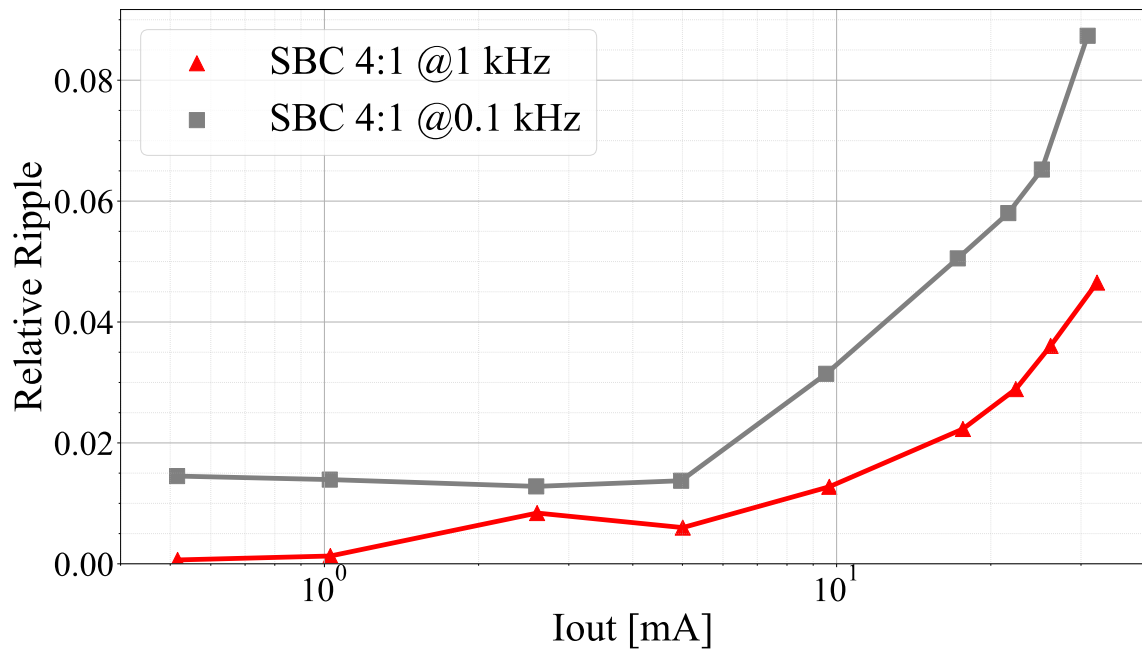
A high output voltage ripple ( $\gg 5\%$ ) is considered unacceptable for most applications of DC-DC converters [1], making it a natural performance benchmark to evaluate the SBC using multiple batteries. Ripple is significantly impacted by the operating frequency, especially when considering a limited dimension of the flying component. As the SBC works at low and ultra-low frequency without an output capacitor, it is key to evaluate that it presents acceptable levels of output voltage ripple when operating with multiple batteries.

Fig. 4.6 illustrates the relationship between the output voltage ripple and the output current for the 3:1 and 4:1 SBC topologies at 100 Hz and 1 kHz, respectively. Once again, these measurements were conducted without the presence of any output capacitor.

Fig. 4.6a demonstrates that the output voltage ripple of the 3:1 SBC stays below 5% even at a low switching frequency of 100 Hz, with an output current of approximately 30 mA. Notably, this ripple level is lower than the corresponding value obtained with the 2:1 SBC under the same output current conditions. The contribution of the batteries to the voltage ripple is advantageous due to their internal impedance, even when two batteries are connected in series during phase  $\phi_3$ . This contribution can be equated to the term  $V_{IR}$  as depicted in Fig. 3.10b. Unlike the 2:1 SBC, which operates with only two phases, the 3:1 SBC employs three phases of equal duration. Consequently, the switching frequency of the 3:1 SBC is 1.5 times higher than that of the 2:1 SBC for the same cycle period. The higher switching frequency has a minor yet beneficial impact on the output voltage ripple at the same operating frequency.



(a)



(b)

Figure 4.6 | Output voltage ripple of (a) 3:1 SBC and (b) 4:1 SBC at 100 Hz and 1 kHz respectively



For the 4:1 SBC in Fig. 4.6b, we can see an output voltage ripple of less than 9% at the low frequency of 100 Hz at the same output current of approximately 30 mA. An operation over four phases represents a switching frequency 2 times higher than in the 2:1 SBC for the same cycle duration. However, the operation with three phases instead of four phases of equal duration changes the dynamic, as there is a longer settling time during the longer phase. Uneven settling times lead to uneven behavior during each phase, and higher output voltage ripple. Batteries used in the 4:1 SBC present lower individual internal resistance than the batteries used in the 2:1 SBC, however in phases  $\phi_2$  and  $\phi_3$  batteries B2 and B3 are connected in series, leading to a higher equivalent resistance. This higher equivalent series resistance leads to a greater  $V_{IR}$  contribution, increasing the output voltage ripple.

## ii Efficiency

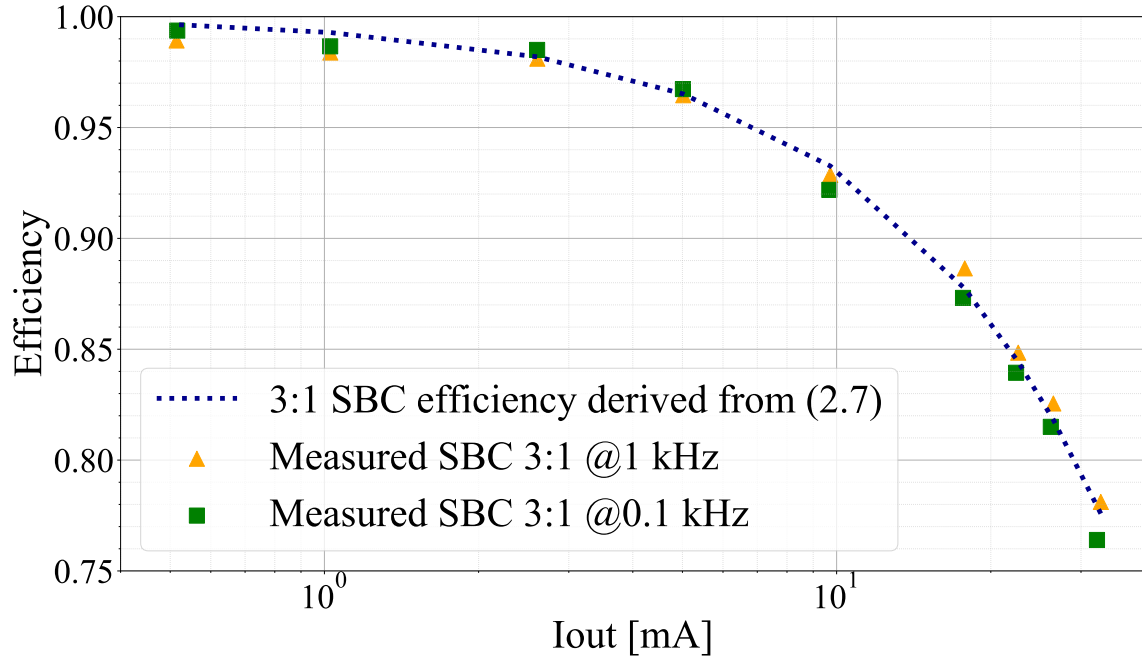
The efficiency of both the 3:1 and 4:1 SBC configurations were evaluated at 100 Hz and 1 kHz. Since the control is externally generated, the focus of the analysis was on conduction efficiency rather than overall efficiency, as previously done for the 2:1 SBC. On future implementations some driving losses need to be taken into account due to the higher effective switching frequency.

Fig. 4.7 illustrates the measured and calculated efficiency for the 3:1 and 4:1 SBC configurations for various output currents. The measured values are provided for both configurations at both frequencies, while the calculated efficiency utilizes the previously determined frequency-independent equivalent output resistance for each topology. Such output resistance is obtained using (2.7), requiring only structural parameters of the circuit.

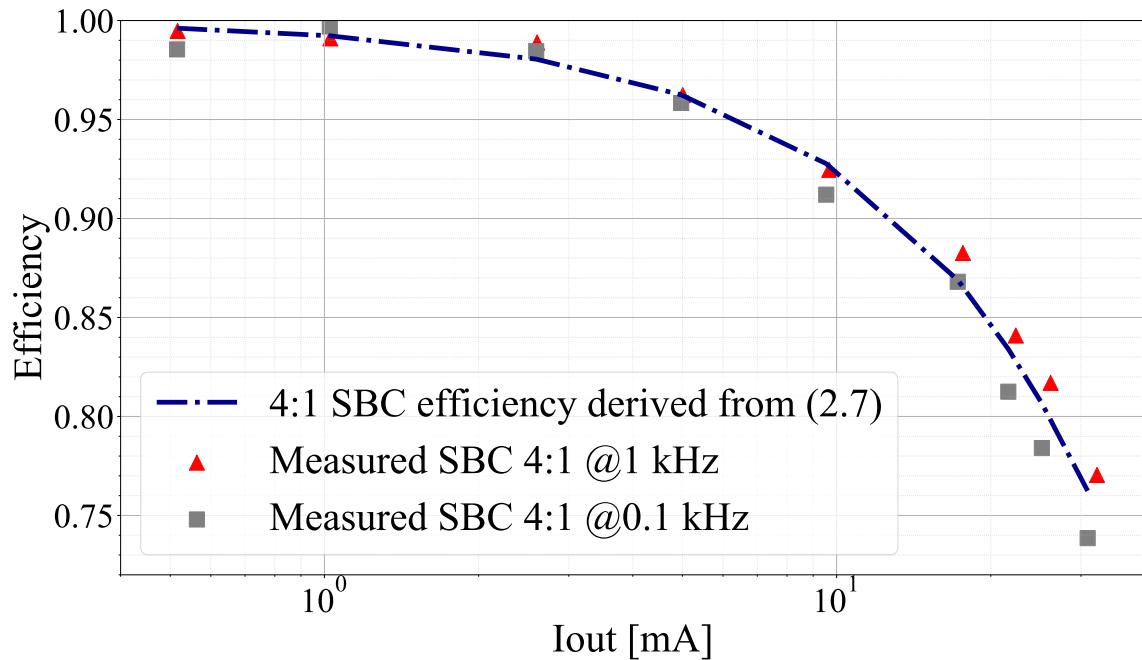
Figure 4.7a presents the efficiency for the 3:1 SBC configuration. The average difference between the measured efficiency and the calculated efficiency is less than 1%. Indicating that the calculated efficiency provides a reliable estimation of the actual performance. Similarly to the 2:1 SBC configuration discussed in Chapter 2, the efficiency performance of the 3:1 SBC is relatively unaffected by frequency, as long as it remains within the limitations imposed by the range of ion mobility in the batteries.

Notably, the 3:1 SBC achieves a high conduction efficiency ( $>90\%$ ), when operating at an output current exceeding 10 mA, even at a low switching frequency of 100 Hz, and without the presence of any output capacitance. At this high efficiency and frequency, the 3:1 SBC delivers an output power of 15 mW, corresponding to a power density of  $14 \mu\text{W}/\text{mm}^3$  (considering only the volume occupied by the batteries). This power volume density is thirty times lower compared to the one of the 2:1 SBC, which utilizes a different battery type.

Such power density value is expected as the 3:1 SBC employs twice the number of batteries (with both connected in series during phase  $\phi_3$ ) than the 2:1 configuration and each battery has larger dimensions, contributing to an increase in overall size and complexity. The implementation also necessitates additional switches (10 compared to the 4 in the 2:1 SBC), which adds to the complexity and potential limitations of the achievable power density.



(a)



(b)

Figure 4.7 | Conversion efficiency of (a) 3:1 SBC and (b) 4:1 SBC at 100 Hz and 1 kHz, respectively

For the 4:1 SBC, the efficiency results are shown in Fig. 4.7b. The average efficiency difference between the measured and theoretical values is 0.65% and 1.22% for the operating frequency of 1 kHz and 100 Hz, respectively. Similarly to the 3:1 and 2:1 SBC configurations, the efficiency also remains relatively frequency-independent, provided that the operation remains within the physical and chemical limits for ion mobility presented by the batteries.

The 4:1 SBC exhibits higher conduction efficiency at lower power output, as shown in Fig. 4.7b, while maintaining a high efficiency (>90%) up until an output current of 10 mA for both studied frequencies. At this level of efficiency, the 4:1 SBC yields an output power of 13 mW, corresponding to a power density of 8  $\mu\text{W}/\text{mm}^3$  (considering only the volume occupied by the batteries). This density is fifty times lower than the one achieved by the 2:1 SBC. The battery used as B3 for the 4:1 SBC alone has more than double the volume of the batteries compared to the 3:1 configuration. However, this limitation can be easily addressed with access to a wider range of off-the-shelf batteries. Despite the batteries of the 4:1 SBC occupying a higher volume than the other experimentally tested configurations, it still uses the same number of switches (10) as the implemented 3:1 SBC, despite higher complexity.

### iii Overall Performances

The SBC operation with multiple batteries presents a similar behavior as the more simple implementation of a 2:1 SBC. Both configurations of 3:1 and 4:1 conversion ratios offered low output voltage ripple even at the relatively low frequency of 100 Hz. The measured conduction efficiency of 3:1 and 4:1 SBC closely resemble the one obtained with (2.7) for calculating the equivalent output resistance of the circuits. Such efficiency is kept high (>90%) even at output currents of 10 mA. The efficiency of both topologies is highly frequency independent, highlighting the robustness of the 3:1 SBC's efficiency under different operating conditions.

Even operating with multiple batteries, the SBC present the BVSA behavior during settling time, expanding the operating range of family topology. Each battery independently present the BVSA behavior, similar to the 2:1 SBC opening more flexible approaches to the SBC. The voltage conversion ratio can be kept constant with same batteries even if changing input and output voltages, presuming that they respect the voltage range accepted by each battery.

A long term validation also confirmed the behavior initially presented by the 2:1 SBC that even after several millions of  $\mu$ -cycles, the batteries retained their behavior and performance. Even some minor mismatch of duty cycle can be tolerated by the system (knowing that they are not strictly perfect). It brings the possibility of future exploration of cycles with less strict constraints about charge balance during each cycle.

## II Possible control approaches

The implementation of the SBC circuits operates so far in open-loop mode, and future research is necessary to explore closed-loop configurations for regulating the output voltage. In this context, we can

investigate various traditional control approaches and their potential implementation in the SBC topology family. However, it is important to notice that the time constant of the converter is strongly linked to the slow battery behavior. A close loop approach around the converter will easily present a faster response than the battery dynamic posing regulation challenges.

In Chapter 2, we introduced the SBC representation as a converter with a transformer model and an output resistance. The input voltage undergoes conversion based on the transformer ratio, and the resulting output voltage is obtained by subtracting the voltage drop in the output resistance. However, under non-zero load conditions, the output voltage never reaches the ideal ratio due to the voltage drop across the output resistance. If targeting more than 90% efficiency, the output voltage will be around 10% less than the voltage obtained under no-load conditions, relaxing the need of control in regulation under certain conditions.

Given this understanding, we can outline some basic approaches for a control strategy. Similarly to what is employed in SCCs, the SBC can benefit from a two-stage control strategy, consisting of a coarse grain control and a fine grain control. The coarse grain control involves modifying the circuit's phase configuration, analogous to the gearbox SCC approach [7]. This coarse grain control enables the converter to operate close to the optimal ratio, thereby maximizing efficiency.

On the other hand, the fine grain control focuses on directly modulating the output resistance to achieve the exact desired output voltage. However, it is essential to recognize that fine grain control cannot be achieved without incurring some power dissipation. This situation is akin to a linear regulator, where efficiency is limited by the ratio between the output and input voltages [5]. This section explores strategies for the fine grain control.

### a Frequency Modulation

In traditional SCCs, frequency modulation has emerged as a popular control solution [6]. By varying the switching frequency over a wide range, fine grain regulation of the output voltage can be achieved. This flexibility allows the converter to maintain constant efficiency for a given regulated output voltage, which is advantageous. It can also be combined with other technologies for fast responses [2].

However, frequency modulation also has its drawbacks. One significant impact concerns the output voltage ripple, which tends to increase with the variation of switching frequency. Despite its effectiveness in SCCs, this control approach faces limitations when applied to SBCs.

Unlike SCCs, the SBC exhibits a largely frequency-independent output impedance. Additionally, the range of feasible operating frequencies for SBCs is more constrained. These limitations make frequency modulation less practical for SBCs, as it may not provide the desired level of control and stability.

Due to the unique characteristics and limitations of the SBC topology, exploring alternative control strategies that better suit its inherent properties becomes essential.

## b Duty Cycle Modulation

Widely used in inductive DC-DC converters through pulse-width modulation (PWM), it has also found application in SCCs [4] when operating in the FSL region, where resistive losses dominate the equivalent output resistance. Traditionally duty cycle modulation is limited to a small range but grant fine grain regulation [3].

Fig. 4.9 illustrates the impact of duty cycle asymmetry on the output and battery voltages of a 2:1 SBC (converting 2.6 V down to 1.3 V). As shown in Fig. 4.8, duty cycle asymmetry refers to the difference in time between the charging semi-period ( $\phi_1$ ) and the discharging semi-period ( $\phi_2$ ) within a  $\mu$ -cycle. Positive asymmetry implies that the charging period is longer than the discharging period, while negative asymmetry indicates the opposite. A duty cycle imbalance of 0% means that the  $\mu$ -cycle is symmetrical, with equal time between both semi-periods. The plot presents relative voltage values for asymmetries of 5%, 10%, and 20% for both positive and negative cases. A restriction when applied to the SBC topology is that a duty cycle asymmetry can lead to unbalanced operation (the batteries receiving and providing an unequal amount of charge).

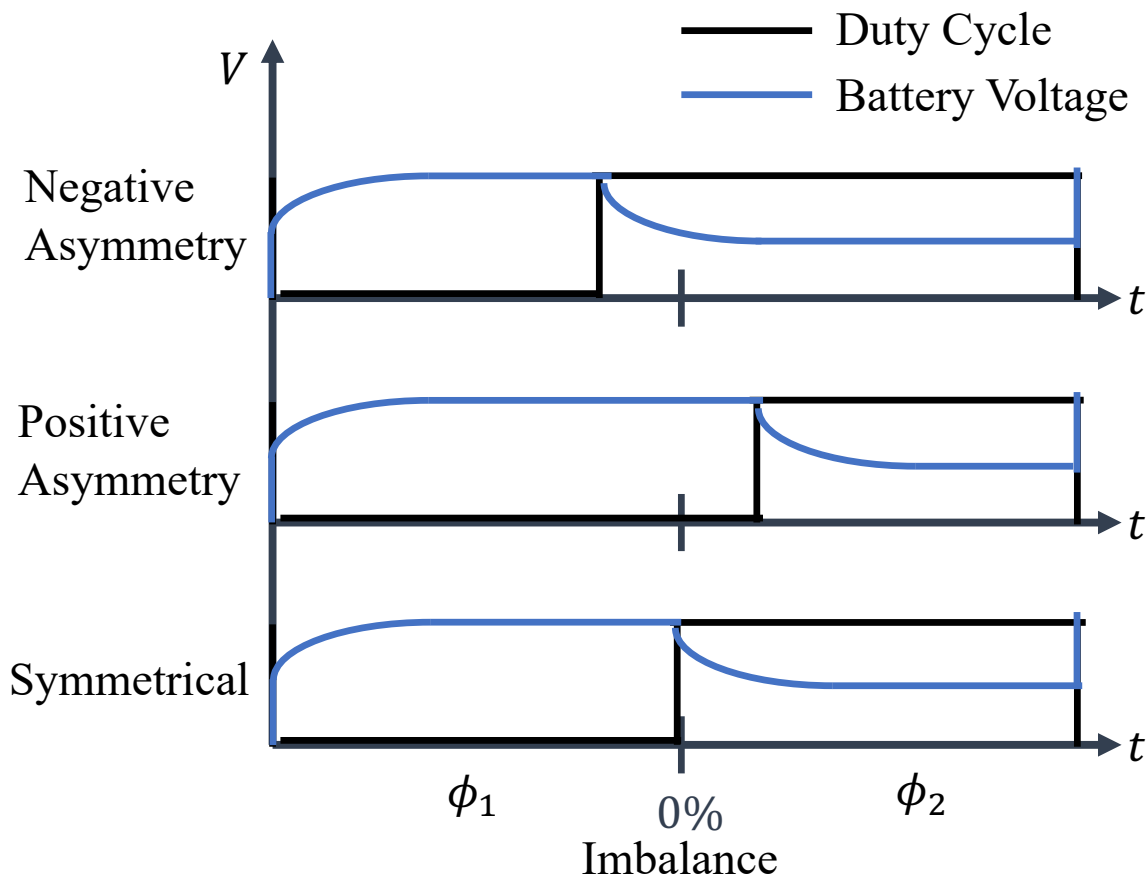


**Figure 4.8** | Positive and negative duty cycle asymmetries on 2:1 SBC.

When analyzing the impact of the duty cycle asymmetry on the average voltage value, we can see that

it follows a linear behavior for negative duty cycle asymmetries. Here, the value of the relative voltage of 100% represents that the voltage is exactly the value obtained with a symmetrical cycle pattern. In the case of the implemented 2:1 SBC, output voltage and battery voltage average values are equal 1.3 V under a symmetrical steady-state operation. We can see that a negative asymmetry of the duty cycle, represents an equivalent reduction on the battery's average voltage value, however, the tendency does not follow for positive duty cycle asymmetry. We can relate that to the fact that, for positive asymmetries, the equivalent voltage value is close to the absolute limits of the battery and outside of its usual working voltage values. For the output voltage, we can see an impact of the duty cycle asymmetry, however much less prominent, limiting the scope of regulation.

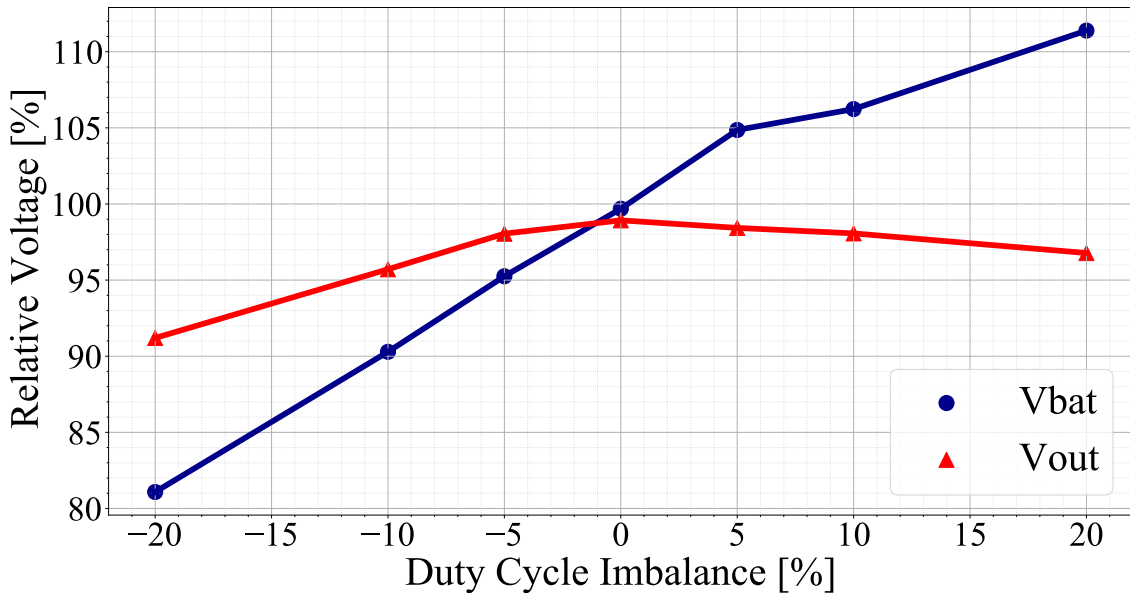


**Figure 4.9** | 2:1 SBC battery voltage and output voltage variation due to duty cycle modulation at 100 Hz and output current of 2.5 mA.

As shown in Fig. 4.10, the efficiency presents a symmetrical behavior around the point of zero duty cycle imbalance. As expected, there is a negative impact on efficiency with the highest value of duty cycle asymmetry, with the impact being higher for a positive asymmetry as we work closer to the physical voltage potential of the battery. The impact in efficiency close to 0% of duty cycle imbalance is limited, highlighting the interest of duty cycle modulation only on a limited range.

The duty cycle asymmetry also impacts the output voltage ripple. As the average voltage of the battery changes, it proportionally changes the voltage difference between input, voltage and output. It generates a voltage asymmetry on the output during each semi-cycle (as the 2:1 SBC operates without output capacitor). This imbalance between voltages is a direct cause for greater output voltage ripple, since output voltage is either directly connected to battery voltage (during phase  $\phi_2$  or is the difference between input voltage and battery voltage (in phase  $\phi_1$ ).

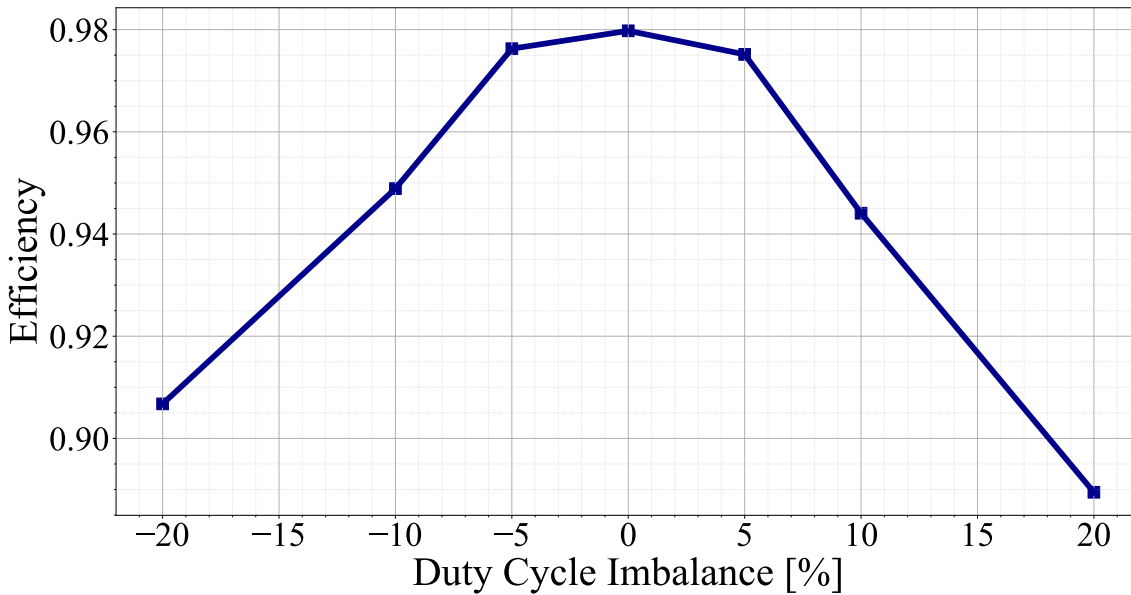


**Figure 4.10** | Duty cycle modulation impact on efficiency of a 2:1 SBC at 100 Hz and output current of 2.5 mA.

It is clear that the best approach for the control of the SBC is similar to the one of the SCC in a two stage control strategy with a coarse grain control and a fine grain control. For the fine grain control of the SBC the duty cycle modulation is a better alternative than frequency modulation, however it still presents a huge penalty in efficiency and a limited operation range. Some other approaches focus outside of the SBC power stage adding a new stage, like the use of an LDO at the output or a hybrid route, adding an output inductance and applying duty cycle modulation to the inductance.

### III Conclusion

This chapter explored the concept of SBC topologies, specifically focusing on topologies using multiple batteries. To study such topologies, it focused on 3:1 and 4:1 SBC configurations. Through a comprehensive analysis, we gained valuable insights into the performance and efficiency of these novel power stage circuits.

The 3:1 SBC was demonstrated to convert an input voltage of 3.75 V into 1.25 V with a remarkable output voltage ripple of below 5% even at a low switching frequency of 100 Hz. By employing three phases of equal duration, the 3:1 SBC maintained high conduction efficiency, exceeding 90% for output currents exceeding 10 mA. This efficiency was relatively unaffected by frequency, making the 3:1 SBC a robust solution under different operating conditions. However, the design's increased complexity and the need for additional switches limits its achievable power density, providing nearly six times lower power volume density compared to the 2:1 SBC.

The 4:1 SBC, on the other hand, demonstrated the ability to convert voltages in a 4:1 ratio with batteries operating at different voltage levels (2.5 V and 3.75 V). The efficiency performance of the 4:1

### III. CONCLUSION

---

SBC was also relatively frequency-independent, achieving high conduction efficiency ( $>90\%$ ) up to an output current of 10 mA for both studied frequencies. Despite achieving lower power volume density than the 2:1 SBC, the 4:1 SBC still present interesting performance benchmarks.

Both SBC configurations with multiple batteries demonstrated unique characteristics. It includes the BVSA introduced in the 2:1 SBC, where the batteries self-adjust their voltages to the required levels during steady-state operation. Such behavior is not typically seen in conventional DC-DC converters. The presence of the BVSA behavior on the SBC topologies for higher conversion ratio, and the performance demonstrated by such implementations expand the application range of the SBC family topology.

However, every implementation of the SBC circuits operates in open-loop. Exploring close-loop configurations to regulate the output voltage is important for the SBC application. Similar to the SCC the SBC benefits of a two stage control strategy: a coarse grain control implemented by a change in the circuit phases configuration (akin to the gearbox approach of the SCC), and a fine grain implemented by a more direct control strategy (like the frequency modulation used in the SCC). For the SBC frequency modulation did not showed promising results as the SBC is highly frequency independent. A more promising approach is the duty cycle modulation, however it also presents some limitations. The implementation of an LDO at the output of the circuit or the exploration of hybrid solutions can also present possible control solutions.

Every SBC implementation up until now used the same chemistry technology, next chapter explores the possible effects that different battery technologies can bring to the SBC. It also explores the use of fuel cells as intermediate passive device for the circuit, due to similarities with batteries.





# Bibliography

- [1] Tom Van Breussegem and Michiel Steyaert. A 82voltage doubler. In *2009 Symposium on VLSI Circuits*, pages 198–199, 2009.
- [2] Hanh-Phuc Le, John Crossley, Seth R. Sanders, and Elad Alon. A sub-ns response fully integrated battery-connected switched-capacitor voltage regulator delivering 0.19w/mm<sup>2</sup> at 73In *2013 IEEE International Solid-State Circuits Conference Digest of Technical Papers*, pages 372–373, 2013.
- [3] Wonseok Lim, Byungcho Choi, and Yonghan Kang. Control design and closed-loop analysis of a switched-capacitor dc-to-dc converter. In *2001 IEEE 32nd Annual Power Electronics Specialists Conference (IEEE Cat. No.01CH37230)*, volume 3, pages 1295–1300 vol. 3, 2001.
- [4] B.W.-K. Ling, C. Bingham, H.H.-C. Iu, and Kok Lay Teo. Combined optimal pulse width modulation and pulse frequency modulation strategy for controlling switched mode dc-dc converters over a wide range of loads. In *IET Control Theory & Applications*, pages 1973–1983, 2012.
- [5] A. Samir, E. Kussener, W. Rahajandraibe, H. Barthélemy, and L. Girardeau. A 90-nm cmos high efficiency on chip dc-dc converter for ultra-low power low cost applications. In *2013 IEEE Faible Tension Faible Consommation*, pages 1–5, 2013.
- [6] Thomas Souvignet, Bruno Allard, and Severin Trochut. A fully integrated switched-capacitor regulator with frequency modulation control in 28-nm fdsoi. *IEEE Transactions on Power Electronics*, 31(7):4984–4994, 2016.
- [7] Tom Van Breussegem and Michiel Steyaert. A fully integrated gearbox capacitive dc/dc-converter in 90nm cmos: Optimization, control and measurements. In *2010 IEEE 12th Workshop on Control and Modeling for Power Electronics (COMPEL)*, pages 1–5. IEEE, 2010.

## BIBLIOGRAPHY

---

## CHAPTER 5

# Different Passive Technologies Exploration and Impact

A drawback associated with the SBC lies in the strong relationship between the output voltage ( $V_{out}$ ) and the battery (or batteries) voltage. Despite the battery's inherent self-adjustment mechanism presented in Chapter 3, and despite the potential relaxation of this constraint with higher voltage conversion ratios as presented in Chapter 4, this characteristic remains inherently limiting. The batteries' operating voltage limits can significantly constrain the versatility of the SBC. To explore different output voltage values, one potential solution is the adoption of alternative battery chemistries, such as Lithium-Ion (Li-Ion), for instance. Embracing such different battery chemistries can also introduce additional advantages and disadvantages when integrated into the SBC framework.

Furthermore, the concept and experimental validation of the SBC can potentially be extended to other energy storage devices sharing similar characteristics. Fig. 5.1 presents a Ragone plot that illustrates diverse energy storage technologies, delineating various battery chemistries while also encompassing fuel cells. Notably, fuel cells exhibit comparable attributes to batteries, including elevated gravimetric energy density. Consequently, fuel cells emerge as prospective candidates for deployment as intermediate energy storage components within low-frequency DC-DC converters.

This chapter focuses on the exploration of such technologies of energy storage. Evaluating their viability inside the SBC concept and possible expansion of application possibilities.

### I Impact of Different Chemistries

Studying the behavior of various battery chemistries within the SBC framework, we can gain insights into their suitability for different applications. This knowledge will help optimizing the performance and efficiency of the SBC by identifying the most compatible and efficient battery chemistries for specific use cases.

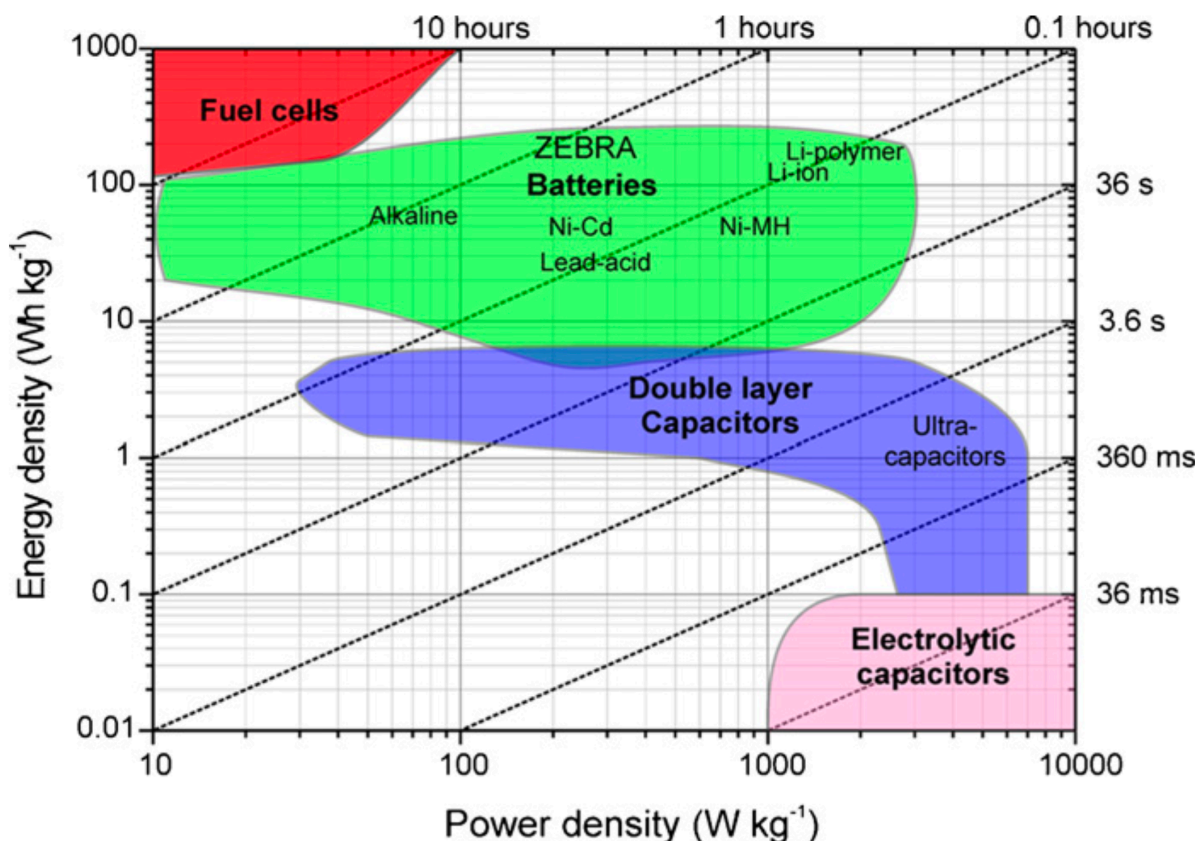


**Figure 5.1** | Ragone plot of various storage chemistries. Diagonal perforated lines represent the relation between energy and power. [1]

### a Lithium-ion (Li-Ion)

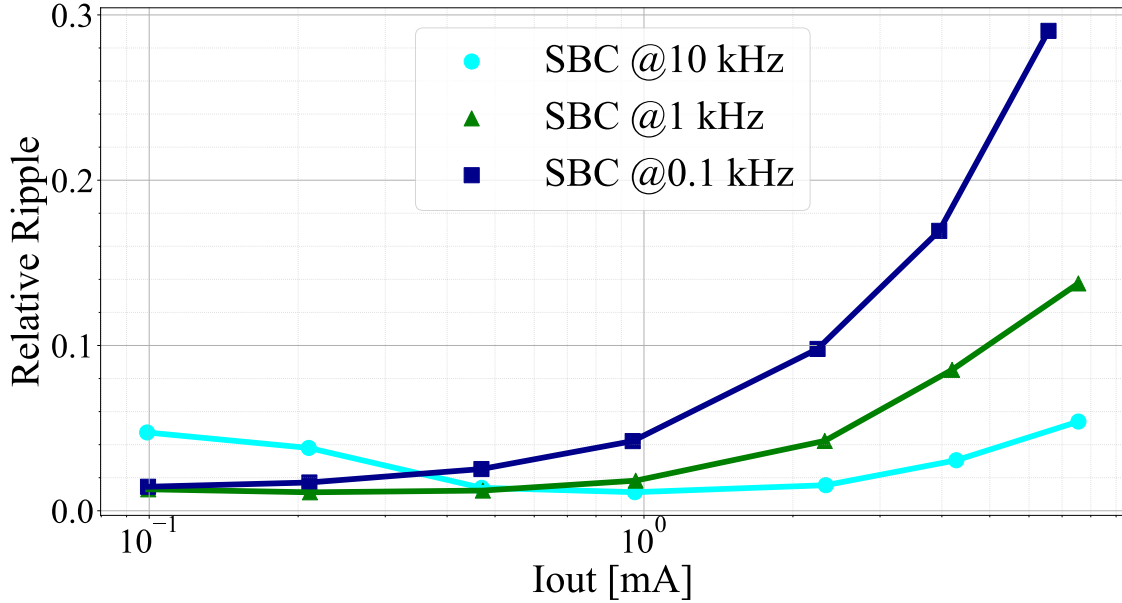
In Chapter 3 lithium-ion (Li-ion) batteries are presented as a potential battery technology to be implemented in an SBC. They are a preferred choice for many electronic applications due to good combination of characteristics like energy storage density, lightweight design, and rechargeable capabilities. As shown in Fig. 5.1, Li-ion batteries offer high energy density and high power density compared to other battery technologies, contributing to their widespread use in electronic applications and also strengthens their potential use applied to the SBC.

The circuit used to experiment with a Li-ion battery is the same as the one presented in Chapter 3, Section III. An off-the-shelf battery known as TS621E with similar dimensions to the previous NiMH device is experimented. The battery's nominal voltage is 1.5 V and it has a nominal capacity of 2.5 mAh.

Despite the higher operating voltage range (between 1.0 V and 1.5 V) of the Li-ion battery, the 2:1 SBC will use the same voltage levels as for the NiMH, converting an input voltage of 2.6 V down to 1.3 V. The circuit operating frequency spans from three orders of magnitude from 100 Hz up to 10 kHz. The circuit operates without any output capacitor.

The output voltage ripple is shown in Fig. 5.2. The lower battery capacity is generally related to a higher internal impedance, which is the case for the Li-ion battery. Such higher internal impedance caused

a much higher observed output voltage ripple than with the NiMH 2:1 SBC, featuring a maximum ripple of almost 30% at 100 Hz and an output current of 7 mA.



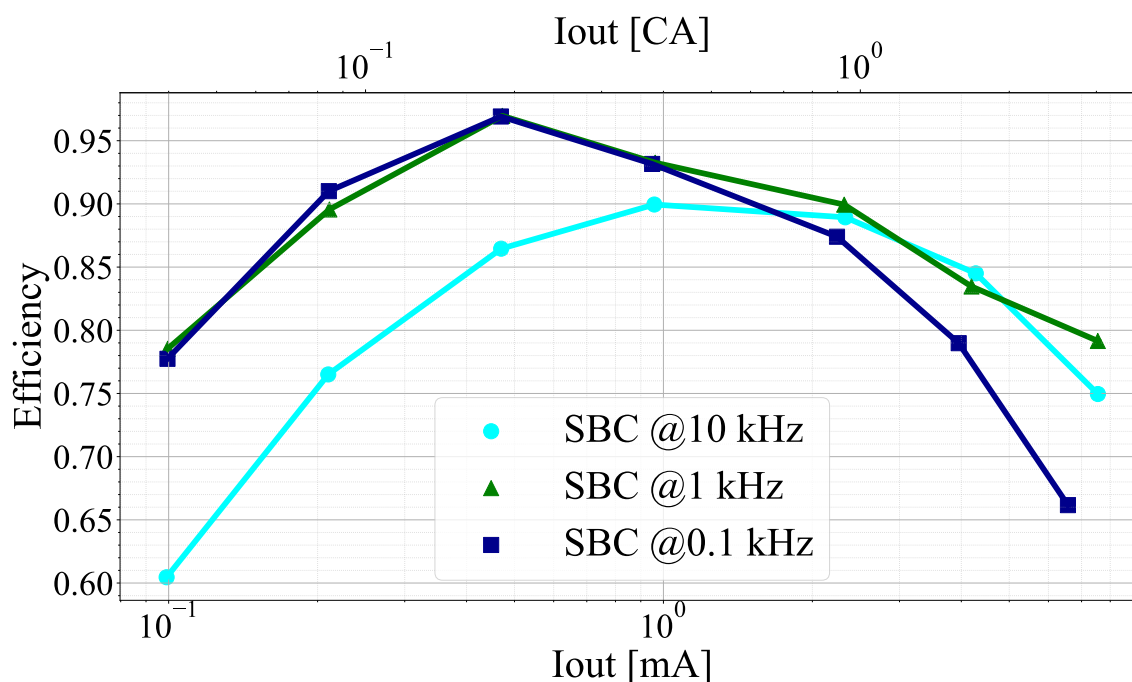
**Figure 5.2** | Relative output voltage ripple of 2:1 SBC using TS621E Li-ion battery at different operating frequencies

Fig. 5.3 presents the efficiency of the 2:1 SBC using Li-ion battery at different frequencies. Despite a lower nominal capacity than the NiMH counterpart (2.5 mAh against 6 mAh), the Li-ion battery is still under  $\mu$ -cycle behavior even at peak output current and lowest operating frequency, as it represents a DoD of  $\sim 10$  ppm. The Li-ion 2:1 SBC still managed to maintain high efficiency ( $>90\%$ ) for an output current range of 2 mA at frequencies of 100 Hz and 1 kHz. With such high efficiency, it reaches a peak output power of 2.57 mW at 100 Hz and 2.74 mW at 1 kHz, representing a power volumetric density at 100 Hz of  $34.7 \mu\text{W}/\text{mm}^3$  (referring solely to the battery's volume). A peak efficiency of 97% is achieved despite the lower power density. Long experimental setups reinforce the lower impact of  $\mu$ -cycle operation against high SoC charge and discharge cycles on cycle-life of batteries inside a SBC, including for Li-ion batteries.

The battery's nominal capacity is not expected to affect the power output at first order, but at second order the reduction in the nominal battery capacity creates an increase in the internal impedance. The Li-ion battery did not intrinsically present advantages to the SBC, however it remains a valid battery technology option.

## b Solid-state batteries (SSBs)

Solid-state batteries (SSBs) are presented in Chapter 3 as a promising technology for next-generation energy storage systems and also for possible use inside the SBC family topology. These innovative batteries utilize solid-state electrolytes, which can take the form of ceramics, polymers, or composite



**Figure 5.3** | Efficiency of 2:1 SBC using TS621E Li-ion battery at different operating frequencies

materials, to facilitate the transport of ions between the cathode and anode, thereby eliminating the need for liquid electrolytes on the one hand and geometry variation on the other hand. In comparison to traditional liquid electrolyte batteries, SSBs offer a host of advantages, including enhanced safety, heightened energy density, and extended cycle life [3].

One of the SSBs under investigation is an off-the-shelf thin film battery (TFB) developed by STMicroelectronics, recognized as EFL1K0AF39. This particular battery features a  $\text{LiCoO}_2$  cathode, a LiPON ceramic electrolyte, and a lithium anode. With a nominal voltage of 3.9 V and a capacity of 1 mAh, the TFB deviates in form factor from the other battery technologies previously examined. Notably, the TFB features a low thickness of 160  $\mu\text{m}$  (including packaging) and a large surface area measuring 743  $\text{mm}^2$ . Given its lower nominal capacity, the battery naturally exhibits a relatively higher internal resistance, approximately ten times that of the NiMH battery (80  $\Omega$ ). Its pulse current capacity is rated at 15 CA, however this regimen presumes only a 10% conduction time by the battery in each cycle. During regular operation it is rated at most to 5 CA, already presenting a significant impact on discharge capacity ( $\sim 0.5$  mAh).

The TFB is implemented in the same 2:1 SBC circuit as for the other battery technologies. However, due to the SSB's voltage range spanning from 3.0 V to 4.2 V, the 2:1 SBC featuring the TFB transforms an input voltage of 7.6 V into an output voltage of 3.8 V. The TFB enables 2:1 SBC conversions ranging from 8.4 V to 4.2 V down to 6 V towards 3 V. This circuit operates across a wide range of operating frequencies, spanning three orders of magnitude from 100 Hz to 10 kHz.

Illustrated in Fig. 5.4 is the output voltage ripple observed in the 2:1 SBC configuration employing the

TFB and no output capacitor. Notably, the elevated internal resistance of the lithium TFB significantly influences the output voltage ripple, primarily due to the increased ohmic IR drop,  $V_{IR}$ , as presented in Chapter 3. However, the output voltage ripple still remains under 5% for output currents under 2 mA for all three studied operating frequencies. And even at 100 Hz the SBC has less than 10% voltage ripple for output currents under 4 mA.

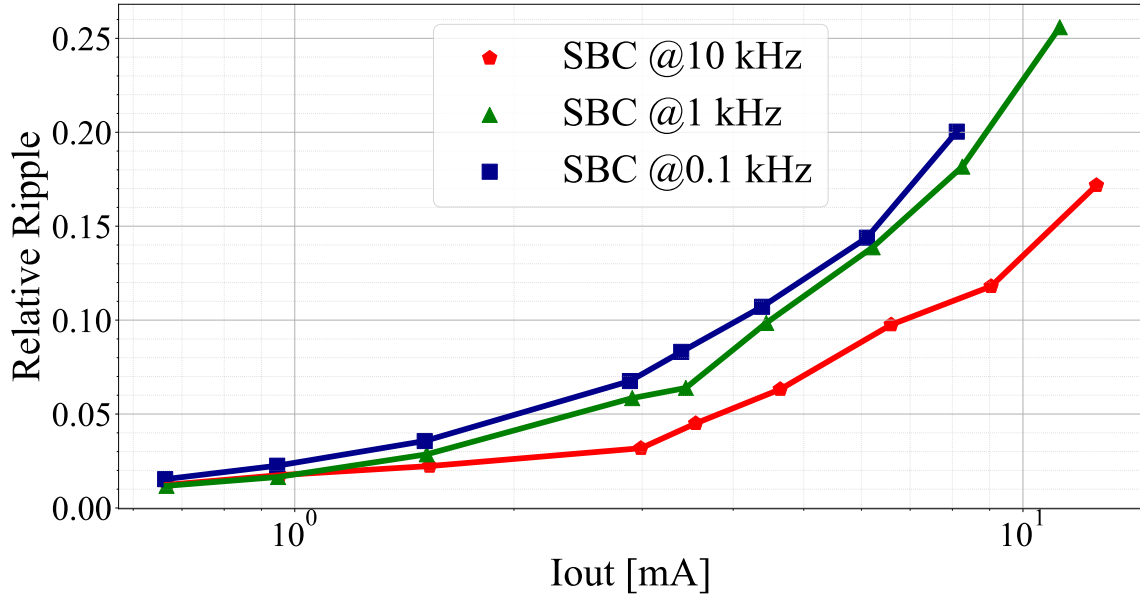


**Figure 5.4** | Relative output voltage ripple of 2:1 SBC using off-the-shelf EFL1K0AF39 thin-film battery at different operating frequencies

Fig. 5.5 illustrates the efficiency profile in relation to the output current. In comparison to the liquid electrolyte batteries, the overall efficiency of the SSB is notably lower, attaining a peak efficiency of 78% at 1 kHz and 76.8% at 100 Hz for an output current of 2 mA. Such peak efficiency is approximately 15% lower than the results achieved by the NiMH and Li-ion batteries (the output current levels are not directly comparable due to nominal capacity differences). At 10 kHz the battery reaches 80% efficiency for an output current of 9 mA and an output power of approximately 30 mW. Focusing on low frequency operation, while maintaining an efficiency of 70%, the TFB demonstrates the capability to yield an output power of approximately 24 mW at both frequencies of 100 Hz and 1 kHz, reaffirming its independence from frequency variations while still inside the ionic mobility regime.

This magnitude of output power translates to a power volumetric density of 200  $\mu\text{W}/\text{mm}^3$  (6x of the Li-ion battery and one third that of the NiMH). The larger density against Li-ion can be attributed to the TFB’s distinctive form factor and its elevated operating voltage. However, due to the limited capacity, it limits current delivery, and consequently output current and power, which puts it into disadvantage against the NiMH battery. Despite the TFB’s lower energy storage capacity, even at the lowest operation frequency and higher output current it still represents a DoD less than 0,005%.



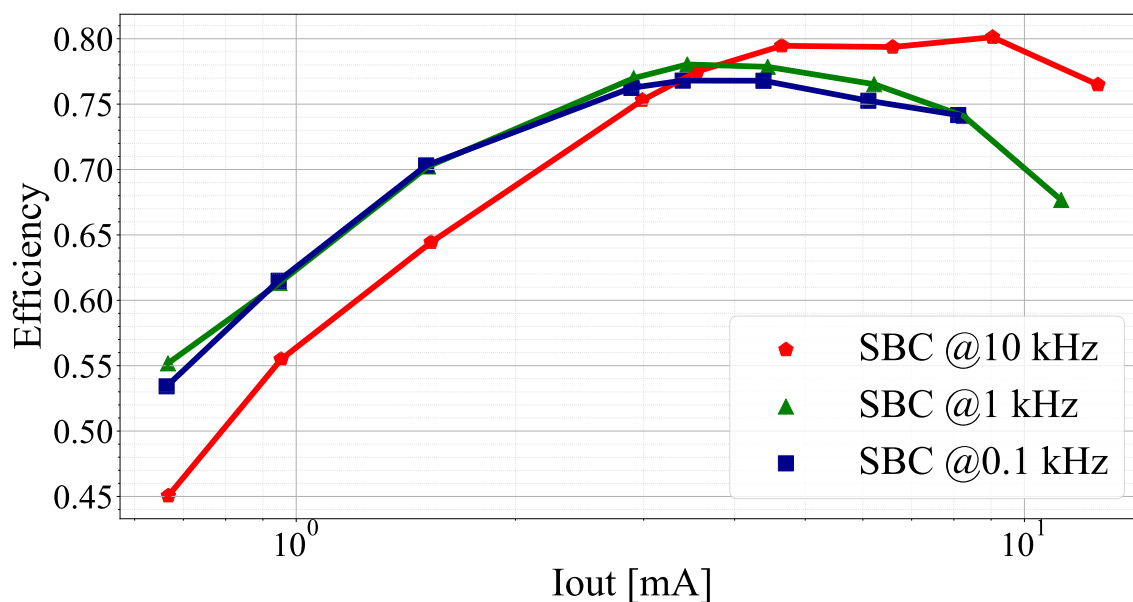


**Figure 5.5** | Efficiency of 2:1 SBC using off-the-shelf EFL1K0AF39 thin-film battery at different operating frequencies

In addition to the commercially available solid-state battery (SSB) investigated earlier, an exploratory analysis was conducted on a millimeter-scale thin-film battery (TFB) developed within CEA-Leti, aimed at achieving high-density energy storage [3]. This TFB showcases a cathode composed of  $\text{LiCoO}_2$  (20  $\mu\text{m}$ ) and LiPON (4  $\mu\text{m}$ ), encompassing a total surface area of 1.575  $\text{mm}^2$ , with the cathode's active pattern spanning 0.48  $\text{mm}^2$  giving an energy storage capacity of around 4.8  $\mu\text{Ah}$ .

In similarity to the previous battery evaluations, the latter TFB was integrated into the 2:1 switched-capacitor (SBC) configuration. The 2:1 SBC involving the Leti TFB transforms a 7.6 V input voltage to a 3.8 V output voltage. The study encompassed two operating frequencies: 100 Hz and 1 kHz. Nonetheless, due to constraints imposed by the battery being unpackaged, both the circuit and battery required a controlled environment with exceedingly low oxygen concentration.

Fig. 5.6 depicts the efficiency of the 2:1 SBC employing the TFB for varying output currents across the two operating frequencies. Notably, the Leti-TFB presents a considerably higher internal resistance compared to other examined technologies, largely due to its dimensions. This elevated internal resistance significantly influences TFB performance, leading to limitations in maximum output current, substantial output voltage drop, and an overall reduction in system efficiency. The peak efficiency of the 2:1 SBC utilizing the TFB is under 10% at both 100 Hz and 1 kHz. This low efficiency can be attributed to two primary factors:

- The off-the-shelf commercial IC requires a bias current consumption of at least 120  $\mu\text{A}$  solely for the oscillator at 100 Hz, with an even higher value at 1 kHz;
- The battery's internal impedance is estimated to range from  $\text{k}\Omega$  to tens of  $\text{k}\Omega$ , which is several orders

of magnitude higher than the other studied batteries.

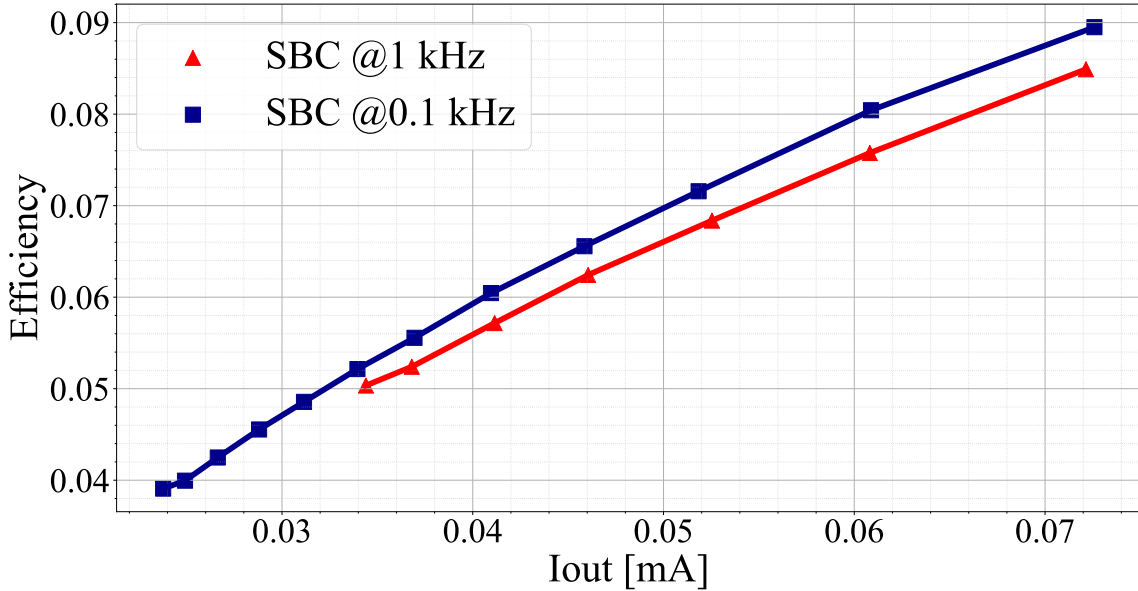


**Figure 5.6** | Efficiency of 2:1 SBC using millimeter-scale Leti thin-film battery at 100 Hz and 1 kHz operating frequency.

Due to the battery's substantial internal impedance, the average output voltage experiences a significant decline with increasing output current. To maintain the battery's operational conditions, which keeps the voltage within the safety range, the output current must be restricted, consequently limiting the output power. At the measured peak output power, the battery voltage nears the lower limit (3 V) for the battery. This limitation in output power explains the particular efficiency curve with no decrease at high output currents in Fig. 5.6.

Despite these challenges, the SBC with the diminutive battery dimensions still attains an output power density of  $1.78 \text{ mW/mm}^3$  (considering only the overall battery volume) at both tested frequencies, under peak efficiency conditions. These values surpass those of the other studied SSB by a considerable margin, nearly tenfold higher, despite lower efficiency. However at an ultra-low power output of  $200 \text{ }\mu\text{W}$ .

A deeper comprehension of the TFB SBC's low efficiency becomes clearer as the chosen off-the-shelf IC LM2663 is rated for 200 mA operation, whereas the circuit exhibits a peak output current that is over 2000 times lower. Designing an specific circuit focusing on such low power can profoundly affect the TFB SBC's performance. In addition, currently battery's primary design goal of achieving greater energy storage density [3] rather than high output power results in higher internal impedance, directly impacting power. efficiency. The potential demonstrated here suggests that addressing these design challenges could significantly influence the feasibility of expanding the SBC domain towards a fully integrated on-chip solution.

## II Exploration of weak MFCs

Fuel-cells are similar to batteries as both are electrochemical cells. In the case of fuel-cells they convert the chemical energy of a fuel and an oxidizing agent (usually oxygen [13]) into electricity through a pair of redox reactions [14]. Their main difference to regular batteries is their need of a continuous source of fuel and oxidizing agent to sustain the chemical reaction while in batteries the chemical energy is already stored inside the battery. A fuel-cell can produce electricity continuously as long as fuel and oxidizing agent are being supplied.

Due to the similarities between fuel-cells and batteries, they present themselves as candidates for intermediary storage device in DC-DC converters replacing batteries in a SBC. We explore the use of a subset of fuel-cells for this use, microbial fuel-cells.

### a Microbial Fuel-Cell

Microbial Fuel-Cell (MFC) is a type of fuel-cell that operates on a principle quite similar to other fuel-cell variants, such as hydrogen fuel-cells. There are two main types of MFCs, single-chamber and dual-chamber. A dual-chamber MFC is divided in two compartments, the first compartment houses the anode, containing the fuel (organic matter), and microorganisms in a low-oxygen environment. In contrast, the second compartment houses the cathode and is rich in oxygen. An exchange membrane impermeable to oxygen but permeable to the ions separates these two compartments.

In the anode compartment, microorganisms spontaneously adhere to the electrode surface and form a bacterial biofilm. Electro-active bacteria within this biofilm oxidize the surrounding organic matter in the absence of oxygen and transfer the electrons to the anode. These electrons then flow through a conductor to the cathode, where they react with the oxygen produced by the water (reduction of the oxygen). Both electrodes are constructed with conductor materials to ensure the efficient collection and transfer of electrons.

When a load is connected between the anode and the cathode, the chemical energy produced by the oxidation of the organic fuel can be converted into electrical energy. The power generated by the MFC is continuous but limited by factors such as the quantity of organic matter and its renewal around the anode, or the transport of hydrogen ions to the exchange membrane.

Particularly for single-chamber MFCs the cathode chamber and membrane are removed, and one side of the cathode is directly exposed to oxidants, commonly to the atmosphere (air cathode), and the other side to the anode, this is the type of MFC used here. Furthermore, for the remaining of the research single-chamber batch-mode MFCs are considered as opposed to in-flow MFC. The MFC is then a sealed reactor where nutrients have been incorporated along with waste material or purposely with ad hoc chemical compounds.

### **i Common Applications of MFCs**

Due to the potential of MFCs for energy scavenging and harvesting, a significant area of interest lies in their application as power supplies for sensors [10]. However, the contexts brought by distinct characteristics of MFCs give rise to various approaches in their use. Different MFC types, such as Benthic MFCs, Plant MFCs, or waste-water-based MFCs, result in diverse designs and electrical performances. Numerous studies have reported improvements in the power density of MFC reactors within each of these contexts [16]. The power density, measured using the cathode effective area as a reference metric, typically ranges from 50 mW/m<sup>2</sup> to 2000 mW/m<sup>2</sup>. Researchers explore combining elementary MFC reactors to achieve higher peak voltage or power levels, aiming to meet the power requirements of sensor payloads. Serially connected MFCs have been investigated in the literature, which shows that an active balance scheme becomes necessary to address the variability between individual MFCs [8].

### **ii MFC's Electrical Behavior and Performance**

In order to understand the electrical behavior of a single MFC or an array of MFCs, its I-V curve is analyzed, in which the fuel-cells work as a voltage source delivering power through a quite significant internal impedance. However, measuring the I-V curve of an MFC is quite challenging. One of the commonly used methods for such characterization is the potentiostat method [9]. It involves applying a defined resistive load at the MFC output and observing the variation of the output voltage. The measurement results in an I-V curve, which is shown in Fig. 5.7. The presence of microorganisms introduces specific time-constants, leading to an overall particular system response. Similar results are obtained through other characterization approaches [5].

Irrespective of the MFC technology or the method used for I-V curve evaluation, the electrical behavior is comparable to the typical I-V characteristic shown in Fig. 5.8. An output resistive load is varied and the effective MFC output power is evaluated. Under nominal conditions, the open-circuit voltage of an MFC typically ranges from 0.2 V to 1.2 V, with simple MFC reactors exhibiting about 0.8 V (e.g., waste water with 1 g/dm<sup>3</sup> acetate). The internal impedance of MFCs falls within the range of 100  $\Omega$  to 1000  $\Omega$  for specific configurations (e.g., waste water, single chamber, batch-mode MFC).

The internal impedance observed from the electrical output significantly impacts the electrical interface for energy scavenging, representing a major constraint. As an MFC weakens, its open-circuit voltage and overall electrical performance degrade, especially in batch-mode reactors as can be seen in Fig. 5.9. Temperature variations can also influence electrical performance in a similar manner. At a certain point, the open-circuit voltage and/or the MPP value may no longer be sufficient to operate a standard electrical interface, however its usage as an intermediate energy storage in a DC-DC converter is not discarded.

### **iii Energy Scavenging and DC-DC Converter for MFCs**

Efficiently scavenging energy from MFCs requires establishing Maximum Power Point (MPP) conditions, where the electrical interface connected to the MFC presents an input impedance similar to the MFC's

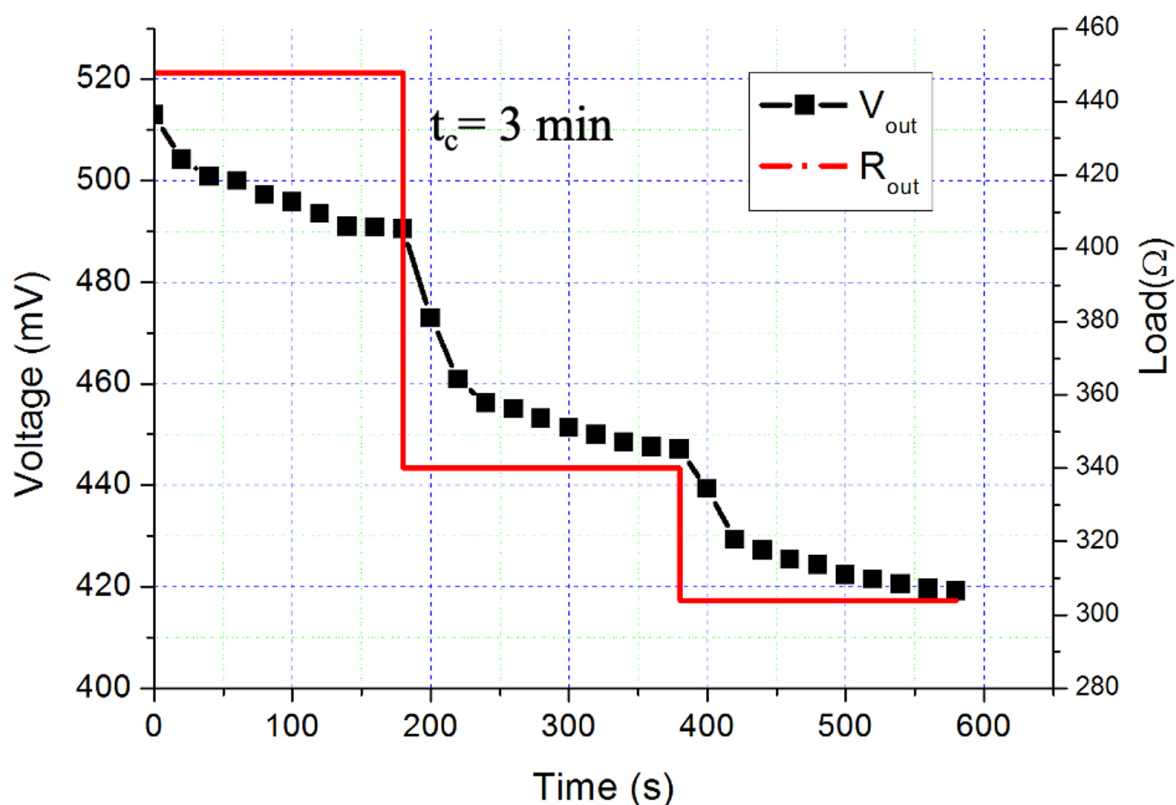


**Figure 5.7** | Electrical behaviour of an MFC under sudden changes of the output resistive load. 3 min delay is introduced between successive changes. [2]

internal impedance. Several DC-DC converter topologies have been explored for energy harvesting [6, 12, 17, 18].

In [12], it has been demonstrated that the combination of a BQ25505 IC with a TPS61200 IC results in an electrical interface capable of achieving an efficiency of 59.6%. However, for this setup to operate, an input voltage greater than 236 mV is required. The BQ25505 IC, designed by Texas Instruments, is specifically tailored for ultra-low-power battery charging with low-impedance low-power sources, with a maximum impedance of 100  $\Omega$ . On the other hand, the TPS61200 IC, also manufactured by Texas Instruments, serves as a high-efficiency synchronous DC-DC boost converter, allowing the output voltage to be configured between 1.8 V and 5.5 V.

Similar limitations are found in other commercially available integrated circuits, such as AEM10941 E-PEAS, NH2D0245 NOWI, and CITIUS CHIP. These integrated circuits exhibit relatively high open-circuit voltages and have MPP schemes that might not be optimally adapted to the dynamic behavior of MFCs, as illustrated in Fig. 5.7. Additionally, substantial research effort has been directed to address miniaturizing DC-DC converters. For instance, in the context of switched-capacitor voltage converters, advancements have been made using 3D silicon capacitors [11]. Similarly, in the case of magnetic voltage converters, 3D inductance has been explored [15]. Mimicking a specific input inductance is the main feature of the Flyback DC-DC converter in discontinuous conduction mode [4, 7]. However, the flyback's main transistor

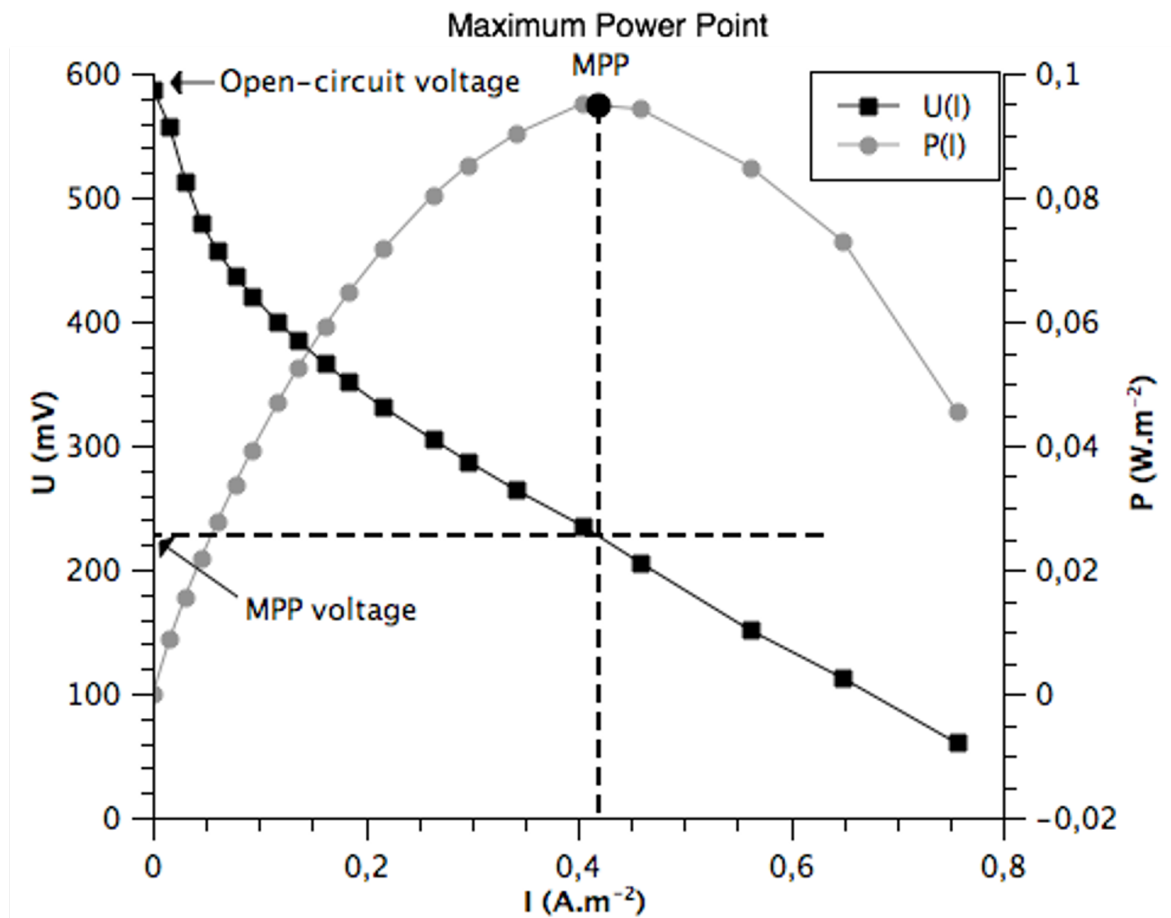


Figure 5.8 | MFC typical I-V characteristic. [2]

requires a nominal gate voltage that one MFC is not able to deliver alone. Usually requiring the use of cold-start circuits. But even then due to steady-state losses, the minimum cold start-up voltage is reported to be in the 120 mV to 180 mV in literature, which can be too high for weak MFCs.

In the context of weak MFCs, the utilization of such conventional DC-DC converters, presents strong limitations. These commercially available integrated circuits have a relatively high open-circuit voltage requirement, making them unsuitable for low-power sources like weak MFCs. An MFC is able to supply an ultra-low power IoT system but continuous operation is difficult to ensure. A group or plant of MFCs may be sufficient but it would render the system bulky. However, despite a weak MFC being rendered unsuitable for the use as a continuous energy source for such scenarios, its use as an intermediate energy storage device in a DC-DC converter can still be explored.

Since a weak MFC can't be used as the unique source to keep supplying a payload, the switched fuel-cell converter (SFC) studies the possibility of the MFC supporting a principal voltage source. Such main source could be also an MFC. Next section details the proposed converter and study if further energy is scavenged from this MFC and up to what level.

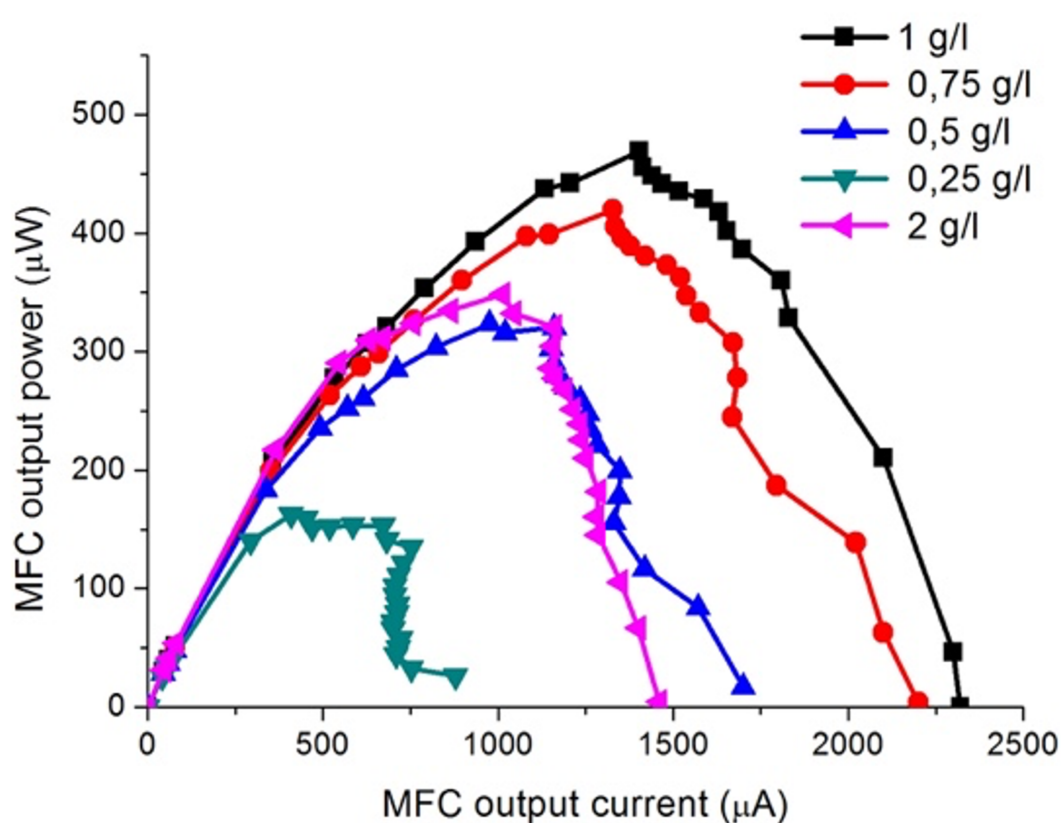


Figure 5.9 | Electrical performances of a single-chamber batch-mode MFC with various level of acetate density. [2]

## b Switched Fuel-Cell Converter (SFC)

The concept of switched-capacitor topology has been extended to batteries with the SBC. Such converter topology has the main interest in enhancing effective efficiency by a very low switching frequency in low power scenarios. The concept of the SBC is expanded further here by replacing the battery by a weak MFC, effectively creating the switched fuel-cell converter (SFC).

As weak MFCs already generate very small voltage values, a step-up converter proves to be a more suitable option. In this study, a voltage-doubler circuit is implemented, utilizing a single chamber MFC as the intermediate energy storage (Fig. 5.10). The voltage doubler circuit of a SFC, SBC and SCC have strong similarities due to the simplicity of employing a single intermediate energy storage device.

Derived from the SBC, the SFC operates within a  $\mu$ -cycle context. During phase  $\phi_1$ , the MFC receives a minimum amount of charge,  $\Delta Q$ . In phase  $\phi_2$ , the principal voltage source and the MFC jointly supply an amount of charge to the output capacitor and the load. During steady-state operation, the charge delivered by the MFC remains constant at  $\Delta Q$ , effectively delivering an amount of charge of  $-\Delta Q$  to the circuit. The implemented SFC converts a principal input voltage ( $V_{in}$ ) of 0.8 V into an output voltage of 1.6 V, with a switching frequency of 4 Hz, 10 Hz, 100 Hz, and 1 kHz. The goal of this implementation is to investigate the performance of the SFC and its potential as an effective energy converter utilizing weak MFCs, which would effectively extend their lifetime.

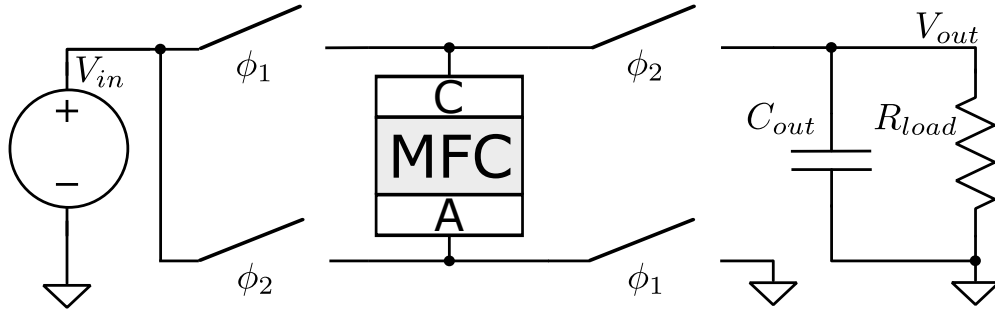


Figure 5.10 | Switched DC-DC voltage doubler using MFC.

### i Experimental Setup

As for the 2:1 SBC presented in Chapter 3, the circuit is implemented experimentally using the off-the-shelf switched-capacitor voltage converter integrated circuit LM2663 as shown in Fig. 5.11.

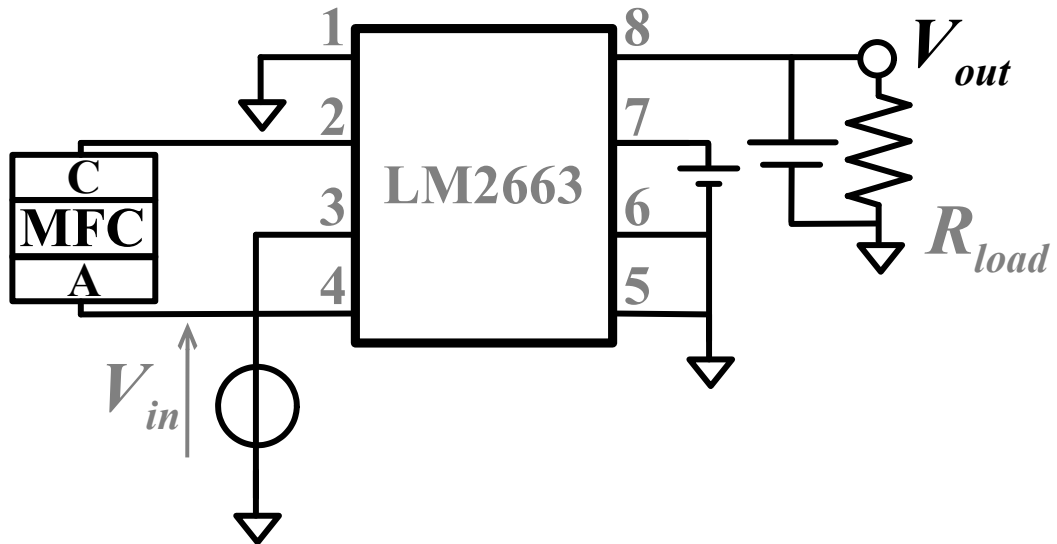


Figure 5.11 | Electrical circuit under study.

A lab-scale, batch-mode, one-chamber depleted MFC is used ( $V_{OC} < 300$  mV). The principal voltage source is a low-impedance power supply set to 800 mV. Despite the MFC's initial open-circuit voltage being significantly low, upon the SFC reaching steady-state, the MFC reaches an operating point where its effective voltage is close to the voltage imposed by the principal voltage source (800 mV). An MFC features a capacitive behavior related to its electrical electrodes. This behavior resembles closely the BVSA phenomena present in the SBC and presented in Chapter 3.

The LM2663 has an internal oscillator with an adjustable frequency, which can be externally tuned using a network of capacitors. Table 5.1 shows the values of the equivalent capacitor network  $C_{osc}$  for operating frequencies between 4.2 Hz and 10 kHz.

The cold-start conditions of the system have not been addressed. The output capacitor,  $C_{out}$ , is



**TABLE 5.1** | CAPACITOR NETWORK VALUE FOR OPERATION OF LM2663 WITH THE MFC

Frequency [Hz]	4.2	10	100	1k	10k
Capacitance [nF]	800	405	22.5	3.5	0.4

precharged to 1.6 V prior to any evaluation. The input voltage is set at a fixed value of 800 mV to simulate a scenario where the primary battery (working as  $V_{in}$ ) becomes depleted gradually over a long-term period. It is assumed that the system will continue to operate even as the input voltage decreases. However, the commercial IC LM2663 requires a minimum output voltage of 1.2 V (on voltage doubler configuration) for a proper start-up. Such condition is not met from a strict point-of-view. Therefore, precharging the output capacitor serves as a rapid solution to overcome the startup issue and ensure the successful operation of the system.

For any frequency, a sufficient transient time is allowed for reaching a steady-state. Said otherwise the depleted MFC is allowed to perform the voltage self-adjustment behavior until its output voltage settles to 800 mV, the voltage imposed by the principal source.

## ii Performance

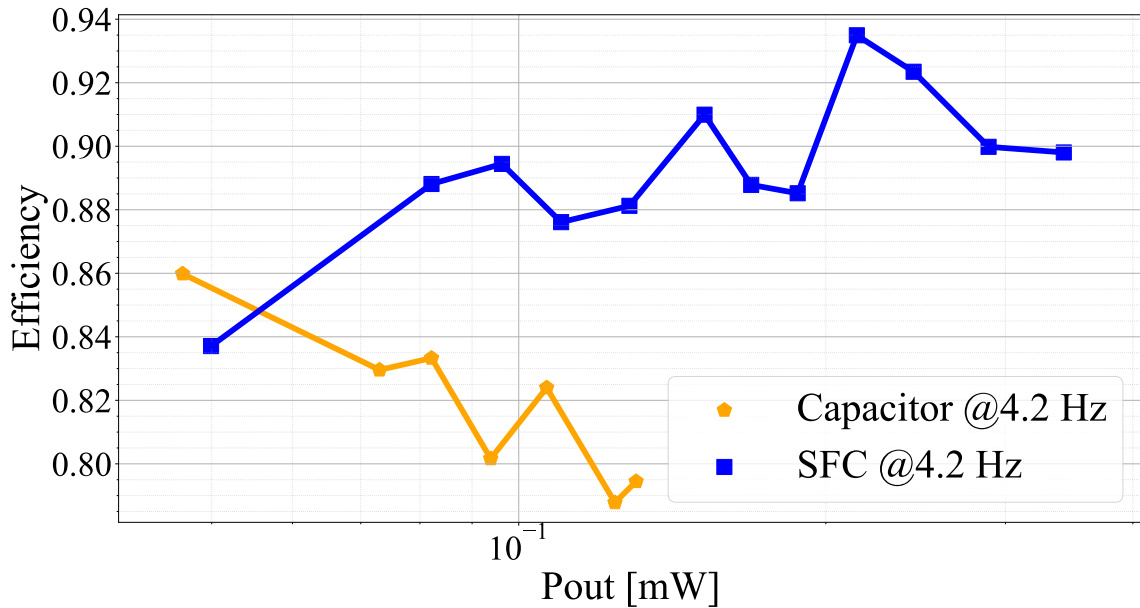
The output current  $I_{out}$  in the load resistor  $R_{load}$  varies between 30  $\mu$ A and 1 mA under different experimental conditions. To evaluate the efficiency, the current delivered by the principal source  $V_{in}$  is measured using a series shunt resistor of 10  $\Omega$ . During phase  $\phi_1$  of operation, the MFC absorbs a certain amount of energy, while it desorbs another amount of energy during phase  $\phi_2$ . One of the main interest is to assess whether the effective action of the MFC is akin to that of a passive capacitor, or if energy is indeed scavenged from the MFC during its operation in the SFC. To address such question the operation of the SFC is compared to that of an equivalent SSC. However, determining the equivalent capacitance of the MFC is not a straightforward task.

Fig. 5.12 provides a primary comparison between the SFC with a depleted MCF and an SSC equipped with a capacitor of 110  $\mu$ F at an operating frequency of approximately 5 Hz. The relatively large capacitor value seems to support the notion of capacitive behavior exhibited by the MFC, as observed from an impedancemetry point of view.

At low frequency, the internal impedance of a SCC is, as expected, quite high. It impacts in a decrease of efficiency with larger output current amplitude. The SFC does not present a similar behaviour which proves that:

- the MFC does not operate exclusively as a capacitor (similarly to what happens with the battery in the SBC);
- the MFC, though depleted, is able to provide a certain amount of energy to the output.

Considering this behavior by the SFC, makes that the classic relation of efficiency demonstrated by the ratio of output power over input power of the circuit is not strictly held. In this case the efficiency can be considered as a pseudo-efficiency, considering that there energy being independently provided by the MFC.



**Figure 5.12** | Comparison between an SFC and an SCC with corresponding conditions at 4.2 Hz.

Fig. 5.13 presents the efficiency of the voltage-doubler SFC with respect to output power ( $P_{out}$ ) at various operating frequencies. The SFC, employing a depleted MFC, achieves a peak output power of 1.4 mW while maintaining high efficiency ( $>90\%$ ). Notably, the SFC maintains an efficiency greater than 90% across an output power range exceeding 1.2 mW, with a peak efficiency of 97.25% observed at an operating frequency of 100 Hz. In the power range of 0.2 mW to 1.2 mW, the SFC demonstrates an effective efficiency surpassing 94%. When compared to an equivalent SCC operating under similar conditions, the SFC presents a better operation than the SCC counterpart. Regardless of the type of capacitor employed to substitute the MFC, the resultant efficiency is consistently lower. Additionally, the SFC exhibits reduced output voltage ripple across all operating frequencies. These findings collectively suggest that the behavior of the MFC in this setup is not purely analogous to that of a passive capacitor, as evidenced by the somewhat higher efficiency compared to the SCC.

The operating frequency has an impact on efficiency, as depicted in Fig. 5.13. Surprisingly, a lower frequency appears to affect the LM2663 driver as the static consumption should be lower, which is not experimentally confirmed. Nevertheless, the circuit maintains remarkable efficiency levels at 10 Hz, with efficiency exceeding 90% for output powers ranging from 155  $\mu$ W to 814  $\mu$ W. Notably, even at a modest output power of 50  $\mu$ W, an efficiency of over 75% is sustained at 10 Hz, emphasizing the robustness of the SFC under varying operating conditions.

Fig. 5.14 presents the output voltage ripple of the SFC under various operating frequencies and compares it to the output voltage ripple of a conventional SCC at 10 Hz. As expected, lower frequencies result in increased output voltage ripple, as shown in Fig. 5.14a. Furthermore, the figure reveals that at

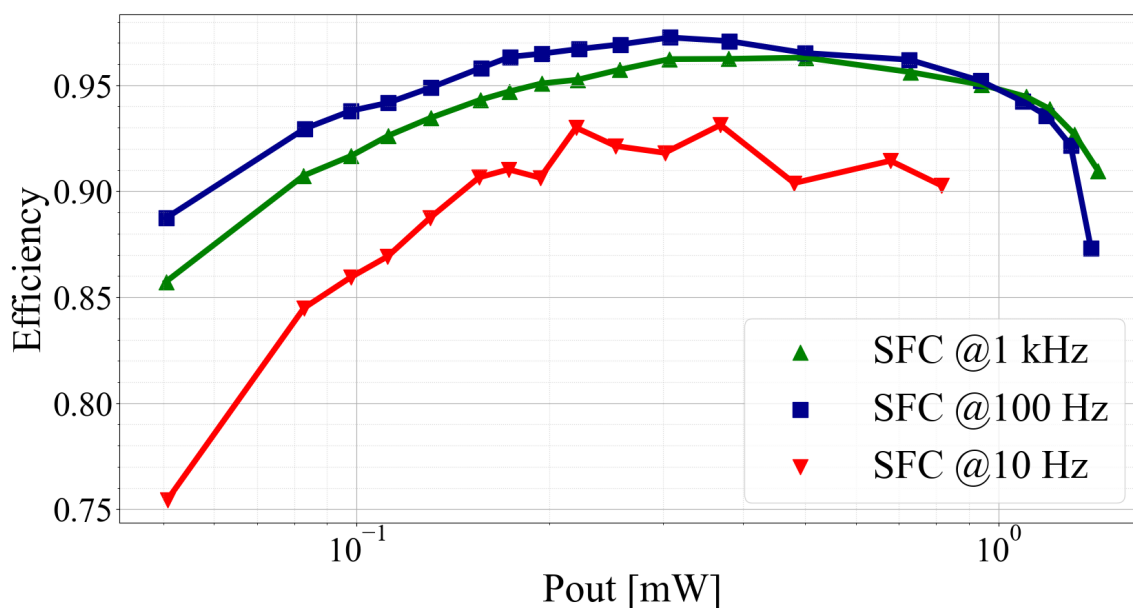


**Figure 5.13** | Efficiency of voltage-doubler SFC against output power at different frequencies.

each specific frequency, higher power output corresponds to higher output voltage ripple. For instance, at an operating frequency of 4.2 Hz, the output voltage ripple reaches 7.8% while having a maximum output power of 342  $\mu$ W. Similarly, at 10 Hz the SFC has a maximum output power of 841  $\mu$ W, and the ripple reaches nearly 10% of the output voltage. In contrast, at higher operating frequencies, the ripple diminishes to below 0.6%, an acceptably low value for most DC-DC applications. These high-frequency conditions allow the output power to achieve levels as high as 1.4 mW. The ability to achieve higher output power at higher frequencies is attributed to the reduced ripple, which prevents momentary voltage excursions that might be unsupported by the off-the-shelf IC. At high frequency, the charge exchanged by the MFC is smaller and better suits the MFC operation.

It is noteworthy that, despite the primary input source contributing to the majority of the output power regardless of the operating frequency, the MFC's behavior is perturbed at very high frequency. Nevertheless, there is promising indications for a successful exploitation of MFCs in a SFC configuration, despite 10 Hz still being a relatively high frequency when compared to the time-constants of regular MFCs.

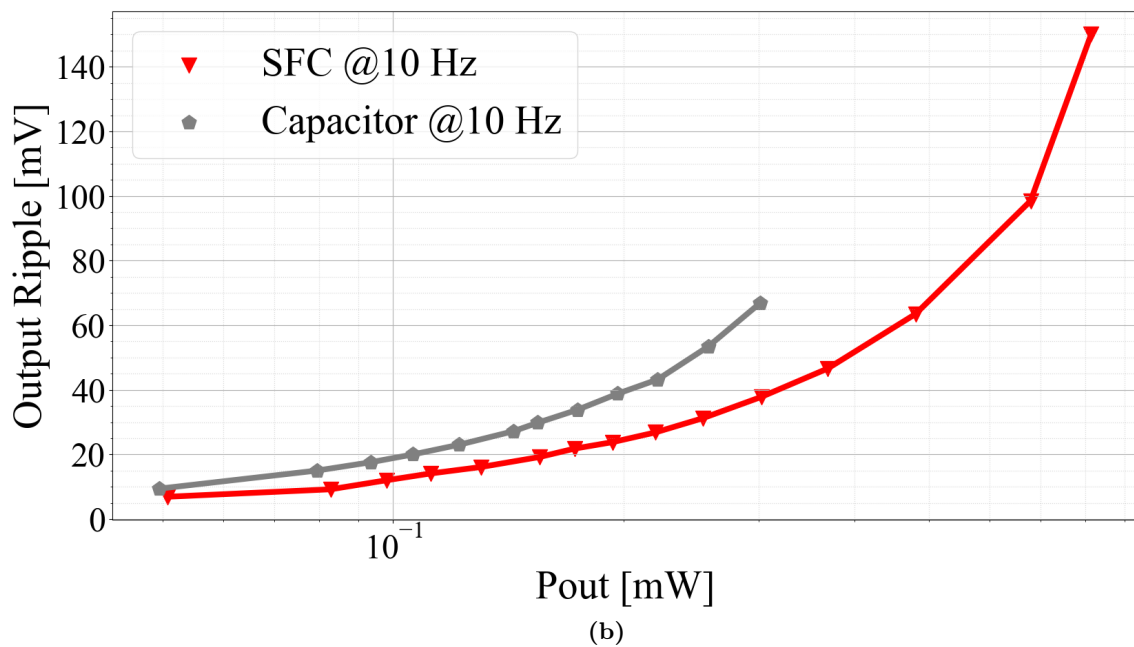
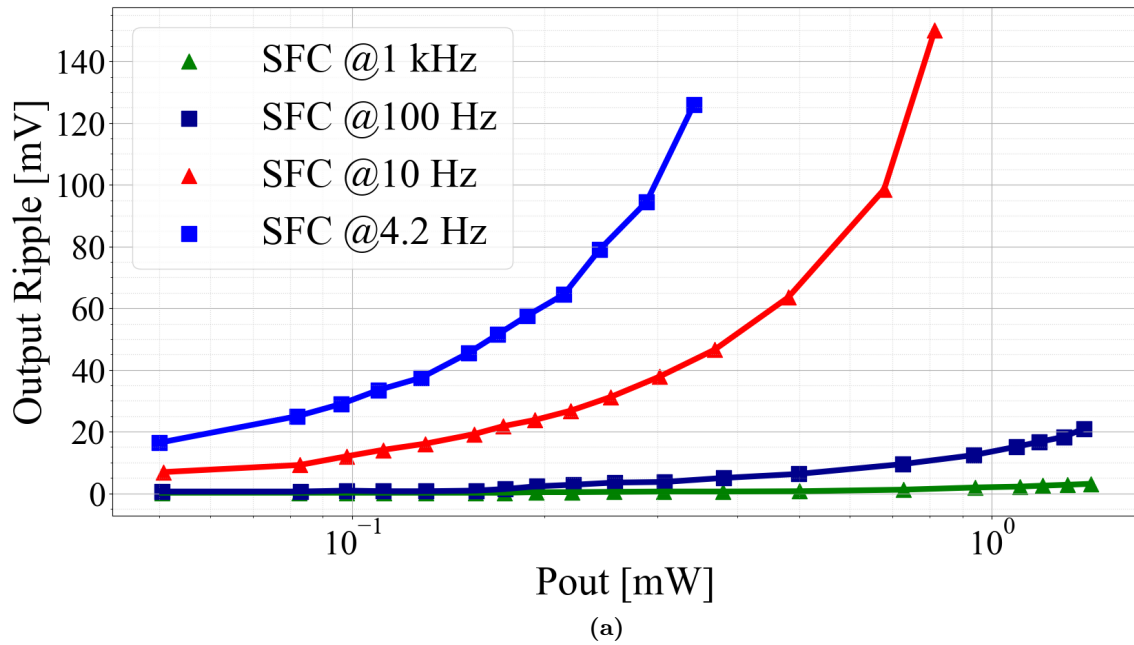


Figure 5.14 | Output voltage ripple of SFC (a) comparison against SCC and (b) response to operating frequency

The potential capacitive behavior of the MFC can be speculated at tested operating frequencies. Fig. 5.14b provides a comparison between the SFC and an SCC featuring a 110  $\mu\text{F}$  capacitor, a value close to the effective capacitance of the MFC. At 10 Hz, the SFC consistently exhibits lower output voltage ripple compared to its SCC counterpart. Although 10 Hz represents a relatively high frequency relative to the MFC's natural time-constants, as elucidated earlier, the MFC's behavior does not entirely align with that of a standard capacitor. The SFC's superiority in maintaining lower output voltage ripple allows it to achieve substantially higher output power than the SCC counterpart (300  $\mu\text{W}$  by the SCC against 841  $\mu\text{W}$  of the SFC).

The results underscore the feasibility of utilizing a weak or depleted MFC within the SFC framework, allowing for effective energy scavenging. Despite the challenging electrical characteristics posed by a depleted MFC in traditional energy harvesting interface circuits, the SFC topology presents an innovative solution to address these challenges.

### III Conclusion

This chapter focused on exploring other battery chemistry options for the SBC and to entertain the possibility of the use of MFCs as intermediate storage device in place of batteries in the SBC. It extends from established chemistries like Li-Ion to innovative Solid-State Batteries (SSBs), revealing their unique potential contributions to the SBC's operation.

While each battery chemistry holds its distinct traits, a recurring constraint of the SBC framework is the close connection between output voltage ( $V_{out}$ ) and battery voltage range. Despite the dynamic self-adjustment mechanism detailed in Chapter 2, and the potential relaxation of this constraint with higher voltage conversion ratios elucidated in Chapter 4, this attribute remains a foundational limitation. Operating voltage limits intrinsic to batteries can wield considerable influence on the versatility of the SBC. To circumvent these constraints and explore diverse output voltage values, the adoption of alternative battery chemistries, like Li-Ion, emerges as a potential solution. This introduces an avenue for further investigation, probing the advantages and drawbacks of integrating such chemistries into the SBC paradigm.

The exploration expands to the domain of Solid-State Batteries (SSBs), an emergent technology boasting solid-state electrolytes as a safer, more energy-dense, and long-lasting alternative. The study encompasses both commercial and experimental SSBs, with a focus on their behavior within the 2:1 SBC circuitry. These SSBs, with their distinct characteristics, exhibit their efficacy in different operating scenarios, underlining their viability as candidates for energy storage within the SBC framework. The outcomes, as evidenced by ripple and efficiency profiles, showcase their unique potential, where TFBs particularly excel in power density despite limitations in efficiency.

Common to the studied battery technologies is that the obtained results show that they can give acceptable performances to the 2:1 SBC, as long as they are kept operating with a very small DoD, even for batteries with low capacity. An exception is made for the millimetric TFB as the performance was degraded due to the non-optimal circuit and predominant static losses.

### III. CONCLUSION

---

Lower energy storage capacity of the batteries is linked with a higher internal resistance impacting on a smaller output current range when operating at high efficiency and consequently lower maximum output power. The higher voltage operating range benefits when exploring higher output power to some degree, as the capacity and internal resistance still limit the achievable output current. Some batteries also present a wider voltage range, favoring the exploration of flexible operating conditions. Nevertheless, as the tested batteries also presented the self-adjustment behavior described in Chapter 2, it is clear that they successfully enable a wider operating voltage range for the 2:1 SBC.

The chapter pivots to the integration of weak Microbial Fuel Cells (MFCs) into the SBC paradigm. This innovative concept introduces a pioneering avenue that not only optimizes energy scavenging but also extends primary battery lifespan. The interplay between MFCs and batteries yields benefits that cannot be attained by conventional converters. However, while these findings present a remarkable stride forward, further investigations beckon. Deeper analyses of the MFC behavior over time, exploration of multi-source configurations, and enhanced circuit designs are some of future investigations needed for the use of MFCs as intermediate energy storage devices in DC-DC converters.



# Bibliography

- [1] Q. Cai, D.J.L. Brett, D. Browning, and N.P. Brandon. A sizing-design methodology for hybrid fuel cell power systems and its application to an unmanned underwater vehicle. *Journal of Power Sources*, 195(19):6559–6569, 2010.
- [2] Armande Capitaine, Gael Pillonnet, Thibaut Chailloux, Adrien Morel, and Bruno Allard. Impact of switching of the electrical harvesting interface on microbial fuel cell losses. In *2017 IEEE SENSORS*, pages 1–3, 2017.
- [3] Jacopo Celè, Sylvain Franger, Yann Lamy, and Sami Oukassi. Minimal architecture lithium batteries: Toward high energy density storage solutions. *Small*, 19, 01 2023.
- [4] T. Chailloux, Armande Capitaine, Benjamin Erable, and G. Pillonnet. Autonomous sensor node powered by cm-scale benthic microbial fuel cell and low-cost and off-the-shelf components. *Energy Harvesting and Systems*, 3:205 – 212, 2016.
- [5] Ka Yu Cheng, Ralf Cord-Ruwisch, and Goen Ho. A new approach for in situ cyclic voltammetry of a microbial fuel cell biofilm without using a potentiostat. *Bioelectrochemistry*, 74(2):227–231, 2009.
- [6] Nicolas Degrenne, Bruno Allard, François Buret, Florent Morel, Salah-Eddine Adami, and Denis Labrousse. Comparison of 3 self-starting step-up dc:dc converter topologies for harvesting energy from low-voltage and low-power microbial fuel cells. In *Proceedings of the 2011 14th European Conference on Power Electronics and Applications*, pages 1–10, 2011.
- [7] Nicolas Degrenne, Marilyne Boileau, Florent Morel, Firas Khaled, Olivier Ondel, Francois Buret, and Bruno Allard. Association of flyback converters to harvest energy from multiple hydraulically connected biofuel cells. In *2012 IEEE International Conference on Green Computing and Communications*, pages 664–667, 2012.
- [8] Firas Khaled, Olivier Ondel, Bruno Allard, and François Buret. Voltage balancing strategies for serial connection of microbial fuel cells. *The European Physical Journal Applied Physics*, 71(1):10904, 2015.
- [9] Catarina Lousa Marques. *Theoretical Analysis of a Potentiostat for Studying Microbial Fuel Cells*. PhD thesis, Universidade da Beira Interior (Portugal), 2021.
- [10] Edith Osorio-de-la Rosa, Javier Vázquez-Castillo, Alejandro Castillo-Atoche, Julio Heredia-Lozano, Andrea Castillo-Atoche, Guillermo Becerra-Nuñez, and Romeli Barbosa. Arrays of plant microbial fuel



- cells for implementing self-sustainable wireless sensor networks. *IEEE Sensors Journal*, 21(2):1965–1974, 2021.
- [11] Emeric Perez, Yasser Moursy, Sami Oukassi, and Gaël Pillonnet. Silicon capacitors opportunities for switched capacitor converter. In *2022 IEEE 23rd Workshop on Control and Modeling for Power Electronics (COMPEL)*, pages 1–6, 2022.
- [12] Celso Recalde, Denys López, Diana Aguay, and Víctor J. García. Environmental sensing in high-altitude mountain ecosystems powered by sedimentary microbial fuel cells. *Sensors*, 23(4), 2023.
- [13] Kaustav Saikia, Biraj Kumar Kakati, Bibha Boro, and Anil Verma. *Current Advances and Applications of Fuel Cell Technologies*, pages 303–337. Springer Singapore, Singapore, 2018.
- [14] R.S.K.R.S. Sedha. *Materials Science*. S. Chand Limited, 2008.
- [15] Chandra Shetty and Daniel C. Smallwood. Design, modeling, and analysis of a 3-d spiral inductor with magnetic thin-films for pwr soc/pwr sip dc-dc converters. *IEEE Access*, 10:92105–92127, 2022.
- [16] Wanjing Wu, Duwei Zhang, and Ping Fang. Advance in improving the electrical performance of microbial fuel cell. *IOP Conference Series: Earth and Environmental Science*, 555(1):012004, aug 2020.
- [17] Heng Xiao, Nanjian Qi, Yajiang Yin, Shijie Yu, Xiangzheng Sun, Guozhe Xuan, Jie Liu, Shanpeng Xiao, Yuan Li, and Yizheng Li. Investigation of self-powered iot sensor nodes for harvesting hybrid indoor ambient light and heat energy. *Sensors*, 23(8):3796, 2023.
- [18] Haoquan Zhang, Konstantin Martynov, Duanhui Li, and David J. Perreault. A cmos-based energy harvesting approach for laterally-arrayed multi-bandgap concentrated photovoltaic systems. In *2019 IEEE Energy Conversion Congress and Exposition (ECCE)*, pages 3394–3401, 2019.

# Conclusion

In the pursuit of efficient and sustainable energy solutions for modern electronics, this work pursued an exploration of low-power DC-DC converters. Spanning five chapters, each meticulously crafted to contribute unique insights and advancements, this research journey has unfolded with the ultimate aim of revolutionizing the field of low-power energy conversion.

First Chapter 1 established a foundation to the work by investigating the ever-expanding demand for energy-efficient power solutions in our increasingly electronic-dependent world. It introduced the pivotal role played by DC-DC converters in facilitating the seamless transformation of electrical energy between varying voltage levels, an essential function for the operation of a diverse array of electronic components. The chapter briefly presented the two classes of DC-DC converters: linear and switched. While linear converters depend on resistive voltage drops for voltage regulation, switched converters harness the power of energy storage and periodic release to achieve precise voltage transformations. For the remaining of the work the focus relies towards switched DC-DC converters, which revolve around central passive devices, traditionally capacitors and inductors. Next is the exploration of the specific challenges encountered in the realm of low-power switched DC-DC converters. Describing how the aiming for heightened efficiency, reduced footprint and enhanced power density becomes increasingly demanding as power budgets shrink. This category of converters finds applications in a myriad of industries, ranging from the realm of medical devices and wireless sensor networks to the realm of portable consumer electronics and the integration of renewable energy sources into power grids.

Efficiency, power, and footprint emerged as the defining characteristics of low-power DC-DC converters. It is a poignant reminder that sustaining high efficiency at ultra-low power levels can pose an intricate challenge due to the newfound significance of previously overlooked factors, such as leakage and switching losses.

Stepping into the spotlight, SCCs took center stage as the go-to solution for achieving high power density in low-power applications. However, the complex balance between efficiency and footprint remains an important step in the world of SCCs. The relentless pursuit of high efficiency often led to the enlargement of converter footprints, and the integration of high-density capacitors do not always yield the expected enhancements.

This exploration of the state of the art of low-power DC-DC converters transitioned seamlessly to Chapter 2, where a spotlight is pointed on the concept of incorporating batteries as the central intermediate

energy storage device in DC-DC converters. The chapter presents the benefits of working at low frequencies for low-power applications. As the output power of batteries remains fundamentally frequency-independent at first order, they offer a distinct advantage over capacitor and inductor-based converters in these domains. This emphasis on low frequencies was necessitated by the formidable challenge posed by traditional passive technologies, which demand considerable footprints, thereby sacrificing power density.

In response to the limitations inherent to batteries, Chapter 2 presented a novel family of converter topologies known as Switched-Battery Converters (SBCs). These innovative converters use batteries as flying energy storage devices, providing an alternative approach to the persistent challenges posed by low-frequency, low-power applications. The chapter detailed the processes required to establish valid phases and working cycles within these SBC topologies, underscoring the importance of reliability and operational efficiency.

Moreover, Chapter 2 briefly ventured into the realm of optimization for these operational cycles, offering potential strategies to enhance practical implementation and physical performance. These optimization techniques promised to elevate the overall efficiency, reliability, integrability, and effectiveness of converter systems employing batteries as flying passive devices.

Chapter 3 presented the experimental verification of the SBC's viability, substantiating its claim to deliver efficient and reliable power conversion, particularly excelling in the low-frequency domain. It went further offering a comparative analysis of the new SBC topologies against existing SCC architectures in practical scenarios. In this realm, the SBC outshone its predecessor, the SCC, by exhibiting superior performance in terms of output voltage ripple, efficiency, and power density.

The validation of the SBC in an open-loop 2:1 converter configuration not only validated its capabilities but also set the stage for deeper exploration and development. The chapter introduced some unique characteristics of the SBC, notably the Battery Voltage Self-Adjustment (BVSA) mechanism, and its operation with an extremely low Depth of Discharge (DoD), which held the promise of significantly extending battery lifespans. However, some questions were left unanswered, especially regarding the long-term impact of SBC operation on battery performance and degradation.

While the initial validation primarily focused on single flying element configurations, it paved the way for Chapter 4's exploration of SBC topologies featuring multiple flying batteries. By incorporating more than one flying battery, higher conversion ratios could be achieved, expanding the range of potential applications for the SBC, especially with the BVSA mechanism. This exploratory journey was grounded in principles patented during the thesis research, lending further credence to the SBC as a promising alternative to conventional DC-DC converters in low-power, low-frequency scenarios.

Furthermore, Chapter 3 acknowledged the need to delve into closed-loop operation and control strategies for SBC circuits, recognizing that this exploration would maximize their performance and stability, opening doors to a wider range of load conditions.

Chapter 4 then transitioned into the realm of topologies with multiple batteries, notably the 3:1 and 4:1 SBC configurations. With meticulous analysis, this chapter offered valuable insights into the performance and efficiency of these novel power stage circuits.

---

The 3:1 SBC emerged as a capable contender, converting input voltages with precision and maintaining remarkable output voltage ripple even at low switching frequencies. It confirmed once again the SBC frequency independence by maintaining high conduction efficiency irrespective of operating frequency. However, the chapter also acknowledges the inherent complexity of the design and its impact on achievable power density, which lagged behind its 2:1 counterpart.

On the other hand, the 4:1 SBC showed its ability to convert voltages in a 4:1 ratio while making use of batteries operating at different voltage levels. Its efficiency performance, notably frequency independence, strengthened the claim for expanding SBC applications. While it didn't match the power volume density of the 2:1 SBC, the 4:1 SBC presented intriguing performance benchmarks.

Both configurations with multiple batteries confirmed the unique characteristics, notably the BVSA mechanism's persistence, a behavior seldom observed in conventional DC-DC converters. Nevertheless, Chapter 4 reminded us of a crucial aspect—every SBC implementation thus far had operated in an open-loop system.

Chapter 4 then focuses towards exploring control strategies for SBC circuits. It was discussed that the best strategy seems to be a two-stage control, as employed in SCCs. It involves a coarse grain control, consisting in changes in circuit phases and cycles, similar to a SCC gearbox approach, and a fine grain control, as a frequency modulation used in SCCs. However, frequency modulation do not align with the SBC's highly frequency-independent nature, requiring alternative approaches, like duty cycle modulation or the possible integration of Low Dropout Regulators (LDOs) at the output.

As this chapter concluded, it promises the the exploration of diverse battery chemistries and their impact on SBC performance in Chapter 5.

Chapter 5 explores alternative battery chemistries, ranging from the established Li-Ion batteries to the innovative Solid-State Batteries (SSBs). Each chemistry brought its unique characteristics to the table, and yet, a common constraint persisted, the intricate relationship between the SBC's output voltage and battery voltage, a link that remained foundational to the SBC framework. Despite the dynamic self-adjustment mechanism, the constraints imposed by battery operating voltage limits stood as a factor complicating the expansion of the SBC's versatility.

Li-Ion batteries entered the spotlight as a potential solution, promising higher output power capabilities and enabling exploration of diverse output voltage values. This presented an exciting avenue for research, promising to uncover the advantages and drawbacks of integrating such chemistries into the SBC paradigm.

The exploration also investigated Solid-State Batteries (SSBs), a technology boasting solid-state electrolytes and offering a safer, energy-dense, and long-lasting alternative. Commercial and experimental SSBs were tested with the 2:1 SBC, revealing their efficacy under different operating scenarios. The outcomes, characterized by ripple and efficiency profiles, showcased their potential, with Thin Film Batteries (TFBs) particularly excelling in power density despite certain efficiency limitations.

This exploration underscored a common thread: these battery technologies exhibited acceptable performances in the 2:1 SBC, provided they operated with a minimal Depth of Discharge (DoD). Exceptions were made for millimetric TFBs, whose performance was compromised due to non-optimal circuit designs

and predominant static losses at the output power level. The chapter highlighted the intriguing interplay between energy storage capacity, internal resistance, output current range, and voltage operating range, with batteries showcasing adaptability through the BVSA behavior, expanding the operating voltage range for the 2:1 SBC.

However, the study was not limited only to batteries. It expanded the concept of the SBC to explore integrating Microbial Fuel Cells (MFCs) as energy storage devices, pushing the boundaries of energy scavenging and primary battery lifespan extension. The relationship between MFCs and batteries unveiled benefits that can transcend conventional converters, opening space to even expand their use in energy harvesting.

This chapter ended setting the stage for further investigations. Deeper analyses of MFC behavior over time, exploration of multi-source configurations, and enhanced circuit designs points towards promising fields in the utilization of MFCs as intermediate energy storage devices in DC-DC converters.

In summation, this thesis has been an intellectual journey through the intricate world of low-power DC-DC converters, spearheaded by the innovative SBC topology. From its inception in Chapter 1 to the promising possibilities unveiled in Chapter 5, this research has not only expanded our understanding of energy conversion but also opened new horizons for sustainable and efficient power solutions. The future research directions outlined in each chapter hold the promise of further enhancing the SBC's capabilities, broadening its applications, and paving the way for a greener and more efficient future in the realm of low-power electronics.



## FOLIO ADMINISTRATIF

### THESE DE L'INSA LYON, MEMBRE DE L'UNIVERSITE DE LYON

NOM : BERLITZ

DATE de SOUTENANCE : 20/12/2023

Prénoms : Carlos Augusto

TITRE : Switched Battery DC-DC Converters for Low-Power Applications

NATURE : Doctorat

Numéro d'ordre : 2023ISAL0118

Ecole doctorale : 160 - Électronique, Électrotechnique, Automatique (EEA)

Spécialité : Électronique, micro et nanoélectronique, optique et laser

RESUME : Avec la popularisation récent des dispositifs électroniques portables, des capteurs sans fil et de l'Internet des objets (IoT), la demande de solutions de gestion d'alimentation efficaces et adaptables a atteint des sommets sans précédent. Les applications à faible puissance, couvrant un large éventail de domaines et sont devenues essentielles à notre mode de vie moderne. Ces applications, souvent alimentées par des ressources énergétiques limitées, présentent un ensemble unique de défis et d'opportunités dans le domaine de l'électronique de puissance. Alors que les convertisseurs CC-CC traditionnels ont démontré leur efficacité dans de nombreuses situations, leurs conceptions conventionnelles pourraient ne plus suffire à répondre aux exigences distinctes et strictes des systèmes à faible et ultra-faible puissance. La recherche des nouveaux convertisseurs CC-CC commuté spécifiquement adaptés aux applications à faible puissance est au cœur de cette thèse.

Traditionnellement, les convertisseurs CC-CC reposent sur des inducteurs ou des condensateurs pour une conversion à haute efficacité. Cependant, malgré les avancées dans des nombreux domaines de l'électronique de puissance, certaines limitations physiques et intrinsèques subsistent dans le domaine de faible-puissance, telles que les pertes de partage de charge ou la difficulté de miniaturisation des inducteurs. De telles contraintes appellent à des solutions innovantes pour ce genre d'application des convertisseurs CC-CC.

Cette thèse propose une solution pour relever les défis intrinsèques aux convertisseurs CC-CC traditionnels, une nouvelle famille de topologies de convertisseurs CC-CC à basse fréquence et faible puissance basée sur des batteries en tant que dispositif passif volant. Cette nouvelle famille de topologies est validée expérimentalement avec des avantages par rapport aux convertisseurs CC-CC traditionnels dans les mêmes conditions. Cela ouvre également un nouveau domaine d'étude pour les technologies passives jusqu'alors non explorées dans ce contexte, comprennent des batteries et piles à combustible.

MOTS-CLÉS : convertisseur CC-CC, faible-puissance faible-fréquence, batteries, convertisseur commuté

Laboratoire (s) de recherche : Ampère UMR CNRS 5005

Directeur de thèse: Bruno Allard, Professeur des Universités, INSA de Lyon

Président de jury :

Composition du jury :

Cousineau, Marc, Maître de Conférences, Toulouse INP  
Prodic, Aleksandar, Full Professor, University of Toronto  
Vinassa, Jean-Michel, Professeur d'Université, Bordeaux INP  
Dumont, Romane, Docteur, ST Microelectronics

Allard, Bruno, Enseignant chercheur, INSA Lyon  
Pillonet, Gaël, Directeur de Recherche, CEA-LETI  
Oukassi, Sami, Ingénieur Chercheur, CEA-LETI